On the role of air-sea interaction parameters in the formation of convective systems over north Indian Ocean during El-Niño, La-Niña and IOD years

A Thesis submitted to Goa University for the award of the Degree of

DOCTOR OF PHILOSOPHY

in

MARINE SCIENCES

By

Mr. Sumesh. K.G.

Research Guide

Dr. M. R. RAMESH KUMAR

Goa-University

Taleigao - Goa

(2017)

Dedicated to my wife Manjusha and daughter Neha...

Contents

Chapter 3: A climatology of the convective systems over northern Indian Ocean

Chapter 4: Convective systems over NIO during the El-Niño and El-Niño Modoki years

Chapter 5: Convective systems over NIO during the La-Niña and La-Niña Modoki years

Chapter 6: Convective systems over NIO during the Indian Ocean Dipole and Neutral years

LIST OF TABLES

LIST OF FIGURES

LIST OF ABBREVIATIONS

NIO: ....North Indian Ocean
AS: ....Arabian Sea
BB: ....Bay of Bengal
IMD: ....India Meteorological Department
SST: ....Sea Surface Temperature
ENSO: ....El-Niño Southern Oscillation
SO: ....Southern Oscillation
EN: ....El-Niño
ENM: ....El-Niño Modoki
LN: ....La-Niña
LNM:...La-Niña Modoki
IOD: ....Indian Ocean Dipole
PIOD: ....Positive Indian Ocean Dipole
NIOD: ....Negative Indian Ocean Dipole
NU: ....Neutral
MON: ....Monsoon season
NON: ....Non-monsoon seasons
LLRV: ....Low Level Relative Vorticity
LLC: ....Low Level Convergence
VWSC: ....Vertical Wind Shear Coefficient
U: ....Zonal Wind
MTI: ....Mid Tropospheric Instability
CI: ....Convective Instability parameter
HUM: ....Humidity parameter

Statement

As required under the University Ordinance 0.19.8 (vi), I state that the present thesis entitled **"On the role of Air-Sea interaction parameters in the formation of convective systems over north Indian Ocean during El-Niño, La-Niña and IOD years"** is my original research work carried out at the National Institute of Oceanography, Goa and that no part there of has been submitted for any other degree or diploma in any University or Institution. The literature related to the problem investigated has been cited. Due acknowledgements have been made wherever facilities and suggestions have been availed of.

Mr. Sumesh. K.G.

Certificate

This is to certify that the thesis entitled "**On the role of Air-Sea interaction parameters in the formation of convective systems over north Indian Ocean during El-Niño, La-Niña and IOD yearS**" submitted by Sumesh. K.G., for the award of the degree of Doctor of Philosophy in the Department of Marine Sciences is based on his original studies carried out by him under my supervision. The thesis or any part there of has not been previously submitted for any degree or diploma in any University or Institution.

Ramesh Kumar

Dr. M.R. Ramesh Kumar

All the corrections suggested by Referees have been incorporated

21-07-2017

Ramesh Kumar 21/7/17

21/07/17

Acknowledgments

First of all I express my sincere love, respect and gratitude to my research guide Dr. M.R.Ramesh Kumar, without his continuous support and encouragement, this thesis would have never been completed successfully. I express my sincere gratitude to former Directors of NIO Dr. S.R. Shetye, Dr. S.W.A. Naqvi, Dr. S. Prasanna Kumar, Dr. V.S.N. Murty and to the present Director Dr. S.K. Singh for providing all the necessary facilities to carry out my Ph.D research work at NIO. Sincere thanks to Dr. M. Rajeevan (former Director of IITM-Pune) for providing the necessary computer facilities at IITM. I am very much grateful to University Grants Commision New Delhi for providing me a research fellowship.

The suggestions and critical comments from Dr. V.V. Gopalkrishna as Vice Chancellor's nominee, during each stage of my research are greatly acknowledged. I thank all the Scientists at Physical Oceanography Division of NIO especially Dr. A.S. Unnikrishnan, Dr. P. Vethamony, Dr. S. Prasanna Kumar and Dr. P.M. Muraleedharan for their help, support and encouragement during the period of my research. I have received sincere help from Mr. G.S. Michael Technical officer at POD on the preparation of GMT plots which is also greatly acknowledged. Special thanks to Dr. V.K. Banaker and Mr. V. Krishnakumar for their help and support through the HRM division. I extend my sincere gratitude to my friend and mentor Dr. S. Abhilash, Asst. Professor, Dept. of Atmospheric Sciences, CUSAT for helping me in the development of the new index and I am grateful to Professor Ramola Antao for the english correction of my thesis.

Sincere thanks to Mr. Midhun Raj for his timely assistance in the plagiarism checking and similarity matching through NIO library more over that he has provided many important research articles related to the research work for reference. I had a wonderful and memorable research time at NIO, I have received helps from my friends at all the stages of my research. Heartfelt thanks to my all NIO friends Dr. Shyam, Divya, Chinnu, Remya, Vijith, Byju, Glejin Johnson, Saji Pjilip, Haris, Charles, Subeesh, Nideesh,

Joshua, Gopika, Swathy and Gourav for their help and friendship.

Sincere thanks to my mother and brother. My father is no more to see this achievement, but I am sure that he will bless me from the heaven. I am extremely grateful to my beloved wife Manjusha for her whole hearted love, help, care and support. Kisses to my most loving daughter Neha. Finally I thank all those who have helped me to achieve this goal.

Above all I thank the almighty god for the blessings all the time ....

Sumesh. K.G.

List of Publications

Publications related to the Ph.D Thesis

1. **K. G. Sumesh** and M. R. Ramesh Kumar, 2013: Tropical Cyclones over north Indian Ocean during El Nino Modki years. Natural Hazards, DOI: 10.1007/s11069-013-0679-x. 68(2), 1057-1074.

2. **K. G. Sumesh** and M. R. Ramesh Kumar, 2015: Tropical cyclones over north Indian Ocean during La-Niña Modoki years. Indian Journal of Geo Marine Sciences.Vol. 44(7), July, 2015, 977-983.

3. **K. G. Sumesh,** S. Abhilash and M. R. Ramesh Kumar, 2016: Relative roles of individual variables on a revised convective system genesis parameter over north Indian Ocean with respect to distinct background state. Natural Hazards (communicated).

ABSTRACT

Tropical cyclones are the most disastrous weather systems over the globe. They generally form within the Inter Tropical Convergence Zone where the relative vorticity and atmospheric convection are always present and the magnitude of the vertical wind shear is minimum. They cause severe damage to the life and property in the coastal areas of their landfall. These catastrophic convective systems die if there is a lack of warm moist air supply as they approach the land.

The genesis and intensification of these convective systems are highly influenced by various air-sea interaction parameters. The role of these cyclogenesis parameters in the formation and intensification of the convective systems over northern Indian Ocean (NIO) in various climatic modes has been investigated in this research work. The convective systems formed over NIO in the period of 1979 to 2008 are considered in this study and classified them into three categories, namely depressions, cyclones and severe cyclones. The convective systems, further grouped with respect to the origin of their genesis (Arabian Sea & Bay of Bengal) and analysed with respect to climatic modes, namely: the El-Niño, El-Niño Modoki, La-Niña, La-Niña Modoki, Positive IOD, Negative IOD and Neutral (devoid of ENSO and IOD) conditions.

A new cyclogenesis index has been developed as a part of the present study and named as the Convective System Genesis Parameter (CSGP). The relative role of each individual variable on CSGP has been analysed separately for different categories of the storms over both Arabian Sea and Bay of Bengal. The composite structure of the CSGP for different categories of the storms is further evaluated separately for distinct large scale background state. The present study shows that the CSGP is capable of providing the location of cyclogenesis and distinguish different categories of the storms.

Chapter 1

Introduction

1.1 Introduction

Tropical cyclones are the most dangerous weather systems that form over the warm ocean surfaces where the Sea Surface Temperature (SST) is greater than 26°C. They influence the weather and climate over many of the tropical countries. They can cause severe damage to the life and property in the regions of their landfall. Northern Indian Ocean (NIO) comprising Arabian Sea (AS) and Bay of Bengal (BB) is one of the most important cyclone prone basins among the world ocean basins. NIO is known for its potential to produce the most intense tropical cyclones in the world. On an average 80-85 tropical cyclones form over the globe in each year. Every year 3-5 tropical cyclones form over NIO and it accounts for 6-7% of the global tropical cyclones. Depending upon the various thermodynamic properties over both AS and BB more number of tropical cyclones form over BB than AS. Amato and Carmago (2010) showed that on an average 1-2 tropical cyclones form over AS every year and furthermore, the number of cyclones forming in the BB is about four times higher than in the AS (Dube 1997).

1.2 Conditions favourable for the formation of the tropical cyclones

A tropical cyclone generally forms in the vicinity of the Inter Tropical Convective Zone (ITCZ) or near equatorial trough, where the relative cyclonic vorticity is already present and the tropospheric vertical shear of horizontal wind is a minimum or zero (Gray 1968). The easterly waves also influence the formation of the tropical cyclones in various basins (Landsea 1993, Frank and Roundy 2006). Even though the formation of tropical cyclone is less understood it is known that some physical conditions are required for the formation of the tropical cyclones. Gray (1975 and 1998) has introduced the ocean atmospheric parameters which are responsible for the formation of tropical cyclones, they are: 1) high magnitude of Coriolis force, 2) high magnitude of low level relative vorticity, 3) low magnitude of vertical wind shear, 4) high magnitude of ocean thermal energy, 5) a conditionally unstable atmosphere and 6) high magnitude of relative humidity.

1.3 The evolution of tropical cyclones

The tropical cyclone has a definite life cycle and it evolves in four phases, namely the formative stage, immature stage, mature stage and the dissipation stage. In the formative stage a tropical disturbance will establish in a large area of the ocean surface where the SST is greater than 26°C. The disturbance will slowly develop into the Low Pressure Area (LPA) with high speed winds. The intensity of the LPA would increase to its later stages namely depression, deep depression, cyclonic storm and severe cyclonic storm, as it experiences the favourable ocean-atmospheric conditions for its development. High amount of moisture supply will be there for all the stages of the convective system. The formative stage extends from the establishment of LPA to the stage of the severe cyclonic storm.

In the immature stage there is a rapid fall of central pressure and it will reach the lowest limit. The huge convective clouds will get organized into spiral bands. The pressure falls to its lowest point and the winds attain maximum speed during this period. In the mature stage the pressure fall will be stopped and there will not be further increase in the wind speed. The circulation expands outward and starts moving towards the land. In the dissipation stage the entire system will start to decay as the system approaches towards the land. The system dies when it enters the land or an oceanic area where the SST is below 26°C because the warm moist air supply is drastically stopped.

1.4 The structure of a mature tropical cyclone

Tropical cyclones exhibit much variations in their size and intensity with respect to the origin and season of their genesis. Several authors have studied the variations in the size intensity for tropical cyclones (Shea and Gray (1973 a,b), Frank 1976, Emmanual 1985 and 2005, Holland 1997, Merril 1983). A mature tropical cyclone typically consists of a warm core vortex circulation, cyclonic in the lower and anti cyclonic in the upper layer of the troposphere, with a core of intense winds and precipitation (Frank 1976).

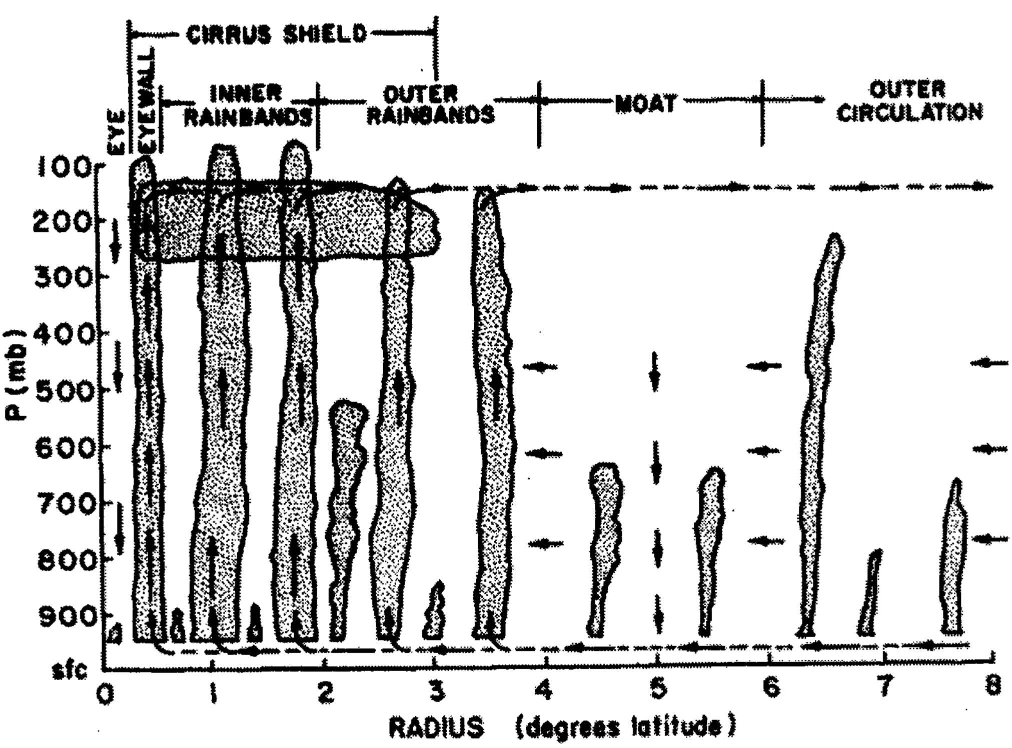

Figure: 1.1 The schematic diagram of a mature tropical cyclone (Frank 1976)

The diameter of a mature tropical cyclone can extend upto 1500-2000 km. The central part of the tropical cyclone is called the eye of the cyclone, the radius of the eye is about 50-60 km. The eye is a cloud free region since there exist calm winds and weak convection. Surrounded by the eye there is eye wall which has 10-20km thickness, which exhibits extremely strong cyclonic wind flow and intense convection. The eye wall is the region of towering cumulonimbus clouds, severe thunder storms and torrential rainfall. Beyond the eye wall cloud the cyclonic winds gradually diminish with the radius, and active convection is confined primarily to intense cyclonically curving squall lines known as spiral bands or feeder bands. The schematic diagram of a mature tropical cyclone is shown in figure (1.1).

1. 5 Previous studies on the storms and depressions over north Indian Ocean (NIO)

The thermodynamic properties and ocean-atmospheric conditions favourable for the development of the convective systems are highly variable over AS and BB. The physical processes and frequency variations of the convective systems, namely depressions, cyclones and severe cyclones over NIO have been subject to many studies by various authors. Studies have found that there is a decreasing tendency in the frequency of the depressions over NIO (Rajeevan et. al 2000a,b) during the monsoon season for the period of 1951-1998. Xavier and Joseph (2000) showed that the frequency of depressions / storms depends on the vertical wind shear. The SST has much influence on the formation of the convective systems over NIO. Pai and Rajeevan (1998) found that the organized convection over NIO increases as the SST increases from 26.4° C and reaches a maximum up to 29.0° C and the convections decrease as the SST increases to more than 29.0° C. This study reveals that overheating of the ocean surface will diminish the large scale convection and suppress the formation of the convective systems.

Studies on the frequency of cyclonic storms over NIO reveal that there is an increasing trend in the frequency of intense tropical cyclones over NIO (Singh et al. 2000; Singh 2007; Srivastav et al. 2000). Srivastava et al. (2000) show that there was a significant decreasing trend in the frequency of cyclonic storms over NIO during the period of 1891-1997; this study further suggests that the weakening of Hadley circulation may be one of the causes of decreased cyclonic activity. A negative trend has been observed in the year to year fluctuations in the frequency of the cyclonic storms since 1950 (Mandal 1991). Patwardhan and Bhalme (2001) observed a negative trend in the frequency of cyclones during the recent years. Ramesh Kumar and Syam (2010) have studied the impact of global warming on the cyclonic storms over NIO, and state that the frequency of storms and severe storms do not show any dramatic rise despite increase over the sea surface temperature in the BB from 1951-2007 compared to the 1901-1951. This study further states that there is a large decrease in the mid tropospheric humidity over the BB during the period 1951-2007 and the atmospheric parameters such as low level vorticity, mid tropospheric humidity and vertical wind shear, all play an important role on the genesis and intensification of storms over this basin. Ramesh Kumar and Baiju (2010) have studied the ocean atmospheric conditions leading to the formation of cyclones over AS, and it states that better spatial and temporal satellite estimates of OLR, SST, Precipitable Water, blended Objectively Analysed Air Sea Flux (OAFlux), European Centre for Medium Range Weather Forecast (ECMWF) data products, and new tools, such as moored buoys and Argo floats would be useful for the study of cyclones over the Arabian Sea. Ramesh Kumar et. al (2009) have studied the role of convective systems over north west Pacific Ocean and monsoon activity over the Indian subcontinent. It states that in the years of deficit rainfall and prolonged breaks in the monsoon season, the systems (about 69%) formedfurther south than in the case of excess monsoon years.

The frequency of severe cyclonic storms during the period of 1877-1977 has been studied by Mooley (1980,1981), who found that the percentage of storms intensifying into severe cyclonic storms were high during the period of 1965-77. Muni Krishna (2009) has shown that the frequency of the severe cyclone is increasing during the summer monsoon season. The study shows that the weakening of Tropical Easterly Jet (TEJ) gives suitable environmental conditions for the formation of severe cyclones during the summer monsoon season. The north-ward movements of the severe cyclones over BB during the dry Indian summer monsoon episodes have been studied by Joseph et.al (2016). the results show that the dry monsoon conditions are associated with the cold phase of the Atlantic Multidecadal Oscillation (AMO).

Table 1.1 Classification of convective systems by India Meteorological Department (IMD)

Sl. No:	**Convective Systems**	**Wind speed in knots / (kmph)**
1	Low Pressure Area (LPA)	<17 / (<32)
2	Depression (D)	17-27 / (32-50)
3	Deep Depression (DD)	28-33 / (51-59)
4	Cyclonic Storm (CS)	34-47 / (60-90)
5	Severe Cyclonic Storm (SCS)	48-63 / (90-119)
6	Very Severe Cyclonic Storm (VSCS)	64-119 / (119-220)
7	Super Cyclone (SC)	>119 / (>220)

Table 1.1 gives the IMD classification of the convective systems over NIO. As per India Meteorological Department (IMD), the area in the atmosphere in which the pressures are lower than those of the surrounding region at the same level and is represented on a synoptic chart by a system of one closed isobar when the system is at sea or one closed isobar in the radius of 3 degrees from the centre over land. In this region the surface wind speed will be 17 Knots (32 Kmph). This region is called a Low Pressure Area (LPA). These LPAs are producing enough rainfall in the coastal and inland regions over the Indian peninsula. Three categories of convective systems (depressions and deep depressions, cyclonic storms and severe cyclonic storms and above) have been considered in this study.

1. 6 Depressions

Depressions are the convective systems in which the wind speed is (17-27 knots) or (32-50 kmph). The depressions are the most important synoptic scale disturbances that generally form during the monsoon season (June-September) and contribute to about 10% of the Indian summer monsoon rainfall. The depressions also bring good amount of rainfall during the non-monsoon seasons. A study (Rajeevan et. al 2000b) stated that 7-8 monsoon depressions form over NIO every year. Several studies have shown that there is a decreasing trend in the frequencies of the monsoon depressions over NIO. A significant decreasing trend for the depressions is noticed (Dash 2004) for the depressions over NIO. In this category the depressions and deep depressions are considered. As per the IMD criteria, the convective system represented on a synoptic chart by two closed isobars at 2 hPa interval is called a depression. Deep depression is a convective system represented on a synoptic chart by three closed isobars at 2 hPa and the surface wind speed will be 28 to 33 Kts (51 – 59 Kmph) at sea. They also bring heavy rainfall to the coastal and inland areas over the Indian subcontinent. The frequency of these systems is more during the monsoon season compared to the non-monsoon seasons. Further it is observed that there are more depressions and deep depressions over BB than the AS.

1. 7 Cyclones

The cyclones are intense convective systems represented on a synoptic chart by four or more closed isobars at 2 hPa intervals and in which the wind speed on surface level is between 34 – 47 Kts. The cyclonic storms and higher intensities are generally called tropical cyclones in NIO. The energy of a cyclone is the latent heat produced inside each cumulonimbus tower. The heat stored in the oceans helps the large scale cumulonimbus convection to initiate cyclogenesis. These tropical cyclones will die as they approach the land or move through a cold ocean surface.

1. 8 Severe cyclones

There are three more intense convective systems according to IMD criteria based on the wind speeds. If the cyclones experience a favourable environment such as the warm ocean surface to pump fuel to the cyclone, high magnitude of relative vorticity, low magnitude of vertical wind shear and a highly unstable atmosphere, they will get intensified into a severe cyclone. The size of the severe cyclones will be smaller than the cyclones. But the sustained wind speed and rainfall will be more than the cyclones. These severe cyclones can cause severe damage to the life and property in the coastal areas of their land fall. According to IMD, the Severe cyclonic storm is the intense convective system with wind speed on surface level is between 48 – 63 Kts. If the sustained wind speed on surface level is between 64 – 119 Kts this category of the convective system is called the Very severe cyclonic storm. The most severest of the convective system is the Super cyclone, in which the sustained wind speed on surface level is more than 119 Kts and above.

1. 9 Importance of the study

The convective systems forming over NIO affect the weather, climate and well being of the people in India. The convective systems such as depressions and deep depressions produce a good amount of rainfall mainly in the monsoon season and in turn meets the water requirement for India. At the same time other intense convective systems such as cyclonic storms, severe cyclonic storms, very severe cyclonic storms and super cyclones are producing torrential rainfall, flash floods, storm surges and other damage to the life and property in the coastal areas of their land fall. The NIO is known for its potential to produce the most intense tropical cyclones in the world. A better forecasting of these convective systems would be very important because we can save a good number of lives and property from the hazards of the cyclones. Various cyclogenesis indices are used to forecast these tropical storms over various basins including NIO. In this aspect a revised Convective System Genesis Parameter (CSGP) has been proposed to identify the regions favourable for the storm genesis and to forecast their intensity. The revised CSGP can be used to forecast all categories of convective systems such as depressions, cyclones and severe cyclones over NIO during the monsoon as well as non-monsoon seasons.

1.10 Objectives of the study

This study addresses how the large scale back ground state of the basin influences the formation and intensification of the convective systems. The frequencies of the convective systems during climatic modes namely like El-Niño, El-Niño Modoki, La-Niña, La-Niña Modoki, PIOD, NIOD and neutral years are also analyzed. A new cyclogenesis index namely the convective system genesis parameter (CSGP) has been developed as a part of the present study. This index looks at the relative roles of various cyclogenesis parameters namely, low level relative vorticity, low level convergence, vertical wind shear co-efficient, mid tropospheric relative humidity and convective instability. The characteristics of this index for all the convective systems formed over NIO during the period from 1979 to 2008 have been investigated. The composite structure of the CSGP for different categories of convective systems is further evaluated separately for distinct large scale background state. The results show that this index is capable of distinguishing different categories of convective systems. The CSGP exhibits large variability during distinct large scale background state. It is also found that the individual variables contribute in a different way during the monsoon and non-monsoon seasons. The specific objectives of the present study are to understand the role of various air-sea interaction parameters in the formation of convective systems over NIO during the 1) El-Niño years, 2) La-Niña years and 3) IOD years.

Chapter 2

Data and methodology

In order to achieve the specific objectives mentioned in chapter 1, we have studied different types of convective systems (Depressions, Deep depressions, Cyclones, Severe cyclones, Very severe cyclones and Super cyclones) over the north Indian Ocean (Arabian Sea and Bay of Bengal) during different seasons (Monsoon and Non-monsoon) for the study period 1st January, 1979 to 31st December, 2008. The in-situ data pertaining to the formation of various convective systems (dates, frequencies, genesis locations and tracks) have been extracted from the cyclone e-Atlas (IMD). The NCEP/NCAR Reanalysis 2 (Kanamitsu et. al 2002) data set has been used to study the characteristics of the air-sea interaction parameters for the convective systems formed over NIO. It is also used to develop the new cyclogenesis index.

We have obtained the cyclone frequencies for various basins from the Unisys Weather (http://weather.unisys.com/hurricane/). The Outgoing Long-wave Radiation (OLR) data (Liebmann and Smith, 1996) from National Oceanic and Atmospheric Administration (NOAA) is used in the thesis. The data is measured by Advanced Very High Resolution Radiometer (AVHRR) aboard the NOAA Polar Orbiting satellites available from 1974 onwards with gaps filled with temporal and spatial interpolation. The data contains a major gap of several months during 1978 due to the failure of satellite. The data has a spatial resolution of 2.5° latitude-longitude grids and monthly and daily fields are available. Generally geostationary-derived OLR data is suitable for cyclone studies requiring high temporal resolution, but they lack global coverage. Compared with it NOAA interpolated OLR provide better accuracy, global coverage and have multi-decade record which makes it suited for studies of low-frequency variability.

Hadley Centre Sea Ice and Sea Surface Temperature data Hadley Centre sea ice and sea surface temperature data (Rayner et al, 2003) version 1.1 (HadISST V1.1) developed at the Met Office Hadley Centre for Climate Prediction and Research is used in this thesis. The data has global coverage with a resolution of 1° x 1° latitude-longitude grid and is available from 1871. Gaps in the SST data have been interpolated. Care has to be taken when using 32 HadISST-1 for studies of climatic variability, particularly in some data sparse regions, because of the limitations of the interpolation techniques (Rayner et al, 2003).

The extended reconstructed sea surface temperature (ERSST) (Smith and Reynolds 2003) was constructed based on the International-Comprehensive OceanAtmosphere Data Set (I - COADS). ERSST Version 3 (Smith and Reynolds 2008) is used in this thesis. The data has a spatial resolution of 2° latitude - longitude and monthly means are available. Although there are differences due to both the use of different historical bias corrections as well as different data and analysis procedures, the large-scale variations of ERSST are broadly consistent with those associated with the HadISST (Smith and Reynolds 2003). Each month the ERSST analysis is updated with the available GTS ship and buoy data. The anomalies are computed with respect to 1971-2000 month climatology (Xue et. al 2003). ERSST version 2 was an improved extended reconstruction of ERSST version 1. However ERSST version 3 differs form ERSST version 2 by the inclusion of satellite data.

The monthly Nino 3.4 SST indices obtained from the NOAA Climate Prediction Center (CPC) website (www.cpc.noaa.gov) is used for defining the El-Niño and La-Niña years. The index is created from ERSST version 3b and the SST anomalies are calculated for the Nino 3.4 region (5°N – 5°S, 120° – 170°W) based on centered 30-year base periods updated every 5 years. El-Niño (La-Niña) years are defined such that the October-

December averaged SST anomaly of the region is above (below) a threshold value of 0.5°C and the condition should persist for a minimum of 5 consecutive over-lapping months.

The IOD index, also known as Dipole Mode Index (DMI) is obtained from Japan Agency for Marine-Earth Science and Technology (JAMSTEC) website (www.jamstec.go.jp). Intensity of the IOD is represented by anomalous SST gradient between the western equatorial Indian Ocean (50°E–70°E and 10°S–10°N) and the south eastern equatorial Indian Ocean (90°E–110°E and 10°S–0°). When the DMI is positive then, the phenomenon is refereed as the positive IOD and when it is negative, it is refereed as negative IOD. The index used in the thesis is derived from HadISST and monthly index is available from 1958.

The latent heat flux used in the present study has been extracted from OAFlux (Yu and Weller, 2007). The OAFlux project uses objective analysis approach to take into account data errors in the development of enhanced global flux fields. The objective analysis denotes the process of synthesizing measurements/estimates from various sources. Such process reduces error in each input data source and produces an estimate that has the minimum error variance.

2.1 In- Situ data

IMD has digitized the hard copy editions of the widely referred atlas "Tracks of Storms and Depressions in the Bay of Bengal and the Arabian Sea", which were published by IMD in the years 1964, 1979 and 1996. This electronic version is named the Cyclone e-Atlas. This product was released in the year 2008. This in-situ data set gives substantial information on the frequency, date of formation and dissipation, genesis locations and the tracks of all the convective systems, namely depressions, cyclones and severe cyclones formed over NIO. This has been designed in such a way that the frequencies of the depressions, cyclones and severe cyclones are expressed in tabular form as well as bar diagrams. The intensity variations of the convective systems from the date of formation to the date of dissipation are also available in this package.

2.2 The NCEP/NCAR Reanalysis II

The NCEP/NCAR Reanalysis II (Kanamitsu et. al 2002) is a continually updated gridded data set representing the state of the earth's atmosphere. This data set is developed by incorporating the surface and upper-air observations and Numerical Weather Prediction (NWP) outputs. This product is the outcome of a collaborative research project between two leading national research organizations of America, namely the National Centre for Environmental Prediction (NCEP) and the National Centre for Atmospheric Research (NCAR). NCEP Reanalysis II is an improved version of the NCEP Reanalysis I (Kalnay et. al 1996). It has fixed the errors of the NCEP Reanalysis I. The parameterization schemes of the physical processes have been updated in this new version. Daily averaged data for all the weather parameters in 17 standard pressure levels are available in this data set. The values of the variables derived from the reanalysis have varying degrees of influence from observations and models. Output variables are classified into four classes (A, B, C and D), depending on the degree to which they are influenced by the observations and the model. Class A variables indicate that the analysis variable is strongly influenced by the observed data and hence it is in the most reliable class (for example, upper air temperature and wind); the class B indicates that although there are observational data that directly affect the value of the variable, the model also has a very strong influence on it (for example, humidity and surface temperature). The class C indicates that there are no observations directly affecting the variable and that derives only by the data assimilation to remain close to the atmosphere (for example, clouds, precipitation and surface fluxes). Further the class D represents a field obtained from purely climatological values and does not depend upon the model. The spatial resolution of this data set is 2.5° x 2.5° and it covers a large area between 90°N to 90°S and 0°E to 357.5°E.

2.3 Methodology

The studies and observations show that various climatic episodes namely El-Niño and La-Niña (Trenberth 1997, Clark et.al 2014, Li et.al 2011), El-Niño Modoki and La-Niña Modoki (Ashok et. al 2007, Hsu et. al 2013), Positive IOD, Negative IOD (Saji et. al 1999, Webster et. al 1999, Kripalani and Pankaj Kumar 2004, Pervez and Henebry 2015) and neutral (Pervez and Henebry 2015) conditions have got high influence on the frequencies and intensities of the convective systems over NIO. The role of air-sea interaction parameters in the formation and intensification of the convective systems formed over NIO during the period between 1979 and 2008 has been investigated in this study. The cyclogenesis parameters defined and tested over NIO by various authors (Gray 1975, Zehr 1992, Kotal 2009) such as the low level relative vorticity (LLRV) at 850 hPa level, low level convergence (LLC) at 850 hPa level, vertical wind shear coefficient (VWSC), mid tropospheric relative humidity (HUM) and the convective instability (CI) have been used to analyze the influence of the said climatic episodes in the formation and intensification of the convective systems over this basin. The average values for all these parameters for every system has been obtained from the day of formation to the day of dissipation. The low pressure systems have been classified into three categories, namely depressions, cyclones and severe cyclones and further grouped with respect to the origin of their genesis. Finally the systems are grouped again with respect to the large scale state of the ocean.

2.4 The selected years of various climatic episodes

Table (2.1) gives the list of selected years of various climatic modes. There were four El-Niño years, seven El-Niño Modoki years, six La-Niña years, two La-Niña Modoki years one PIOD year, three NIOD years and four neutral years during the study period. These years have been obtained form various research articles.

Table 2.1 List of selected years of various climatic modes

Sl. No	El-Niño	El-Niño Modoki	La-Niña	La-Niña Modoki	PIOD	NIOD	Neutral
1	1982	1986	1981	2000	2007	1989	1979
2	1983	1990	1984	2008		1993	1980
3	1987	1991	1988			1996	1985
4	1997	1992	1998				2001
5		1994	1999				
6		2002	2005				
7		2004					

2.5 Role of cyclogenesis parameters in the formation of the tropical cyclones

Five cyclogenesis parameters have been considered in this study, namely 1) low level relative vorticity (LLRV), 2) low level convergence (LLC), 3) vertical wind shear co-efficient (VWSC), 4) mid tropospheric relative humidity parameter (HUM) and the convective instability parameter (CI). It is observed that the tropical cyclones form only in regions where the magnitude of LLRV is positive. In such regions there will be strong inflow of warm moist air into the centre of the low pressure system. This inflow of warm moist air produces cyclonic spin-up and it will enhance the development of convective clouds.

There exists a deep LLC from the surface to 400 hPa for all categories of convective systems. The LLC enhances the convective currents and helps the formation of huge cumulonimbus clouds in the cyclone. Normally tropical cyclones do not form over NIO during the monsoon months. The monsoon current in the lower atmosphere and strong Tropical Easterly Jet (TEJ) in the upper levels of the atmosphere makes strong vertical wind shear over this region, hence there is hardly any tropical cyclone during this period. The formation of tropical cyclones requires a small magnitude of vertical wind shear hence the maximum frequency of the tropical cyclones is found over NIO during the pre-monsoon and post-monsoon seasons. It is observed that, if the magnitude vertical wind shear is large the formation of tropical cyclone is limited and there is no further intensification for the existing cyclone.

Tropical cyclones do generally form over the warm ocean surfaces where the SST is greater than 26°C. It requires a warm thermal oceanic layer of 60m depth to supply the warm moist air. The source of energy of tropical cyclone is the moisture from this warm surface water and the latent heat of condensation. This warm thermal layer over the ocean makes a region of large scale convection and produces huge number of towering convective clouds. The environmental moisture has been considered an important parameter for the formation and intensification of the tropical cyclones (Gray 1975, Wu 2015). Theoretical and modelling studies show that the high magnitude of environmental moisture is conducive for the formation and intensification of the tropical cyclones (Emanuel 2004, Kimball 2006). As one of the skilful predictors the Relative Humidity (RH) at 850 hPa as the area averaged 200 to 800 km from the storm centre has been used in the Statistical Hurricane Intensity Prediction Scheme (SHIPS) at the National Hurricane Centre (Kaplan 2010).

The formation of the tropical cyclones also requires a conditionally unstable atmosphere. Equivalent potential temperature (θ_e) is a measure of instability in the atmosphere. If the magnitude of θ_e is decreasing with altitude then the atmosphere is unstable and convection occurs over there. Sikora (1976) suggested that the equivalent potential temperature at 700 hPa level in a developing tropical cyclone is an excellent parameter to measure the total thermodynamic energy of the tropical cyclone at a particular time because it accounts for both sensible and latent heat energy. This study further suggests that abnormally high values of equivalent potential temperature (> or = 370° K) for the formation of tropical cyclones can herald a period of subsequent explosive deepening. The magnitude of the equivalent potential temperature is maximum in the eye wall.

Studies show that there should be a well-established vertical coupling of the lower and upper tropospheric flow patterns for the formation of the tropical cyclone. Cumulonimbus convection acts as the primary mechanism for this vertical coupling. Cumulonimbus convection is typically associated with a substantial decrease of θ_e between the boundary layer and the middle troposphere. Normally the θ_e gradients are taken between the surface and 500 hPa; they typically range between 15 and 20 °K. All these parameters have been considered in this study to investigate the influence of these ocean-atmospheric parameters in the frequency and intensity variations over NIO during various climatic episodes.

2.6 Cyclogenesis Indices

Cyclogenesis index is a mathematical expression of the cyclogenesis parameters which are used to forecast the formation and intensification of a tropical cyclone. Various authors (Gray 1975, Zehr 1992, Royer 1998, McBride and Zehr 1981, Emanuel and Nolan 2004, Kotal, 2009) have used different combinations of these ocean-atmospheric parameters to make better indices to forecast the genesis of the tropical cyclones in a more accurate way and they are being used to forecast tropical cycones all over the world. A new cyclogenesis index has been developed as a part of this study.

2.7 Seasonal Genesis Parameter (SGP)

Gray (1975) developed the first cyclogenesis index using the six physical parameters, namely (1) low level relative vorticity, (2) coriolis parameter, (3) inverse of the vertical shear of the horizontal wind between the lower and upper tropsphere, (4) ocean thermal energy or sea temperature above 26°C to a depth of 60m, (5) vertical gradient of equivalent potential temperature between the surface and 500 hPa level and (6) mid tropospheric relative humidity (RH). The first three parameters are called the dynamic parameters and the last three parameters are called the thermodynamic parameters. The product of all these parameters is called the Seasonal Genesis Parameter (SGP). It is hypothesized that tropical cyclone formation will be most frequent in the regions and in the seasons when the product of the six primary genesis parameters are maximum. The Seasonal Genesis Parameter (SGP) is defined as

SGP = [(Vorticity parameter) x (Coriolis parameter) x (Vertical shear parameter)] x [(Ocean energy parameter) x (Moist stability parameter) x (Humidity parameter)]. In other words Seasonal genesis parameter is the product of the dynamic potential and thermodynamic potential. That is SGP = [(Dynamic potential) x (Thermal potential)]

Dynamic potential is expressed in units of ($10^{-11}s^{-2}$ ((ms^{-1} / 750 hPa))), and thermal potential is expressed in units of (10^5 cal/cm^2 °K /(500 hPa)). The SGP is expressed in units of 10^{-8}cal Ks^{-1} cm^{-3}. Compared with the results of Gray (1979) and Ryan et.al (1992), this is found to be a good predictor of the number of tropical cyclones formed per 5°x5° latitude-longitude square per 20 years. The SGP is usually calculated from the seasonally averaged climatological data of the atmosphere or the oceanic fields for each of the seasons: winter (JFM), spring (AMJ), summer (JAS) and autumn (OND).

2.8 Yearly Genesis Parameter (YGP)

Gray (1975) proposed a Yearly Genesis parameter (YGP) and it is calculated as the sum of the four SGPs in four seasons. The thermal potential of the SGP delimits the regions and the seasons of possible tropical cyclone formation. The dynamical factors determine the synoptic conditions favourable to the formation of tropical cyclones. The YGP which incorporates both thermal and dynamical parameters, is able to identify the regions having a high probability of tropical cyclone formation on climatological time scales.

Gray (1979) validated YGP against observations of the reported detection locations of storm systems which later became tropical cyclones, according to WMO criteria, during 1958-1977. The calculations made by Gray are based on climatological observations averaged over the same period, and have shown that the SGP is able to reproduce remarkably the seasonal frequency distribution of observed tropical cyclones and their distribution over the different ocean basins. It is noticed that the average cyclogenesis is reasonable in the northern hemisphere and in the southern hemisphere, the cyclone frequencies are over estimated by the YGP especially in southern Indian Ocean and south west Pacific. Royer et.al (1998) modified Gray's YGP by replacing the thermal potential with the convective potential. The convective potential is defined as

Convective potential = k x P_c over the oceans and for $|\emptyset| \leq 35°$ lat.

Where P_c is the seasonal mean convective precipitation in mm/ day computed by the model, and Ø is the latitude, and the numerical value of k is 0.145. This modified YGP is called the "Convective Yearly Genesis Parameter (CYGP)", which is found as successful as the original YGP for reproducing the main areas of tropical cyclone genesis.

2.9 Daily Genesis Parameter (DGP)

McBride and Zehr (1981) introduced a Daily Genesis Parameter (DGP). This parameter is calculated as the difference of relative vorticity at the upper level (200 hPa) and the lower level (900 hPa). It is defined as (ζ 900 hPa - ζ 200 hPa). This parameter could describe that: (1) The developing and non-developing systems are warm core in the upper levels. The temperature gradients are more pronounced in the developing systems, but the magnitudes are so small that the differences would be difficult to measure for individual systems. (2) The developing or pre-typhoon cloud cluster exists in a warmer atmosphere over a large horizontal scale. (3) There is no obvious difference in vertical stability for moist convection between the systems. (4) There is no obvious difference in moisture content or moisture gradient. (5) The pre-typhoon and pre-hurricane systems are located in large areas of high values of low level relative vorticity. The low level vorticity in the vicinity of a developing cloud cluster is approximately twice as large as that observed with non developing cloud clusters. (6) The mean divergence and vertical motion for the typical western Atlantic weather system is well below the magnitudes found in pre-tropical storm systems. (7) Once a system has sufficient divergence to maintain

100 hPa or more per day upward vertical motion over a 4° radius area, there appears no relationship between the amount of upward vertical velocity and the potential of the system for development. (8) cyclogenesis takes place under conditions of zero vertical wind shear near the system centre. (9) There is a requirement for large positive zonal shear to the north and negative zonal shear close to the south of a developing system. There is also a requirement for southerly shear to the west and northerly shear the east. The scale of this shear pattern is over a 10° latitude radius circle with maximum amplitude at ~6° radius.

2.10 Genesis Parameter (GP)

Zehr (1992) introduced a parameter called Genesis Parameter (GP) to quantify the cyclogenesis over the north-west Pacific Ocean. GP is the product of three dynamic parameters such as Low Level Relative Vorticity at 850 hPa, Low Level Convergence (negative of Divergence) at 850 hPa and Shear Co-efficient. This study showed that this genesis parameter was useful in differentiating between the non-developing and developing systems in the western North Pacific. Roy Bhowmic (2003) used this genesis parameter to study the developing and non-developing systems over NIO, and observed that GP values around 20×10^{-12} S^{-2} against T-No: 1.5 have the potential to develop into a severe cyclonic storm.

2.11 Genesis Potential Parameter (GPP)

Kotal et.al (2009) proposed a new cyclogenesis parameter for the Indian Seas, termed the Genesis Potential Parameter (GPP). This parameter is defined as the product of four variables, namely vorticity at 850 hPa, mid tropospheric relative humidity, mid tropospheric instability and inverse of vertical wind shear. The parameter is tested with a sample dataset of 35 non-developing and developing low pressure systems that formed over the Indian Seas during the period of 1995-2005. The result shows that there is a distinction between GPP value is found to be around three to five times greater for developing systems than for non-developing systems. The analysis of the parameter at early development stage of a cyclonic storm appears to provide a useful predictive signal for intensification of the system.

2.12 Convective System Genesis Parameter (CSGP)

A new cyclogenesis index has been developed as a part of this reserch work, it can be used to forecast the possible areas of genesis and intensity of the convective systems over NIO. This index is named as the Convective System Genesis Parameter (CSGP). This is different from the above mentioned indices such as Genesis Parameter (GP) defined by Zehr (1992) and the Genesis Potential Parameter (GPP) defined by Kotal et. al (2009). This index is defined as

$$CSGP = (LLRV_{850} \bullet LLC_{850} \bullet VWSC \bullet HUM \bullet CI)$$

Where

1) $LLRV_{850}$= Low Level Relative Vorticity at 850 hPa

2) LLC_{850}= Low Level Convergence (negative of Divergence) at 850 hPa

3) VWSC= Shear Co-efficient = $[25.0 - ((U_{200}-U_{800}) / 20.0)]$

4) HUM = [RH – 40] / 30, mid tropospheric relative humidity. (Where RH is the mean relative humidity between 700 and 500 hPa)

5) CI = (θ_e at 1000 hPa – θ_e at 500 hPa), Vertical gradient of Equivalent potential temperature between two levels.

The shear parameter has been kept at the maximum magnitude of 25 ms^{-1}, if the magnitude is greater than 25 ms^{-1} it will reduce CSGP to zero. The unit of this index is $10^{-10}s^{-2}$ °K. The characteristics of this index (CSGP) for all the three categories of the convective systems have been analyzed and the relative role of each individual variable on CSGP is also studied separately for different categories of the storms over both AS and BB. The composite structure of the CSGP for different categories of storms is further evaluated separately for distinct large scale background state. The results show that the revised CSGP is capable of distinguishing different categories of storms. The CSGP exhibits great variability during distinct large scale background state of the ocean. It is also found that the individual variables contribute in a different way during monsoon and non-monsoon seasons. Hence it is suggested that the revised CSGP can be used to forecast all categories of convective systems such as depressions, cyclones and severe cyclones over NIO during the monsoon as well as non-monsoon seasons.

Table 2.2. Total convective systems over NIO formed in both seasons during the study period

Category	**Arabian Sea**		**Bay of Bengal**		**Total over NIO**
	Monsoon (Jun - Sep)	Non-monsoon (Oct - May)	Monsoon (Jun - Sep)	Non-monsoon (Oct - May)	
Depressions	10	17	63	44	134
Cyclones	3	5	8	27	43
Severe cyclones	6	10	3	42	61

Table (2.2) gives the total number of the convective systems formed in both seasons over NIO for the study period. There have been 10 depressions in the monsoon season and 17 depressions in the non-monsoon seasons over AS. Whereas 63 depressions were formed in the monsoon season and 44 depressions formed in the non-monsoon seasons over the BB. The frequencies of the cyclones and severe cyclones over AS were fewer than the frequencies of these convective systems over BB. There were 3 cyclones formed in the monsoon season and 5 cyclones formed in the non-monsoon seasons over AS. In the case of BB, there have been 8 cyclones in the monsoon season and 27 cyclones in the non-monsoon seasons. An increase in the frequency in the severe cyclones have been observed in both seasons over AS. But the increase in the frequency of the severe cyclones has been observed only in the non-monsoon seasons over BB. There have been 6 severe cyclones in the monsoon season and 10 severe cyclones in the non-monsoon seasons over AS. Whereas only 3 severe cyclones formed in the monsoon season and 42 severe cyclones formed in the non-monsoon seasons over BB. Because of the high magnitude of the vertical wind shear over NIO during the monsoon season the frequency of the cyclones and severe cyclones are limited over this basin.

Chapter 3

A climatology of the convective systems over northern Indian Ocean

---

3.1 Introduction

A brief climatological analysis on the monthly frequencies and tracks of the convective systems has been presented in this chapter. Further the climatology of the ocean parameters, namely sea surface temperature, outgoing long wave radiation and latent heat flux are also analyzed. The entire study period is considered as three decades (1979-1988, 1989-1998 and 1999-2008) and further sub divided into the monsoon season and non-monsoon seasons. The decadal as well as seasonal (monsoon and non-monsoon) climatology of the ocean-atmospheric parameters are also investigated; further the trends of each parameter have been analysed.

3.2 Annual cycle of the convective systems over NIO during the study period

The monthly occurrence of various convective systems over NIO based on the e-Atlas data prepared by IMD is shown in the figure (3.1). Figure 3.1 (a, b) shows the monthly frequencies of the convective systems over AS and BB during the study period. Consistent with the previous studies it is seen that there are significant differences in the convective activity as well as the number of convective systems over AS and BB. The frequency of convective systems over BB has two peaks (May – June) and (October – November), with a low frequency during January – April. Further it is seen that the maximum number of the VSCS form in the months of May, November and October respectively. Unlike in the AS, the influence of VWSC is not that much in BB, and hence a few of them do form in BB.

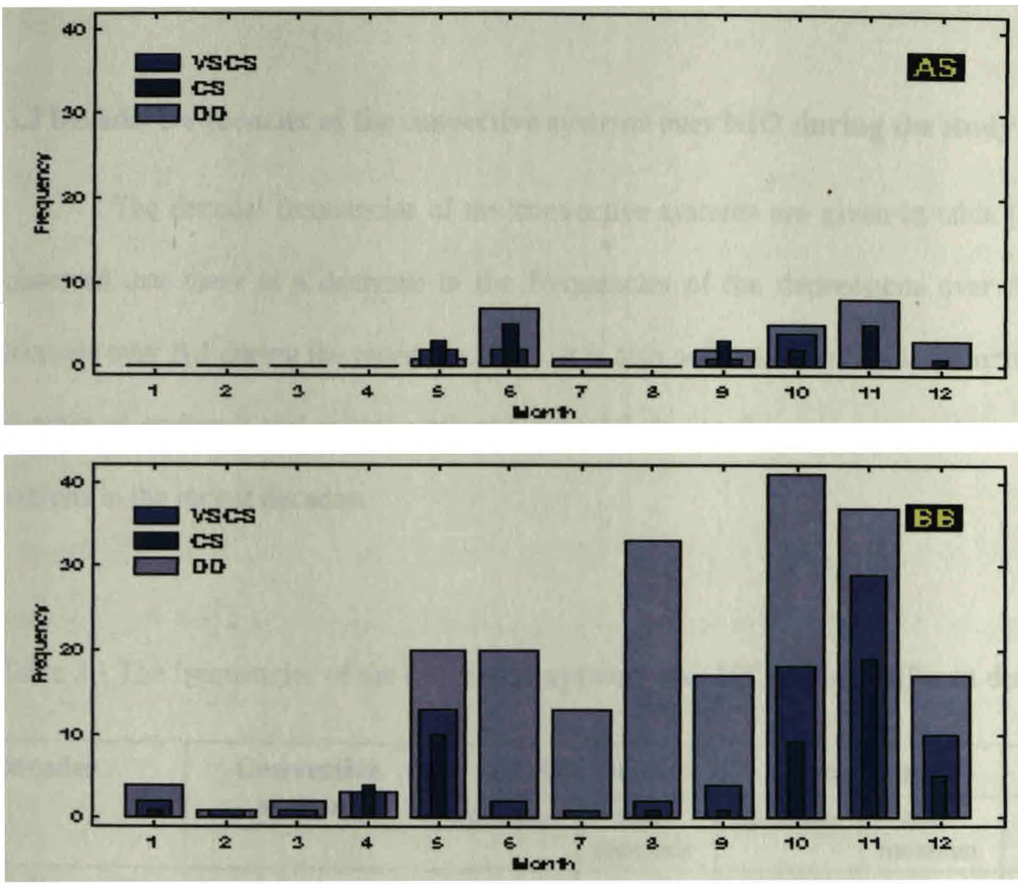

Figure 3.1 The monthly frequencies of the convective systems over NIO (a) Arabian Sea and (b) Bay of Bengal for the study period

From figure 3.1 (a), it is observed that the frequency of the depressions are more over AS during the months of June, September, October, November and December. It is noticed that the frequency of the cyclones is more during October and the frequency of severe cyclones is more in the months of June and November. From figure 3.1 (b), it is observed that the cyclones and severe cyclones are formed over BB during the winter months (January and February). It is observed that the frequency of the depressions is more during the months of May, June, July, August, September, October, November and

December. It is also noticed that the frequency of the cyclones and severe cyclones is more during the months of May, October and November.

3.3 Decadal frequencies of the convective systems over NIO during the study period

The decadal frequencies of the convective systems are given in table (3.1). It is observed that there is a decrease in the frequencies of the depressions over AS and an increase over BB during the recent decades. It is also noticed that there is an increase in the number of cyclones and severe cyclones over AS during the monsoon and non-monsoon seasons in the recent decades.

Table 3.1 The frequencies of the convective systems over NIO during different decades

Decades	**Convective systems**	**Arabian Sea**		**Bay of Bengal**		**Total**
		Monsoon	**Non-monsoon**	**Monsoon**	**Non-monsoon**	
1979-1988	Depressions	5	9	8	12	34
	Cyclones	0	1	4	12	17
	Severe cyclones	2	2	2	17	23
1989-1998	Depressions	2	6	23	27	58
	Cyclones	1	3	1	3	8
	Severe cyclones	3	1	4	16	24
1999-2008	Depressions	3	2	35	19	59
	Cyclones	2	2	0	12	16
	Severe cyclones	2	5	0	11	18

3.4 Monthly occurrence of the convective systems over NIO

It is observed that the the convective systems do not form over AS during January, February and March, but few convective systems do form over BB during this period. These convective systems over BB normally form between 5°N - 8°N, move in a westerly or north-westerly direction and strike the northern Tamil Nadu coast or the east coast of Sri Lanka. They have a tendency to weaken and dissipate over the ocean. In the month of April most of the convective systems over BB form over the area 8°N and 13°N and east of 85°E. These systems will initially move towards north-west or north; later they re-curve towards north-east and strike the Aracan coast of Myanmar. The general direction of the tracks of the convective systems in the AS is similar to that of the convective systems over BB.

The frequency of the convective systems are more in the month of May. Most of the convective systems over BB form over the area between 10°N and 15°N, they move initially in a north-westerly or northerly direction and then re-curve towards the north-east. The whole of the east coast of India, the coastal areas of Bangladesh and Arakan coast of Myanmar are liable to occurrence of the cyclones and severe cyclones in this month. The convective systems over AS take a north-west track and move towards the coast of Arabia and a few of them move in a northerly direction towards the coasts of Maharashtra and Gujarat. The frequency of the convective systems are further increased during the month of June. Almost all the convective systems over BB form over the area between 16°N and 21°N and west of 92°E. Most of the convective systems over BB move towards north-west direction and weaken into depressions after crossing the coast. In the course of further movement the tracks curve towards north or north-northeast. In the case of AS most of the convective systems are formed over north of 15°N and east of 65°E.

In the month of July most of the convective systems over BB form north of 18°N and west of 90°E and they move generally in a west-northwesterly direction. It is noticed that the intensification of the cyclones to severe cyclones is limited during this month. At the same time there is drop in the frequencies of the convective systems over AS during this month. In the month of August the tracks of the convective systems over BB are similar to those of July and it is also noticed that there are no convective systems over AS during this month. In the month of September it is seen that most of the convective systems over BB form north of 15°N and west of 90°E. These systems move initially in a west to north-westerly direction and later re-curve towards north-northeast. It is found that the frequency of the convective systems over AS is low in this month.

In the month of October the convective systems over BB form over the area between 8°N and 14°N. They move initially in a north-westerly direction, most of them later re-curve and move towards the north-easterly direction. The coastal areas of northern Tamil Nadu, Andhra Pradesh and Bangladesh are highly vulnerable to the occurrence of cyclones and severe cyclones during this month. It is seen that most of the convective systems over AS generally move west-ward and few of them are moving initially north to north-westward and re-curve to the north-east direction and hits the northern coasts of Maharashtra and Gujarat.

In the month of November most of the convective systems over BB form over the area between 8°N and 13°N, they move in a west-northwesterly direction and hit the coastal areas of northern Tamil Nadu and southern Andhra Pradesh. It is seen that few of these convective systems enter into AS and re-intensify. In the AS the initial movement of the convective systems is north-westerly but few systems re-curve to the north-east direction and hit the coastal regions of northern Maharashtra and south Gujarat. In the month of December there is a decrease in the frequency of the convective systems over NIO. In the case of BB most of the convective systems form over the area between 5°N and 10°N. The convective systems form over the south-west Bay, move initially in a north-westerly direction and hit the coastal areas of northern Tamil Nadu and north-eastern parts of Sri Lanka. The convective systems over the south-east Bay, generally move in a north to north-westerly direction and later re-curve towards the north-easterly direction. These systems show a tendency to weaken and dissipate during this north-easterly movement.

3.5 Decadal change in the tracks of the convective systems over NIO during the study period

The changes in the genesis locations and tracks of the convective systems during the monsoon and non-monsoon seasons of different decades are analyzed. Figure (3.2) gives the decadal changes of the genesis locations and tracks of the depressions over NIO during different decades. It is observed that there is a north-ward shift in the genesis locations of the depressions during the monsoon season and a south-ward shift in the non-monsoon seasons of the three decades. Further it is noticed that the genesis locations of the depressions during the non-monsoon seasons are much more wide spread but it well organized during the monsoon season. From figure 3.2 (a, c, e) it is seen that most of the depressions over BB during the monsoon season have moved towards north to north-westerly direction, but the tracks of the depressions over BB during the non-monsoon seasons do not show a general pattern and they have moved into many directions (figure 3.2 (b, d, f)). In the case of AS most of the depressions have a north-west to westerly tracks during both the monsoon as well as non-monsoon seasons.

Figure (3.3) shows the changes in the genesis locations and tracks of the cyclones over NIO during the monsoon and non-monsoon seasons of different decades. It is observed that the cyclones over AS move generally from west to northwest directions during the monsoon and non-monsoon seasons of these decades. It is observed that the cyclones over BB during the monsoon season move in a north to north-easterly direction. A north-east ward deflection is observed in the tracks of the cyclones over BB during the non-monsoon seasons.

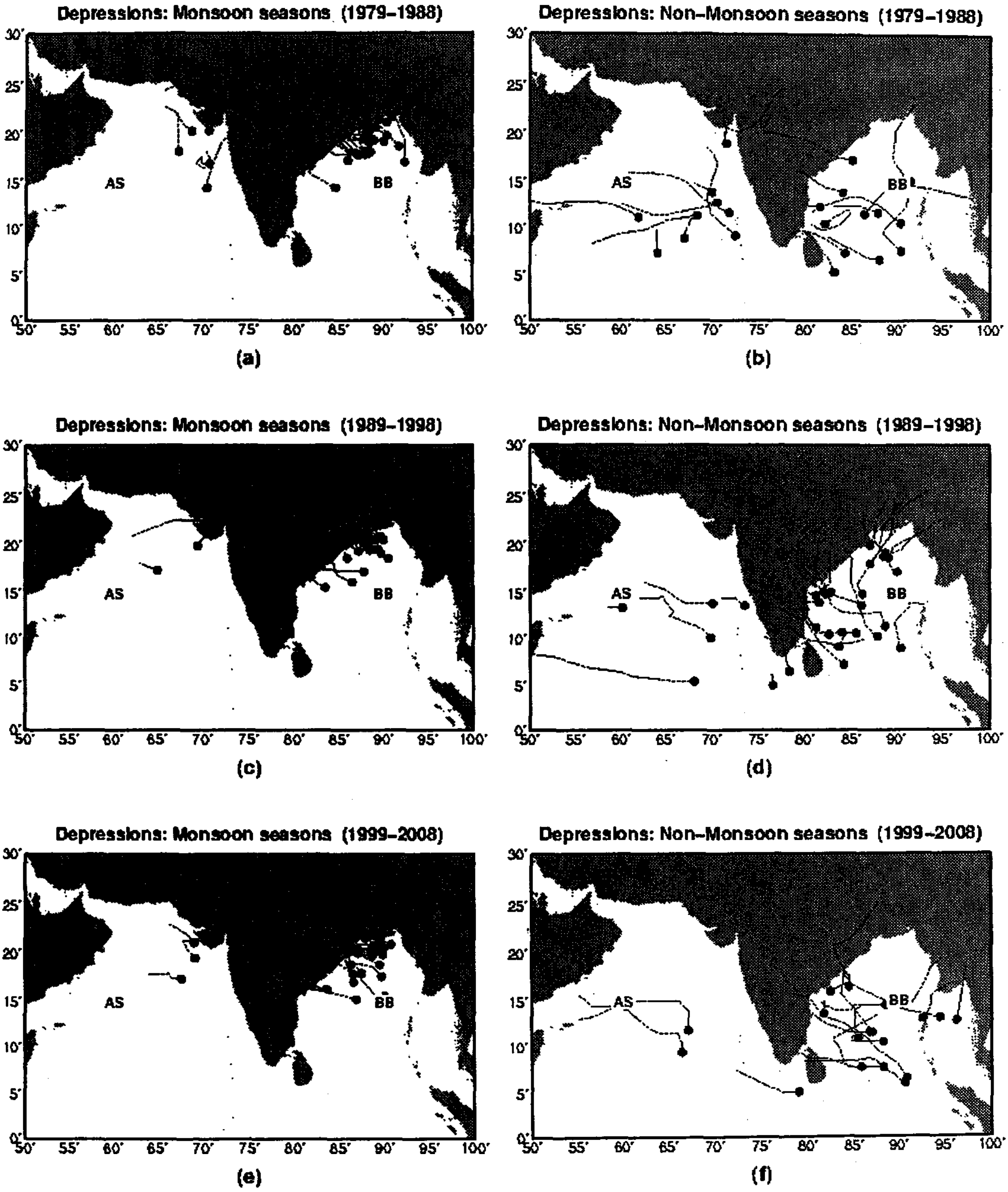

Figure 3.2 The decadal change of the tracks of the depressions over NIO during the monsoon and non-monsoon seasons of different decades

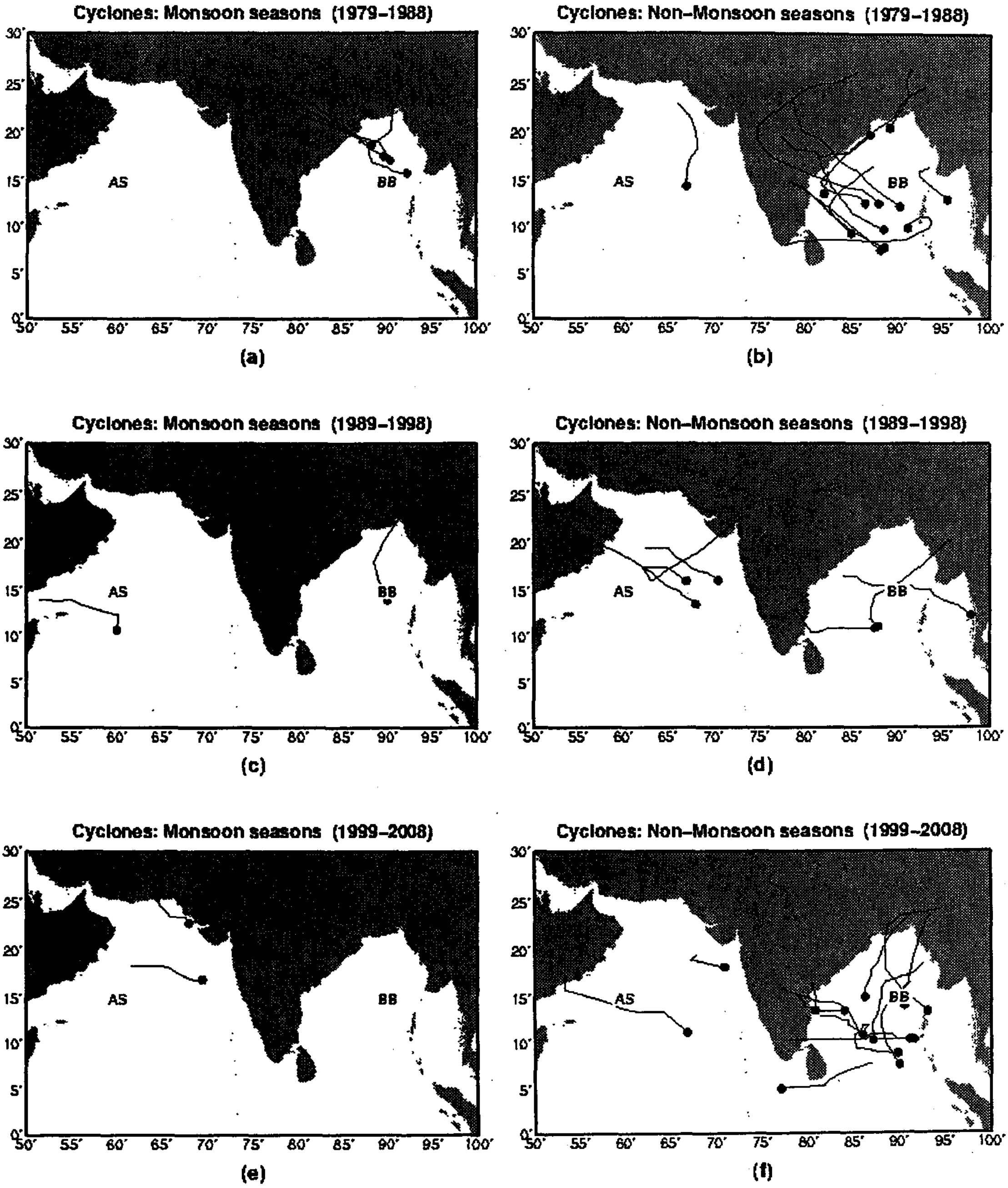

Figure 3.3 The decadal change of the tracks of the cyclones over NIO during the monsoon and non-monsoon seasons of different decades

Figure (3.4) gives the changes in the genesis locations and tracks of the convective systems over NIO during the monsoon and non-monsoon seasons of different decades. It is observed that the severe cyclones over NIO moved in a north-westerly direction during the monsoon season of the decade 1979-1988 while during the non-monsoon season they have deflected from their initial north-west direction to north-east direction in this decade. It is seen that the tracks of the severe cyclones over NIO during the monsoon season show a north-east ward movement. While during the non-monsoon seasons it is observed that the north-east ward deflections of the tracks are limited and most of the severe cyclones moved in a northerly direction in the decade 1989-1998. In the decade 1999-2008, it is observed that most of the severe cyclones over BB during the non-monsoon seasons have taken a north-westerly track in the initial stages and later deflected towards north-east direction. It is also noticed that there is a tendency for the severe cyclones to dissipate over the ocean or decay immediately after the landfall.

3.6 Climatology of the air-sea interaction parameters over NIO during the study period

The climatology of the air-sea interaction parameters such as sea surface temperature, outgoing long-wave radiation, latent heat flux, low level convergence, low level relative vorticity, vertical wind shear co-efficient, mid tropospheric relative humidity, convective instability are obtained during the monsoon and non-monsoon seasons of the different decades in the study period. Further the variations of SST over the Indo-Pacific Ocean during the monsoon and non-monsoon seasons of different climatic modes have also been presented in this chapter.

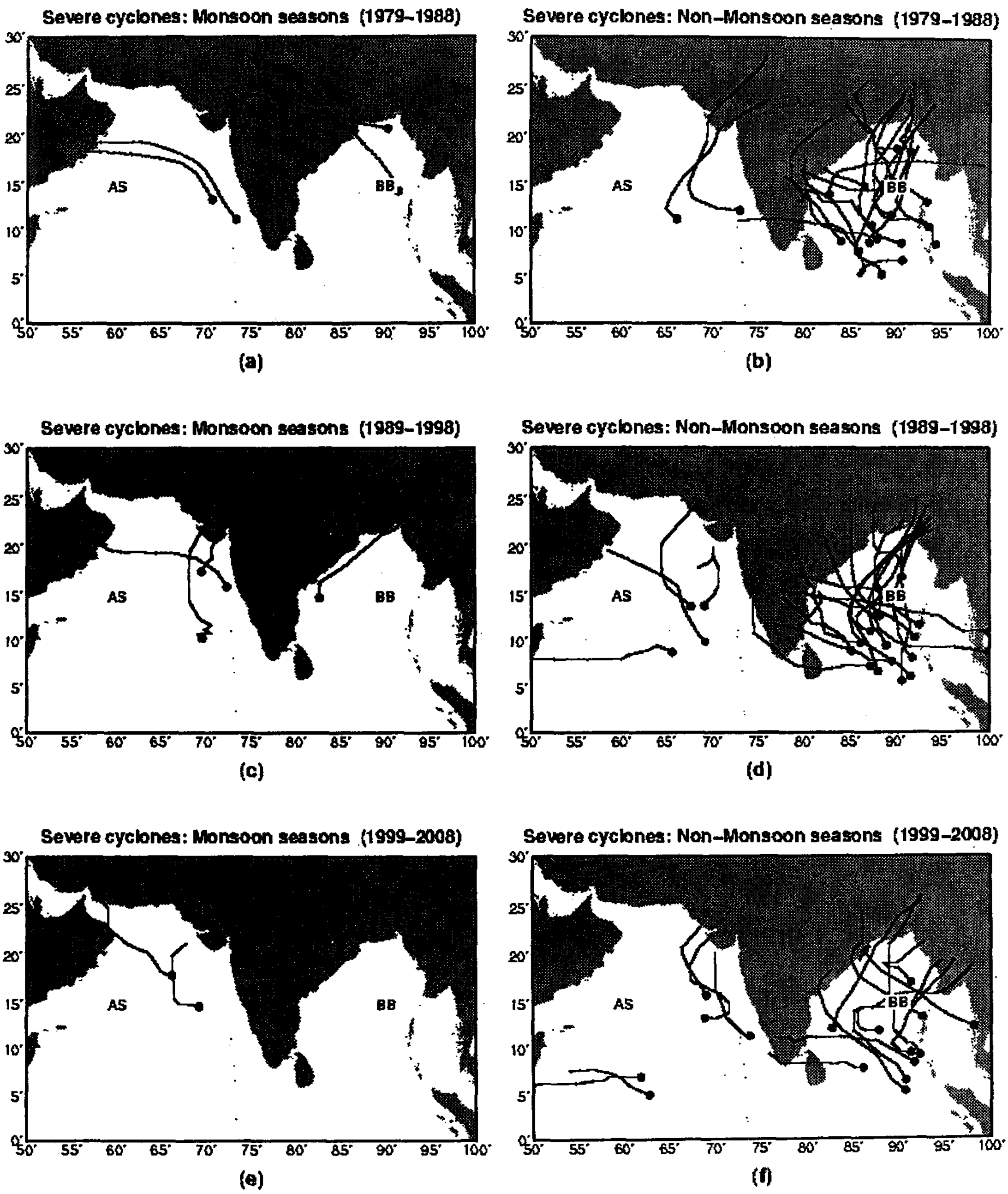

Figure 3.4 The decadal change of the tracks of the severe cyclones over NIO during the monsoon and non-monsoon seasons of different decades

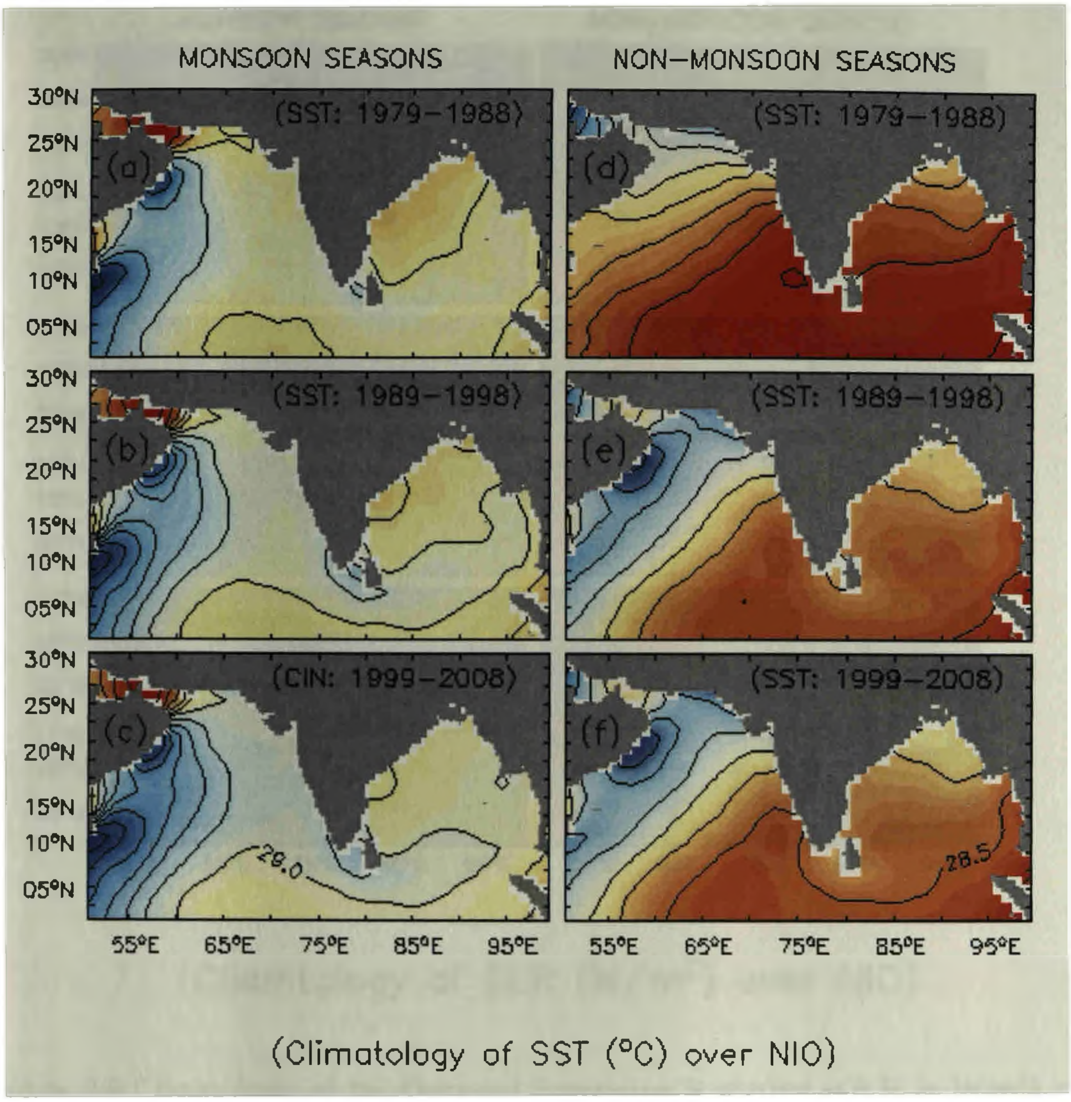

Figure 3.5 Climatology of Sea Surface Temperature (SST in °C) over NIO during different decades in the study period

Figure (3.5) gives the climatology of SST over NIO during the different decades in the study period. From figure 3.5 (a, b, c) it is observed that there was a shift of cooler SST from the western and north-western AS to the eastern AS during the monsoon season of all the decades. From figure 3.5 (d, e, f) it is observed that the NIO was warmer during the non-monsoon seasons of the decades 1979-1988. A shift of cooler SST from the north-western AS to the central AS is found during the non-monsoon seasons of the decades 1989-1998 and 1999-2008.

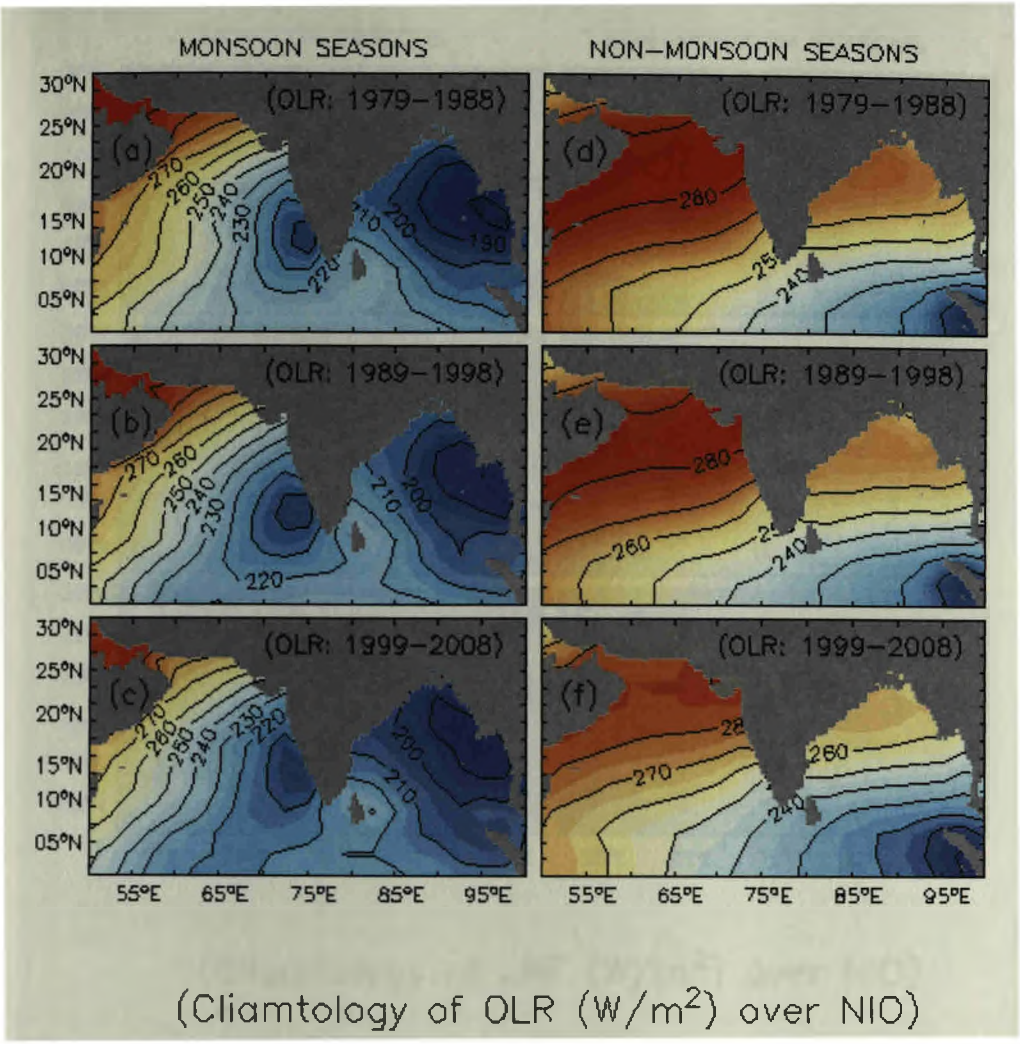

Figure 3.6 Climatology of the Outgoing Longwave Radiation (OLR in W/m^2) over NIO during the monsoon and non-monsoon seasons of different decades in the study period

Figure (3.6) gives the climatology of the outgoing long-wave radiation during different decades in the study period. From figure 3.6 (a, b, c) low magnitudes of the OLR are observed over the eastern AS and north-eastern BB during the monsoon season of the decades 1979-1988, 1989-1998 and 1999-2008. From figure 3.6 (d, e, f) it is observed that the higher magnitudes of the OLR are concentrated over the northern AS and BB during the non-monsoon seasons of these decades. It is also observed that the lower magnitudes of the OLR are concentrated over the south-east of BB during the non-monsoon seasons of these decades.

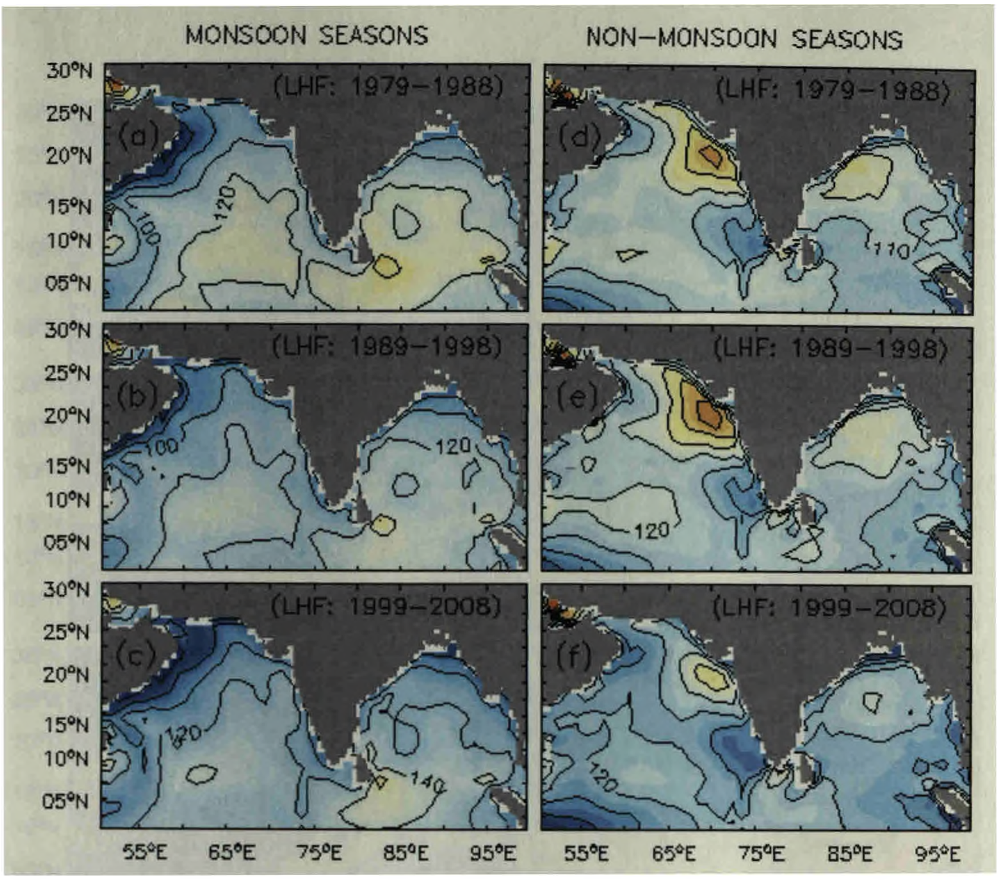

(Cliamtology of LHF (W/m^2) over NIO)

Figure 3.7 Climatology of the LHF (W/m^2) over NIO during the monsoon and non-monsoon seasons of different decades in the study period

Figure (3.7) gives the climatology of the LHF over NIO during the monsoon and non-monsoon seasons of the different decades. From figure 3.7 (a) it is observed that the maximum magnitude of the LHF is observed during the monsoon season for the decade 1979-1988. From figure 3.7 (b, c), it is noticed that the magnitude of the LHF has decreased further during the monsoon season of the decades 1989-1998 and 1999-2008. From figure 3.7 (d, e) it is noticed that the maximum magnitude of the LHF is observed over north-east AS during the non-monsoon seasons of the decades 1979-1988 and 1989-1998. But the magnitude of LHF has decreased over NIO during the non-monsoon seasons of the decade 1999-2008.

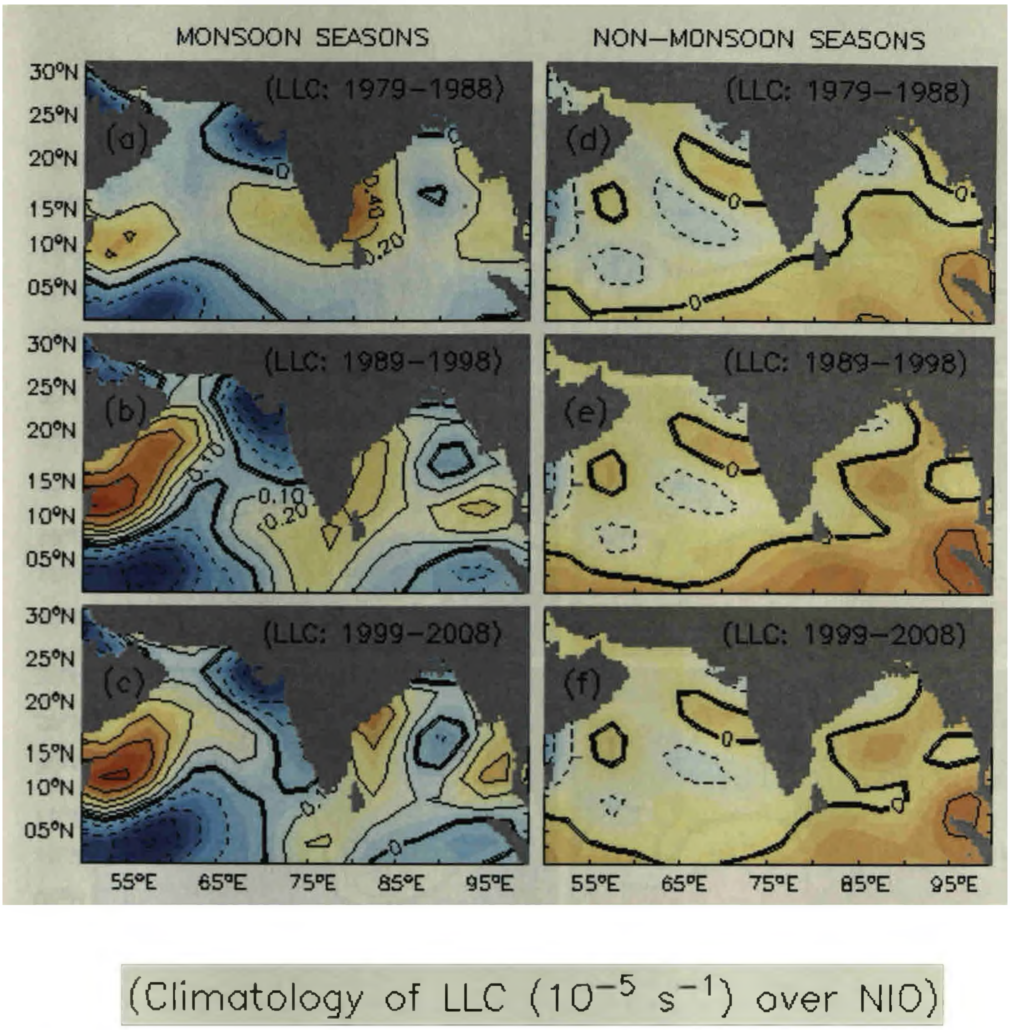

Figure 3.8 Climatology of low level convergence (LLC) over NIO during the monsoon and non-monsoon seasons of the different decades in the study period

Figure (3.8) gives the climatology of the low level convergence (LLC) during the monsoon and non-monsoon seasons of the different decades in the study period. From figure 3.8 (a, b, c) it is observed that the magnitude of LLC is more over NIO during the monsoon season of the decade 1989-1998. From figure 3.8 (d, e, f) the high magnitude of LLC is found for the non-monsoon seasons of the decade 1989-1998. It is also noticed that there is large scale divergence over the central and southern AS during the monsoon and non-monsoon seasons of these decades.

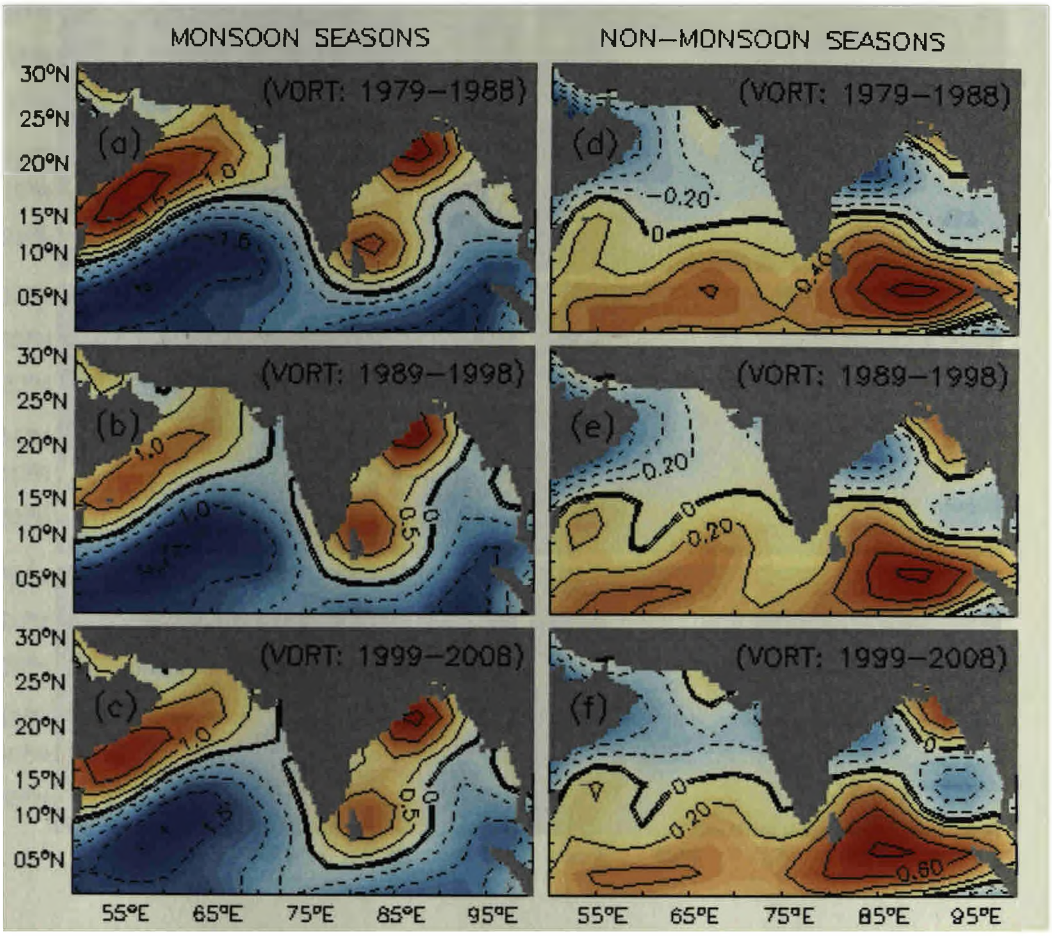

(Climatology of VORT (10^{-5} s^{-1}) over NIO)

Figure 3.9 Climatology of low level relative vorticity (LLRV) over NIO during the monsoon and non-monsoon seasons of the different decades in the study period

Figure (3.9) gives the climatology of the low level relative vorticity (LLRV) over NIO during the monsoon and non-monsoon seasons of the different decades in the study period. From figure 3.9 (a) it is observed that the higher magnitudes of the LLRV are found over the southern AS. From figure 3.9 (b, c, d, e, f) it is noticed that the higher magnitudes of LLRV is found over the north-western AS, northern BB and southern BB during the monsoon and non-monsoon seasons of all the decades.

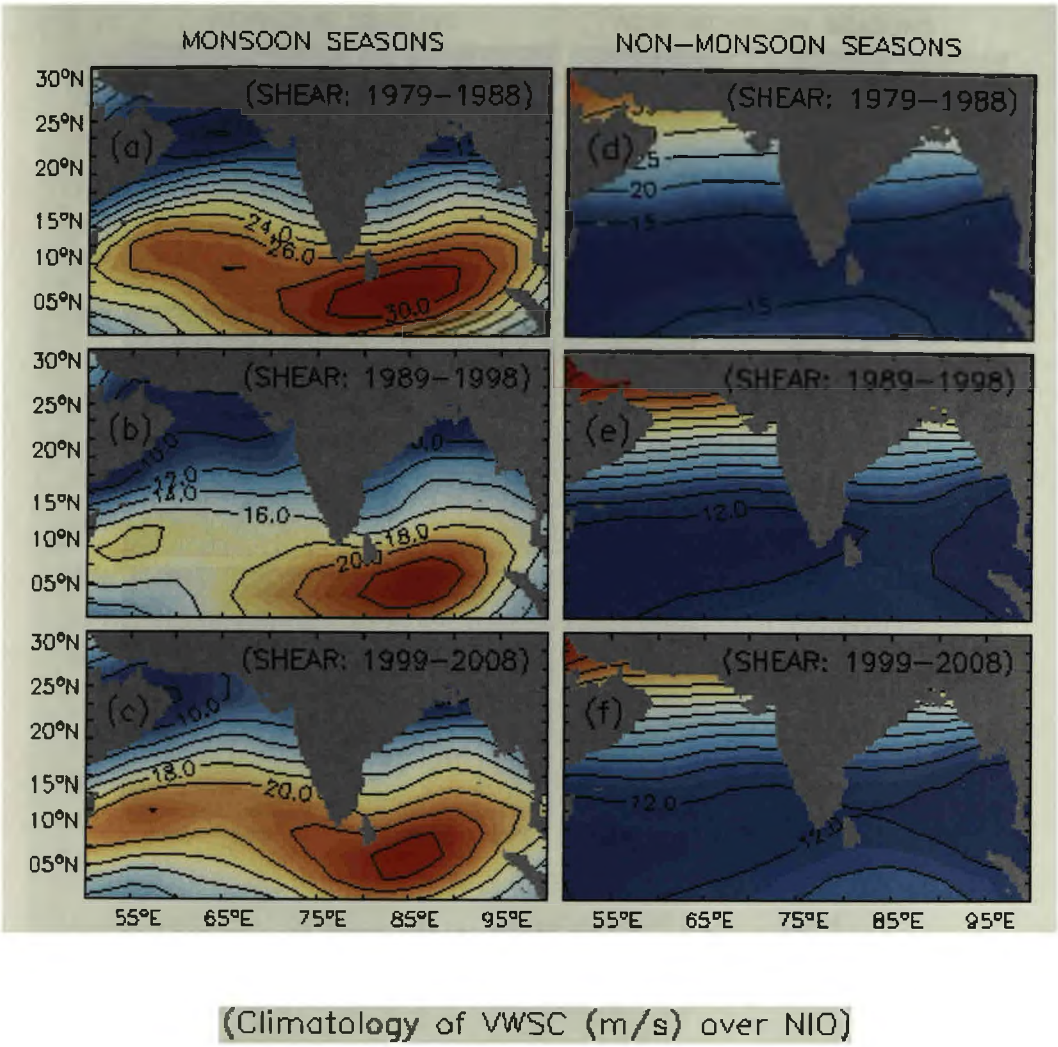

Figure 3.10 Climatology of vertical wind shear co-efficient (VWSC) over NIO during the monsoon and non-monsoon seasons of different decades in the study period

Figure (3.10) gives the climatology of the vertical wind shear coefficient (VWSC) during the monsoon and non-monsoon seasons of the different decades in the study period. From figure 3.10 (a, b, c) it is observed that the higher magnitudes of the VWSC are concentrated over the southern parts of NIO and lower magnitudes are concentrated over the northern parts of the NIO during the monsoon season of all the decades. A reverse situation is observed during the non-monsoon seasons. From figure 3.10 (c, e, f) it is found that the lower magnitudes of VWSC are concentrated over the southern parts of NIO and higher magnitudes of VWSC are concentrated over the northern parts of NIO.

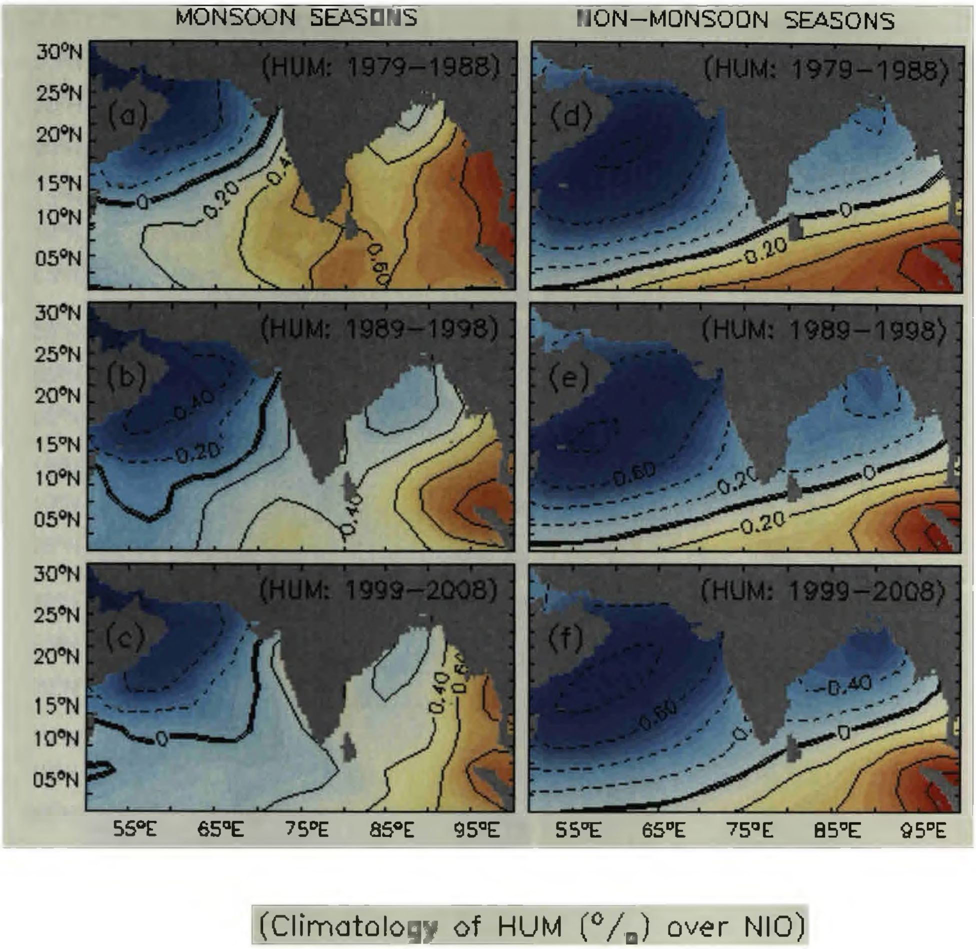

Figure 3.11 Climatology of Humidity parameter (HUM) during the monsoon and non-monsoon seasons of different decades in the study period

Figure (3.11) gives the climatology of the mid tropospheric relative **humidity** (HUM) during the monsoon and non-monsoon seasons of different decades. From figure 3.11 (a), the higher magnitude of HUM is found over the eastern AS and BB during the monsoon season of the decade 1979-1988. The lower magnitudes of HUM are found over the north-east AS. From figure 3.11 (b, c, d, e, f) it s observed that the higher magnitude of HUM is found over the eastern and south eastern BB during the monsoon and non-monsoon seasons of all the decades.

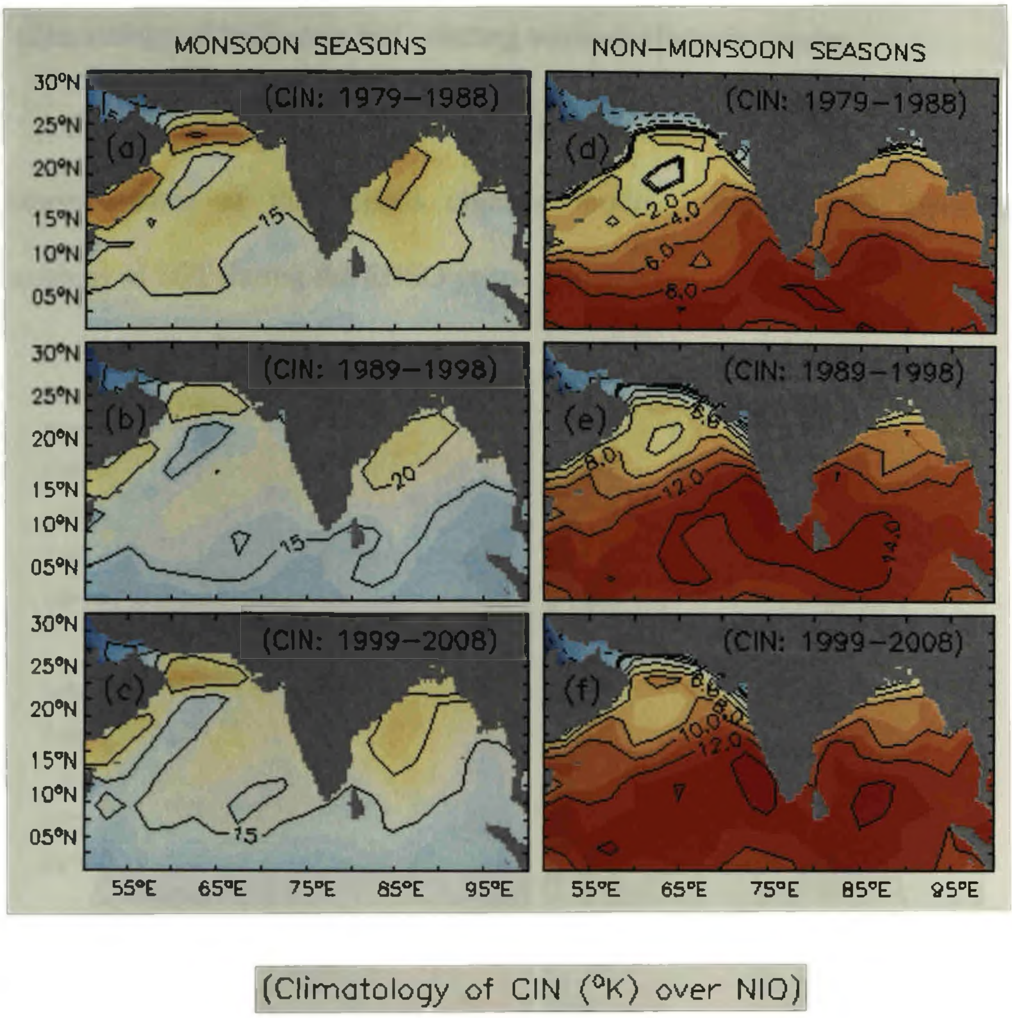

Figure 3.12 Climatology of Convective Instability parameter (CI) during the monsoon and non-monsoon seasons of different decades of the study period

Figure (3.12) gives the climatology of the convective instability (CI) during the monsoon and non-monsoon seasons of different decades in the study period. From figure 3.12 (a) it is found that the magnitude of CI is more during the monsoon season of the decade 1979-1988. From figure 3.12 (b, c), a lower magnitude of CI is noticed over NIO during the monsoon season of the decades 1989-1998 and 1999-2008. From the figure 3.12 (d, e, f) it is observed that a higher magnitude of CI is found over NIO during the non-monsoon seasons of all the decades.

3.7 Climatology of SST over NIO during various climatic modes

The climatology of the SST and LHF are presented during the monsoon and non-monsoon seasons of the various climatic modes. Figure 3.13 gives the seasonal climatology of SST during the ENSO years.

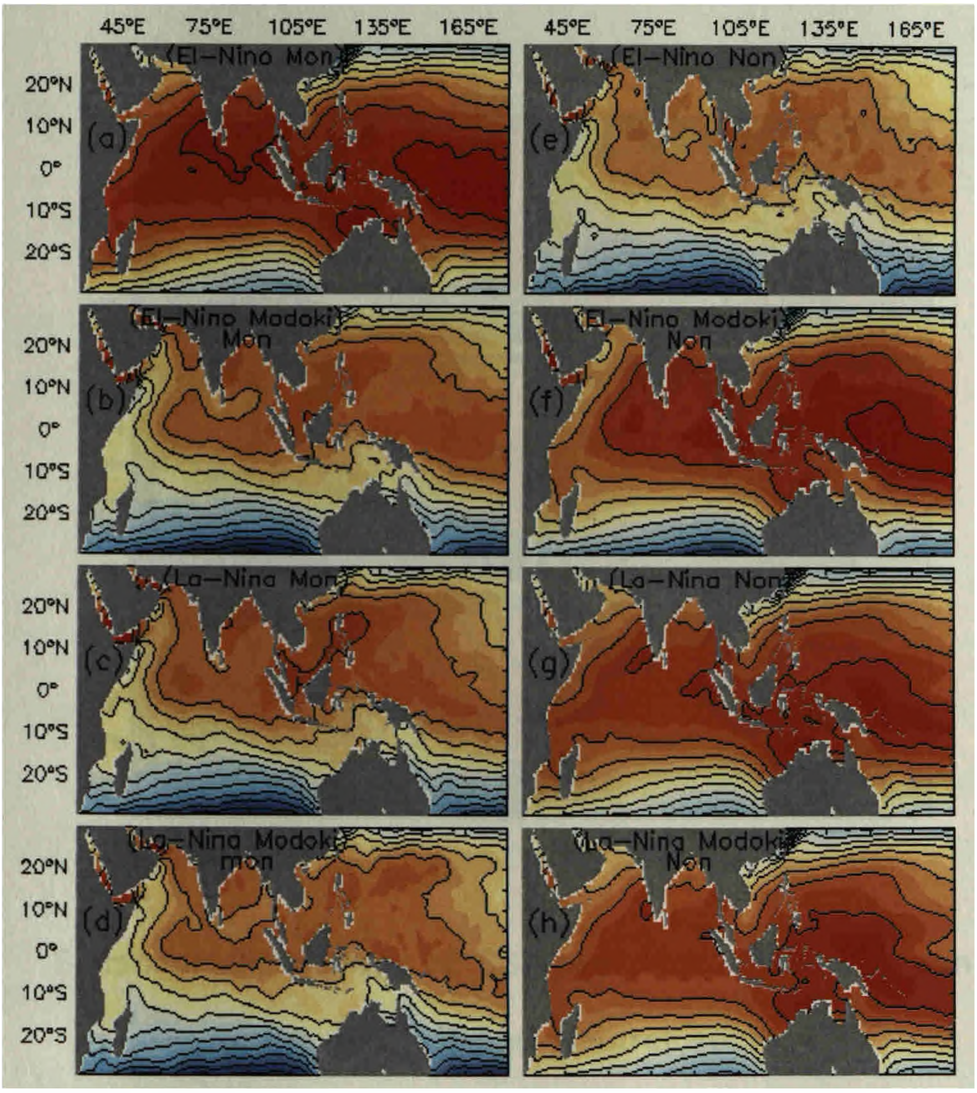

Seasonal climatology of SST over the Indo-Pacific ocean during different climatic modes

Figure 3.13 Climatology of SST over NIO during the monsoon and non-monsoon seasons of different climatic modes

From figure 3.13 (a, e) it is observed that the SST is higher during the monsoon season of the El-Niño years than during the non-monsoon seasons. From figure 3.13 (b, f) it is noticed that the non-monsoon seasons of the El-Niño Modoki years are warmer than the monsoon season.

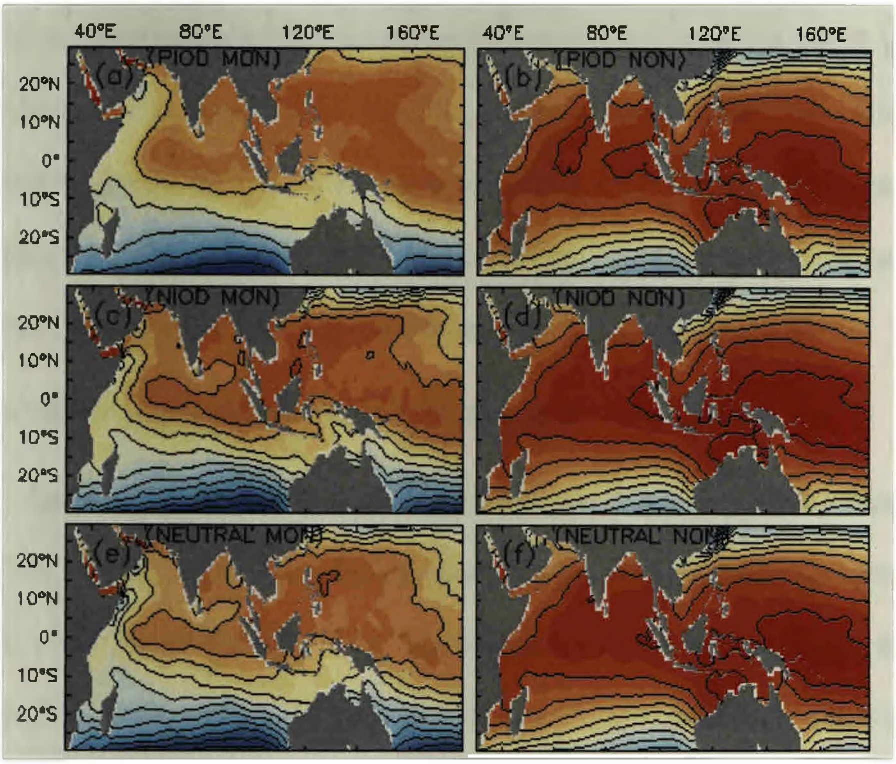

Seasonal climatology of SST over Indo–Pacific ocean

during the IOD and Neutral years

Figure 3.14 Climatology of SST during the monsoon and non-monsoon seasons of the IOD and neutral years

From figure 3.13 (c, g) it is observed that the SST is found to be higher during the non-monsoon seasons than during the monsoon season of the La-Niña years. From figure 3.13 (d, h), it is noticed that the non-monsoon season of the La-

Niña Modoki has a higher magnitude of SST than the monsoon season.

Figure (3.14) shows the climatology of SST during the monsoon and non-monsoon seasons of the IOD and neutral years. From figure 3.14 (a, b) it is observed that the magnitude of SST is high over NIO during the non-monsoon seasons than the monsoon season. From figure 3.14 (c, d) the higher magnitudes of SST are observed over NIO during the non-monsoon seasons than the monsoon season during the NIOD years. From figure 3.14 (e, f) it is observed that the magnitude of SST is higher over NIO during the non-monsoon seasons than the monsoon season of the neutral years. It is also noticed that the magnitude of SST is found to be low over NIO during the monsoon season of the neutral years compared to the monsoon season of the PIOD and NIOD years.

3.8 Most intense storms formed over NIO during the study period

Figure (3.15) shows the most intense cyclones formed over NIO during the study period. The names and tracks of the cyclones and the corresponding background state of the ocean also given in the table (3.2). There have been three super cyclones and nine very severe cyclonic storms with hurricane intensity were formed during the study period. The super cyclones are namely Gonu, Orisssa cyclone and the third super cyclone is termed SCS (H). The H in brackets denotes that the cyclone has a core of hurricane intensity winds. The super cyclone Gonu was formed on 1st June over AS and moved towards Oman coast and dissipated on 7th June during 2007. The lowest recorded central pressure of Gonu was 920 hPa and the maximum wind speed was 127 knots. The next super cyclone is the Orissa cyclone, which was formed over south China Sea on 25th October, 1999, moved northwest-ward and intensified over BB on 31st October and slowly reached the Orissa coast. It is noticed that the maximum wind speed of this severe cyclone was 80 knots and the central pressure was 912 hPa at its maximum intensity. After the landfall it drifted towards south and dissipated on 31st October, 1999. This severe cyclone caused tremendous damage to the coastal areas of Orissa state.

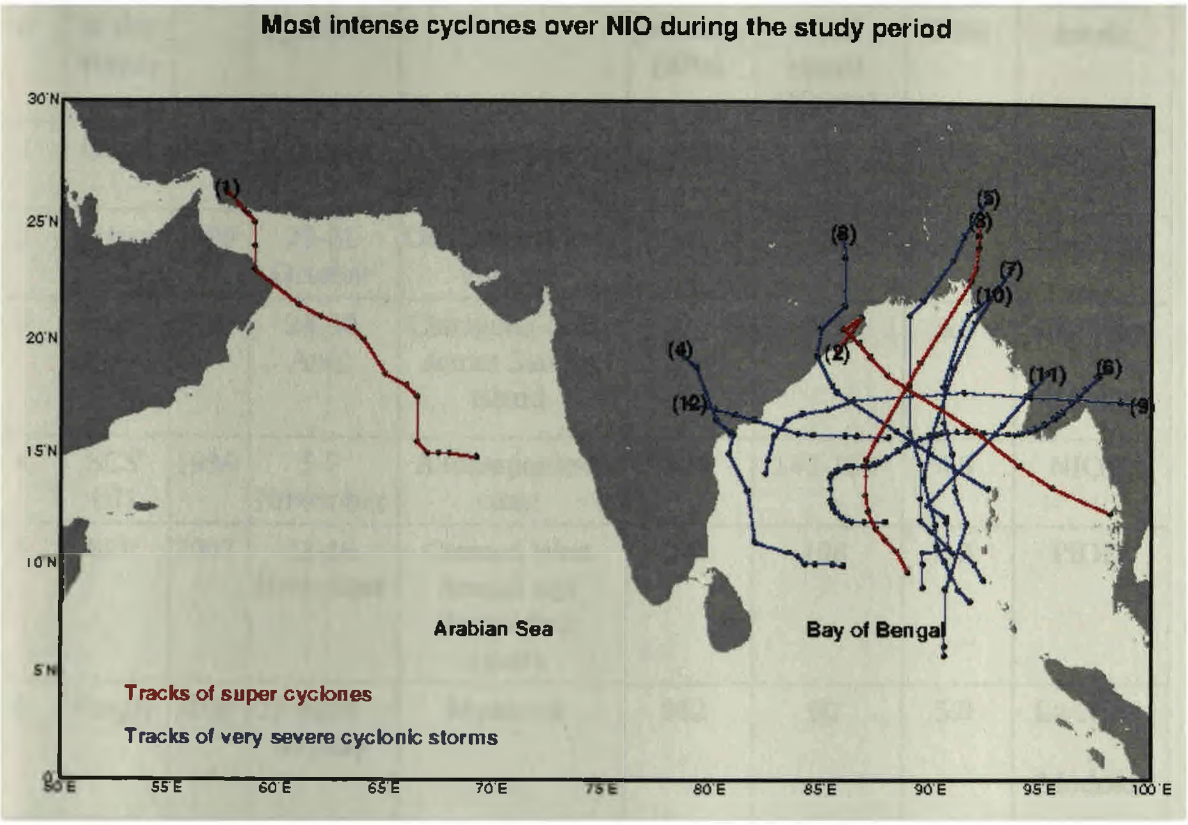

Figure 3.15 Most intense cyclones formed over NIO during the study period

The third super cyclone was termed the SCS (H). It was formed on 24th April and dissipated on 30th April. It moved to Chitagong coast across the Sandwip island. This has marked a lowest central pressure of about 920 hPa and the maximum wind speed was 98 knots. A highest T-No of 6.5 has also been recorded for this super cyclone. The fourth cyclone is named the SCS (H), it was formed on 5th November, 1996 and made landfall over the Andhra Pradesh coast. The name of the next severe cyclone was "Sidr" which was formed over BB on 11th November, 2007.

Table 3.2 Most intense cyclones formed over NIO during the study period

Sl.No	Name of the Storm	Year	Life period	Place of landfall	Lowest pressure (hPa)	Maximum wind speed (Knots)	Highest T.No	Climatic mode
1	Gonu	2007	1-7 June	Crossed Oman and Mercan coast	920	127	6.5	PIOD
2	Orissa cyclone	1999	25-31 October	Orissa coast near Paradip	912	80	7.0	La-Niña
3	SCS (H)	1991	24-30 April	Chitagong coast across Sandip island	920	98	6.5	El-Niño Modoki
4	SCS (H)	1996	5-7 November	Andhrapradesh coast	974	140-150	4.5	NIOD
5	Sidr	2007	11-16 November	Crossed West Bengal and Bengladesh coasts	944	108	6.0	PIOD
6	Nargis	2008	27 April – 03 May	Myanmar	962	90	5.0	La-Niña Modoki
7	SCS (H)	1990	5-11 May	Machilipattanam	912	70	6.5	El-Niño Modoki
8	SCS (H)	1994	29 April – 03 May	North Myanmar coast	940	--	6.0	El-Niño Modoki
9	SCS	1982	1-5 May	Myanmar	997	95-115	6.5	El-Niño
10	SCS (H)	1997	15-20 May	Bengladesh coast	965	126	5.0	El-Niño
11	Mala	2006	25-29 April	Arakan coast	950	102	5.5	PIOD+El-Niño
12	VSCS	1999	15-18 October	Orissa coast	--	--	5.0	La-Niña

It took a north-easterly track and moved to Bangladesh and dissipated on 16th November over the coasts of Bangladesh. Severe cyclone "Nargis" formed over BB on 27th April 2008 and moved towards Myanmar and dissipated on 3rd May. The seventh severe cyclone is named SCS (H), it formed over BB on 5th May 1990 and dissipated over Machilipattanam on 11th May. The severe cyclone SCS (H) was formed over BB on 1st May 1982 and dissipated over Myanmar coast on 5th May. The severe cyclone SCS (H) formed over BB on 15th May 1997 and it dissipated over Bangladesh coast on 20th May. The severe cyclone "Mala" was formed over BB on 25th April 2006 and dissipated over Arakan coast on 29th April. A very severe cyclonic storm VSCS was formed over BB on 15th October 1999. This was the second very severe cyclone over BB during these years. This also made landfall over the Orissa coast on 18th October.

3.9 Variations of CSGP for the convective systems over NIO during the study period

The variations of the Convective System Genesis Parameter (CSGP) for the convective systems over NIO during the study period have been analyzed. Figure (3.16) shows the variations of the depressions formed in both the seasons over NIO during the study period. The black dots represent the genesis locations of the depressions. Figure 3.16 (a) gives the variations of CSGP for the depressions formed over AS during the monsoon season of the study period. There have been 10 depressions over AS during the monsoon season. From this figure it is found that all the depressions over AS during the monsoon season were formed against low values of CSGP (~ -0.5 to 0.0 $x10^{-10}s^{-2}\,^{o}K$). Figure 3.16 (b) shows the variations of CSGP for the depressions over AS during the non-monsoon seasons of the study period. There have been 17 depressions over AS during the non-monsoon season. From this figure it is observed that almost all the depressions have formed against the low values of CSGP (~ -0.5 to 0.0 $x10^{-10}s^{-2}\,^{o}K$). But there is an increase in the values of the CSGP over BB. Figure 3.16 (c), gives the variations of CSGP for the depressions over BB during the monsoon season of the study period. There have been 63 depressions over BB during this period and it is noticed that most of the depressions have formed against the low positive values of CSGP (~ 0.0 to 0.5 $x10^{-10}s^{-2}\,^{o}K$). Figure 3.16 (d) shows the variations of CSGP for the depressions over BB during the non-monsoon seasons of the study period. There have been 44 depressions over BB during this period and it is found that all the depressions have formed against the low values of CSGP (~ -0.5 to 0.0 $x10^{-10}s^{-2}$ °K). From these figures it is understood that all the depressions over NIO, during both the seasons, have formed against low magnitudes of CSGP (~ -0.5 to 0.5 $x10^{-10}s^{-2}$ °K).

Variations of CSGP for the Depressions over NIO

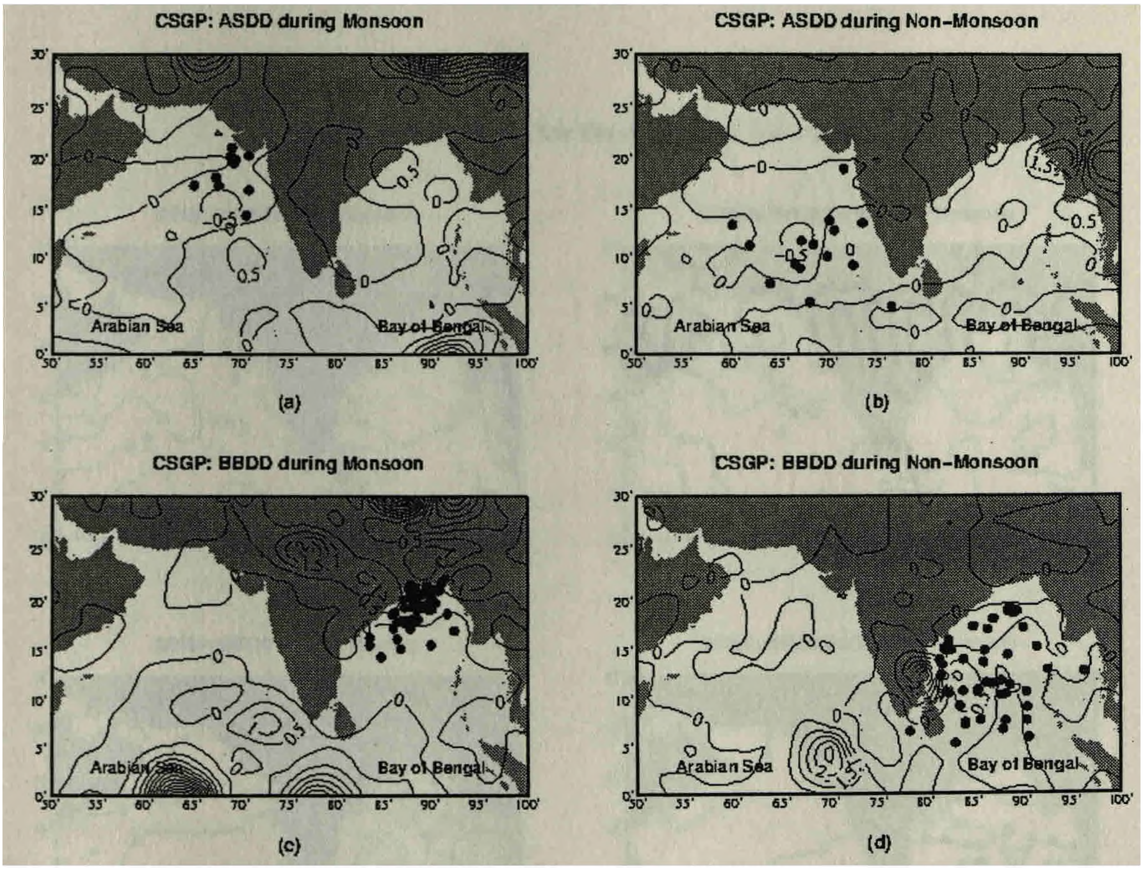

Figure: 3.16 Variations of CSGP for the Depressions formed over NIO during the monsoon and non-monsoon seasons

Figure (3.17) shows the variations of CSGP for the cyclones formed in both the seasons over NIO during the study period. Figure 3.17 (a) shows the variations of CSGP for the cyclones formed over AS during the monsoon season of the study period. There have been 3 cyclones over AS during this period and it is found that all the cyclones have formed against the low positive values of CSGP (~ 0.0 to 0.4 $x10^{-10}s^{-2}\,^{o}K$). Figure 3.17 (b) gives the variations of CSGP for the cyclones formed over AS during the non-monsoon seasons of the study period. There have been 5 cyclones over AS during this period and it is observed that all the cyclones have formed against the low positive values of CSGP (~ 0.0 to 0.4 $x10^{-10}s^{-2}\,^{o}K$). Figure 3.17 (c) shows the variations of CSGP for the cyclones over BB during the monsoon season of the study period.

Variations of CSGP for the Cyclones over NIO

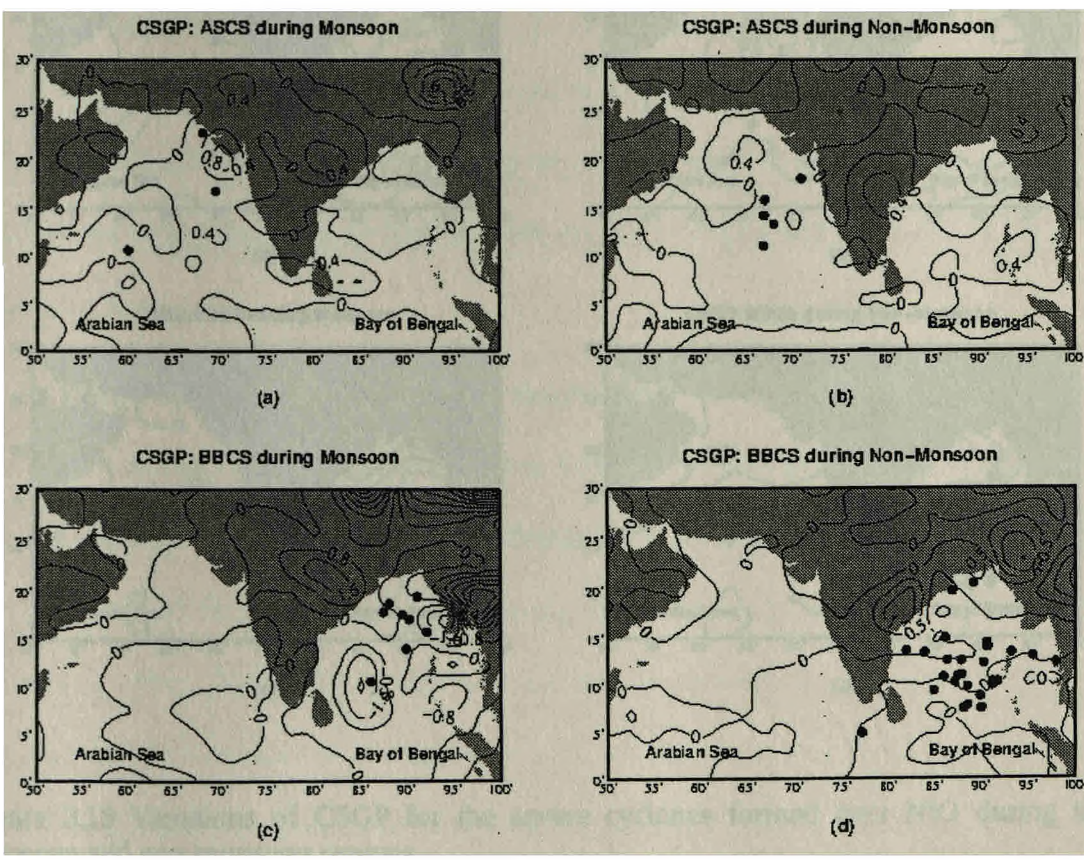

Figure. 3.17 Variations of CSGP for the Cyclones formed over NIO during the monsoon and non-monsoon seasons

There have been 8 cyclones over BB during this period and it is noticed that most of the cyclones over BB were formed against the low positive values of CSGP (~ 0.0 to 0.5 $x10^{-}$

$^{10}s^{-2}$ °K). Figure 3.17 (d) gives the variations of CSGP for the cyclones over BB during the non-monsoon seasons. There have been 27 cyclones over BB during this period and it is found that all the cyclones have formed against the low positive values of CSGP (~ 0.0 to 0.5 x$10^{-10}s^{-2}$ °K). From these figures it is clear that the cyclones over NIO have formed against low positive magnitudes of CSGP (~ 0.0 to 0.5 x$10^{-10}s^{-2}$ °K).

Variations of CSGP for the Severe cyclones over NIO

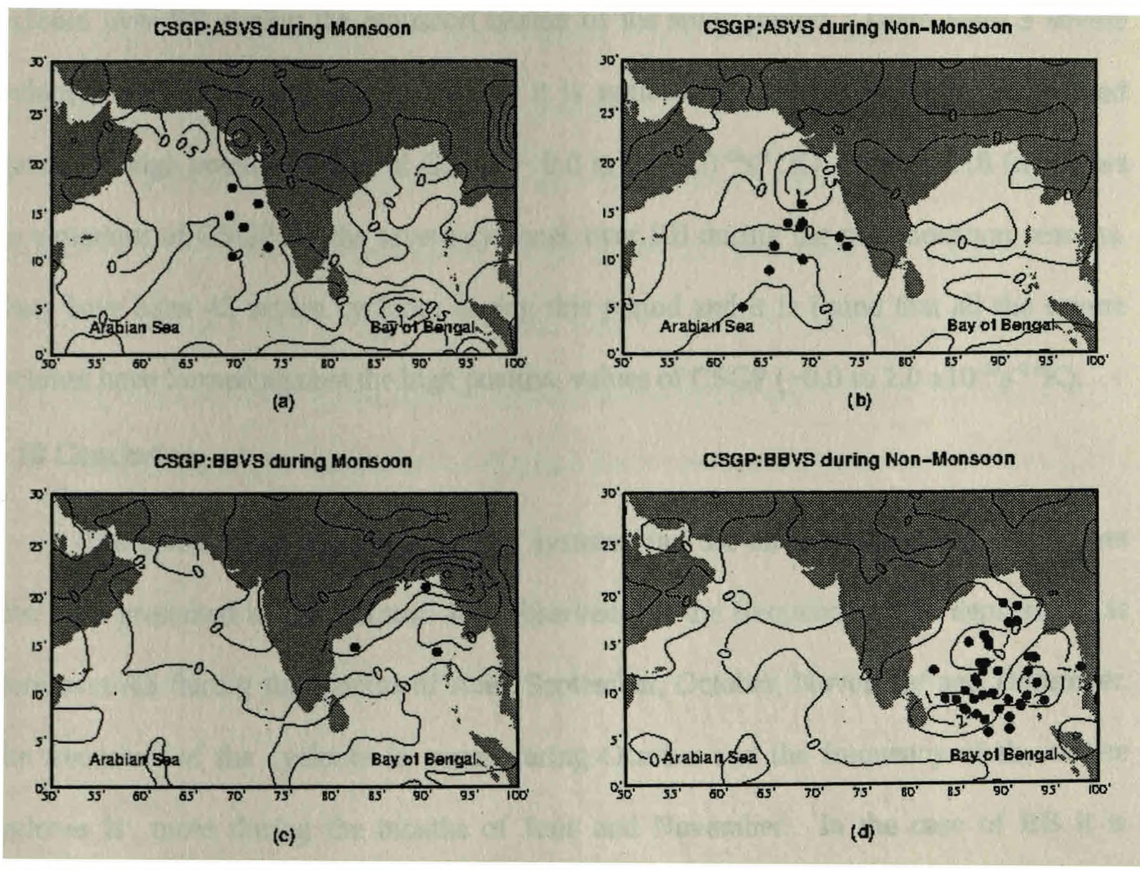

Figure 3.18 Variations of CSGP for the severe cyclones formed over NIO during the monsoon and non-monsoon seasons

Figure (3.18) shows the variations of CSGP for the severe cyclones formed in both seasons over NIO during the study period. Figure 3.18 (a) gives the variations of CSGP for the severe cyclones over AS during the monsoon season of the study period. There were 6 severe cyclones over AS during this period and it is found that all the severe cyclones *formed against the low magnitudes of CSGP (~ 0.0 to 0.2 $x10^{-10}s^{-2}$ °K).* Figure 3.18 (b) shows the variations of CSGP for the severe cyclones formed over AS during the non-monsoon seasons of the study period. An increase in the magnitude of CSGP is noticed for the severe cyclones over NIO. In the case of the severe cyclones over AS in the non-monsoon seasons, there have been 10 severe cyclones over AS during this period and it is observed that all the severe cyclones have formed against the high positive values of CSGP (~ 0.0 to 1.0 $x10^{-10}s^{-2}$ °K). Figure 3.18 (c) gives the variations of CSGP for the severe cyclones over BB during the monsoon season of the study period. There were 3 severe cyclones over BB during this period and it is noticed that the severe cyclones formed against the high positive values of CSGP (~ 0.0 to 3.0 $x10^{-10}s^{-2}$ °K). Figure 3.18 (d) shows the variations of CSGP for the severe cyclones over BB during the non-monsoon seasons. There have been 42 severe cyclones during this period and it is found that all the severe cyclones have formed against the high positive values of CSGP (~0.0 to 2.0 $x10^{-10}s^{-2}$ °K).

3. 10 Conclusion

The climatology of the convective systems and the air-sea interaction parameters have been presented in this chapter. It is observed that the frequency of the depressions is more over AS during the months of June, September, October, November and December. The frequency of the cyclones is more during October and the frequency of the severe cyclones is more during the months of June and November. In the case of BB it is observed that the frequency of the depressions is more during the month of May, June, July, August, September, November and December. It is also found that the frequencies of the cyclones and severe cyclones are more during the months of May, October and November.

There is a reduction in the number of depressions over AS during the recent decades. An increase in the number of cyclones and severe cyclones (during the non-monsoon seasons) is noticed over AS. A general west to north-west direction in the tracks of the depressions is noticed. Further a northeast-ward deflection for the tracks of the cyclones and severe cyclones is found during the decades 1979-1988 and 1999-2008. It is noticed that there is a trend for the severe cyclones to dissipate over the ocean or decay immediately after the landfall.

An east-ward shift of the cooler SST from the western AS to the eastern parts of AS has been observed during the monsoon season. The higher SST is found over NIO during the decade 1979-1988 and it has decreased in the later decades. Higher magnitudes of OLR are noticed over AS during the non-monsoon seasons of the recent decades. The magnitude of LHF is more during the non-monsoon seasons of al the decades. This can be attributed to the increased frequency of the convective systems over AS these seasons. The magnitudes of LLC are more during the decade 1989-1998 compared to the other decades. The magnitude of LLRV is high during the decades of 1989-1998 and 1999-2008. A decreasing trend in HUM is also noticed during the recent decades. The SST is found to be high during the monsoon season of the El-Niño years and it is found to be high during the non-monsoon seasons of the other climatic modes. Finally the characteristics of CSGP for all the categories of convective systems have been analyzed. The results show that the CSGP is capable of distinguishing different categories of the convective systems over NIO.

Chapter 4

Convective systems over northern Indian Ocean during the El-Niño and El-Niño Modoki years

4.1 Introduction

The Southern Oscillation (SO) is defined as a periodical seesaw fluctuation in sea surface pressure between the south-east Pacific Ocean and Australian-Indonesian region (Philander 1983). The fluctuations in the SST over tropical Pacific Ocean are associated with a phenomenon named the El-Niño. The average period of SO is 3 years and the period of El-Niño events varies from 2 to 10 years. Hence the phases of SO at which the SST is high and surface pressure difference is low across the tropical Pacific Ocean are now considered as the independent events referred to as the El-Niño Southern Oscillation (ENSO) events. The ENSO events are now considered as the most important climatic forcing that influence the global climate. It is observed that the variations in the magnitudes of the north-east and south-east trade winds and the seasonal fluctuations of the sea surface temperature and pressure over both eastern and western parts of the tropical Pacific Ocean cause this phenomenon. El-Niño and La-Niña events are the most important phases of the ENSO phenomenon. These ocean-atmospheric conditions develop over this basin depending up on the variations in the magnitudes of above-mentioned parameters from the normal conditions.

In the normal conditions the trade winds will push off the surface water from the east to the western Pacific Ocean. Hence the western Pacific Ocean has larger exposure to the solar radiation than the eastern Pacific Ocean. This causes the western Pacific Ocean to be warmer than the eastern part of the Pacific Ocean. This results in the large scale atmospheric convection of warm, moist and less dense air in the western Pacific Ocean. The piled up warm water in the western Pacific Ocean cannot flow through the surface to bring the required equilibrium in the surface of the tropical Pacific Ocean, because the magnitude of the trade winds pushes more water from the western to eastern Pacific Ocean. Hence the piled up warm water in the western Pacific Ocean will follow an undercurrent and upwell over the east Pacific Ocean to maintain the equilibrium. This undercurrent will bring much more cold water from the bottom of the ocean to the eastern Pacific Ocean. The atmosphere over the eastern Pacific Ocean will become cold and dry as the cold water reaches the eastern Pacific Ocean. The cold dry air in the eastern Pacific Ocean makes a large scale air subsidence over this region.

The convergence over western Pacific Ocean and divergence over eastern Pacific Ocean will establish a convective loop over the tropical Pacific Ocean with an ascending limb in the western Pacific Ocean and a descending limb in the eastern Pacific Ocean. This convective loop is called the Walker circulation. The ascending limb of the Walker circulation is associated with large scale atmospheric convection and high rainfall anomalies in the western Pacific Ocean and descending limb is associated with large scale divergence and drought like situations in the eastern Pacific Ocean. This is called the normal condition. The fluctuations in the magnitudes of the trade winds cause abnormal warming and cooling of SST and result in the development of El-Niño and La-Niña conditions over the tropical Pacific Ocean.

4. 2 Definitions of El-Niño and El-Niño Modoki

An El-Niño event occurs when the magnitude of the north-east and south-east trade winds is decreased. Hence the trade winds will not push off the surface waters from east to the western Pacific Ocean. The piled up warm water in the western Pacific Ocean will start flowing through the surface from western Pacific Ocean and it will reach the eastern Pacific Ocean. By this time the atmosphere over the tropical eastern Pacific Ocean will get heated up and make large scale atmospheric convections over there. The heat energy stored over the western Pacific Ocean gets reduced and the entire atmosphere becomes cold and dry. The Walker circulation gets modified during this time as the ascending limb and the convection zones shifted from the western to eastern Pacific Ocean and the descending limb shifts from the eastern to western Pacific Ocean. This condition is called the El-Niño condition. The modification of the Walker circulation results in heavy convective activity enhanced rainfall over the eastern Pacific Ocean and drought like situations in the west Pacific Ocean. The counter-part of El-Niño is called the La-Niña. An El-Niño event has been quantified as the SST anomalies over Niño 3.4 region (5° N - 5° S, 170° - 120° W) exceeding the threshold 0.4° C for six months (Trenberth 1997).

Since the geographical position of NIO is very close to the western Pacific Ocean region the formation and intensification of the tropical cyclones is greatly affected by the El-Niño event. The large scale convection over the warm tropical oceans is a major part of the driving energy for the general circulation of the atmosphere (Graham and Barnet 1987) it influences the general circulation and in turn influences the global climate system. Studies and observations (Landsea 2000, Chu 2004) show that the frequency and intensity of the cyclones are highly influenced by these air-sea interaction processes. Two different kinds of air-sea interaction processes also exist associated with the ENSO system namely the El-Niño Modoki and La-Niña Modoki.

The El-Niño Modoki is a coupled ocean-atmosphere phenomenon in the tropical Pacific and it is different from the traditional El-Niño events. It is defined by the anomalous warming over the central Pacific Ocean and cooler SST anomalies in both west and east along the equator (Ashok et al. 2007, Ashok and Yamagata 2009). Since there is warmer SST in the central Pacific Ocean the Walker circulation splits into two loops as the ascending limb over the central Pacific Ocean and the two descending limbs over both east and west Pacific Ocean. Then the heavy convective rainfall will be over the central Pacific

Ocean. The name "El-Niño Modoki" was first coined by Prof. Yamagata in various press releases. Researchers of the Climate Variations Research Program of Frontier Research Centre for Global Change (FRCGC) led by Prof. Yamagata documented this phenomenon for the first time. This phenomenon appears as second dominant mode of inter-annual variability in the tropical Pacific Ocean. Ashok et. al (2007) proposed an index to calculate the El-Niño Modoki years, by taking the averaged SST of specific boxes from the tropical Pacific Ocean. The index of El-Niño Modoki is defined as.

$$EMI= [SSTA]_A - 0.5[SSTA]_B - 0.5[SSTA]_C$$

Where the square bracket with a subscript represents the area-mean SST, averaged over one of the three regions specified as the central (C: 165° E–140° W, 10° S–10° N), eastern (E: 110° –70° W, 15° S–5° N), and western (W: 125° –145° E, 10° S–20° N). The three terms on the right hand side of the equation are derived from the area-averaged SST anomaly over each of the regions A (165°E-140°W, 10°S-10°N), B (110°W-70°W, 15°S-5°N), and C (125°E-145°E, 10°S-20°N) respectively.

4. 3 Influence of the El-Niño and El-Niño Modoki events on the global climate

There have been numerous studies on the influence of the El-Niño events in the formation and intensification of the tropical cyclones over various basins. Results show that there is a tendency toward fewer tropical cyclones over the Atlantic ocean, while the opposite occurs in La-Niña years (Gray 1984, Gray and Sheaffer 1991, Gray 1993, Knaff 1997). It is also observed that the ENSO system affects a number of landfalls in the United States (Bove et. al (1998), Pielke and Landsea 1999), hurricane intensity (Landsea 1999) and the genesis locations (Elsner and Kara 1999). The shifts in the tropical cyclone activity over various basins have been studied by various authors, the results show that the causative factors responsible for this shift in the tropical cyclone activity are the vertical wind shear (Shapiro 1987, Goldenberg and Shapiro 1996) and the influence of the thermodynamic variables (Tang and Neelin 2004).

It is observed that there is a south-eastward shift of tropical cyclone activity in the El-Niño years and a north-eastward shift of tropical cyclone activity in the La-Niña years over the western north Pacific Ocean (Chan 1985, Dong 1988, Chia and Ropelewski 2002, Wang and Chan 2002). This north-south shift of tropical cyclone activity has been attributed to the east-ward extension of the monsoon trough and westerlies in the western north Pacific Ocean (Lander 1994, 1996) and the reduction of vertical wind shear (Clark and Chu 2002). The typhoons last longer, become more intense and have more recurved trajectories during the El-Niño years (Wang and Chan 2002, Camargo and Sobel 2005, Camargo et. al 2007), which influences landfall probabilities in the Asian countries (Saunders 2000, Elsner and Liu 2003, Wu 2004). Studies show that more hurricanes formed over central Pacific Ocean during the El-Niño years (Wu and Lau 1992, Chu and Wang 1997, Clark and Chu 2002, Chu 2004).

The studies on the influence of El-Niño events on the tropical cyclones over NIO are limited. The tropical cyclones form over NIO mainly in two seasons, namely the pre-monsoon season (March - May) and the post-monsoon season (October – December). It is observed that the frequency of the intense tropical cyclones is less over NIO during the El-Niño years (Singh 2000). Sumesh and Ramesh Kumar (2013) studied the influence of El-Niño events in the formation and intensification of the tropical cyclones over NIO. The results show that the frequency of the tropical cyclones over AS is lesser than BB during the El-Niño years. Few studies exist on the influence of the El-Niño Modoki events on the formation and intensification of the tropical cyclones over the globe. El-Niño Modoki and its climate impacts are highly different from those of El-Niño (Weng et. al 2007); it is noticed that the El-Niño Modoki event has a large decadal background while the El-Niño event is predominant for inter-annual variability. The El-Niño Modoki event has significant impacts on the temperature and precipitation over many parts of the globe (Ashok et. al

2007). Pradhan (2011) calculated the El-Niño and El-Niño Modoki years during the period 1979-2004. Sumesh and Ramesh Kumar (2013) have studied the frequency variations of the cyclones and severe cyclones over NIO during the El-Niño and El-Niño Modoki years. The results show that the frequency of the tropical cyclones over AS is more than BB during the El-Niño Modoki years. This is attributed to the splitting of the Walker circulation, which has high influence on the formation and intensification of the tropical cyclones over NIO during the El-Niño Modoki years.

4. 4 Convective systems over NIO during El-Niño years

Figure (4.1) gives the genesis locations (black dots) and the tracks of the convective systems over NIO during the monsoon and non-monsoon seasons of the El-Niño years. Figure 4.1 (a,b) shows the genesis areas and tracks of depressions formed over NIO during the monsoon and non-monsoon seasons respectively. From this figure it is seen that the depressions are formed towards the north of AS and BB. During the monsoon season the genesis of the depressions is much more localised over the head bay in BB. But during the non-monsoon seasons the depressions are formed towards the south of AS and BB, and the genesis points are widely spread compared to that in the monsoon season. It is also observed that all the depressions (except one) have taken a north-westerly track and entered the land during the monsoon season and it is found that all the 7 depressions have formed and dissipated in the oceans (AS and BB) during the non-monsoon seasons. All the depressions formed over AS and BB in the monsoon and non-monsoon months of the El-Niño years are presented in the Table (4.1 and 4.2). Figure 4.1 (c,d) shows the genesis points and tracks of the cyclones formed over NIO during the monsoon and non-monsoon seasons of the El-Niño years. It is observed that there were no cyclones over AS during both the monsoon and non-monsoon seasons of the El-Niño years. All the cyclones are listed in table (4.3). One cyclone was formed over BB during the monsoon season. It was formed on 01-Jun-1987 and intensified into cyclone on 03-Jun-1987. It has taken a north-westerly track and further re-curved and moved in a northward direction and made landfall on 05-Jun-1987. There have been 3 cyclones over BB in the non-monsoon seasons. The first cyclone was formed on 02-Oct-1983, it was intensified into cyclone on 03-Oct-1983 and landed on 06-Oct-1983.

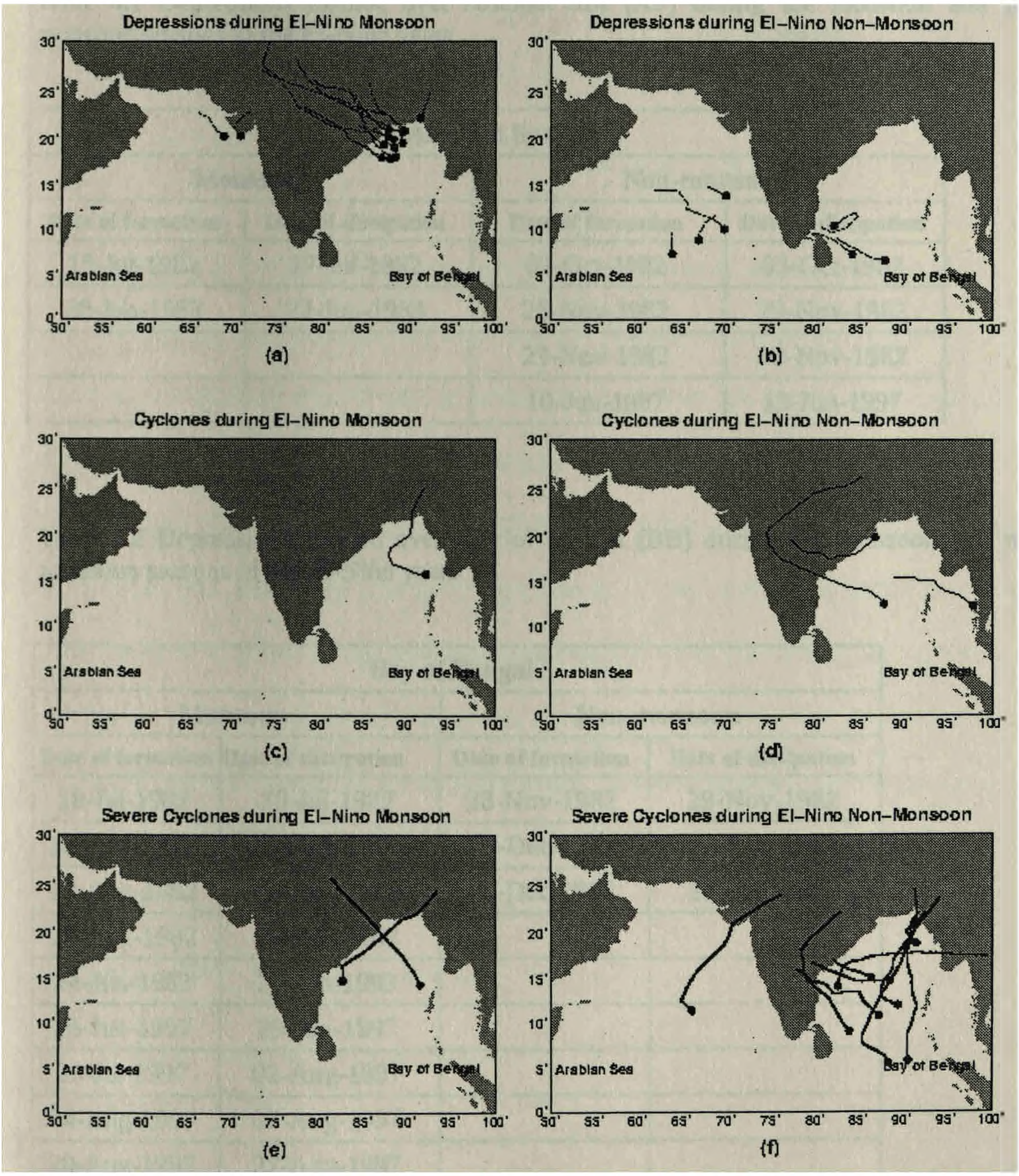

Figure 4.1 Convective systems over NIO during the monsoon and non-monsoon seasons of the El-Niño years

The second cyclone was formed 14-Oct-1987, it was intensified into cyclone on the same day and landed on 19-Oct-1987. The third cyclone was formed on 04-Nov-1997, intensified on the same day and decayed in the ocean on 09-Nov-1997.

Table 4.1 Depressions formed over Arabian Sea (AS) during the monsoon and non-monsoon seasons in the El-Niño years

Arabian Sea			
Monsoon		**Non-monsoon**	
Date of formation	**Date of dissipation**	**Date of formation**	**Date of dissipation**
15-Jul-1982	17-Jul-1982	02-Oct-1982	03-Oct-1982
20-Jun-1983	22-Jun-1983	28-Nov-1982	29-Nov-1982
		29-Nov-1982	30-Nov-1982
		10-Jun-1997	13-Jun-1997

Table 4.2 Depressions formed over Bay of Bengal (BB) during the monsoon and non-monsoon seasons in the El-Niño years

Bay of Bengal			
Monsoon		**Non-monsoon**	
Date of formation	**Date of dissipation**	**Date of formation**	**Date of dissipation**
18-Jul-1982	19-Jul-1982	28-Nov-1982	29-Nov-1982
12-Aug-1982	13-Aug-1982	03-Dec-1982	04-Dec-1982
18-Aug-1982	19-Aug-1982	20-Dec-1982	22-Dec-1982
27-Aug-1982	02-Sep-1982		
24-Jun-1983	27-Jun-1983		
26-Jun-1997	29-Jun-1997		
29-Jul-1997	02-Aug-1997		
04-Aug-1997	07-Aug-1997		
20-Aug-1997	27-Aug-1997		
28-Aug-1997	30-Aug-1997		

Table 4.3 Cyclones formed over BB during the monsoon and non-monsoon seasons in the El-Niño years

Bay of Bengal					
Monsoon			Non-monsoon		
Date of formation	Date of Intensification to Cyclone	Date of dissipation	Date of formation	Date of Intensification to Cyclone	Date of dissipation
01-Jun-1987	03-Jun-1987	05-Jun-1987	02-Oct-1983	03-Oct-1983	06-Oct-1983
			14-Oct-1987	14-Oct-1987	19-Oct-1987
			04-Nov-1997	04-Nov-1997	09-Nov-1997

Figure 4.1 (e,f) shows the genesis points and tracks of the severe cyclones formed over NIO during the monsoon and non-monsoon seasons respectively. There have been only 1 severe cyclone over AS and 11 severe cyclones over BB during the El-Niño years. Table (4.4) gives all the severe cyclones formed over AS during the monsoon season of the El-Niño years. The severe cyclone over AS during the non-monsoon seasons was formed on 05-Nov-1982, intensified into severe cyclone on 05-Nov-1982 and landed on 09-Nov-1982. Table (4.5) gives all the severe cyclones formed over BB during the monsoon and non-monsoon seasons of the El-Niño years. There have been 2 severe cyclones over BB during the monsoon season of the El-Niño years. The first severe cyclone was formed on 31-May-1982 it intensified into severe cyclone on 02-May-1982 and made landfall on 05-May-1982. The second severe cyclone was formed on 23-Sep-1997, intensified into severe cyclone on 26-Sep-1997 and decayed on 27-Sep-1997.

There were 9 severe cyclones over BB during the non-monsoon seasons. In which 3 severe cyclones were formed during the non-monsoon season of 1982, two severe cyclones were formed during the non-monsoon season of 1983, three severe cyclones were formed during the non-monsoon season of 1987 and 1 severe cyclone was formed during the non-monsoon season of 1997. In 1982 there were 3 severe cyclones, the first severe cyclone was formed on 01-May-1982, intensified into severe cyclone on 02-May-1982 and dissipated on 05-May-1982. The second severe cyclone was formed on 15-Oct-1982, intensified into severe cyclone on the same day and decayed on 16-Oct-1982.

Table 4.4 Severe cyclones formed over AS during the monsoon and non-monsoon seasons in the El-Niño years

Arabian Sea					
Monsoon			**Non-monsoon**		
Date of formation	**Date of Intensification to Severe Cyclone**	**Date of dissipation**	**Date of formation**	**Date of Intensification to Severe Cyclone**	**Date of dissipation**
			05-Nov-1982	05-Nov-1982	09-Nov-1982

Table 4.5 Severe cyclones formed over BB during the monsoon and non-monsoon seasons in the El-Niño years

Bay of Bengal					
Monsoon			**Non-monsoon**		
Date of formation	**Date of Intensification to Severe Cyclone**	**Date of dissipation**	**Date of formation**	**Date of Intensification to Severe Cyclone**	**Date of dissipation**
31-May-1982	02-Jun-1982	05-Jun-1982	01-May-1982	02-May-1982	05-May-1982
23-Sep-1997	26-Sep-1997	27-Sep-1997	15-Oct-1982	15-Oct-1982	16-Oct-1982
			17-Oct-1982	17-Oct-1982	21-Oct-1982
			14-Oct-1983	14-Oct-1983	16-Oct-1983
			06-Nov-1983	08-Nov-1983	09-Nov-1983
			30-Jan-1987	31-Jan-1987	04-Feb-1987
			12-Nov-1987	12-Nov-1987	13-Nov-1987
			31-Oct-1987	02-Nov-1987	03-Nov-1987
			15-May-1997	17-May-1997	19-May-1997

The third severe cyclone was formed on 17-Oct-1982, intensified into severe cyclone on the same day and made landfall on 21-Oct-1982. In 1983 there were two severe cyclones, the first severe cyclone was formed on 14-Oct-1983, intensified into severe cyclone on the same day and dissipated on 16-Oct-1983. The second severe cyclone was formed on 06-Nov-1983, intensified into severe cyclone on 08-Nov-1983 and decayed on 09-Nov-1983. In 1987 there were 3 severe cyclones during the non-monsoon seasons. The first severe cyclone was formed on 30-Jan-1987, intensified on 31-Jan-1987 and decayed in the ocean on 04-Feb-1987. The second severe cyclone was formed on 12-Nov-1987, intensified on 12-Nov-1987 and dissipated on 13-Nov-1987. The third severe cyclone was formed on 31-Oct-1987, intensified on 02-Nov-1987 and made landfall on 03-Nov-1987. In 1997 only 1 severe cyclone was formed during the non-monsoon seasons. It formed on 15-May-1997, intensified on 17-May-1997 and decayed on 19-May-1997.

4.5 Variations of CSGP for the convective systems over NIO during the El-Niño years

Figure (4.2) shows the variations of the Convective System Genesis Parameter (CSGP) for the convective systems over NIO during the monsoon and non-monsoon seasons of the El-Niño years. Figure 4.2 (a, b, c, d) shows the variations CSGP for the depressions formed over NIO during this period. From figure 4.2 (a) it is observed that the depressions have formed against the lower positive magnitudes of CSGP and the higher positive magnitudes (0.5 X $10^{-10}s^{-2}$ °K) are found in the southern AS and northern BB is away from the genesis locations. From figure 4.2 (b) it is noticed that the depressions have formed against lower positive magnitudes of CSGP and the higher positive magnitudes are observed over the southern BB. From figure 4.2 (c) it is seen that the depressions were formed against higher positive magnitudes (0.0 to 1.0 X $10^{-10}s^{-2}$ °K) over the head bay and higher positive magnitudes are noticed over the land during this period. From figure 4.2 (d) it is found that the depressions were formed against lower positive magnitudes of CSGP and the higher positive magnitudes are found over the southern AS and the south west BB.

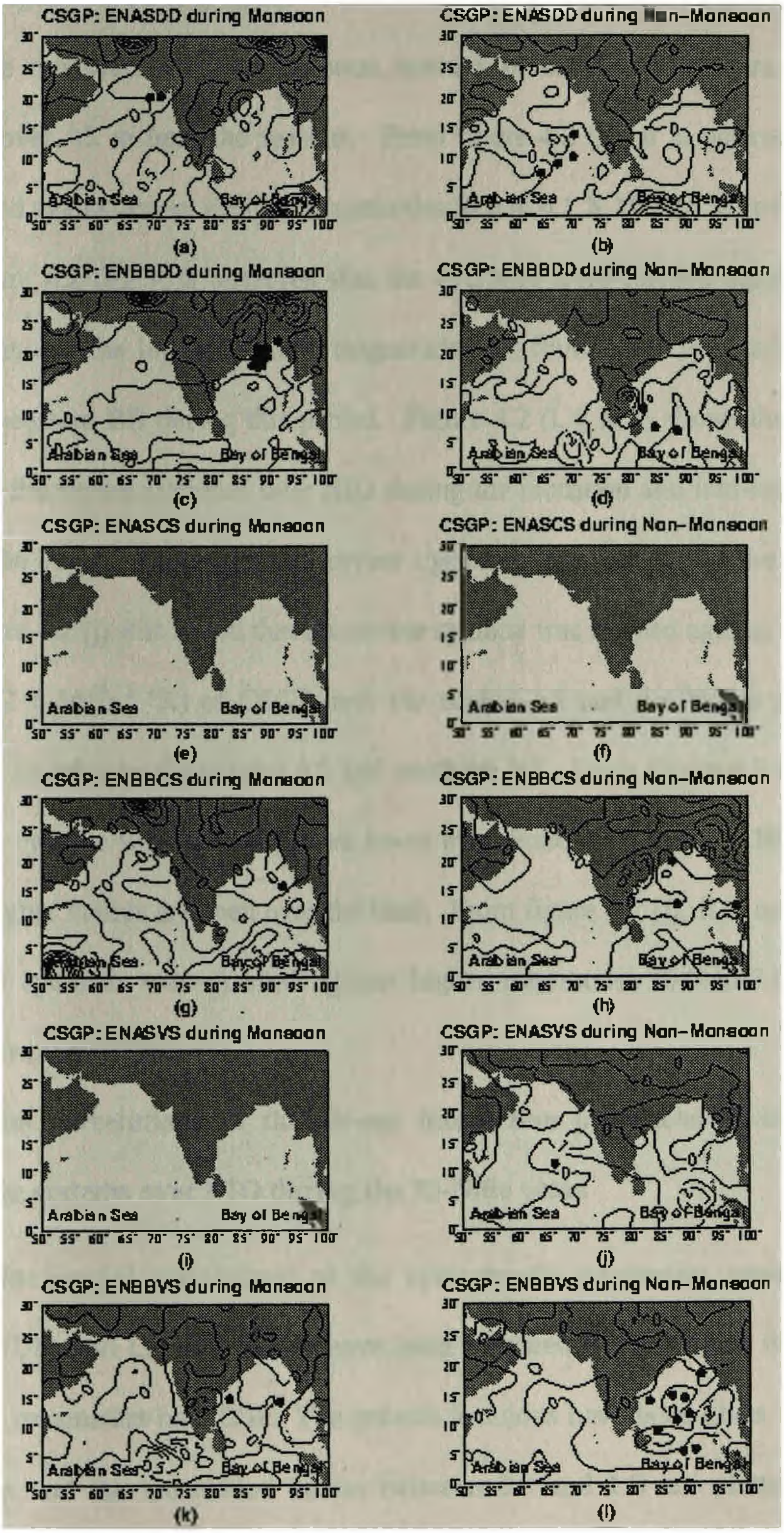

Figure 4.2 Variations of CSGP for the convective systems over NIO during the monsoon and non-monsoon seasons of the El-Niño years

Figure 4.2 (e, f, g, h) shows the variations of the CSGP for the cyclones over NIO during the monsoon and non-monsoon seasons of the El-Niño years. There were no cyclones over AS in both the seasons. From figure 4.2 (g), it is noticed that the cyclone was formed against lower positive magnitudes (0.0 to 0.1 X $10^{-10}s^{-2}$ °K) over the eastern BB. From figure 4.2 (h), it is observed that the cyclones were formed against lower positive magnitudes and the higher positive magnitudes are found over the land near the western and north-eastern BB during this period. Figure 4.2 (i, j, k, l) shows the variations of the CSGP for the severe cyclones over NIO during the monsoon and non-monsoon seasons of the El-Niño years. There were no severe cyclones over AS during the monsoon season. From figure 4.2 (j) it is found that the severe cyclone was formed against lower magnitudes (0.0 to 0.2 x $10^{-10}s^{-2}$ °K) of CSGP over the central AS and the higher positive values of CSGP are found over the eastern AS and southern BB. From figure 4.2 (k) it is found that the severe cyclone was formed against lower magnitudes (0.0 to 0.2 x $10^{-10}s^{-2}$ °K) of CSGP and the higher values are seen over the land. From figure 4.2 (l), it is noticed that most of the severe cyclones were formed against higher magnitudes (0.0 to 2.0 x $10^{-10}s^{-2}$ °K) of CSGP over central BB.

4.6 Spatial correlations of the air-sea interaction parameters with CSGP for the convective systems over NIO during the El-Niño years

The spatial correlations of the cyclogenesis parameters such as LLRV, LLC, VWSC, HUM and CI with CSGP have been obtained to investigate the relative role of individual parameters on CSGP. The genesis locations have been given with a "+" sign in the figures and the correlation values between 0.0 and 1.0 are plotted. This gives the relative roles of the individual parameters on CSGP in the formation and intensification of the convective systems over NIO.

Figure 4.3 (a-e) shows the spatial correlations of the parameters with CSGP for the depressions formed over AS in the monsoon season and figure 4.3 (f-j) shows the spatial correlations of the parameters with CSGP for the depressions formed over AS in the non-monsoon seasons of the El-Niño years.

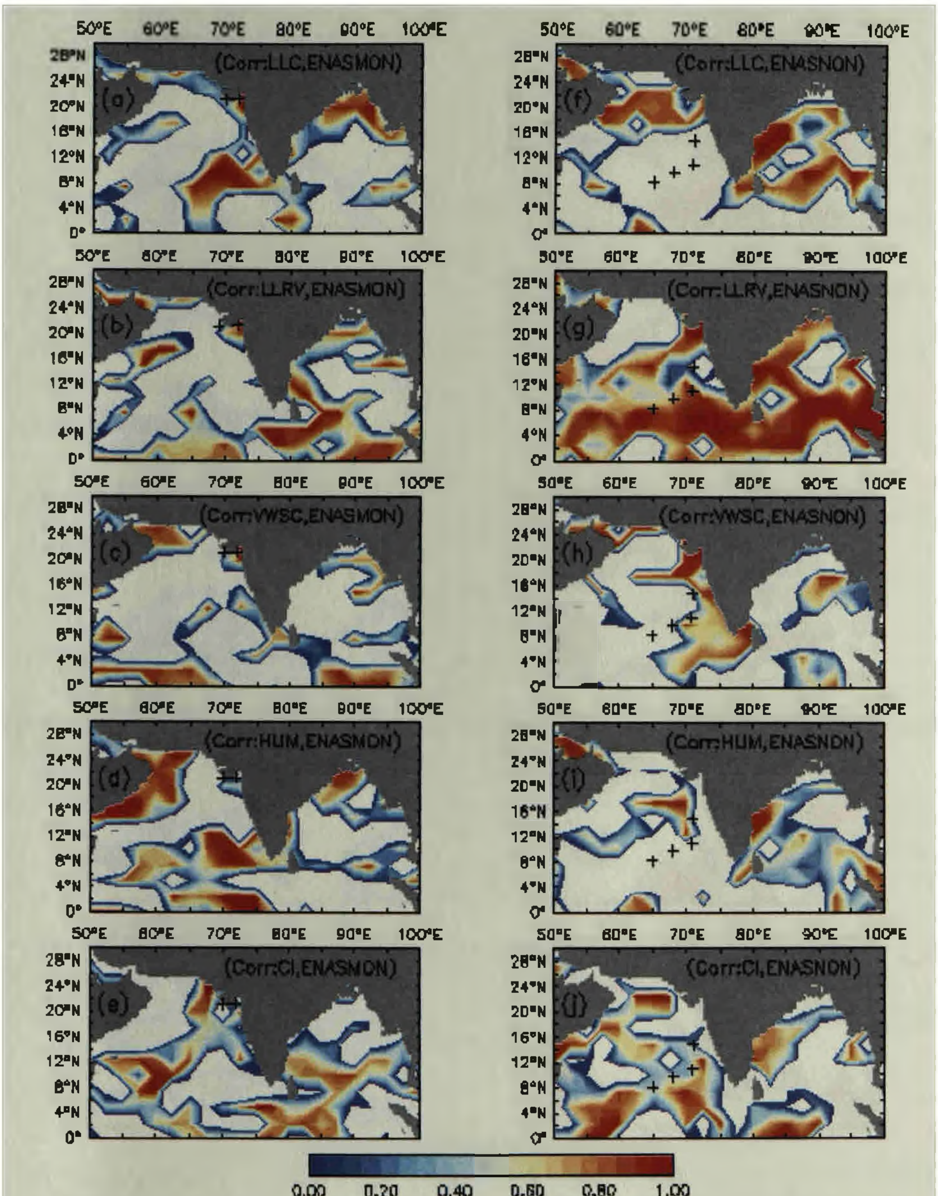

("+" represents the genesis locations of the depressions)
(AS= Arabian Sea, EN=El-Nino, MON=Monsoon, NON=Non-monsoon)

Figure 4.3 Spatial correlations of the parameters with CSGP for the depressions over AS during the monsoon and non-monsoon seasons of the El-Niño years

From figure: 4.3 (a, b, d, e) it is observed that high positive correlations exist for all these parameters namely LLC, LLRV, HUM and CI with the CSGP. Hence all the parameters (except VWSC) help the formation of the depressions over AS during the monsoon season of the El-Niño years.

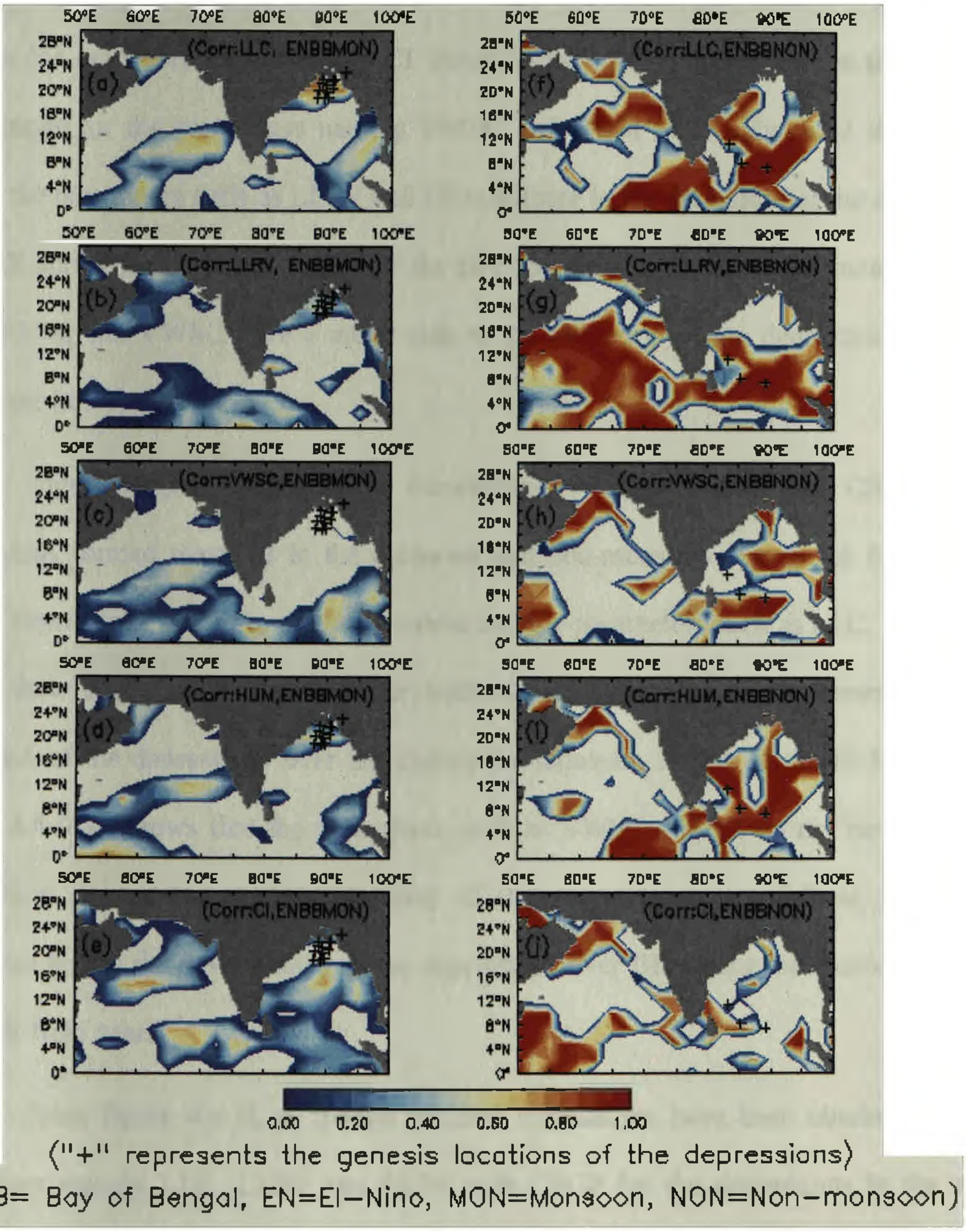

Figure 4.4 Spatial correlations of the parameters with CSGP for the depressions over BB during the monsoon and non-monsoon seasons of the El-Niño years

From figure 4.3 (f) it is clear that the LLC parameter does not have positive correlations around the genesis of the depressions. Hence it is understood that the LLC parameter does not have an important role in the formation of the depressions over AS during the non-monsoon seasons of the El-Niño years. From figure: 4.3 (g, j) it is seen that the high positive correlations do not exist for all the parameters the high positive correlations exist only for LLRV and CI. From figure 4.3 (h,i) it is observed that positive correlations for the parameters namely VWSC and HUM exist only for 2 depressions. Hence the parameters such as LLRV and CI contribute to the formation of the depressions over AS during the monsoon season of the El-Niño years. The other parameters such as LLC, HUM, and VWSC have a minor role in the formation of the depressions over AS during the El-Niño years.

Figure (4.4) shows the spatial correlations of the parameters with CSGP for the depressions formed over BB in the monsoon and non-monsoon seasons of the El-Niño years. From figure 4.4 (a, b, d) it is observed that the parameters such as LLC, LLRV and HUM show high positive correlations with CSGP, hence these parameters help the formation of the depressions over BB during the monsoon season of the El-Niño years. Figure 4.4 (c,e) shows that the parameters such as VWSC and CI do not have positive correlations around the genesis locations of the depressions, hence these parameters contribute less to the development of the depressions over BB during the monsoon season of the El-Niño years.

From figure 4.4 (f, g, i) high positive correlations have been obtained for the parameters namely LLC, LLRV and HUM with CSGP for the depressions in the non-monsoon seasons, hence all these parameters contribute together to the development of depressions over BB in the non-monsoon seasons of the El-Niño years. From figure 4.4 (h,j) positive correlation values are exist only for 2 depressions and negative correlations have been observed for the VWSC and CI parameters with CSGP around the genesis of the depressions hence these parameters contribute less to the development of the depressions over BB during this period.

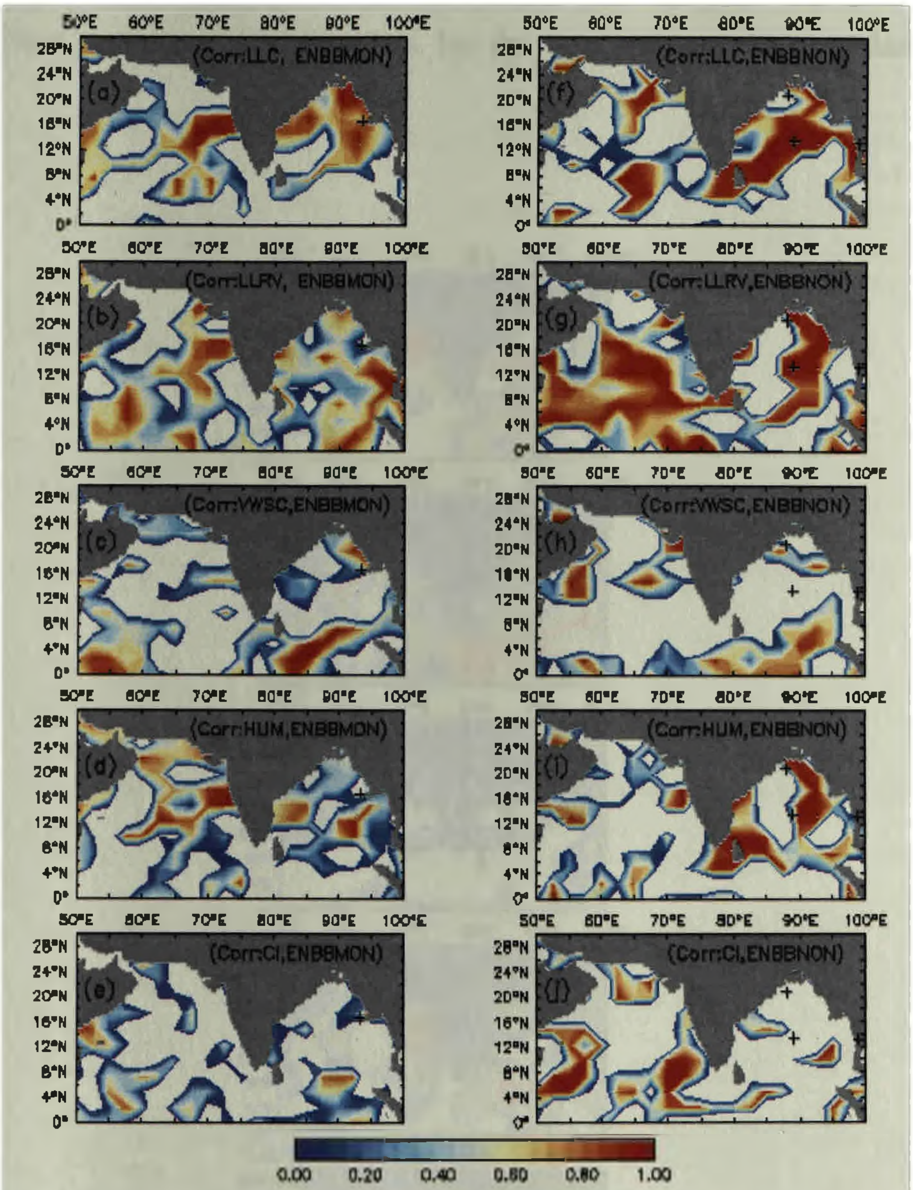

("+" represents the genesis locations of the cyclones)

(BB= Bay of Bengal, EN=El-Nino, MON=Monsoon, NON=Non-monsoon)

Figure 4.5 Spatial correlations of the parameters with CSGP for the cyclones over BB during the monsoon and non-monsoon seasons of the El-Niño years

Figure (4.5) gives the spatial variations of the parameters for the cyclones over BB during the El-Niño years. From figure 4.5 (a), a high positive correlation has been observed for the LLC with CSGP, hence LLC contribute much for the development of the cyclone over BB during the monsoon season of the El-Niño years. From figure 4.5 (b, c, e), parameters such as LLRV, VWSC and CI have low positive correlations with CSGP, hence these parameters contribue less for the development of the cyclone during this period.

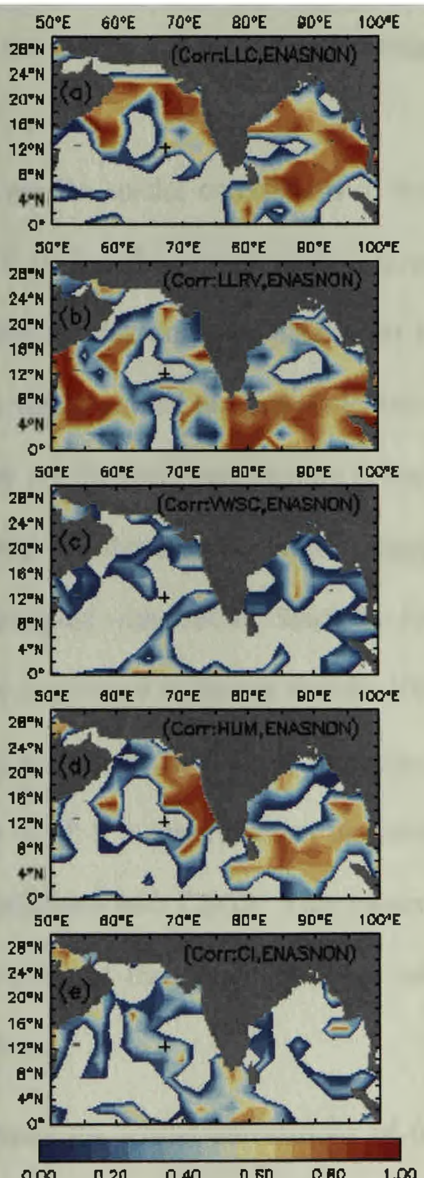

("+" represents the genesis locations of the severe cyclones)
(AS= Arabian Sea, EN=El-Nino, NON=Non-monsoon)

Figure 4.6 Spatial correlations of the parameters with CSGP for the severe cyclones over AS during the non-monsoon seasons of the El-Niño years

From figure 4.5 (f, g, i), a high positive correlation has been observed for the parameters namely LLC, LLRV and HUM, hence these parameters help the formation of the cyclones over BB during the non-monsoon seasons of the El-Niño years. Figure 4.5 (h, j) shows no higher positive values exists for the correlations between the parameters such as VWSC and CI with CSGP around the genesis locations of the cyclones, hence these parameters are contributing less in the formation of the cyclones over BB during this period. There was only one severe cyclone over AS during the non-monsoon seasons of the El-Niño years.

Figure (4.6) gives the spatial correlations of the parameters with CSGP for the severe cyclones over AS during the non-monsoon seasons of the El-Niño years. From figure 4.6 (a, e) it is observed that only two parameters namely LLC and CI have shown high positive correlation values around the genesis locations of the severe cyclone over AS during this period. These are the main contributors in the development and intensification of the severe cyclone over AS during this period. From figure 4.6 (c) it is noticed that VWSC is negatively correlated with CSGP. Since the lower magnitudes are required for the genesis of the severe cyclones it is known that the VWSC parameter is also contribute much for the formation and intencification of the severe cyclones over AS during this period. From figure 4.6 (b, d) it is observed that the parameters such as LLRV and HUM are having negative correlations with CSGP. This means that they contribute less for the formation and intensification of the severe cyclones over AS during the non-monsoon seasons of the El-Niño years.

Figure (4.7) shows the spatial correlations of the air-sea interaction parameters with CSGP for severe cyclones over BB during the El-Niño years. From figure 4.7 (a,b), it is observed that the parameters such as LLC and LLRV show high positive correlations with CSGP. From the figure it is clear that only one severe cyclone has got the benefit of this higher magnitude of LLC and LLRV. From figure 4.7 (d) it is observed that high positive correlations exist between HUM and CSGP, hence the HUM parameter contributes much to the development of the severe cyclones. From figure 4.7 (c), lower values of positive correlations are observed around the genesis locations of the severe cyclones.

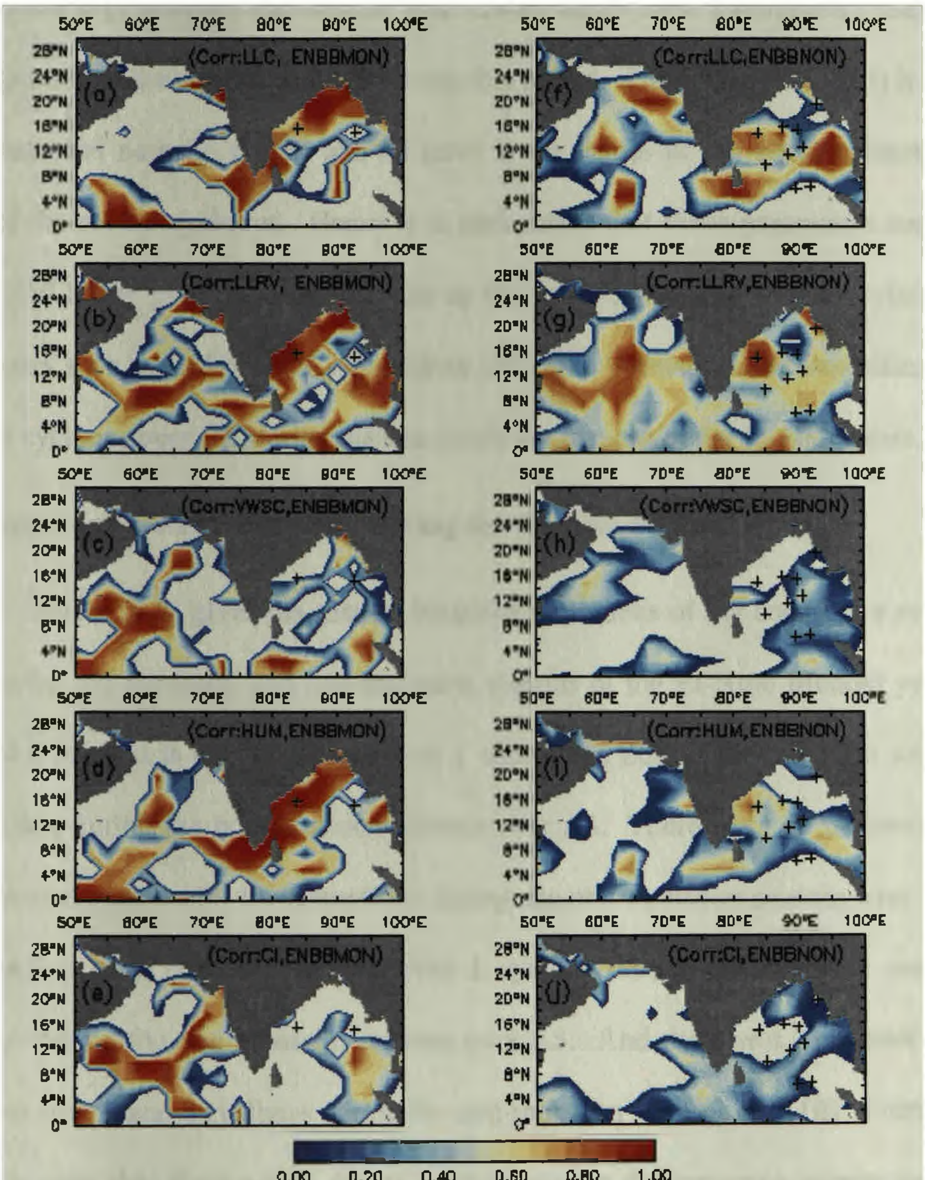

("+" represents the genesis locations of the severe cyclones)
(BB= Bay of Bengal, EN=El-Nino, MON=Monsoon, NON=Non-monsoon)

Figure 4.7 Spatial correlations of the parameters with CSGP for the severe cyclones over BB during the monsoon and non-monsoon seasons of the El-Niño years

From 4.7 (e), no positive values have been observed around the genesis of the severe cyclones. It is understood that the HUM parameter plays an important role in the formation and intensification of the severe cyclones over BB during the El-Niño years.

From figure 4.7 (f, g, i) it is observed that the parameters such as LLC, LLRV and HUM show high positive correlations with CSGP, hence these parameters contribute much to the genesis of the severe cyclones during this period. From figure 4.7 (h, j) it is seen that the parameters namely VWSC and CI have lower values of the positive correlations for most of the severe cyclones. Hence it is understood that these parameters such as LLC, LLRV and HUM play an important role in the formation of the severe cyclones and the parameters such as LLRV and CI contribute less to the formation and intensification of the tropical cyclones over BB during the non-monsoon seasons of the El-Niño years.

4. 7 Convective systems over NIO during the El-Niño Modoki years

Figure (4.8) gives the genesis locations and tracks of the convective systems over NIO during the monsoon and non-monsoon seasons of the El-Niño Modoki years. From figure 4.8 (a,b), it is seen that there was 1 depression during the monsoon season and 5 depressions during the non-monsoon seasons over AS. There were 13 depressions during the monsoon season and 14 depressions during the non-monsoon seasons over BB. From figure 4.8 (c,d) it is seen that there was 1 cyclone during the monsoon season and 2 cyclones during the non-monsoon seasons over AS. And there was 1 cyclone during the monsoon season and 6 cyclones during the non-monsoon seasons over BB. From figure 4.8 (e,f) it is seen that there was 1 severe cyclone during the monsoon season and 4 severe cyclones during the non-monsoon seasons over AS. And there was no severe cyclone during the monsoon season and 9 severe cyclones during the non-monsoon seasons over BB.

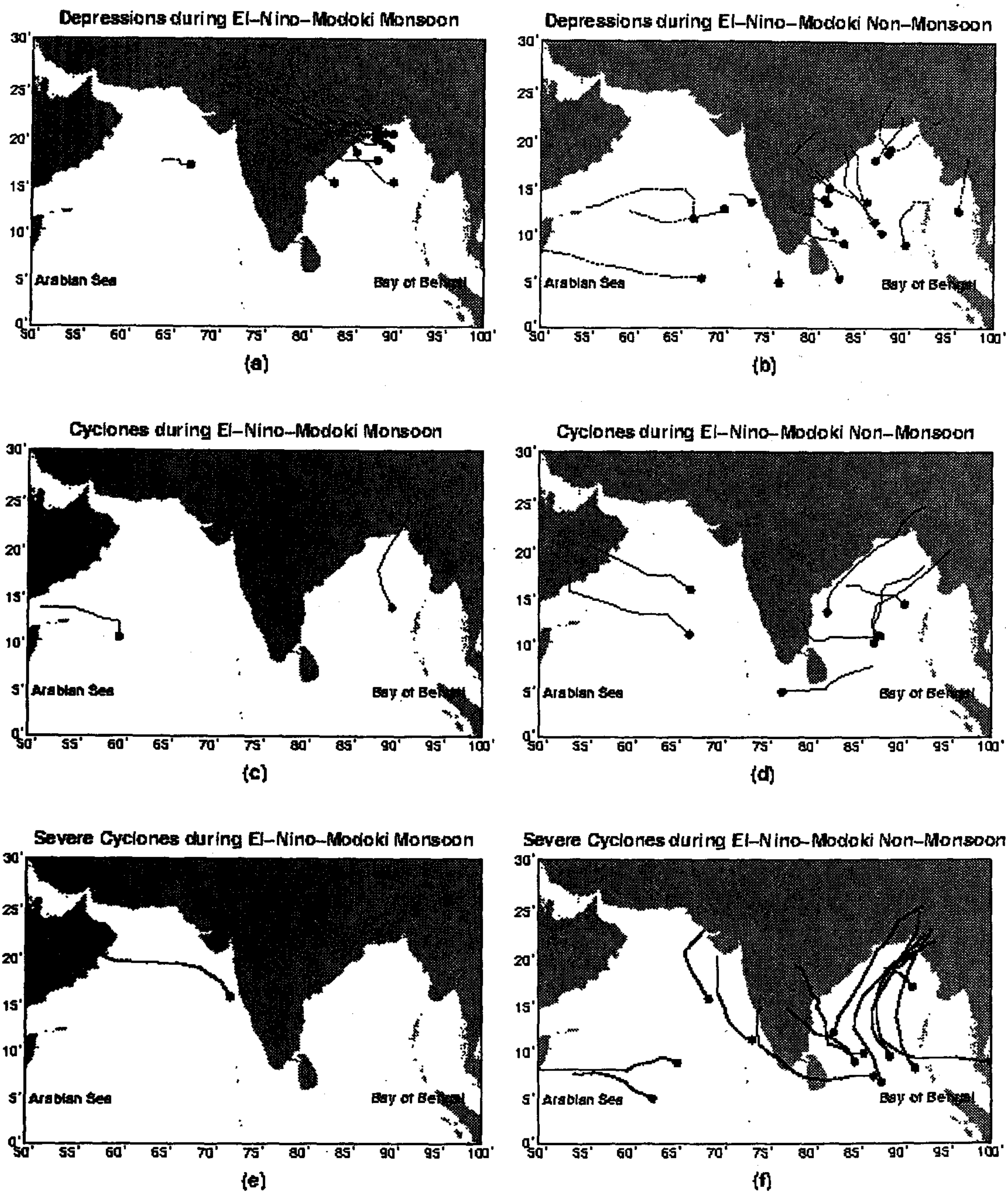

Figure 4.8 Convective systems formed over NIO during the monsoon and non-monsoon seasons of the El-Niño Modoki years

Table (4.6) gives the depressions formed over AS during the monsoon and non-monsoon seasons in the El-Niño Modoki years. There was 1 depression over AS during the monsoon season. This depression formed on 10-Jun-2002 and dissipated on 13-Jun-2002. There have been five depressions over AS during the monsoon and non-monsoon seasons in the El-Niño Modoki years. The first depression was formed on 09-Nov-1986 and decayed on 10-Nov-1986, the second depression was formed on 17-Nov-1990 and dissipated on 18-Nov-1990. In the year 1992 there were two depressions over AS during the non-monsoon season. The first depression was formed on 01-Dec-1992 and decayed on 02-Dec-1992 and the second depression was formed on 21-Dec-1992 and made landfall on 24-Dec-1992. The last depression was formed in the year 2004, it was formed on 02-Nov-2004 and decayed on 07-Nov-2004.

Table 4.6 Depressions formed over AS during the monsoon and non-monsoon seasons in the El-Niño Modoki years

Arabian Sea			
Monsoon		**Non-monsoon**	
Date of formation	**Date of dissipation**	**Date of formation**	**Date of dissipation**
10-Jun-2002	13-Jun-2002	09-Nov-1986	10-Nov-1986
		17-Nov-1990	18-Nov-1990
		01-Dec-1992	02-Dec-1992
		21-Dec-1992	24-Dec-1992
		02-Nov-2004	07-Nov-2004

Table (4.7) shows the depressions formed over BB during the monsoon and non-monsoon seasons in the El-Niño Modoki years. There have been 13 depressions during the monsoon season and 14 depressions during the non-monsoon season of the El-Niño Modoki years. The date of formation and dissipation of all the depressions during this period are listed in the table (4.7). In the year 1986, there were four depressions formed over BB, out of which 3 were formed during the monsoon season and one formed during the non-monsoon seasons. The first depression was formed on 11-Aug-1986 and dissipated on 14-Aug-1986, the second depression was formed on 19-Aug-1986 and decayed on 20-Aug-1986, the third depression was formed on 24-Sep-1986 and decayed on 26-Sep-1986. In the year 1990, there were six depressions formed over BB out of this three were formed during the monsoon season and three during the non-monsoon seasons. In the year 1991, there were five depressions formed over BB out of which three were formed during the monsoon season and two formed during the non-monsoon seasons. In the year 1992, there were 4 depressions formed over BB out of which 2 formed during the monsoon season and 2 formed during the non-monsoon seasons.

Table 4.7 Depressions formed over BB during the monsoon and non-monsoon seasons in the El-Niño Modoki years

Bay of Bengal			
Monsoon		**Non-monsoon**	
Date of formation	**Date of dissipation**	**Date of formation**	**Date of dissipation**
11-Aug-1986	14-Aug-1986	08-Jan-1986	09-Jan-1986
19-Aug-1986	20-Aug-1986	07-Oct-1990	09-Oct-1990
24-Sep-1986	26-Sep-1986	31-Oct-1990	04-Nov-1990
14-Jun-1990	16-Jun-1990	14-Nov-1990	15-Nov-1990
15-Aug-1990	16-Aug-1990	12-Oct-1991	14-Oct-1991
20-Aug-1990	24-Aug-1990	28-Oct-1991	30-Oct-1991
27-Jul-1991	31-Jul-1991	07-Oct-1992	09-Oct-1992
22-Aug-1991	26-Aug-1991	20-Oct-1992	22-Oct-1992
21-Sep-1991	22-Sep-1991	21-Mar-1994	24-Mar-1994
17-Jun-1992	20-Jun-1992	04-Oct-1994	07-Oct-1994
26-Jul-1992	30-Jul-1992	04-Nov-1994	05-Nov-1994
17-Aug-1994	20-Aug-1994	11-May-2002	12-May-2002
11-Jun-2004	14-Jun-2004	22-Oct-2002	23-Oct-2002
		02-Oct-2004	04-Oct-2004

In 1994, there were four depressions formed over BB, out of which 1 formed during the monsoon season and three formed during the non-monsoon seasons. In the year 2002, there were two depressions formed over BB, these two were formed during the non-monsoon seasons. In the year 2004, there were 2 depressions formed over BB out of which 1 formed during the monsoon season and 1 formed during the non-monsoon seasons.

Table 4.8 Cyclones formed over AS during the monsoon and non-monsoon seasons in the El-Niño Modoki years

Arabian Sea					
Monsoon			**Non-monsoon**		
Date of formation	**Date of Intensification to Cyclone**	**Date of dissipation**	**Date of formation**	**Date of Intensification to Cyclone**	**Date of dissipation**
08-Jun-1992	11-Jun-1992	12-Jun-1992	01-Oct-1992	01-Oct-1992	03-Oct-1992
			06-May-2002	09-May-2002	10-May-2002

Table 4.9 Cyclones formed over BB during the monsoon and non-monsoon seasons in the El-Niño Modoki years

Bay of Bengal					
Monsoon			**Non-monsoon**		
Date of formation	**Date of Intensification to Cyclone**	**Date of dissipation**	**Date of formation**	**Date of Intensification to Cyclone**	**Date of dissipation**
31-May-1991	01-Jun-1991	02-Jun-1991	07-Nov-1986	08-Nov-1986	09-Nov-1986
			11-Nov-1991	13-Nov-1991	15-Nov-1991
			16-May-1992	17-May-1992	19-May-1992
			03-Nov-1992	04-Nov-1992	06-Nov-1992
			23-Nov-2002	24-Nov-2002	28-Nov-2002
			21-Dec-2002	24-Dec-2002	25-Dec-2002

Table (4.8) shows the cyclones formed over AS during the monsoon and non-monsoon seasons in the El-Niño Modoki years. There have been three cyclones over AS, out of which 1 cyclone was formed during the monsoon season and two cyclones formed during the non-monsoon seasons. One cyclone in the monsoon season formed on 08-Jun-1992, intensified into cyclone on 11-Jun-1992 and dissipated on 12-Jun-1992. During the non-monsoon seasons the first cyclone was formed on 01-Oct-1992, intensified into cyclone on the same day and made landfall on 03-Oct-1992. The second cyclone was formed on 06-May-2002, intensified into cyclone on 09-May-2002 and decayed on 10-May-2002.

Table (4.9) shows the cyclones formed over BB during the monsoon and non-monsoon seasons in the El-Niño Modoki years. There were 7 cyclones over BB out of which 1 cyclone was formed during the monsoon season and 6 cyclones formed during the non-monsoon seasons. The cyclone in the monsoon season formed on 31-May-1991, intensified into cyclone on 01-Jun-1991 and dissipated on 02-Jun-1991. During the non-monsoon seasons the first cyclone was formed on 07-Nov-1986, intensified into cyclone on 08-Nov-1986 and made landfall on 09-Nov-1986. The second cyclone was formed on 11-Nov-1991, intensified into cyclone on 13-Nov-1991 and decayed on 15-Nov-1991. The third cyclone was formed 16-May-1992, intensified into cyclone on 17-May-1992 and dissipated on 19-May-1992. The fourth cyclone was formed on 03-Nov-1992, intensified into cyclone on 04-Nov-1992 and decayed on 06-Nov-1992. The fifth cyclone was formed on 23-Nov-2002, intensified into cyclone on 24-Nov-2002 and decayed on 28-Nov-2002. The last cyclone was formed on 21-Dec-2002, intensified into cyclone on 24-Dec-2002 and made landfall on 25-Dec-2002.

Table (4.10) shows the severe cyclones formed over AS during the monsoon and non-monsoon seasons in the El-Niño Modoki years. There have been 5 severe cyclones over AS out of which 1 severe cyclone was formed during the monsoon season and 4 severe cyclones formed during the non-monsoon seasons. The severe cyclone in the monsoon season formed on 05-Jun-1994, intensified into severe cyclone on 07-Jun-1994 and dissipated on 09-Jun-1994. During the non-monsoon seasons the first severe cyclone was formed on 15-Nov-1994, intensified into severe cyclone on 18-Nov-1994 and decayed on 20-Nov-1994. The second severe cyclone was formed on 05-May-2004, intensified into severe cyclone on 07-May-2004 and dissipated on 10-May-2004. The third severe cyclone was formed on 30-Sep-2004, intensified into severe cyclone on 02-Oct-2004 and made landfall on 03-Oct -2004. The last severe cyclone was formed on 30-Nov-2004, intensified into severe cyclone on 30-Nov-2004 and decayed on 02-Dec-2004.

Table 4.10 Severe cyclones formed over AS during the monsoon and non-monsoon seasons in the El-Niño Modoki years

Arabian Sea					
Monsoon			**Non-monsoon**		
Date of formation	**Date of Intensification to Severe Cyclone**	**Date of dissipation**	**Date of formation**	**Date of Intensification to Severe Cyclone**	**Date of dissipation**
05-Jun-1994	07-Jun-1994	09-Jun-1994	15-Nov-1994	18-Nov-1994	20-Nov-1994
			05-May-2004	07-May-2004	10-May-2004
			30-Sep-2004	02-Oct-2004	03-Oct -2004
			30-Nov-2004	30-Nov-2004	02-Dec-2004

Table (4.11) shows the severe cyclones formed over BB during the monsoon and non-monsoon seasons in the El-Niño Modoki years. There were no severe cyclones over BB during the monsoon season and there were nine severe cyclones have formed during the non-monsoon seasons. There were two severe cyclones in 1990. The first severe cyclone was formed on 05-May-1990, intensified into severe cyclone on 06-May-1990 and made landfall on 11-May-1990. The second severe cyclone was formed on 15-Dec-1990, intensified into severe cyclone on 17-Dec-1990 and dissipated on 18-Dec-1990. There was one severe cyclone in 1991, this was formed on 24-Apr-1991, intensified into severe cyclone on 26-Apr-1991 and decayed on 30-Apr-1991.

Table 4.11 Severe cyclones formed over BB during the monsoon and non-monsoon seasons in the El-Niño Modoki years

Bay of Bengal					
Monsoon			Non-monsoon		
Date of formation	Date of Intensification to Severe Cyclone	Date of dissipation	Date of formation	Date of Intensification to Severe Cyclone	Date of dissipation
			05-May-1990	06-May-1990	11-May-1990
			15-Dec-1990	17-Dec-1990	18-Dec-1990
			24-Apr-1991	26-Apr-1991	30-Apr-1991
			11-Nov-1992	13-Nov-1992	17-Nov-1992
			15-Nov-1992	17-Nov-1992	21-Nov-1992
			29-Apr-1994	30-Apr-1994	02-May-1994
			29-Oct-1994	30-Oct-1994	31-Oct-1994
			10-Nov-2002	12-Nov-2002	12-Nov-2002
			16-May-2004	18-May-2004	19-May-2004

There were 2 severe cyclones in 1992. The first severe cyclone was formed on 11-Nov-1992, intensified into severe cyclone on 13-Nov-1992 and dissipated on 17-Nov-1992. The second severe cyclone was formed on 15-Nov-1992, intensified into severe cyclone on 17-Nov-1992 and decayed on 21-Nov-1992. There were 2 severe cyclones in 1994. The first severe cyclone was formed on 29-Apr-1994, intensified into severe cyclone on 30-Apr-1994 and landed on 02-May-1994. The second severe cyclone was formed on 29-Oct-1994, intensified into severe cyclone on 30-Oct-1994 and made landfall on 31-Oct-1994. There was 1 severe cyclone in 2002, which was formed on 10-Nov-2002, intensified into severe cyclone on 12-Nov-2002 and dissipated on 12-Nov-2002. There was one severe cyclone in 2004, which was formed on 16-May-2004, intensified into severe cyclone on 18-May-2004 and dissipated on 19-May-2004.

4.8 Variations of CSGP for the convective systems over NIO during the El-Niño Modoki years

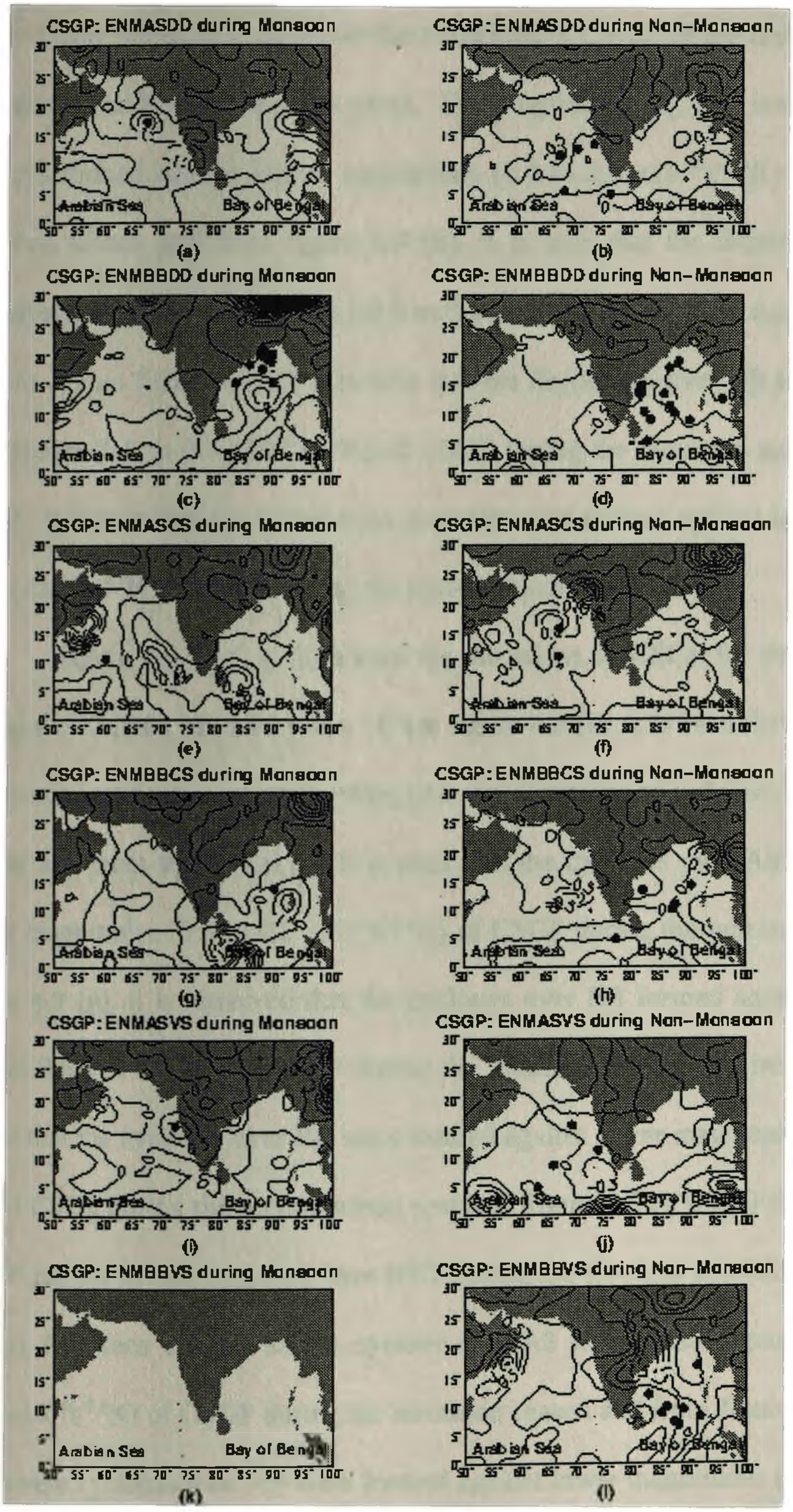

Figure 4.9 Variations of CSGP for the convective systems over NIO during the monsoon and non-monsoon seasons of the El-Niño Modoki years

Figure (4.9) gives the variations of CSGP over NIO during the El-Niño Modoki years. Figure 4.9 (a, b, c, d) shows the variations of CSGP for the convective systems over NIO during the El-Niño Modoki years. From figure 4.9 (a), it is seen that the depression over AS formed against higher magnitudes (1.0 to 2.0 $x10^{-10}s^{-2}$ °K) of CSGP during the monsoon season and from figure 4.9 (b), it is seen that the depressions over AS were formed against lower magnitudes (-0.5 to 0.2 $x10^{-10}s^{-2}$ °K) of CSGP during the non-monsoon seasons. From figure 4.9 (c), it is seen that the depression over BB formed against higher magnitudes (0.0 to 2.0 $x10^{-10}s^{-2}$ °K) of CSGP during the monsoon season and from figure 4.9 (d), it is seen that the depressions over BB were formed against lower magnitudes (0.0 to 0.2 $x10^{-10}s^{-2}$ °K) of CSGP during the non-monsoon seasons.

Figure 4.9 (e, f, g, h) shows the variations of CSGP for the cyclones over NIO during the El-Niño Modoki years. From figure 4.9 (e), it is seen that the cyclone over AS was formed against lower magnitudes (0.0 to 0.5 $x10^{-10}s^{-2}$ °K) of CSGP during the monsoon season and from figure 4.9 (f), it is seen that the cyclones over AS were formed against lower magnitudes (0.0 to 0.5 $x10^{-10}s^{-2}$ °K) of CSGP during the non-monsoon seasons.From figure 4.9 (g), it is observed that the cyclones over BB formed against lower magnitudes (0.0 to 0.5 $x10^{-10}s^{-2}$ °K) of CSGP during the monsoon season and from figure 4.9 (h), it is found that the cyclones over BB were formed against lower magnitudes (0.0 to 0.2 $x10^{-10}s^{-2}$ °K) of CSGP during the non-monsoon seasons. Figure 4.9 (i, j, k, l) shows the variations of CSGP for the severe cyclones over NIO during the El-Niño Modoki years. From figure 4.9 (i), it is seen that the severe cyclone over AS was formed against higher magnitudes (1.0 $x10^{-10}s^{-2}$ °K) of CSGP during the monsoon season and from figure 4.9 (j), it is seen that the severe cyclones over AS were formed against lower magnitudes (0.0 to 0.2 $x10^{-10}s^{-2}$ °K) of CSGP during the non-monsoon seasons. From figure 4.9 (l), it is seen that the severe cyclones over BB were formed against higher magnitudes (0.0 to 0.5 $x10^{-10}s^{-2}$ °K) of CSGP during the non-monsoon seasons.

4. 9 Spatial correlations of the air-sea interaction parameters with CSGP for the convective systems over NIO during the El-Niño Modoki years

Spatial correlations have been obtained for all the parameters with CSGP to analyze the relative role of individual parameters in the formation and intensification of the convective systems over NIO during the El-Niño Modoki years. Figure (4.10) shows the spatial correlations of the cyclogenesis parameters with CSGP for the depressions over AS during the El-Niño Modoki years. From figure 4.10 (a) it is observed that the LLC has high positive correlations with CSGP. From figure 4.10 (b,d) it is observed that the LLRV and HUM have positive correlation values with CSGP around the genesis of the depression. From figure 4.10 (c), it is observed that the VWSC parameter has negative correlations with CSGP around the genesis of the depression. Hence it is understood that the parameters, namely the LLC, LLRV, VWSC and HUM, contribute much to the development of the depression over AS during the El-Niño Modoki years. From figure 4.10 (e), it is observed that CI does not have positive correlations with CSGP around the genesis location of the depression. Hence the CI parameter contributes less to the development of this depression during the monsoon season of the El-Niño Modoki years.

From figure 4.10 (f, g) it is observed that the parameters, namely the LLC and LLRV, show positive correlation with CSGP around the genesis of the depressions. From figure 4.10 (h) it is observed that the VWSC parameter is negatively correlated with CSGP and it is understood that the lower magnitudes of VWSC are required for the formation of the depressions. Hence the parameters namely LLC, LLRV and VWSC contribute much for the formation of the depressions over AS during the non-monsoon seasons of the El-Niño Modoki years. From figure 4.10 (i, j) it is observed that the parameters HUM and CI show negative correlations around the genesis locations of most of the depressions. Hence it is understood that the parameters such as LLC, LLRV and VWSC contribute much to the formation of depressions over AS and the parameters HUM and CI contribute less to the formation of depressions over AS during the non-monsoon seasons of El-Niño Modoki years.

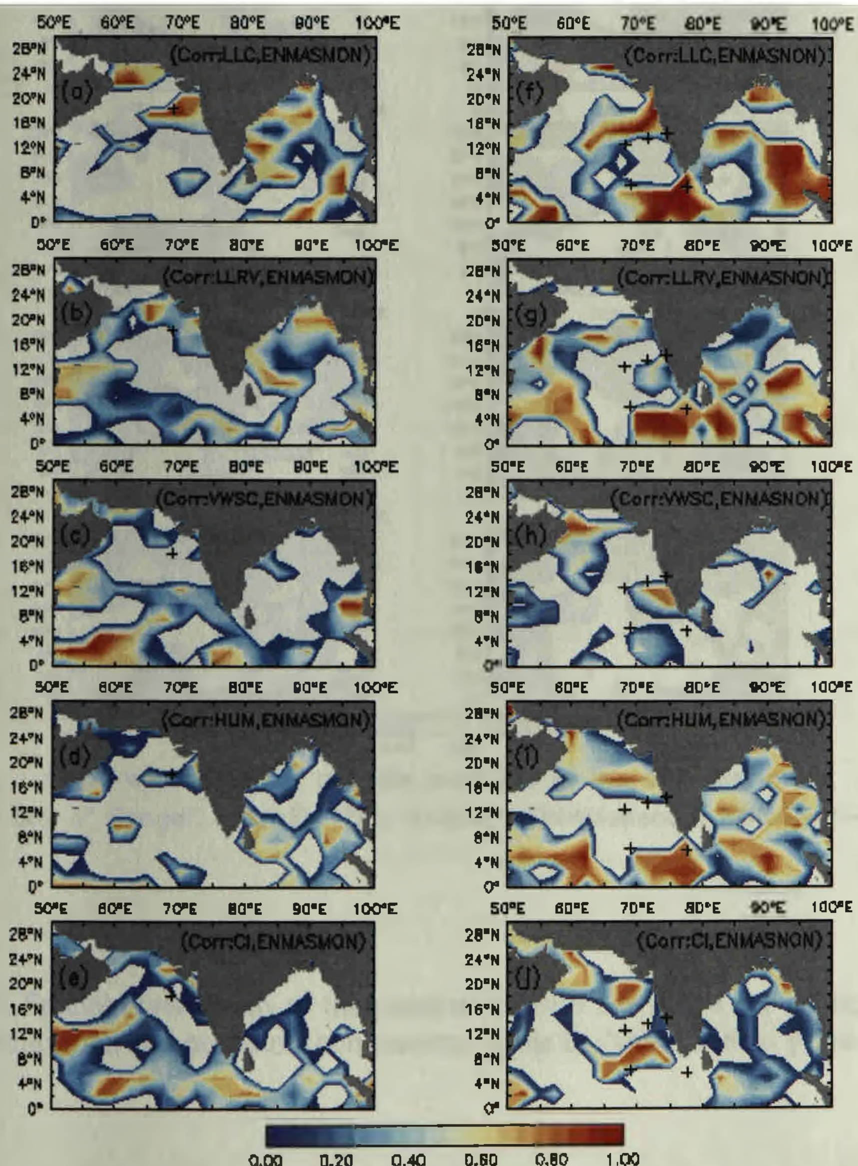

("+" represents the genesis locations of the depressions)

(AS= Arabian Sea, ENM=El-Nino Modoki, MON=Monsoon, NON=Non-monsoon)

Figure 4.10 Spatial correlations of the parameters with CSGP for the depressions over AS during the monsoon and non-monsoon seasons of the El-Niño Modoki years

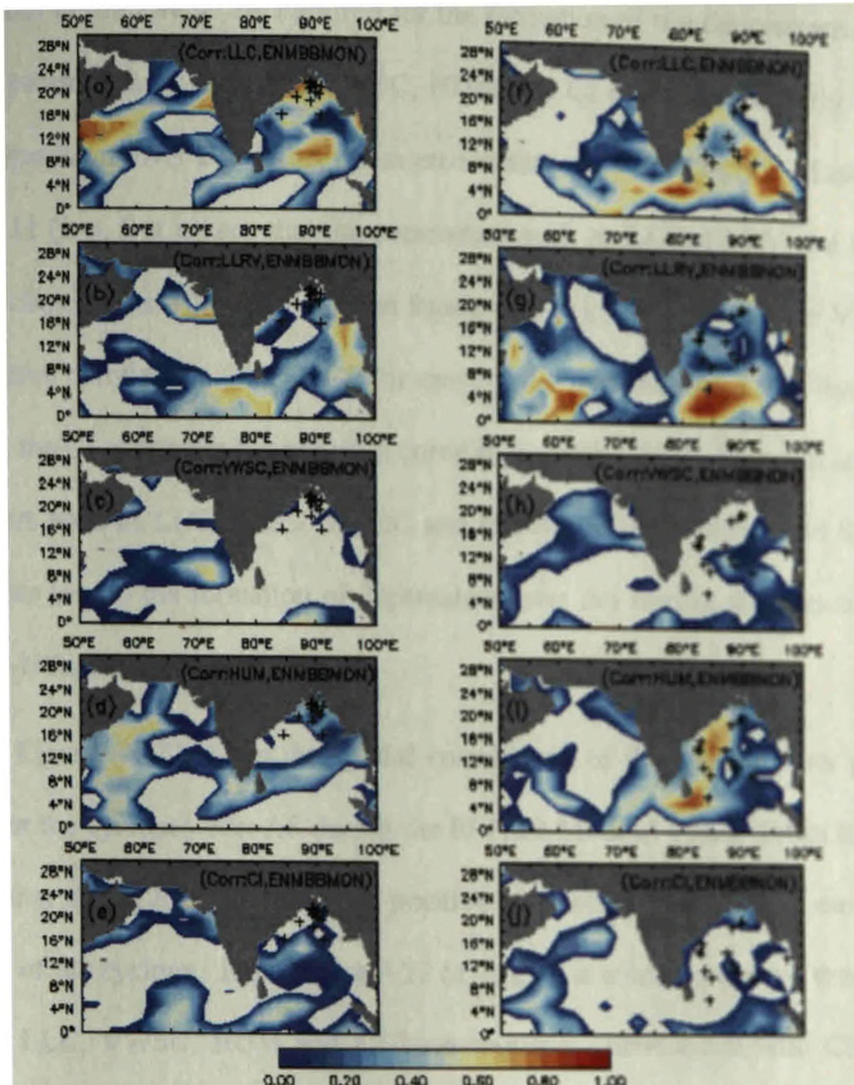

("+" represents the genesis locations of the depressions)
(BB= Bay of Bengal, ENM=El–Nino Modoki, MON=Monsoon, NON=Non–monsoon)

Figure 4.11 Spatial correlations of the parameters with CSGP for the depressions over BB during the monsoon and non-monsoon seasons of the El-Niño Modoki years

Figure (4.11) shows the spatial correlations of the individual parameters with CSGP for the depressions over BB during the El-Niño Modoki years. From figure 4.11 (a, b, d, e) it is observed that the parameters such as LLC, LLRV, HUM and CI have positive correlations with CSGP. From figure 4.11 (c), it is observed that the VWSC parameter does not show positive values around the genesis locations of the depressions. Since lower magnitudes of the VWSC are required for the formation of the depressions, it is understood that the parameters LLC, LLRV, VWSC, HUM and CI contribute equally to the formation of the depressions over BB during the monsoon season of the El-Niño Modoki years. From figure 4.11 (f, g, i) it is seen that the parameters such as LLC, LLRV and HUM have high positive correlations with CSGP. From figure 4.11 (h), it is seen that the VWSC parameter has negative correlations with CSGP for most of the depressions. From figure 4.11 (j), it is seen that the CI parameter has negative correlations with CSGP. Hence it is understood that parameters such as LLC, LLRV, VWSC and HUM contribute more and the CI parameter contributes less to the formation of depressions over AS during the non-monsoon seasons of the El-Niño Modoki years.

Figure (4.12) shows the spatial correlations of the cyclogenesis parameters with CSGP for the cyclones over AS during the El-Niño Modoki years. From figure 4.12 (b), it is seen that the LLRV parameter has positive correlations with CSGP around the genesis location of the cyclone. From figure 4.12 (a, c, d, e) it is also observed that the parameters such as LLC, VWSC, HUM and CI have negative correlations with CSGP around the genesis location of the cyclone. Since the lower magnitudes of the VWSC parameter help the formation of the cyclone. It is understood that the parameters such as LLRV and VWSC contribute more and the other parameters contribute less to the formation and intensification of the cyclone over AS during the monsoon season of the El-Niño Modoki years.

From figure 4.12 (f, g, j) it is observed that the parameters such as LLC, LLRV and CI have high positive correlations with CSGP. From figure 4.12 (h) it is seen that the VWSC parameter has negative correlations around the genesis locations of the cyclones. From figure 4.12 (i) it is seen that HUM has positive correlations with CSGP for one cyclone; there are no positive values around the genesis locations of the other cyclone.

Hence it is known that the parameters such as LLC, LLRV, VWSC and CI have an important role in the formation and intensification of the cyclones over AS during the non-monsoon seasons of the El-Niño Modoki years.

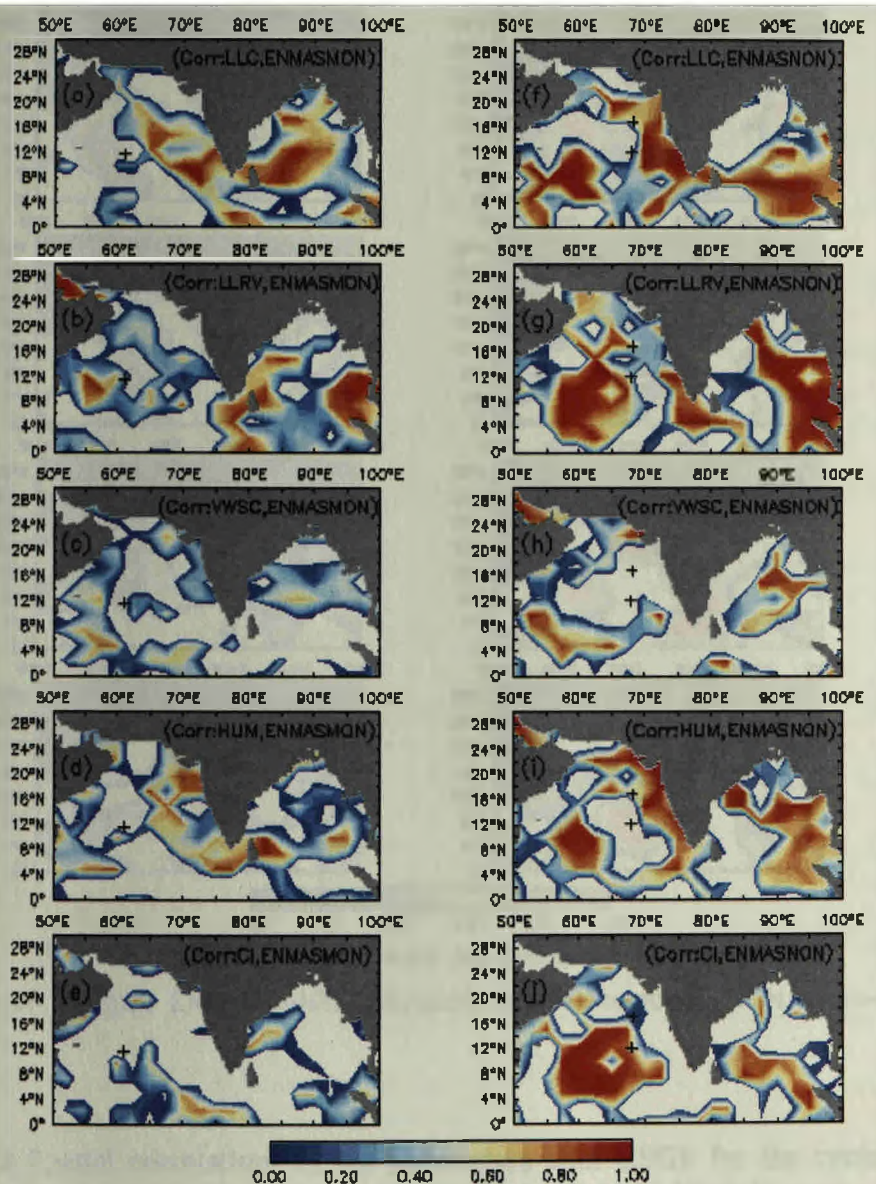

("+" represents the genesis locations of the cyclones)

(AS= Arabian Sea, ENM=El-Nino Modoki, MON=Monsoon, NON=Non-monsoon)

Figure 4.12 Spatial correlations of the parameters with CSGP for the cyclones over AS during the monsoon and non-monsoon seasons of the El-Niño Modoki years

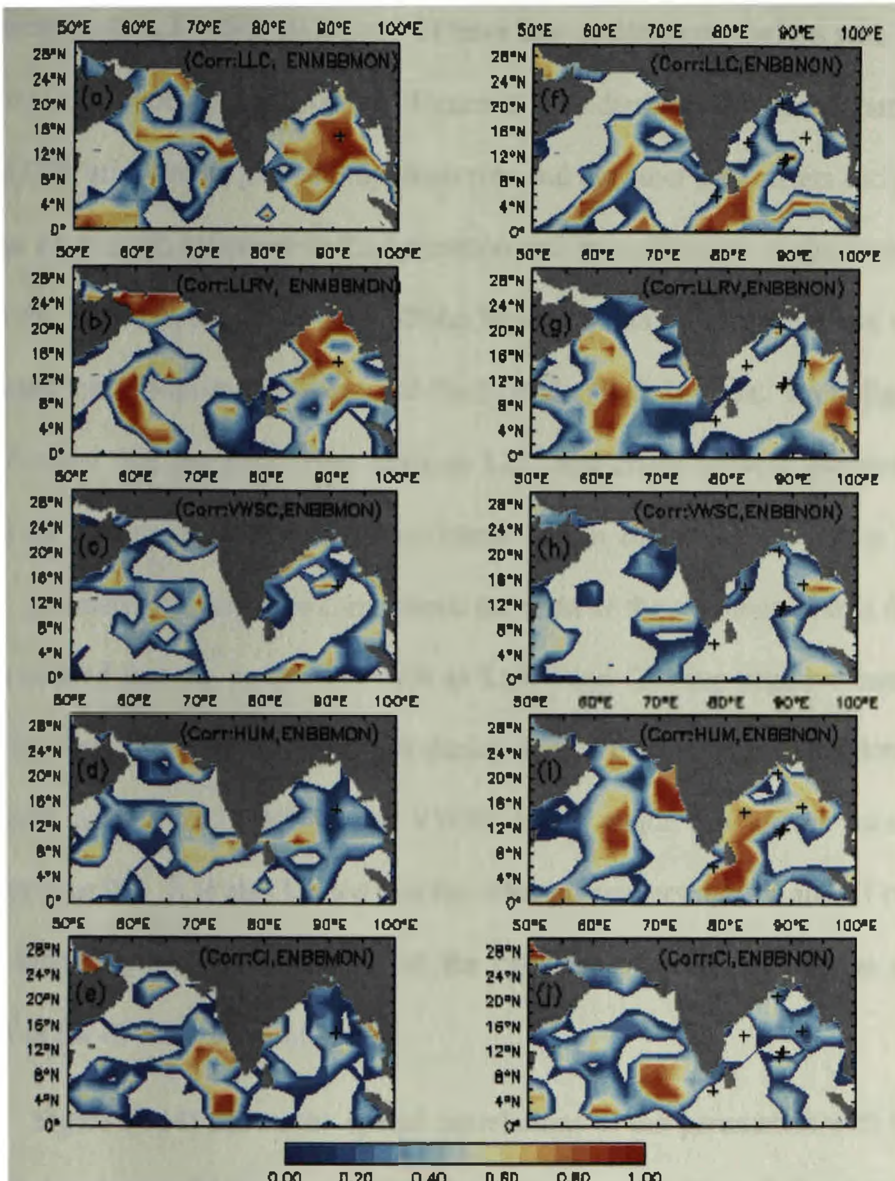

("+" represents the genesis locations of the cyclones)

(BB= Bay of Bengal, ENM=El-Nino Modoki, MON=Monsoon, NON=Non-monsoon)

Figure 4.13 Spatial correlations of the parameters with CSGP for the cyclones over BB during the monsoon and non-monsoon seasons of the El-Niño Modoki years

Figure (4.13) shows the spatial correlations of the parameters with CSGP for the cyclones over BB during the El-Niño Modoki years. From figure 4.13 (a, b), it is observed that the parameters such as LLC and LLRV have high positive correlations with CSGP around the genesis location of the cyclone. From figure 4.13 (c, d, e) it is seen that the parameters such as VWSC, HUM and CI have low positive correlations with CSGP around the genesis location of the cyclone. Hence it is understood that the parameters such as LLC, LLRV and VWSC play an important role and the other parameters such as HUM and CI also have much influence in the formation and intensification of the cyclones over BB during the monsoon season of the El-Niño Modoki years. There were six cyclones over BB during the non-monsoon seasons of the El-Niño Modoki years. From figure 4.13 (f, i) it is observed that the parameters such as LLC and HUM showed positive correlations around the genesis locations of the cyclones. From figure 4.13 (h), it is seen that the VWSC parameter has negative correlations for most of the cyclones. From figure 4.13 (g, j), it is noticed that the parameters such as LLRV and CI have negative correlations with CSGP for most of the cyclones formed during this period. Hence it is understood that the parameters namely LLC, HUM and VWSC has a major role in the formation of the cyclones over BB. It is also known that the other parameters LLRV and CI contribute less to the formation and intensification of the cyclones over BB during the non-monsoon seasons of the El-Niño Modoki years.

Figure (4.14) shows the spatial correlations of the parameters with CSGP for the severe cyclones over AS during the El-Niño Modoki years. From figure 4.14 (a, d, e) it is noticed that the parameters LLC, HUM and CI has positive correlations with CSGP around the genesis location of the severe cyclone. From figure 4.14 (b, c), it is seen that the parameters LLRV and VWSC have negative correlations with CSGP around the genesis location of the severe cyclone. Low magnitudes of the VWSC are required for the formation of the severe cyclones. Hence it is understood that the parameters such as LLC, VWSC, HUM and CI contribute more to the formation and intensification of the severe cyclones over AS during the monsoon season of the El-Niño Modoki years.

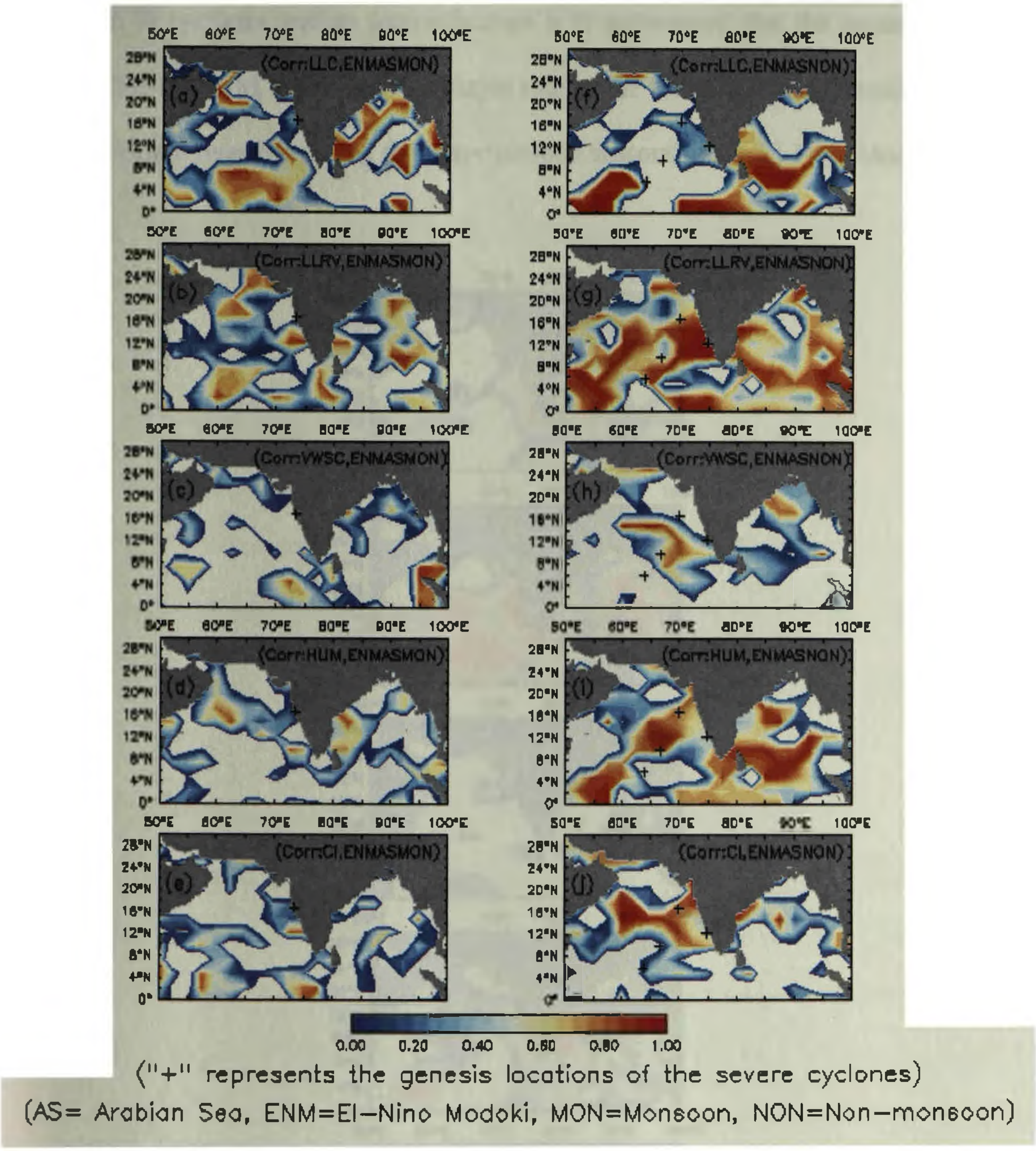

Figure 4.14 Spatial correlations of the parameters with CSGP for the severe cyclones over AS during the monsoon and non-monsoon seasons of the El-Niño Modoki years

From figure 4.14 (g, i, j), it is observed that the parameters LLRV, HUM and CI have high positive correlations with CSGP. High correlation values are observed around the genesis locations of most of the severe cyclones over BB during the non-monsoon seasons of the El-Niño Modoki years. It is also noticed that the parameters namely LLC and VWSC show low positive correlations with CSGP. Since it requires low magnitude of VWSC for the formation of cyclones and its intensification it is understood that the parameters such as LLRV, VWSC, HUM and CI have a major role in the formation and intensification of the severe cyclones over BB during the non-monsoon seasons of the El-Niño Modoki years.

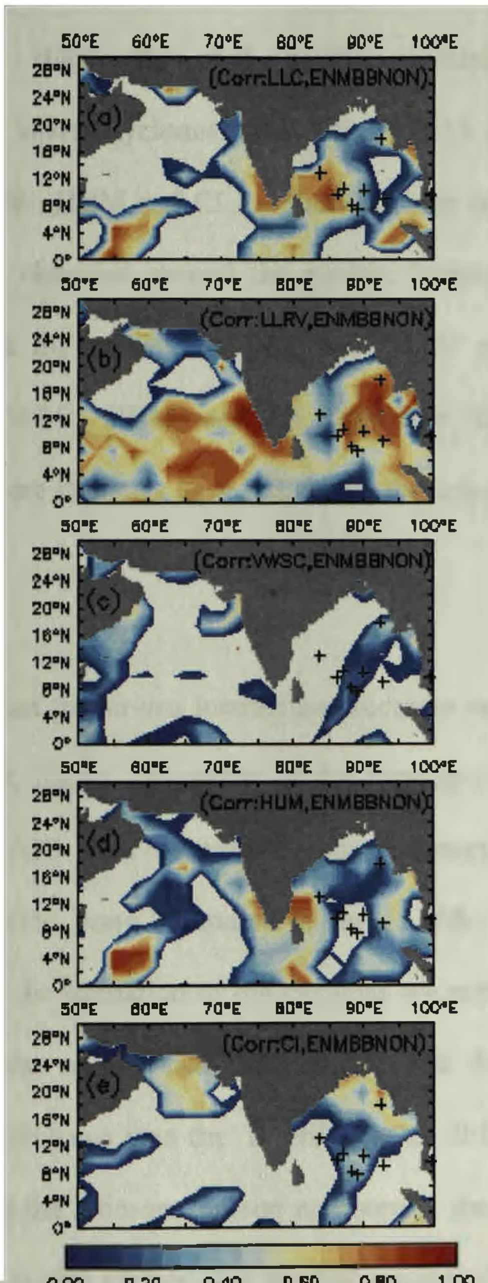

("+" represents the genesis locations of the severe cyclones)
(BB= Bay of Bengal, ENM=El-Nino Modoki, NON=Non-Monsoon)

Figure 4.15 Spatial correlations of the parameters with CSGP for the severe cyclones over BB during the non-monsoon season of the El-Niño Modoki years

Figure (4.15) shows the spatial correlations of the parameters with CSGP for the severe cyclones over BB during the non-monsoon seasons of the El-Niño Modoki years. From figure 4.15 (a, b) it is observed that the parameters LLC and LLRV have high positive correlations with CSGP. High values of the positive correlations are noticed around the genesis locations of the severe cyclones. From figure 4.15 (c, d, e), it is seen that the parameters such as VWSC, HUM and CI have low positive correlations with CSGP. The low positive values are observed around the genesis locations of the severe cyclones. Hence it is known that the parameters LLC and LLRV contribute much, and other parameters such as VWSC, HUM and CI contribute less to the formation and intensification of the severe cyclones over BB during the non-monsoon seasons of the El-Niño Modoki years.

4. 10 Conclusion

It is observed that the air-sea interaction processes such as El-Niño and El-Niño Modoki events have got higher influences in the formation and intensification of the convective systems over NIO. It is observed that the frequency of the depressions over AS is more during the El-Niño years compared to the El-Niño Modoki years in both the seasons. It is found that the formation of the cyclones are suppressed over AS during the El-Niño years and it is also noticed that the frequencies of the severe cyclones are more during the El-Niño Modoki years than the El-Niño years. It is found that the frequencies of the depressions during the monsoon season are more in the El-Niño years than the El-Niño Modoki years. It is also noticed that the frequencies of the depressions during the non-monsoon seasons are more in the El-Niño Modoki years compared to the El-Niño years. The frequencies of the cyclones during the monsoon season are more in the El-Niño years than the El-Niño Modoki years. While the frequencies of the cyclones during the non-monsoon seasons are more in the El-Niño Modoki years than the El-Niño years. It is also observed that the frequencies of the severe cyclones during both the seasons are more in the El-Niño years than the El-Niño Modoki years.

It is understood that during the El-Niño years the Walker circulation gets modified as the ascending limb shifts from the western pacific Ocean to the eastern Pacific Ocean and during the El-Niño Modoki years the Walker circulation gets split into two convective loops where one ascending limb over the central pacific Ocean and two descending limbs over both western and eastern Pacific Oceans. The shifting and splitting of the Walker circulation has greater impacts in the formation and intensification of the convective systems over NIO. During the El-Niño years the large scale convective zones will be over the tropical eastern Pacific Ocean. While during the El-Niño Modoki years the splitting of the Walker circulation shifts the atmospheric convections to the central Pacific Ocean. This affects the convective activities over the NIO and in turn influences the formation and intensification of the convective systems over NIO. It is also observed that there is southward shift of the LLC parameter along with the genesis locations during the El-Niño Modoki years compared to the El-Niño years.

Further it is noticed that there is a northward shift in the genesis locations of the depressions over NIO during the monsoon season of the El-Niño and El-Niño Modoki years. But a southward shift is found during the non-monsoon seasons of the El-Niño years and the genesis loactions of the depressions are much more scattered during the non-monsoon seasons of the El-Niño Modoki years. It is also noticed that all the depressions formed in the monsoon season of the El-Niño Modoki years have taken a north-westerly track. But the depressions formed in the non-monsoon seasons of the El-Niño Modoki years have moved to many directions. In the case of cyclones and severe cyclones it is observed that there is a tendency for the cyclones and severe cyclones to live longer even after the landfall during both seasons of the El-Niño years. But it is noticed that there is tendency for the cyclones and severe cyclones to dissipate over the ocean or immediately after the landfall during both the seasons of the El-Niño Modoki years.

It is observed that the depressions and cyclones over NIO have formed against lower magnitudes of CSGP during the El-Niño and El-Niño Modoki years. It is also noticed that the severe cyclones are formed against higher values of CSGP during the El-Niño years and they formed against lower magnitudes of the El-Niño Modoki years. It is seen that different combinations of the air-sea interaction parameters are influenceing the formation of the convective systems over NIO. During the El-Niño years it is found that the LLC, LLRV and CI are influencing the formation of depressions over AS and LLC, LLRV and HUM are influencing the formation of depressions over BB. It is also found that the LLC and CI are influencing the formation of severe cyclones over AS and LLC, LLRV and HUM are influencing the formation of cyclones and severe cyclones over NIO. During the El-Niño Modoki years it is noticed that, LLC, LLRV and HUM are having major role in the formation of depressions over AS in the monsoon season and depressions over BB during the non-monsoon seasons. It is also noticed that LLC, LLRV, HUM and CI are having important role in the formation of cyclones and severe cyclones over NIO.

Chapter 5

Convective systems over northern Indian Ocean during the La-Niña and La-Niña Modoki years

5.1 Introduction

The counter part of El-Niño is termed as the La-Niña event. This phenomenon occurs when the magnitude of the trade winds increases over the tropical Pacific Ocean. During this period the strong north-east and south-east trade winds will push off a large quantity of the surface water from the east to the western Pacific Ocean. These washed out water will accumulate over the western Pacific Ocean hence there is an anomalous warming over the western Pacific Ocean and it results in the large scale convection in the western Pacific Ocean. The surface area of the piled up water in the western Pacific Ocean will be larger than the normal years. Hence it will follow an undercurrent and up-well over the eastern Pacific Ocean to maintain the equilibrium in the water surface. As a result the cold water will spread in to a larger area over the eastern Pacific Ocean. Hence the atmosphere over the eastern Pacific Ocean will become cold and dry as the cold water spreads out. The cold dry air in the eastern Pacific Ocean makes a large scale air subsidence over this region.

The strong convection over western Pacific Ocean and enhanced divergence over eastern Pacific Ocean will establish an active convective loop (Walker circulation) over the tropical Pacific Ocean with an ascending limb in the western Pacific Ocean and a descending limb in the eastern Pacific Ocean. The active ascending limb of the Walker circulation is associated with enhanced atmospheric convective activities and flood like situations in the western Pacific Ocean and descending limb is associated with large scale air subsidence and drought like situations in the eastern Pacific Ocean during the La-Niña years.

5.2 Definitions of La-Niña and La-Niña Modoki

La-Niña and La-Niña Modoki events are those air-sea interaction processes of anomalous warming and cooling of SST in different parts of the tropical Pacific Ocean. The La-Niña event is defined by warmer than normal SST in the western tropical Pacific Ocean and cooler than normal SST in the eastern tropical Pacific Ocean. The impact of the La-Niña events on the global climate is different from the El-Niño. The La-Niña event is calculated as the SST anomalies over Niño 3.4 region (5° N - 5° S, 170° - 120° W) exceeding the threshold -0.4° C for six months. There have been many studies on the influence of La-Niña events in the formation and intensification of the convective systems over various basins. The results suggest that the La-Niña events enhance the formation of cyclones over various basins.

The La-Niña Modoki (Ashok et. al 2007) event is defined by the cooling over the central Pacific Ocean and flanked by warmer SST anomalies in both west and east along the equator. The influence of La-Niña Modoki events in the formation and intensification of the convective systems are less studied. During La-Niña Modoki events, the two cell walker circulation results in two convective zones and associated high rainfall anomalies over the east and west tropical Pacific Ocean. The La-Niña Modoki and its climate impacts are different from those of La-Niña. The La-Niña Modoki event has got significant impacts on the temperature and precipitation over many parts of the globe.

Shinoda et.al (2011) have found two recent La-Niña Modoki years (2000 and 2008) by using an Index EMI2; it is defined as EMI2 = [SST]A - 0.5[SST]C, where [SST]A and [SST]C are the average SST anomalies over regions A (165°E-140°W, 10°S-

10°N) and C (125°E-145°E, 10°S-20°N) respectively. He also used an Empirical Orthogonal Function (EOF) analysis of surface currents for the period 1993-2009 to find them. Cai and Cowan (2009) showed that La-Niña Modoki events can shift the convection zones towards west of the tropical Pacific Ocean, and it results in heavy rainfall over north-western Australia, rather than over the east as in a conventional La-Niña. Sumesh and Ramesh Kumar (2015) have studied the influence of the La-Niña Modoki events in the formation and intensification of the convective systems over NIO. This study showed that the splitting of the Walker circulation has got greater impacts on the frequencies and intensification of the convective systems over NIO. This study reveals that the ascending limb over the western Pacific Ocean influences the convective activities over BB and enhances the magnitude of Low Level Convergence and it is favorable for the formation and intensification of the convective systems over BB. This study also reveals that there are no cyclones over Arabian Sea during La-Niña Modoki years.

5.3 Convective systems over NIO during the La-Niña years

Figure 5.1 gives the genesis locations and the tracks of the convective systems formed over NIO during the monsoon and non-monsoon seasons of the La-Niña years. Figure 5.1 (a,b) shows the genesis points and tracks of depressions formed over NIO during the monsoon and non-monsoon seasons respectively. From this figure it is seen that the depressions are formed towards the north of AS and BB. During the monsoon season it is more localised near the head bay in BB. But during the non-monsoon seasons the depressions are formed towards the south of AS and BB, and the genesis points are wide-spread compared to the monsoon season. There have been 5 depressions over AS during the monsoon season and there have been 3 depressions over AS during the non-monsoon seasons of the La-Niña years. There have been 15 depressions over BB during the monsoon season and 9 depressions during the non-monsoon seasons of the La-Niña years.

It is observed that almost all the depressions formed in BB during the monsoon season have taken a north-westerly track and entered the land, but except for 1, all the depressions

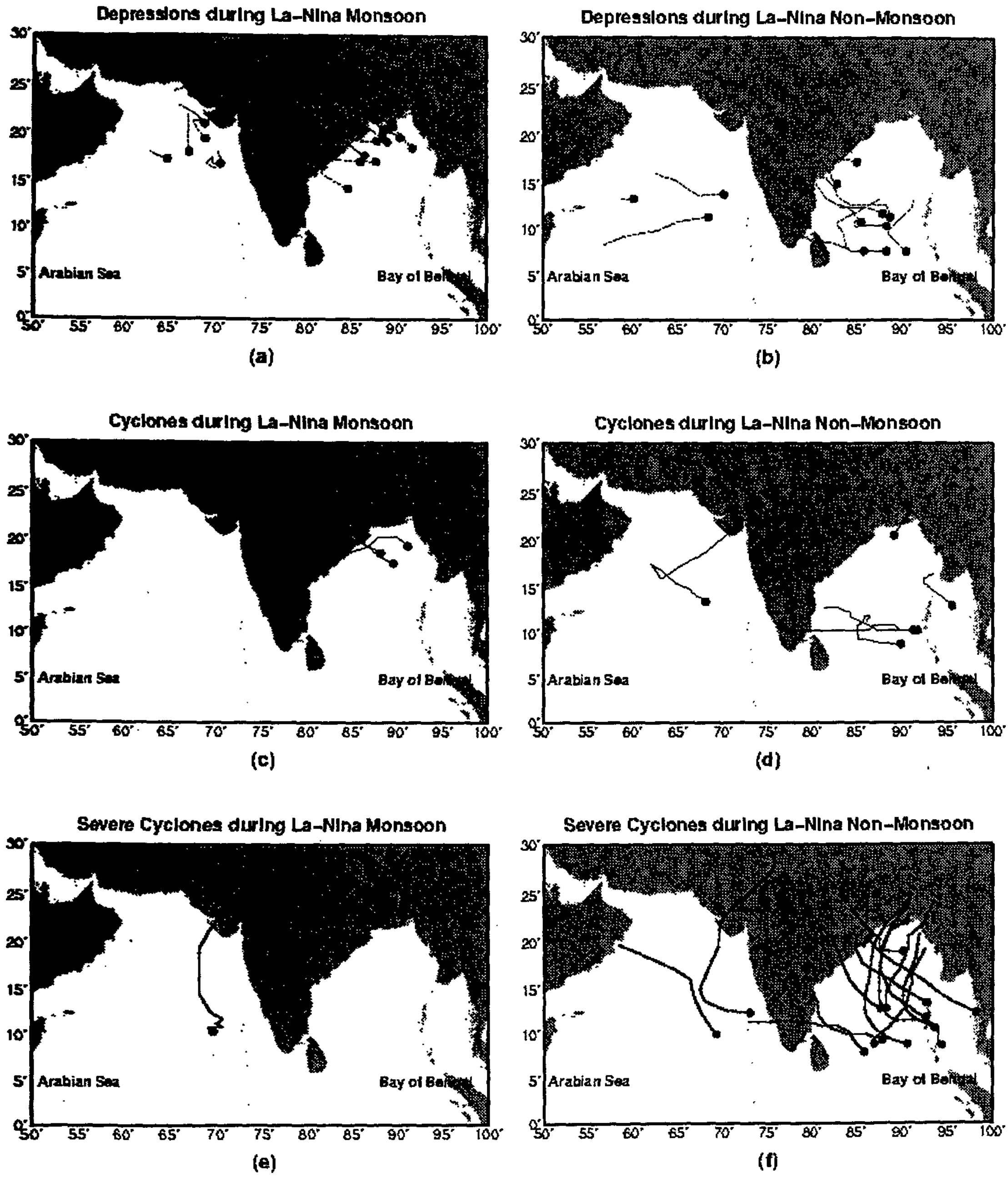

Figure 5.1 Convective systems over NIO during the monsoon and non-monsoon seasons of the La-Niña years

formed in AS have moved towards northwest direction and dissipated in the ocean. During the non-monsoon seasons all the 3 depressions which formed in AS have moved westward and dissipated in the sea. And out of the 9 depressions that have formed over BB only 3 depressions have entered into the land and all the other depressions have dissipated in the ocean.

Figure 5.1 (c,d) shows the genesis points and tracks of the cyclones formed over NIO during the monsoon and non-monsoon seasons respectively. There were no cyclones over AS during the monsoon season but 1 cyclone was formed over AS during the non-monsoon seasons. There have been 3 cyclones over BB during the monsoon season and 5 cyclones during the non-monsoon seasons. All the cyclones formed over BB during the monsoon seasons have taken a long north-westerly track. And the cyclone formed over AS during the non-monsoon season has taken a northwesterly track and suddenly changed its direction and taken a north-easterly track and entered the land. And in BB out of the 5 cyclones, 3 cyclones have moved north-westward and dissipated in the BB itself. In the other two cyclones one cyclone has taken a northerly track and moved towards the land. And the other cyclone has taken a westerly track and moved towards the land.

Figure 5.1 (e,f) shows the genesis points and tracks of the severe cyclones formed over NIO during the monsoon and non-monsoon seasons respectively. There was 1 severe cyclone formed over AS during the monsoon season. And there were 2 severe cyclones over AS during the non-monsoon seasons. There were no severe cyclones over BB during the monsoon season and 12 severe cyclones during the non-monsoon seasons. The severe cyclone formed over AS during the monsoon season has taken a northerly track and turned in a north-easterly direction and entered into the land. During the non-monsoon seasons there were 2 severe cyclones over AS, out of which 1 severe cyclone has taken a north-westerly track and moved to the Oman coast. The next severe cyclone moved towards west and then turned in a northeasterly direction and entered the land. There were no severe cyclones over BB during the monsoon season. During the non-monsoon seasons there were 12 severe cyclones over BB. Out of the 12 severe cyclones over BB almost all the severe cyclones have taken the north-easterly track and entered the land.

Table 5.1 gives the list of all the depressions formed over AS during the monsoon and non-monsoon seasons of the La-Niña years. There have been 5 depressions over AS during the monsoon season and 3 depressions over AS during the non-monsoon seasons. In 1984, 1 depression was formed over AS during the monsoon season and it formed on 06-Jun-1984 and dissipated on 07-Jun-1984. During the non-monsoon season there was 1 depression and it was formed on 04-Dec-1984 and dissipated on 05-Dec-1984. In 1988, 1 depression was formed over AS during the monsoon season and it formed on 09-Jun-1988 and dissipated on 12-Jun-1988. During the non-monsoon season there were no depressions over AS. In 1998, 1 depression was formed over AS during the monsoon season and it formed on 29-Sep-1998 and dissipated on 30-Sep-1998. During the non-monsoon season there were 2 depressions.

Table 5.1 List of Depressions formed over AS during the monsoon and non-monsoon seasons in the La-Niña years

Arabian Sea			
Monsoon		**Non-monsoon**	
Date of formation	**Date of dissipation**	**Date of formation**	**Date of dissipation**
06-Jun-1984	07-Jun-1984	04-Dec-1984	05-Dec-1984
09-Jun-1988	12-Jun-1988	28-May-1998	29-May-1998
29-Sep-1998	30-Sep-1998	06-Oct-1998	09-Oct-1998
21-Jun-2005	22-Jun-2005		
14-Sep-2005	16-Sep-2005		

The first depression was formed on 28-May-1998 and dissipated on 29-May-1998 and the second depression was formed on 06-Oct-1998 and dissipated on 09-Oct-1998. In 2005, 2 depressions were formed over AS during the monsoon season and first depression formed on 29-Sep-1998 and dissipated on 30-Sep-1998. During the non-monsoon season there were 2 depressions. The first depression was formed on 21-Jun-2005 and dissipated on 22-Jun-2005 and the second depression was formed on 14-Sep-2005 and dissipated on 16-Sep-2005. And there were no cyclones over AS during the non-monsoon seasons.

Table 5.2 List of Depressions formed over BB during the monsoon and non-monsoon seasons in the La-Niña years

Bay of Bengal			
Monsoon		**Non-monsoon**	
Date of formation	**Date of dissipation**	**Date of formation**	**Date of dissipation**
20-Jun-1981	24-Jun-1981	31-Oct-1981	02-Nov-1981
03-Aug-1981	04-Aug-1981	01-Oct-1988	03-Oct-1988
12-Aug-1981	16-Aug-1981	07-Dec-1988	08-Dec-1988
17-Sep-1981	18-Sep-1981	13-Oct-1998	15-Oct-1998
30-Jul-1984	06-Aug-1984	26-Oct-1998	30-Oct-1998
15-Aug-1984	19-Aug -1984	08-Dec-1999	10-Dec-1999
09-Jun-1988	10-Jun-1988	26-Oct-2005	29-Oct-2005
17-Jul-1988	18-Jul-1988	20-Nov-2005	22-Nov-2005
02-Aug-1988	06-Aug-1988	15-Dec-2005	21-Dec-2005
13-Jun-1998	15-Jun-1998		
17-Jun-1999	18-Jun-1999		
27-Jul-1999	29-Jul-1999		
06-Aug-1999	08-Aug-1999		
29-Jul-2005	31-Jul-2005		
12-Sep-2005	16-Sep-2005		

Table 5.2 gives the list of all the depressions over BB during the monsoon and non-monsoon seasons of the La-Niña years. There have been 15 depressions over BB during the monsoon season and 9 depressions over BB during the non-monsoon seasons. In the year 1981, there have been 4 depressions during the monsoon season and 1 depression

during the non-monsoon seasons. In the year 1984, there were 2 depressions during the monsoon season and no depression during the non-monsoon seasons. In the year 1988, there were 3 depressions during the monsoon season and 2 depressions during the non-monsoon seasons. In the year 1998, there was 1 depression during the monsoon season and 2 depressions during the non-monsoon seasons. In the year 1999, there were 3 depressions during the monsoon season and 1 depression during the non-monsoon season. In the year 2005, there were 2 depressions during the monsoon season and 3 depressions during the non-monsoon seasons.

Table 5.3 gives the list of all the cyclones over AS during the monsoon and non-monsoon seasons of the La-Niña years. There was only 1 cyclone over AS during the non-monsoon seasons. This cyclone was formed on 11-Oct-1998, intensified into cyclone on 16-Oct-1998 and dissipated on 17-Oct-1998. Table 4.4 gives the list of all the cyclones over BB during the monsoon and non-monsoon seasons of the La-Niña years.

Table 5.3 List of Cyclones formed over AS during the monsoon and non-monsoon seasons in the La-Niña years

Arabian Sea					
Monsoon			**Non-monsoon**		
Date of formation	**Date of Intensification to Cyclone**	**Date of dissipation**	**Date of formation**	**Date of Intensification to Cyclone**	**Date of dissipation**
			11-Oct-1998	16-Oct-1998	17-Oct-1998

There were 3 cyclones during the monsoon season and 5 cyclones during the non-monsoon seasons of the La-Niña years. In the year 1981, 2 cyclones formed over BB in the monsoon season and 1 cyclone in the non-monsoon season. The first cyclone in the monsoon season was formed on 07-Aug-1981, intensified on the same day and dissipated on 10-Aug-1981. The second cyclone in the monsoon season was formed on 25-Sep-1981, intensified on 25-

Sep-1981 and dissipated on 28-Sep-1981. In the year 2005, there were 3 cyclones, out of which 1 cyclone was formed in the monsoon season and 2 cyclones in the non-monsoon seasons. The third cyclone in the monsoon season was formed on 17-Sep-2005, intensified on 18-Sep-2005 and dissipated on 21-Sep-2005. And in the non-monsoon seasons there have been 5 cyclones over BB. The first cyclone in the non-monsoon season was formed in the year 1981. It was formed on 08-Nov-1981, intensified into cyclone on 09-Nov-1981 and dissipated on 10-Nov-1981. The second cyclone was formed in the year 1988. It was formed on 18-Oct-1988, intensified into cyclone on 19-Oct-1988 and dissipated on 20-Oct-1988. The third cyclone was formed in the year 1999; it was formed on 01-Feb-1999, intensified into cyclone on 02-Feb-1999 and dissipated on 03-Feb-1999. The last two cyclones were formed in the year 2005. The first cyclone was formed on 28-Nov-2005, intensified into cyclone on 28-Nov-2005 and dissipated on 02-Dec-2005. The last cyclone was formed on 06-Dec-2005, intensified into cyclone on 07-Dec-2005 and dissipated on 10-Dec-2005.

Table 5.4 List of Cyclones formed over BB during the monsoon and non-monsoon seasons in the La-Niña years

Bay of Bengal					
Monsoon			**Non-monsoon**		
Date of formation	**Date of Intensification to Cyclone**	**Date of dissipation**	**Date of formation**	**Date of Intensification to Cyclone**	**Date of dissipation**
07-Aug-1981	07-Aug-1981	10-Aug-1981	08-Nov-1981	09-Nov-1981	10-Nov-1981
25-Sep-1981	25-Sep-1981	28-Sep-1981	18-Oct-1988	19-Oct-1988	20-Oct-1988
17-Sep-2005	18-Sep-2005	21-Sep-2005	01-Feb-1999	02-Feb-1999	03-Feb-1999
			28-Nov-2005	28-Nov-2005	02-Dec-2005
			06-Dec-2005	07-Dec-2005	10-Dec-2005

Table 5.5 List of Severe cyclones formed over AS during the monsoon and non-monsoon seasons in the La-Niña years

Arabian Sea					
Monsoon			Non-monsoon		
Date of formation	Date of Intensification to Severe Cyclone	Date of dissipation	Date of formation	Date of Intensification to Severe Cyclone	Date of dissipation
04-Jun-1998	06-Jun-1998	10-Jun-1998	29-Oct-1981	30-Oct-1981	03-Nov-1981
			13-Dec-1998	14-Dec-1998	17-Dec-1998

Table 5.6 List of Severe cyclones formed over BB during the monsoon and non-monsoon seasons in the La-Niña years

Bay of Bengal					
Monsoon			Non-monsoon		
Date of formation	Date of Intensification to Severe Cyclone	Date of dissipation	Date of formation	Date of Intensification to Severe Cyclone	Date of dissipation
			16-Nov-1981	18-Nov-1981	20-Nov-1981
			05-Dec-1981	07-Dec-1981	11-Dec-1981
			13-Oct-1984	13-Oct-1984	15-Oct-1984
			10-Nov-1984	11-Nov-1984	14-Nov-1984
			28-Nov-1984	29-Nov-1984	02-Dec-1984
			15-Nov-1988	17-Nov-1988	18-Nov-1988
			24-Nov-1988	25-Nov-1988	29-Nov-1988
			17-May-1998	19-May-1998	20-May-1998
			13-Nov-1998	14-Nov-1998	16-Nov-1998
			19-Nov-1998	21-Nov-1998	22-Nov-1998
			15-Oct-1999	16-Oct-1999	19-Oct-1999
			25-Oct-1999	27-Oct-1999	31-Oct-1999

Table 5.5 gives the list of all the severe cyclones over AS during the monsoon and non-monsoon seasons of the La-Niña years. There was 1 severe cyclone during the

monsoon season and 2 severe cyclones during the non-monsoon seasons. The severe cyclone in the monsoon season was formed on 04-Jun-1998, intensified into severe cyclone on 06-Jun-1998 and dissipated on 10-Jun-1998. The first severe cyclone in the non-monsoon seasons was formed on 29-Oct-1981, intensified into severe cyclone on 30-Oct-1981 and dissipated on 10-Jun-1998. The second severe cyclone was formed on 13-Dec-1998, intensified into severe cyclone on 14-Dec-1998 and dissipated on 17-Dec-1998.

Table 5.6 gives the list of all the severe cyclones over BB during the monsoon and non-monsoon seasons of the La-Niña years. There were no severe cyclones over BB during the monsoon season during the La-Niña years. And there have been 12 severe cyclones over BB during the non-monsoon seasons. In the year 1981, there were 2 severe cyclones. The first severe cyclone was formed on 16-Nov-1981, intensified into severe cyclone on 18-Nov-1981 and dissipated on 20-Nov-1981. The second severe cyclone was formed on 05-Dec-1981, intensified into severe cyclone on 07-Dec-1981 and dissipated on 11-Dec-1981. In the year 1984, there were 3 severe cyclones. The first severe cyclone was formed on 13-Oct-1984, intensified into severe cyclone on the same day and dissipated on 15-Oct-1984. The second severe cyclone was formed on 10-Nov-1984, intensified into severe cyclone on 11-Nov-1984 and dissipated on 14-Nov-1984. The third severe cyclone was formed on 28-Nov-1984, intensified into severe cyclone on 29-Nov-1984 and dissipated on 02-Dec-1984. In the year 1988, there were 2 severe cyclones. The first severe cyclone was formed on 15-Nov-1988, intensified into severe cyclone on 17-Nov-1988 and dissipated on 18-Nov-1988. The second severe cyclone was formed on 24-Nov-1988, intensified into severe cyclone on 25-Nov-1988 and dissipated on 29-Nov-1988. In the year 1998, there were 3 severe cyclones. The first severe cyclone was formed on 17-May-1998, intensified into severe cyclone on 19-May-1998 and dissipated on 20-May-1998. The second severe cyclone was formed on 13-Nov-1998, intensified into severe cyclone on 14-Nov-1998 and dissipated on 16-Nov-1998. The third severe cyclone was formed on 19-Nov-1998, intensified into severe cyclone on 21-Nov-1998 and dissipated on 22-Nov-1998. In the year 1999, there were 2 severe cyclones. The first severe cyclone was formed on 15-Oct-1999, intensified into severe cyclone on 16-Oct-1999 and dissipated on 19-Oct-1999. The second severe cyclone was formed on 25-Oct-1999, intensified into severe cyclone on 27-Oct-1999 and dissipated on 31-Oct-1999.

5.4 Variations of CSGP for the convective systems over NIO during the La-Niña years

Figure (5.2) shows the variations of CSGP for the convective systems over NIO during the monsoon and non-monsoon seasons of the La-Niña years. Figure 5.2 (a, b, c, d) shows the variations of CSGP over NIO for the depressions formed in the monsoon and non-monsoon seasons. From figure 5.2 (a) it is seen that, the depressions were formed against higher magnitude (0.0 to 0.5 x $10^{-10}s^{-2}$ °K) and the higher magnitude of CSGP is found over the land. From figure 5.2 (b), it is seen that the depressions were formed against lower magnitudes of CSGP (0.0 to 0.2 x $10^{-10}s^{-2}$ °K) and the higher magnitude of CSGP is found over the southwest AS. From figure 5.2 (c) it is found that most of the depressions have formed against higher magnitudes of CSGP. From figure 5.2 (d) it is noticed that the depressions have formed agaist the lower magnitudes of CSGP and the higher magnitudes (2.0 x $10^{-10}s^{-2}$ °K) of CSGP are found in the land.

The figure 5.2 (e, f, g, h) gives the variations of the CSGP for the cyclones over NIO during the La-Niña years. From figure 5.2 (f), it is observed that the cyclone was formed against higher magnitude (0.5 x $10^{-10}s^{-2}$ °K). The higher magnitude of CSGP is also found over south-eastern BB. From figure 5.2 (g) it is seen that the cyclones were formed against lower magnitudes of CSGP (0.0 x $10^{-10}s^{-2}$ °K) and higher magnitude of CSGP is found over the land. From figure 5.2 (h) it is noticed that the cyclones were formed against higher magnitudes (0.0 to 0.6 x $10^{-10}s^{-2}$ °K) of CSGP. Figure 5.2 (i, j, k, l) gives the variations of the CSGP for the severe cyclones over NIO during the La-Niña years.

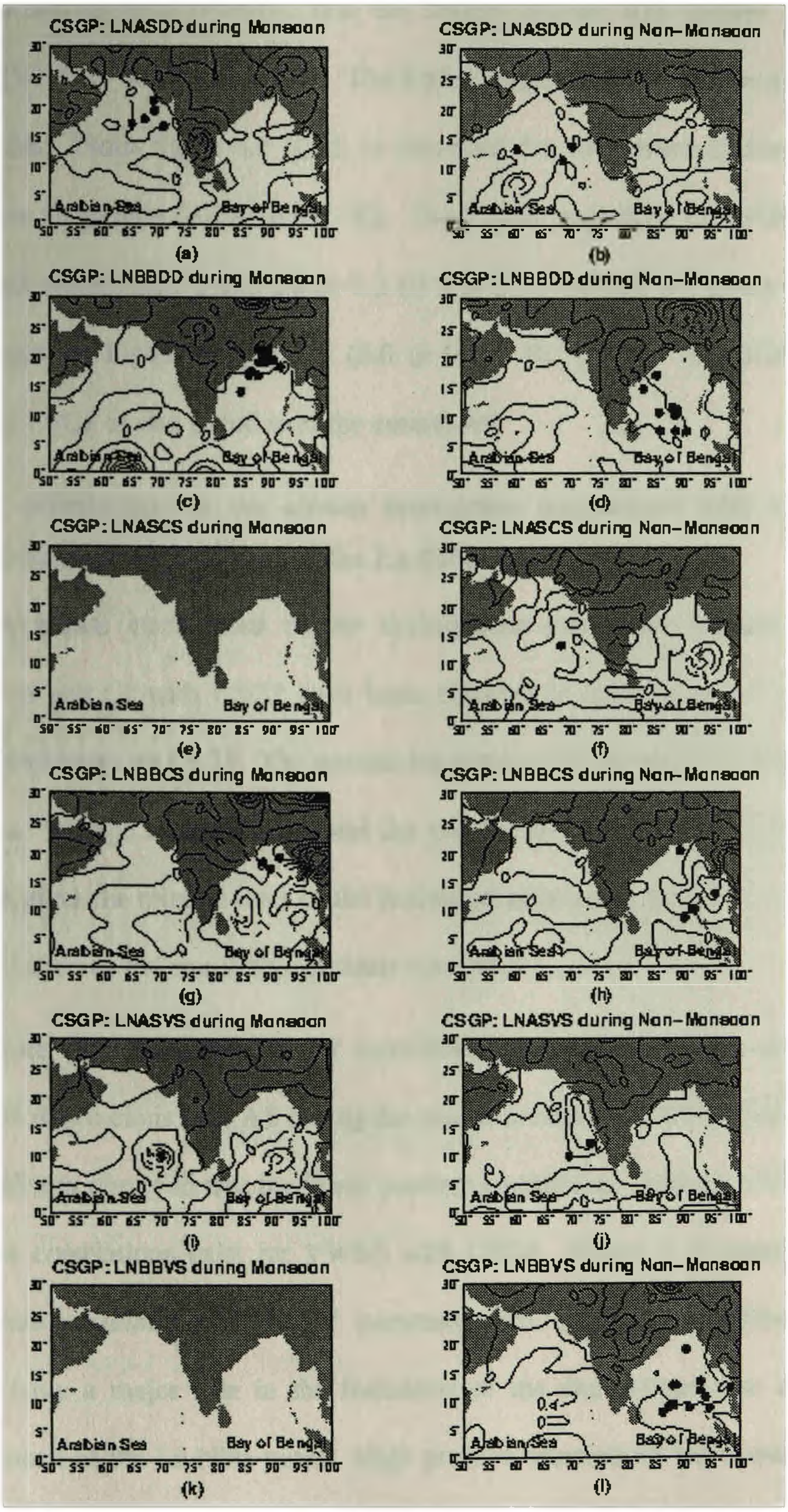

Figure 5.2 Variations of CSGP for the convective systems over NIO during the monsoon and non-monsoon seasons of the La-Niña years

From figure 5.2 (i), it is observed that the severe cyclone was formed against higher magnitude ($5.0 \times 10^{-10} s^{-2}$ °K) of CSGP. The higher magnitude of CSGP is also found over the central BB. From figure 5.2 (j), it is observed that the severe cyclone was formed against higher magnitude ($2.5 \times 10^{-10} s^{-2}$ °K). The higher magnitude of CSGP is also found over the south eastern BB. From figure 5.2 (l) it is observed that the severe cyclones have formed against the higher magnitudes (0.0 to $0.3 \times 10^{-10} s^{-2}$ °K) of CSGP. The higher magnitude of CSGP is also found over the central AS.

5.5 Spatial correlations of the air-sea interaction parameters with CSGP for the convective systems over NIO during the La-Niña years

The spatial correlations of the cyclogenesis parameters namely LLRV, LLC, VWSC, HUM and CI with CSGP have been obtained to investigate the relative role of individual parameters on CSGP. The genesis locations of the convective systems have been given with a "+" sign in the figures and the correlation values between 0.0 and 1.0 are plotted. This gives the relative roles of the individual parameters on CSGP in the formation and intensification of the convective systems over NIO.

Figure (5.3) gives the spatial correlations of the cyclogenesis parameters with CSGP for the depressions over AS during the monsoon season of the La-Niña years. From figure 5.3 (b) it is observed that the lower positive correlations exist for LLRV with CSGP and negative correlations exist for VWSC with CSGP. Hence it is understood that the lower positive correlations of LLRV parameter and negative correlations of VWSC parameter have a major role in the formation of the depressions over AS during the monsoon season of the La-Niña years. High positive correlations have been observed for the parameters namely LLC, LLRV and HUM with CSGP from figure 5.3 (f, g, i). Hence it is clear that these parameters contribute more to the formation of the depressions over AS during the non-monsoon seasons of the La-Niña years.

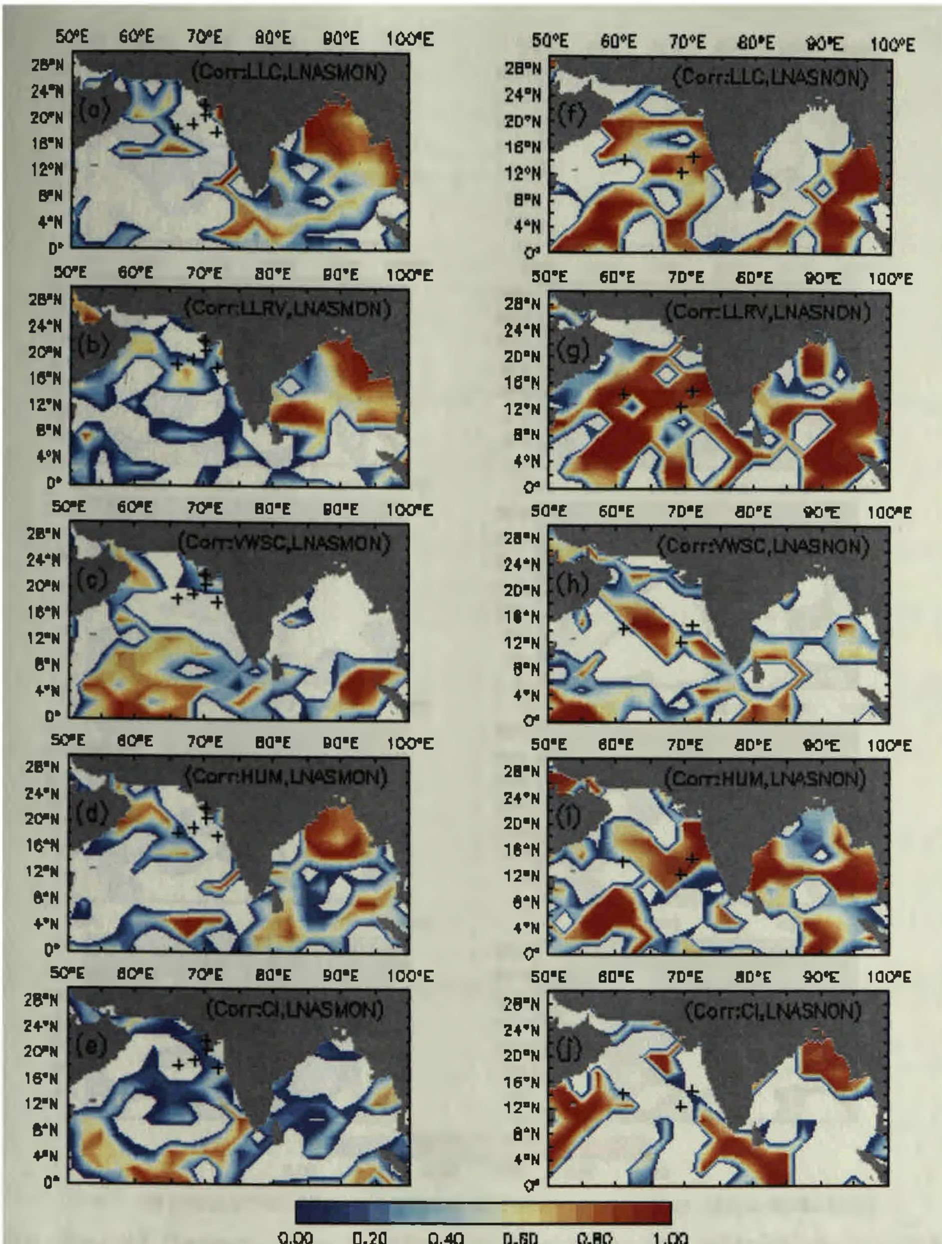

("+" represents the genesis locations of the depressions)

(AS= Arabian Sea, LN=La-Nina, MON=Monsoon, NON=Non-monsoon)

Figure 5.3 Spatial correlations of the parameters with CSGP for the depressions over AS during the La-Niña years

Figure (5.4) gives the spatial correlations of the parameters with CSGP for the depressions during the monsoon and non-monsoon seasons of the La-Niña years. From figure 5.4 (a, b, d) it is observed that the parameters such as LLC, LLRV and HUM have positive correlations with CSGP and from figure 5.4 (c) it is noticed that negative

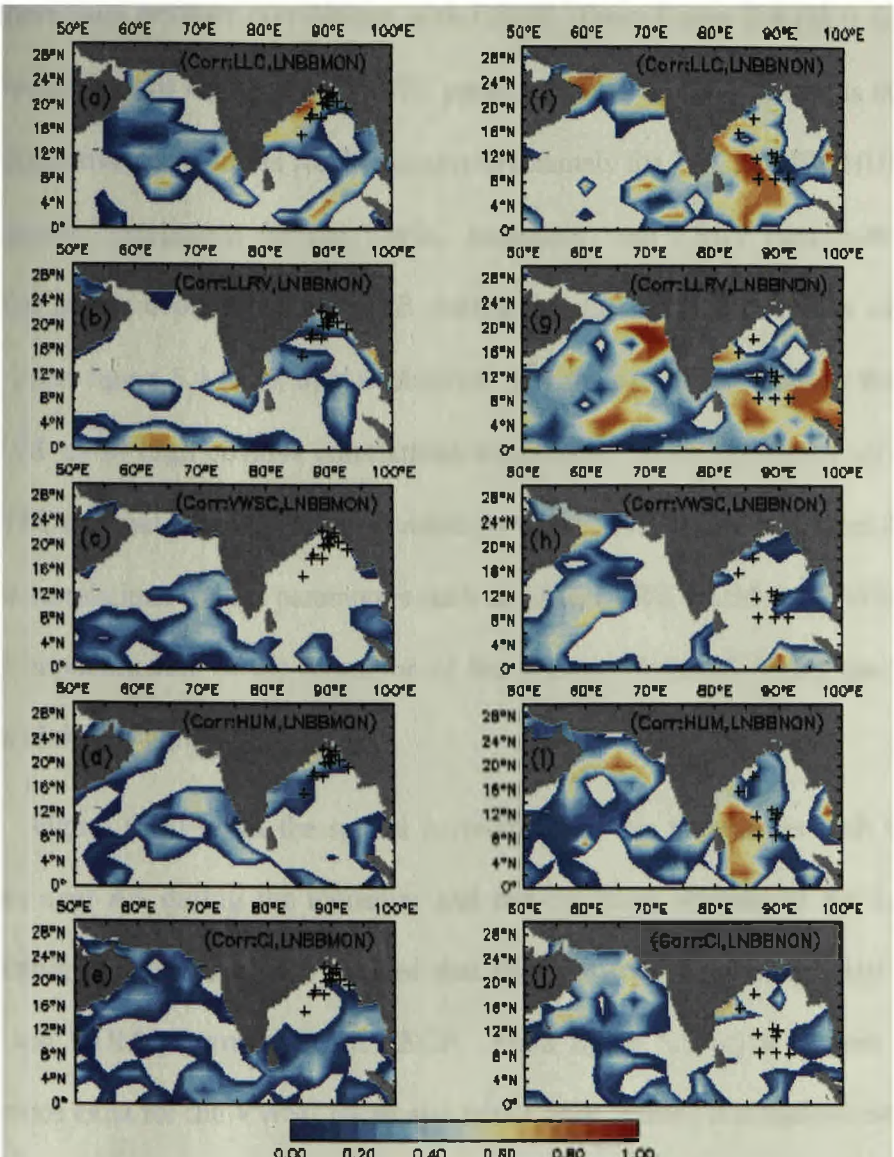

("+" represents the genesis locations of the depressions)
(BB= Bay of Bengal, LN=La-Nina, MON=Monsoon, NON=Non-monsoon)

Figure 5.4 Spatial correlations of the parameters with CSGP for the depressions over BB during the La-Niña years

correlations exist for the VWSC parameter with CSGP. Hence it is known that positive correlations of the parameters such as LLC, LLRV, HUM with CSGP and the negative correlations for the VWSC parameter with CSGP play a major role in the formation of the depressions over BB during the monsoon season of the La-Niña years.

From figure 5.4 (f, g, i) it is observed that the parameters such as LLC, LLRV and

HUM have high positive correlations with CSGP. From figure 5.4 (h) it is seen that the negative correlations exist for the VWSC parameter with CSGP. Hence it is understood that the high positive correlations for the parameters namely the LLC, LLRV, HUM with CSGP and negative correlations for the VWSC parameter with CSGP contribute much to the formation of the depressions over BB during the non-monsoon seasons of the La-Niña years. From figure 5.4 (a, b, d) it is observed that the parameters namely the LLC, LLRV and HUM show high positive correlations with CSGP. From figure 5.4 (c) it is seen that the VWSC parameter has negative correlations with CSGP. Hence it is clear that the higher positive correlations for the parameters such as LLC, LLRV, HUM and VWSC with CSGP play an important role in the formation of the cyclones over AS during the non-monsoon seasons of the La-Niña years.

Figure (5.5) gives the spatial correlations of the parameters with CSGP for the cyclones over AS during the monsoon and non-monsoon seasons of the La-Niña years. From figure 5.5 (a, b, d) it is noticed that high positive correlations exist for the LLC, LLRV and HUM parameters with CSGP. From figure 5.5 (c) it is seen that negative correlations exist for the VWSC parameter with CSGP. Hence it is understood that the high positive correlations of the LLC, LLRV and HUM parameter and the negative correlations of the VWSC with CSGP play an important role in the formation and intensification of the cyclones over BB monsoon seasons of the La-Niña years.

Figure (5.6) gives the spatial correlations of the parameters with CSGP for the cyclones over BB during the monsoon and non-monsoon seasons of the La-Niña years. From figure 5.6 (a) it is observed that the LLC parameter is having high positive correlations with CSGP, hence it is clear that the LLC parameter is influencing the formation of the cyclones over BB during the monsoon season.

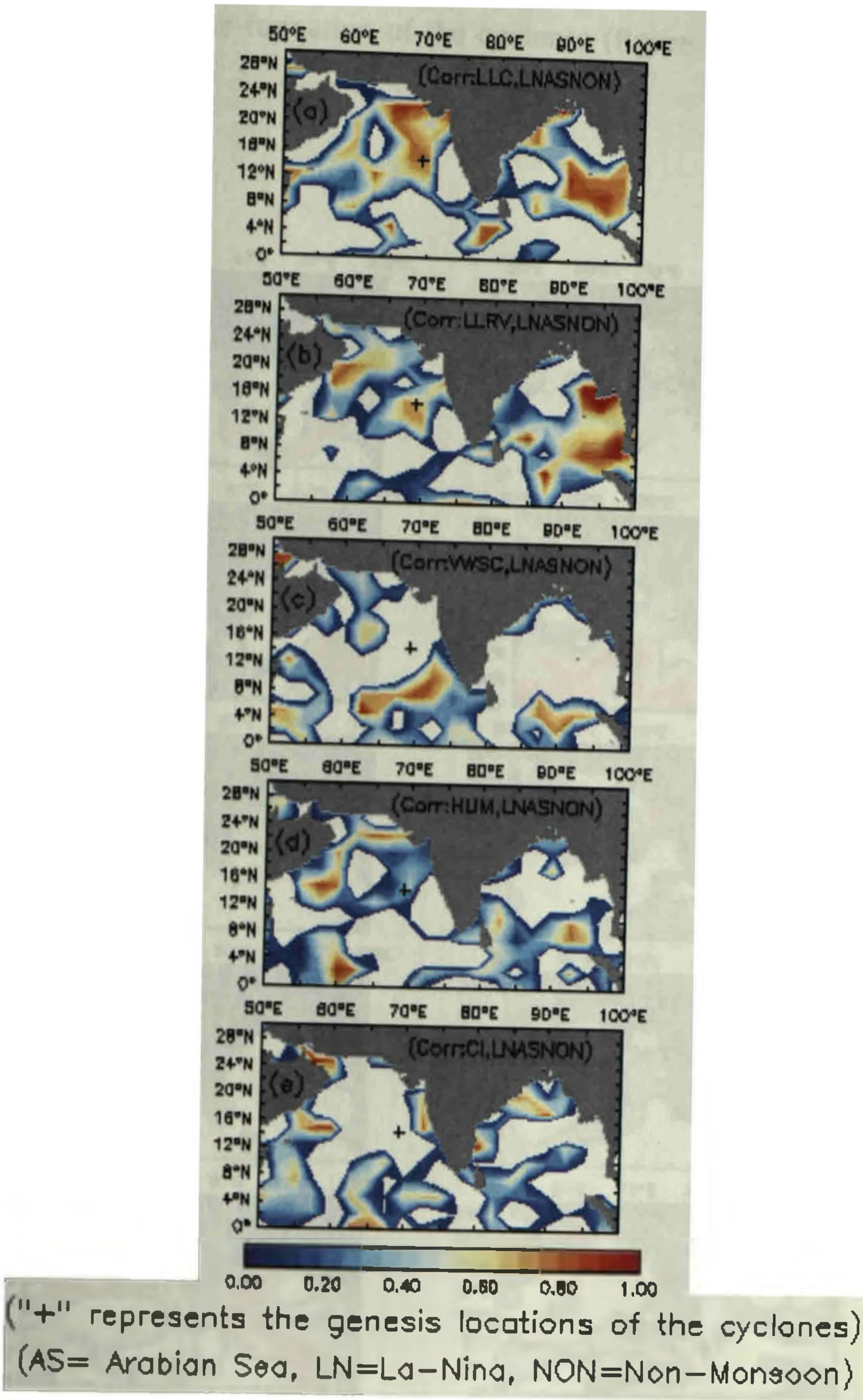

Figure 5.5 Spatial correlations of the parameters with CSGP for the cyclones over AS during the La-Niña years

From figure 5.6 (g) it is observed that the LLRV has high positive correlations with CSGP. From figure 5.6 (j) it is seen that the CI parameter has high positive correlations with CSGP. Hence during the non-monsoon seasons the high positive correlations of LLRV and

CI parameters are hleping the formation of the cyclones (figure 5.6 (g, j)) during the La-Niña years.

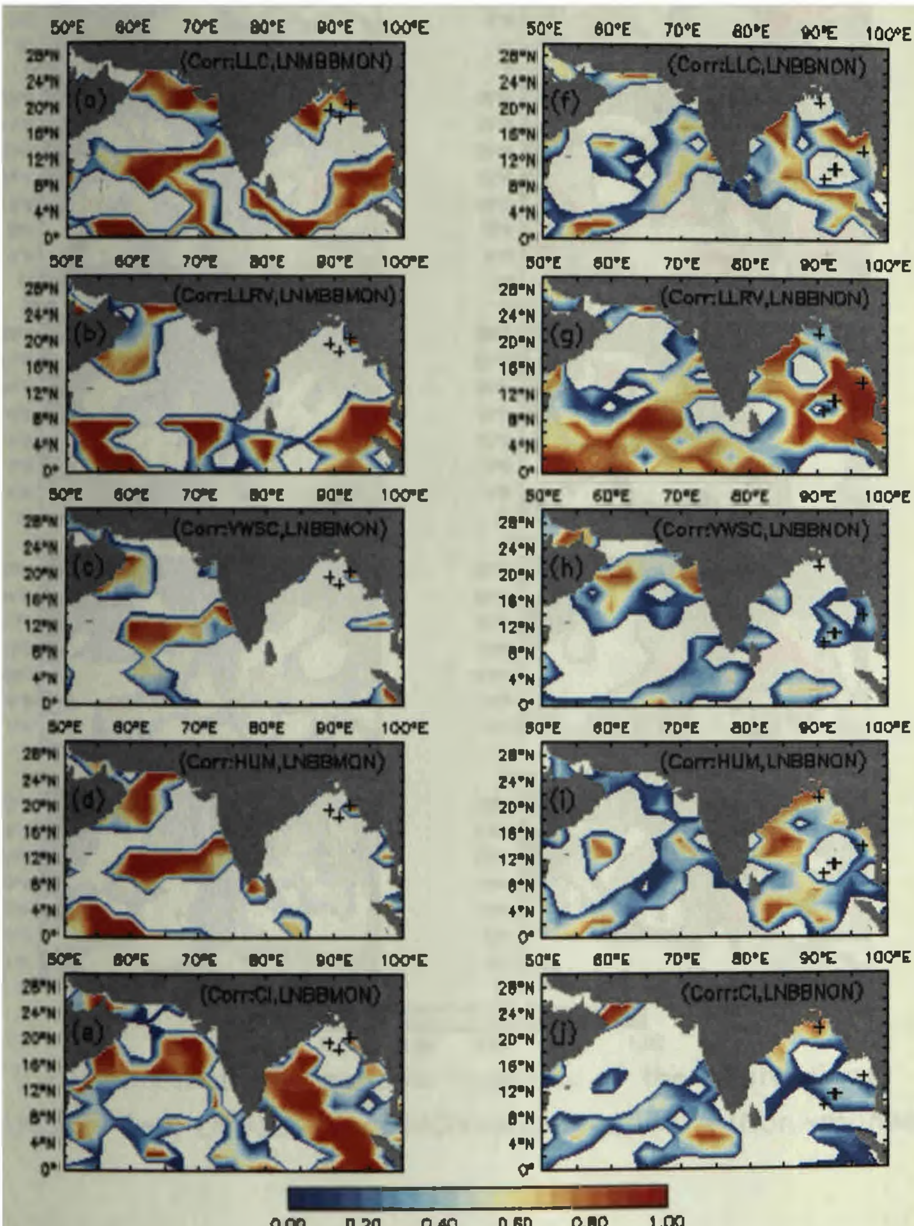

("+" represents the genesis locations of the cyclones)
(BB= Bay of Bengal, LN=La-Nina, MON=Monsoon, NON=Non-monsoon)

Figure 5.6 Spatial correlations of the parameters with CSGP for the cyclones over BB during the La-Niña years

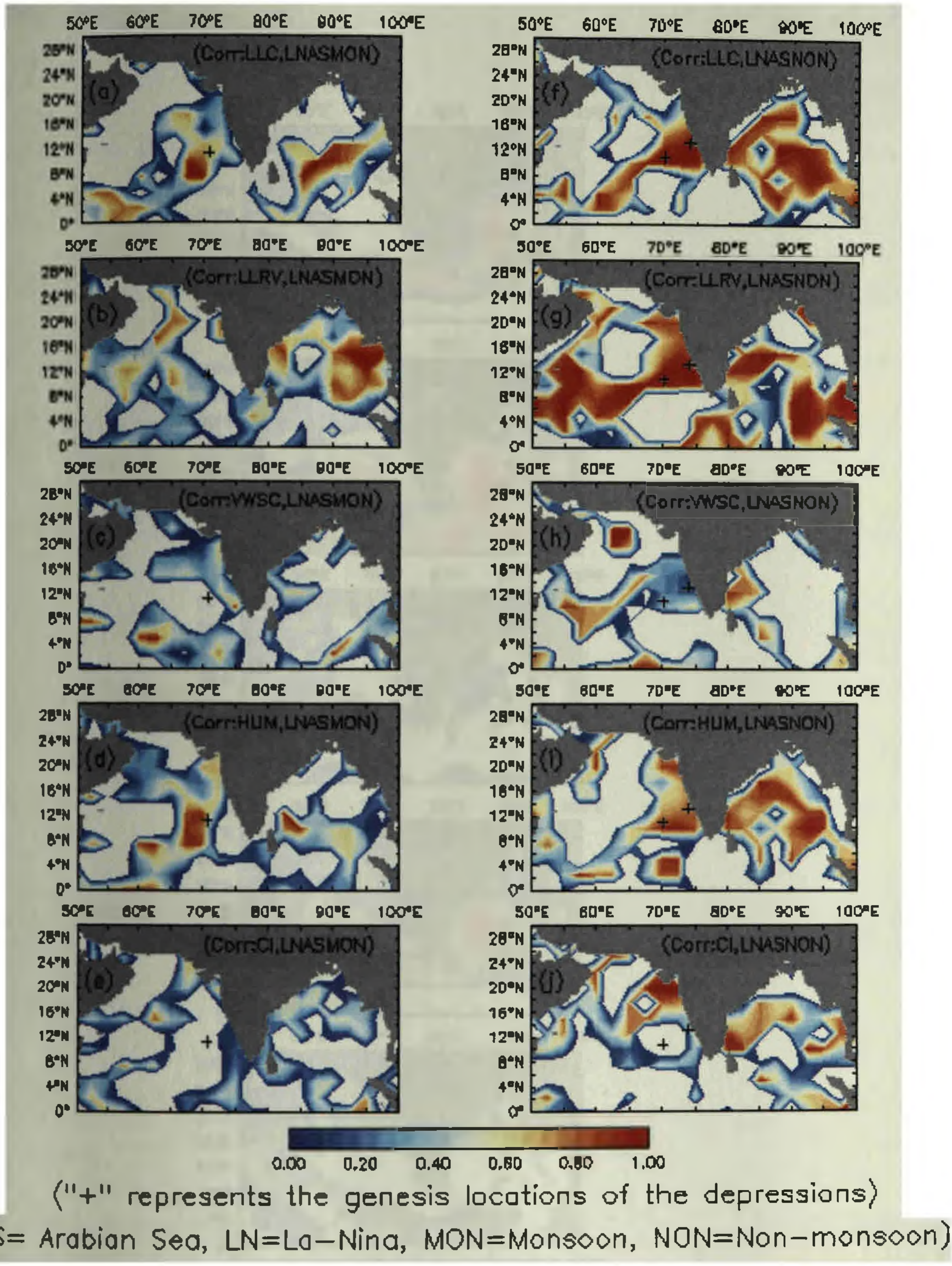

Figure 5.7 Spatial correlations of the parameters with CSGP for the severe cyclones over AS during the La-Niña years

Figure (5.7) gives the spatial correlations of the parameters with CSGP for the severe cyclones over AS during the monsoon and non-monsoon seasons of the La-Niña years. From figure 5.7 (a, d) it is observed that the parameters such as LLC and HUM have high positive correlations with CSGP. From figure 5.7 (c) it is noticed that the VWSC parameter has a negative correlation with CSGP.

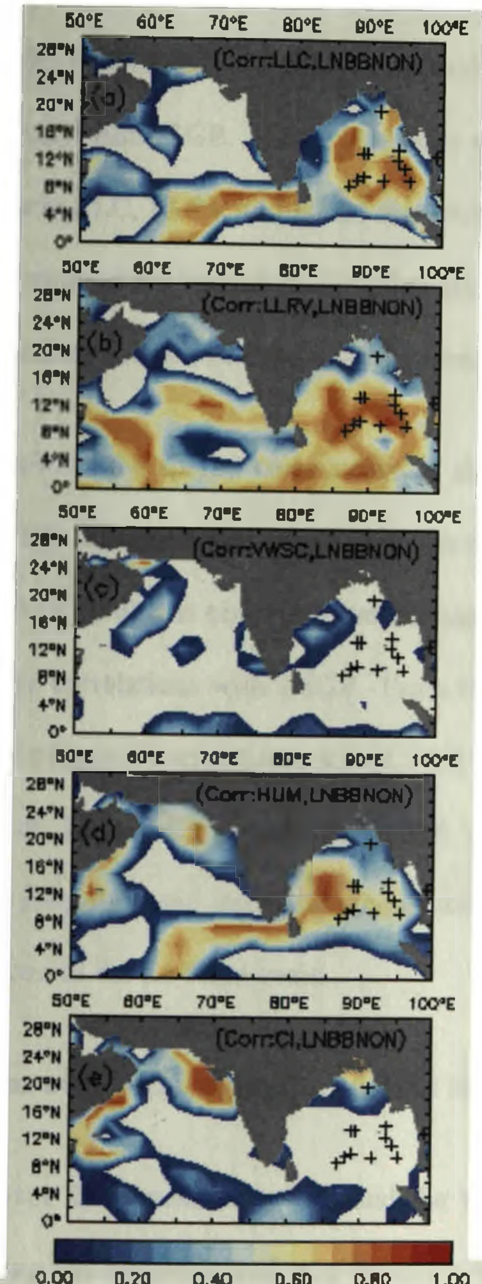

Figure 5.8 Spatial correlations of the parameters with CSGP for the severe cyclones over BB during the La-Niña years

Hence it is understood that the high positive correlations of LLC and HUM and negative correlations of VWSC play an important role in the formation and intensification of the severe cyclones over AS during the monsoon season of the La-Niña years. From figure 5.7 (f, g, i) it is observed that the parameters such as LLC, LLRV and HUM have high positive correlations with CSGP. From figure 5.7 (h) it is noticed that the VWSC parameter has a lower positive correlation with CSGP. Hence it is clear that the high positive correlations of the parameters namely LLC, LLRV and HUM and lower positive correlations of VWSC with CSGP contribute more to the formation and intensification of the severe cyclones over AS during the non-monsoon seasons of the La-Niña years.

Figure (5.8) shows the spatial correlations of the parameters with CSGP for the severe cyclones over BB during the monsoon and non-monsoon seasons of the La-Niña years. From figure 5.8 (a, b, d) it is observed that the parameters such as LLC, LLRV and Hum have high positive correlations with CSGP. From figure 5.8 (c) it is noticed that the VWSC parameter has negative correlations with CSGP. Hence it is clear that the high positive correlations of LLC, LLRV and HUM and negative correlations of VWSC contribute more to the formation and intensification of the severe cyclones over BB during the non-monsoon seasons of the La-Niña years.

5.6 Convective systems over NIO during the La-Niña Modoki years.

Figure 5.9 gives the genesis locations and the tracks of the convective systems formed over NIO during the monsoon and non-monsoon seasons of the La-Niña Modoki years. From figure 5.9 (a), it is seen that there were 4 depressions over BB during the monsoon season. The depressions are formed only over BB and they have moved towards the northwest direction and entered into the land. From figure 5.9 (b), it is seen that, during the non-monsoon seasons there were 2 depressions over BB and they moved towards west and dissipated in BB.

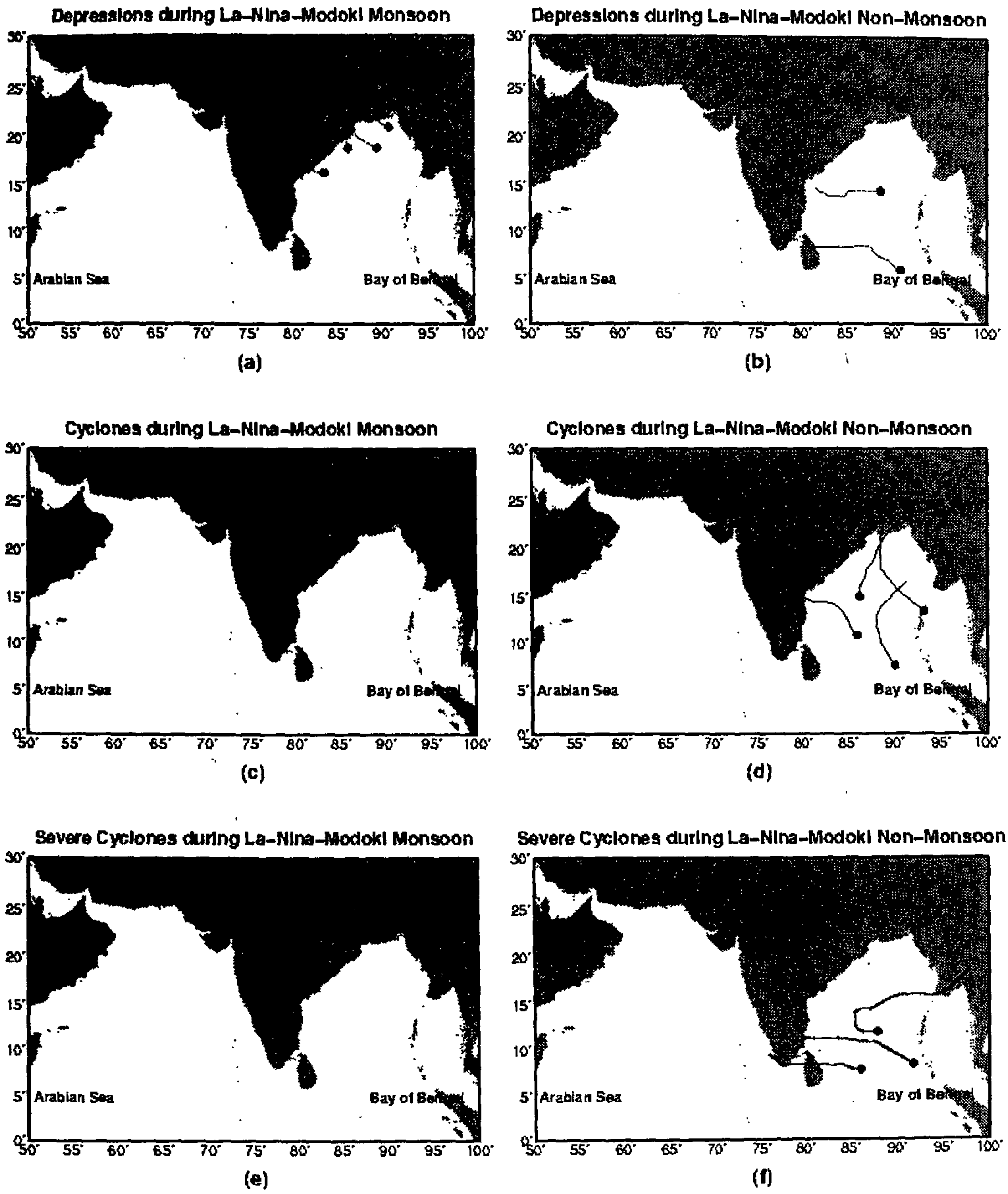

Figure 5.9 Convective systems over NIO during the monsoon and non-monsoon seasons of the La-Niña Modoki years

From figure 5.9 (c), it is seen that there no cyclones over AS and BB during the monsoon season of the La-Niña Modoki years. From figure 5.9 (d) there were no cyclones over AS during the non-monsoon seasons but there have been 4 cyclones over BB during the non-monsoon seasons of the La-Niña Modoki years. Out of these 3 cyclones have moved to the land but 1 cyclone has dissipated over the BB. From figure 5.9 (e), it is seen that there were no severe cyclones over AS and BB during the monsoon season of the La-Niña Modoki years. From figure 5.9 (f), it is seen that there were no severe cyclones over AS during the non-monsoon seasons but there were 3 severe cyclones over BB during the non-monsoon seasons of the La-Niña Modoki years. Out of these 3 severe cyclones 2 severe cyclones moved towards west and entered onto the land. Other severe cyclone moved towards east and entered the Myanmar coast. From these figures it is observed that, the AS was free from convective systems during the monsoon and non-monsoon seasons of the La-Niña Modoki years

Table 5.7 gives the list of depressions formed over BB during the monsoon and non-monsoon seasons of the La-Niña Modoki years. There have been 4 depressions in the monsoon season and 2 depressions over BB during the non-monsoon seasons. In the year 2000, there was 1 depression in the monsoon season on 23-Aug-2000 and dissipated on 24-Aug-2000. In the year 2008, there were 3 depressions in the monsoon- seasons. The first depression was formed on 16-Jun-2008 and dissipated on 18-Jun-2008. The second depression was formed on 09-Aug-2008 and decayed on 10-Aug-2008. The third depression was formed on 15-Sep-2008 and dissipated on 19-Sep-2008. There were 2 depressions over BB in the non-monsoon seasons of the La-Niña Modoki years. The first depression was formed on 15-Oct-2000 and dissipated on 19-Oct-2000. The second depression was formed on 04-Dec-2008 and decayed on 07-Dec-2008. Table 5.8 gives the list of all the cyclones over BB during the non-monsoon seasons of the La-Niña Modoki years. There were no cyclones over BB during the monsoon season of the La-Niña Modoki years. There were 4 cyclones over BB during the non-monsoon seasons of the La-Niña Modoki years.

Table 5.7 List of Depressions formed over BB during the monsoon and non-monsoon seasons in the La-Niña Modoki years

Bay of Bengal			
Monsoon		**Non-monsoon**	
Date of formation	**Date of dissipation**	**Date of formation**	**Date of dissipation**
23-Aug-2000	24-Aug-2000	15-Oct-2000	19-Oct-2000
16-Jun-2008	18-Jun-2008	04-Dec-2008	07-Dec-2008
09-Aug-2008	10-Aug-2008		
15-Sep-2008	19-Sep-2008		

Table 5.8 List of Cyclones formed over BB during the monsoon and non-monsoon seasons in the La-Niña Modoki years

Bay of Bengal					
Monsoon			**Non-monsoon**		
Date of formation	**Date of Intensification to Cyclone**	**Date of dissipation**	**Date of formation**	**Date of Intensification to Cyclone**	**Date of dissipation**
			27-Mar-2000	29-Mar-2000	30-Mar-2000
			25-Oct-2000	27-Oct-2000	29-Oct-2000
			25-Oct-2008	26-Oct-2008	27-Oct-2008
			13-Nov-2008	14-Nov-2008	16-Dec-2008

The first cyclone formed on 27-Mar-2000, intensified into cyclone on 29-Mar-2000 and dissipated on 30-Mar-2000. The second cyclone was formed on 25-Oct-2000, intensified into cyclone on 27-Oct-2000 and dissipated on 29-Oct-2000. The third cyclone was formed on 25-Oct-2008, intensified into cyclone on 26-Oct-2008 and dissipated on 27-Oct-2008. The last cyclone was formed on 13-Nov-2008, intensified into cyclone on 14-Nov-2008 and dissipated on 16-Dec-2008.

Table 5.9 List of Severe cyclones formed over BB during the monsoon and non-monsoon seasons in the La-Niña Modoki years

Bay of Bengal					
Monsoon			Non-monsoon		
Date of formation	Date of Intensification to severe cyclone	Date of dissipation	Date of formation	Date of Intensification to severe cyclone	Date of dissipation
			26-Nov-2000	28-Nov-2000	30-Nov-2000
			23-Dec-2000	26-Dec-2000	28-Dec-2000
			27-Apr-2008	28-Apr-2008	03-May-2008

Table 5.9 gives the list of all the severe cyclones over BB during the non-monsoon seasons of the La-Niña Modoki years. There were no severe cyclones over BB during the monsoon season. There were 3 severe cyclones during the non-monsoon seasons of the La-Niña Modoki years. The first severe cyclone was formed on 26-Nov-2000, intensified into severe cyclone on 28-Nov-2000 and dissipated on 30-Nov-2000. The second severe cyclone was formed on 23-Dec-2000, intensified into severe cyclone on 26-Dec-2000 and dissipated on 28-Dec-2000. The last severe cyclone was formed on 27-Apr-2008, intensified into severe cyclone on 28-Apr-2008 and dissipated on 03-May-2008.

5.7 Variations of CSGP for the convective systems over NIO during the La-Niña Modoki years

Figure (5.10) gives the variations of CSGP for the convective systems over NIO during the monsoon and non-monsoon seasons of the La-Niña Modoki years. Figure 5.10 (a, b, c, d) gives the variations of the CSGP for the convective systems over NIO during the monsoon season of the La-Niña Modoki years.

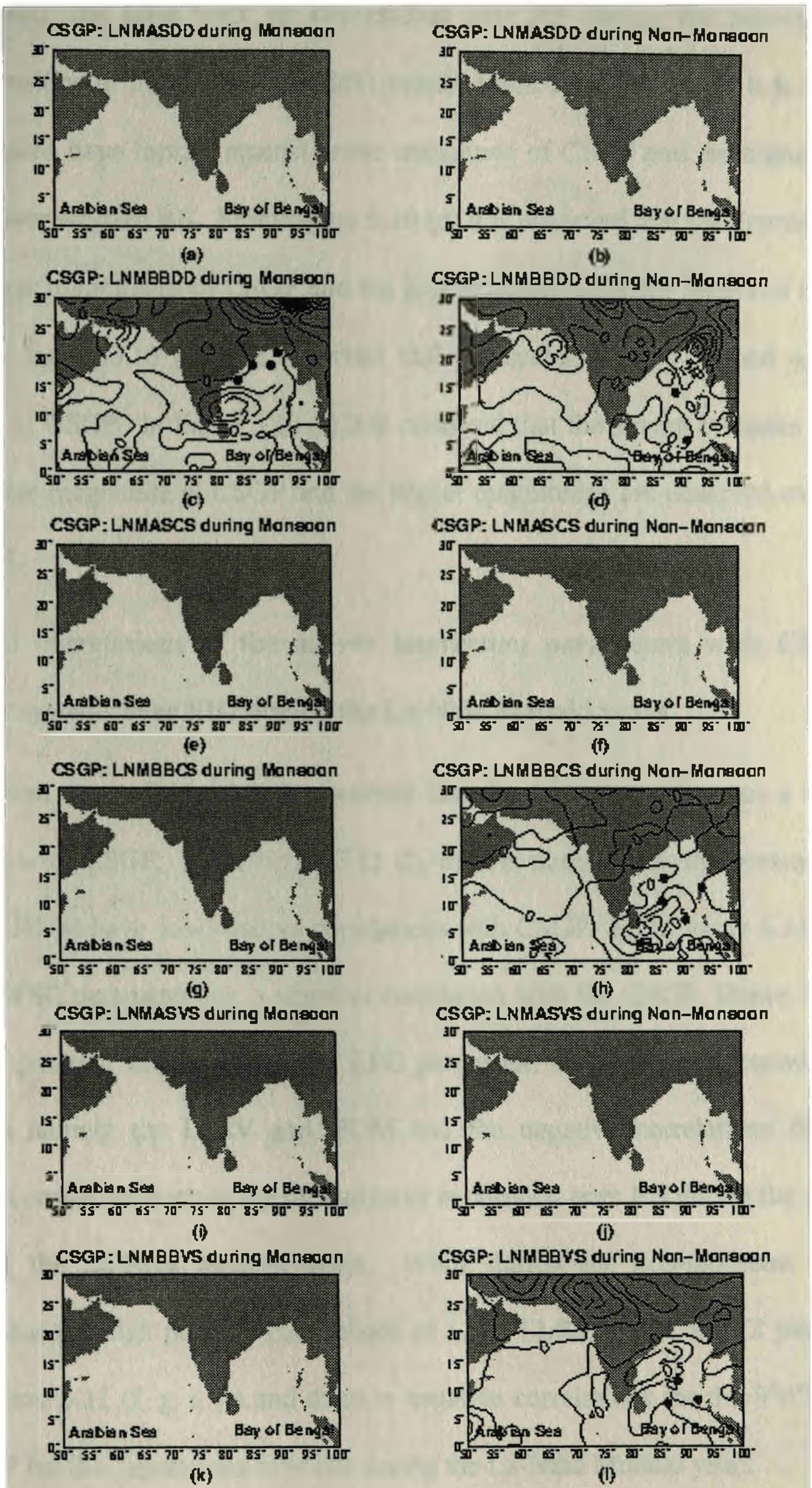

Figure 5.10 Variations of CSGP for the convective systems over NIO during the monsoon and non-monsoon seasons of the La-Niña Modoki years

It is observed that there were no depressions over AS during the monsoon and non-monsoon seasons of the La-Niña Modoki years. From figure 5.10 (c), it is observed that the depressions have formed against lower magnitude of CSGP and the higher magnitudes are found over western BB. From figure 5.10 (d) it is observed that the depressions formed against lower magnitudes of CSGP and the higher magnitudes are observed over northern AS. From figure 5.10 (h) it is observed that the cyclones were formed against higher magnitude of CSGP. In figure 5.10 (l) it is observed that the severe cyclones were formed against lower magnitude of CSGP and the higher magnitudes are observed over the north-western BB.

5.8 Spatial correlations of the air-sea interaction parameters with CSGP for the convective systems over NIO during the La-Niña Modoki years

From figure 5.11 (a) it is observed that the LLC parameter has a high positive correlation with CSGP. From figure 5.11 (b, d) it is noticed that the parameters such as LLRV and HUM have low positive correlations with CSGP. From figure 5.11 (c) it is seen that the VWSC parameter has a negative correlation with the CSGP. Hence it is clear that the higher positive correlation of the LLC parameter, lower positive correlations of the parameters namely the LLRV and HUM and the negative correlations of the VWSC parameter contribute much to the formation of depression over BB during the non-monsoon seasons of the La-Niña Modoki years. While during the non-monsoon seasons it is observed that the high positive correlations of LLC, LLRV, HUM and CI parameters with CSGP (figure 5.11 (f, g, i, j)) and there is negative correlations for the VWSC parameter with CSGP for the depressions over BB during the La-Niña Modoki years.

Figure (5.12) gives the spatial correlations of the parameters with CSGP for the cyclones over BB during the La-Niña Modoki years. From figure 5.12 (b, d) it is observed that the parameters such as LLRV and HUM have high positive correlations with the CSGP.

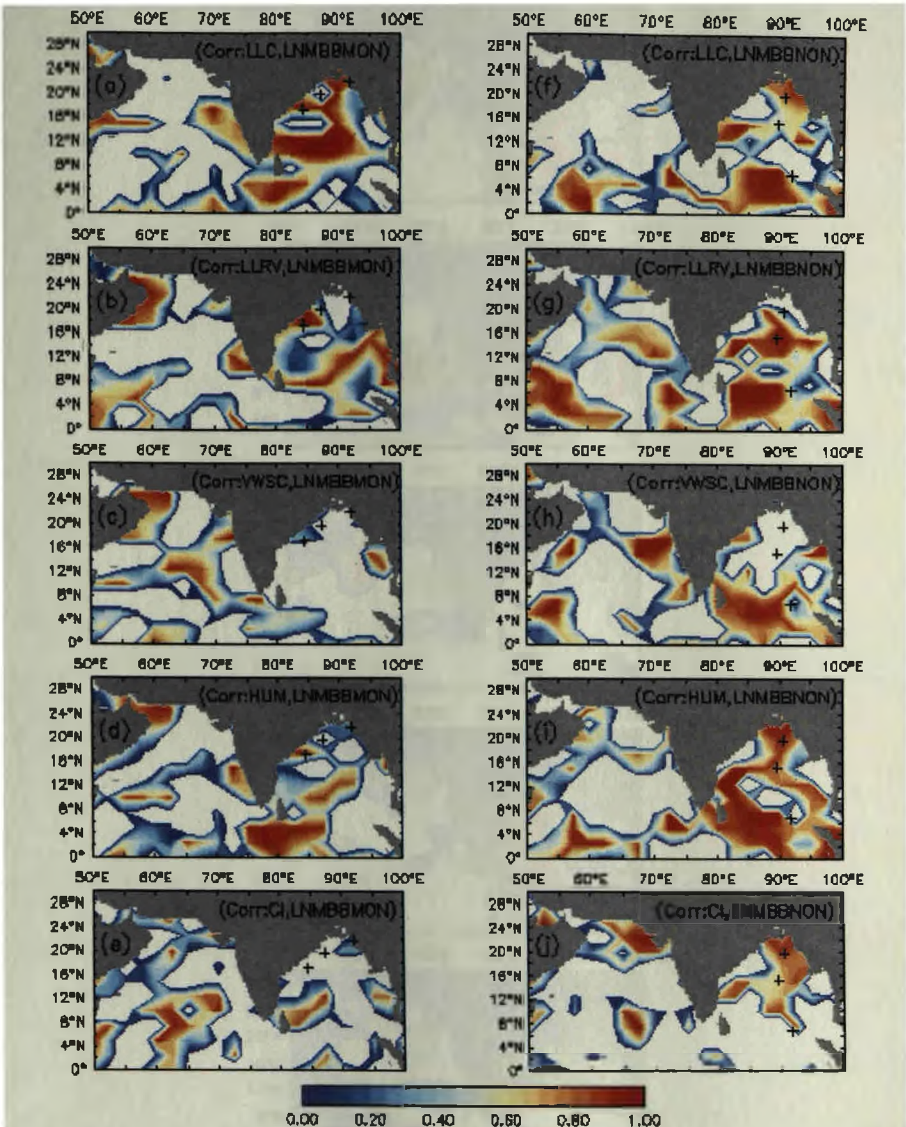

("+" represents the genesis locations of the depressions)

(BB= Bay of Bengal, LNM=La-Nina Modoki, MON=Monsoon, NON=Non-monsoon)

Figure 5.11 Spatial correlations of the parameters with CSGP for the depressions over BB during the La-Niña Modoki years

From figure 5.12 (c) it is noticed that the VWSC parameter has a negative correlation with the CSGP. Hence it is clear that the high positive correlations of the parameters namely the LLRV and HUM and negative correlations of the VWSC with CSGP contribute much to the formation and intensification of the cyclones over BB during the non-monsoon seasons of the La-Niña Modoki years.

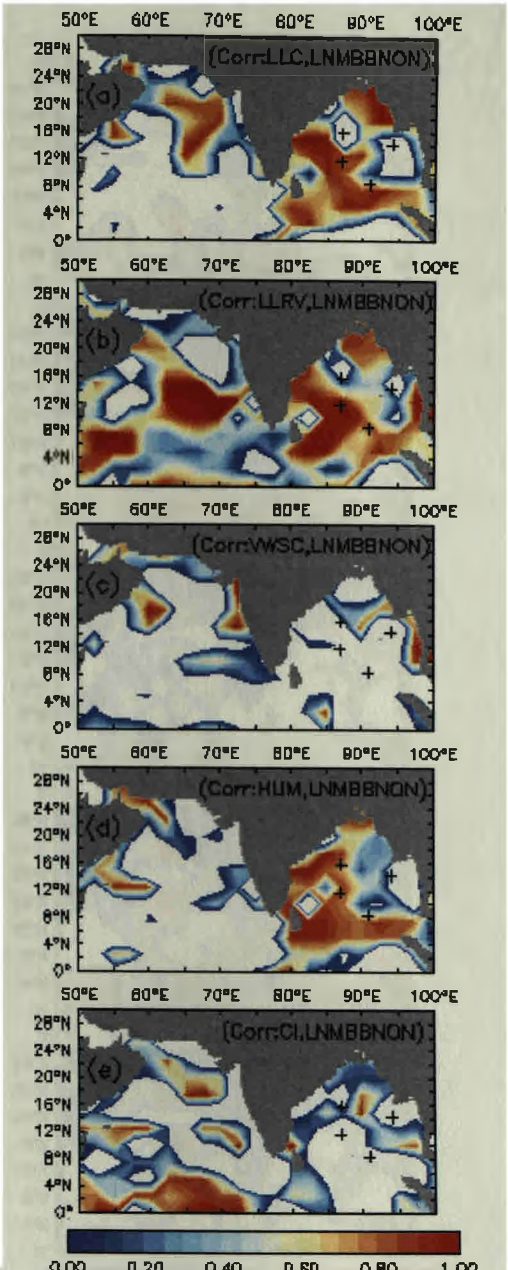

("+" represents the genesis locations of the cyclones)
(BB=Bay of Bengal, LNM=La-Nina Modoki, NON=Non-Monsoon)

Figure 5.12 Spatial correlations of the parameters with CSGP for the cyclones over BB during the La-Niña Modoki years

Figure (5.13) gives the spatial correlations of the parameters with CSGP for the severe cyclones over BB La-Niña Modoki years. From figure 5.13 (a, b, d) it is observed that the parameters such as LLC, LLRV and HUM have low positive correlations with the CSGP.

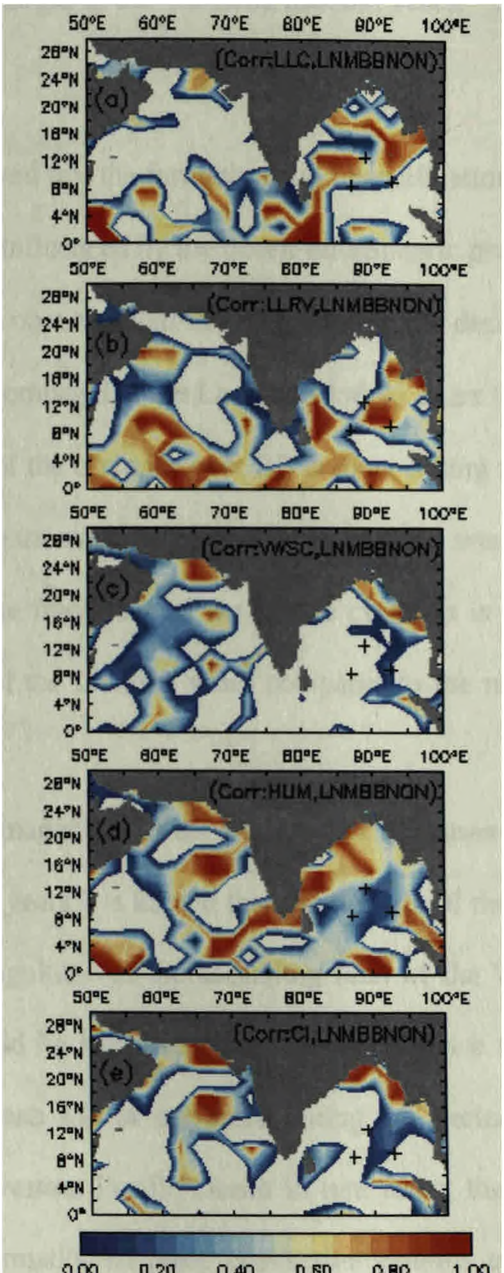

("+" represents the genesis locations of the severe cyclones)
(BB= Bay of Bengal, LNM=La–Nina Modoki, NON=Non–Monsoon)

Figure 5.13 Spatial correlations of the cyclogenesis parameters with CSGP for the severe cyclones over BB during the La-Niña Modoki years

From figure 5.13 (c) it is noticed that the VWSC parameter has a negative correlation with the CSGP. Hence it is clear that the low positive correlations of the parameters such as LLC, LLRV and HUM and the negative correlations of the VWSC contribute much to the formation and intensification of the severe cyclones over BB during the non-monsoon seasons of the La-Niña Modoki years.

5.9 Conclusion

It is observed that the formation and intensification of the convective systems over the NIO are highly influenced by the ocean-atmospheric processes such as La-Niña and La-Niña Modoki. It is observed that the frequency of the depressions over BB is high during the La-Niña years compared to the La-Niña Modoki years in both the seasons. It is noticed that the frequency of the cyclones over BB is more during the non-monsoon seasons of the La-Niña Modoki years compared to the non-monsoon seasons of the La-Niña years. It is also noticed that the frequency of the severe cyclones is more over BB during the non-monsoon seasons of the La-Niña years compared to the non-monsoon seasons of the La-Niña Modoki years.

Since the magnitude of the trade winds increases over the tropical Pacific Ocean during the La-Niña years it is known that the strength of the Walker circulation also will be increased. The magnitude of the ascending limb of the Walker circulation over western Pacific Ocean would be high during this period. Hence the convective activity over the western Pacific Ocean will be enhanced during this period. The large scale atmospheric convections over western Pacific Ocean in turn affect the convective activities over BB. This causes the formation of more convective systems over BB with higher intensities. While during the La-Niña Modoki years, the Walker circulation gets split into two as two convective loops over the tropical Pacific Ocean. This results in two ascending limbs over the western and eastern Pacific Ocean and one descending limb over the central Pacific Ocean. The convective activity increases over the western and eastern Pacific Ocean. The magnitude of the ascending limbs will be less during this period compared to that in the La-Niña years. The ascending limb over western Pacific Ocean generates convective activities over this basin and in turn influences the convective activity over BB. The magnitude of the LLC increases during this period, which is favourable for the formation of the convective systems over BB. Other air-sea interaction parameters such as LLRV, VWSC are also found favourable for the formation of the convective systems over BB.

It is observed that the depressions and cyclones have formed against low magnitudes of CSGP and the severe cyclones have formed against higher magnitudes during the La-Niña years. It is seen that the depressions and cyclones have formed against lower magnitudes of CSGP and the severe cyclones are formed against high magnitudes of CSGP. From the spatial correlations it is observed that the magnitudes of the positive correlations of the LLC parameter with CSGP are found to be high during the La-Niña years compared to those in the La-Niña Modoki years. Hence the formation and intensification of convective systems are decreased over NIO during the La-Niña Modoki years. From the it is noticed that the frequencies of cyclones are more over BB during La-Niña Modoki years than La-Niña years and the frequencies of severe cyclones are more during La-Niña years than La-Niña Modoki years. It also reveals that the La-Niña Modoki events are not conducive for the formation of cyclones over AS. It further states that there is a reduction in the magnitude of LLC over BB during La-Niña Modoki years compared to the La-Niña years; this suppresses the formation of severe cyclonic storms.

It is found that there is a northward shift in the genesis locations of the depressions formed in the monsoon season, but a southward shift is observed during the non-monsoon seasons of the La-Niña and La-Niña Modoki years. It is observed that, the La-Niña conditions help the cyclones and severe cyclones over AS to live longer even after the landfall in both the seasons. It is noticed that the cyclones formed over BB in the monsoon season of the La-Niña years have lived longer after their landfall but it is also noticed that there is a tendency for the cyclones and severe cyclones over BB in the non-monsoon seasons to dissipate over the ocean before the landfall or decay immediately after the landfall. It is found that no convective systems have formed over AS during the La-Niña

Modoki years but in the case of BB it is found that there is a northward shift in the genesis locations of the depressions in the monsoon season and a southward shift in the non-monsoon seasons. The depressions in the monsoon season are having a northwesterly track the depressions in the non-monsoon seasons have a purely westerly track. It is observed that there were no cyclones and severe cyclones over BB during the monsoon season of the La-Niña Modoki years but there were 4 cyclones and 3 severe cyclones during the non-monsoon seasons. It is noticed that the cyclones and severe cyclones have moved towards either west or east. The eastward movement of the track can be atributed to the large scale atmospheric convection over the western Pacific Ocean during the La-Niña Modoki years. It is also seen that there is a tendency for the cyclones and severe cyclones to live longer after their landfall.

Chapter 6

Convective systems over northern Indian Ocean during the Indian Ocean Dipole and Neutral years

6.1 Introduction

Indian Ocean Dipole (IOD) (Saji et al. 1999; Webster et al. 1999) events are considered as the second largest climatic forcing after the ENSO events. This phenomenon is characterized by the anomalous warming and cooling of SST over the western and eastern equatorial Indian Ocean. There are two phases of the IOD events, namely the Positive IOD (PIOD) and the Negative IOD (NIOD). The PIOD event is defined as warmer than normal SST over the western tropical Indian Ocean, and cooler than normal SST over eastern tropical Indian Ocean and the NIOD event is defined as cooler than normal SST over the western tropical Indian Ocean and warmer than normal SST over eastern tropical Indian Ocean.

The studies (Saji and Yamagata 2003b, Behera and Yamagata (2001), Ashok et. al 2003) show that the IOD events have got significant impacts on the weather and climate over various parts of the globe. There have been many studies on the intra seasonal and inter annual variability of IOD events (Saji and Yamagata 2003a) and the tele-connections of the IOD events with ENSO have been studied by Ashok et.al (2003). Francis et.al (2009) shows that a Positive IOD event can be triggered by the occurrence of severe cyclones over Bay of Bengal. Pradhan et.al (2009) showed that the concurrent occurrence of El-Niño Modoki and positive IOD can produce more cyclones over North West Pacific.

Sumesh and Ramesh Kumar (2013) state that the concurrent occurrence of the PIOD and El-Niño events can produce more cyclones over BB than AS. This study further reveals that the concurrent occurrence of the PIOD and El-Niño Modoki events can produce more cyclones over AS than BB. This study proves that the concurrent occurrence of El-Niño Modoki and positive IOD events are conducive to the formation of more tropical cyclones over NIO. Yuan and Cao (2012) showed that during the PIOD event the SST anomalies over NIO are warm in the west and cold in the east, which can weaken the atmospheric convection over the BB and eastern AS. This causes anti-cyclonic atmospheric circulation anomalies at lower levels of the atmosphere and results in the formation of fewer cyclones over NIO. This study further states that during the NIOD event, the SST anomalies over NIO are warm in the east and cold in the west, which can strengthen the atmospheric convection over the BB and eastern AS. This causes cyclonic atmospheric circulation anomalies at lower levels of the atmosphere and results in the formation of cyclone formation over NIO at greater frequencies.

6.2 Convective systems over NIO during the Positive Indian Ocean Dipole (PIOD) years

Figure (6.1) gives the genesis locations (black dots) and the tracks of the convective systems over NIO during the monsoon and non-monsoon seasons of the PIOD years. Figure 6.1 (a,b) shows the genesis points and tracks of depressions formed over NIO during the monsoon and non-monsoon seasons respectively. It is seen that there are no depressions over AS during the monsoon season of the PIOD years. There have been 4 depressions over BB during the monsoon season of the PIOD years. All these depressions have taken a westerly track and entered the land. There was 1 depression formed over AS during the non-monsoon seasons and this depression has taken a north-westerly track and dissipated in the western AS near the Oman coast. There have been 3 depressions over BB during the non-monsoon seasons of the PIOD years. These depressions have moved northward, westward and north-eastward and entered the land.

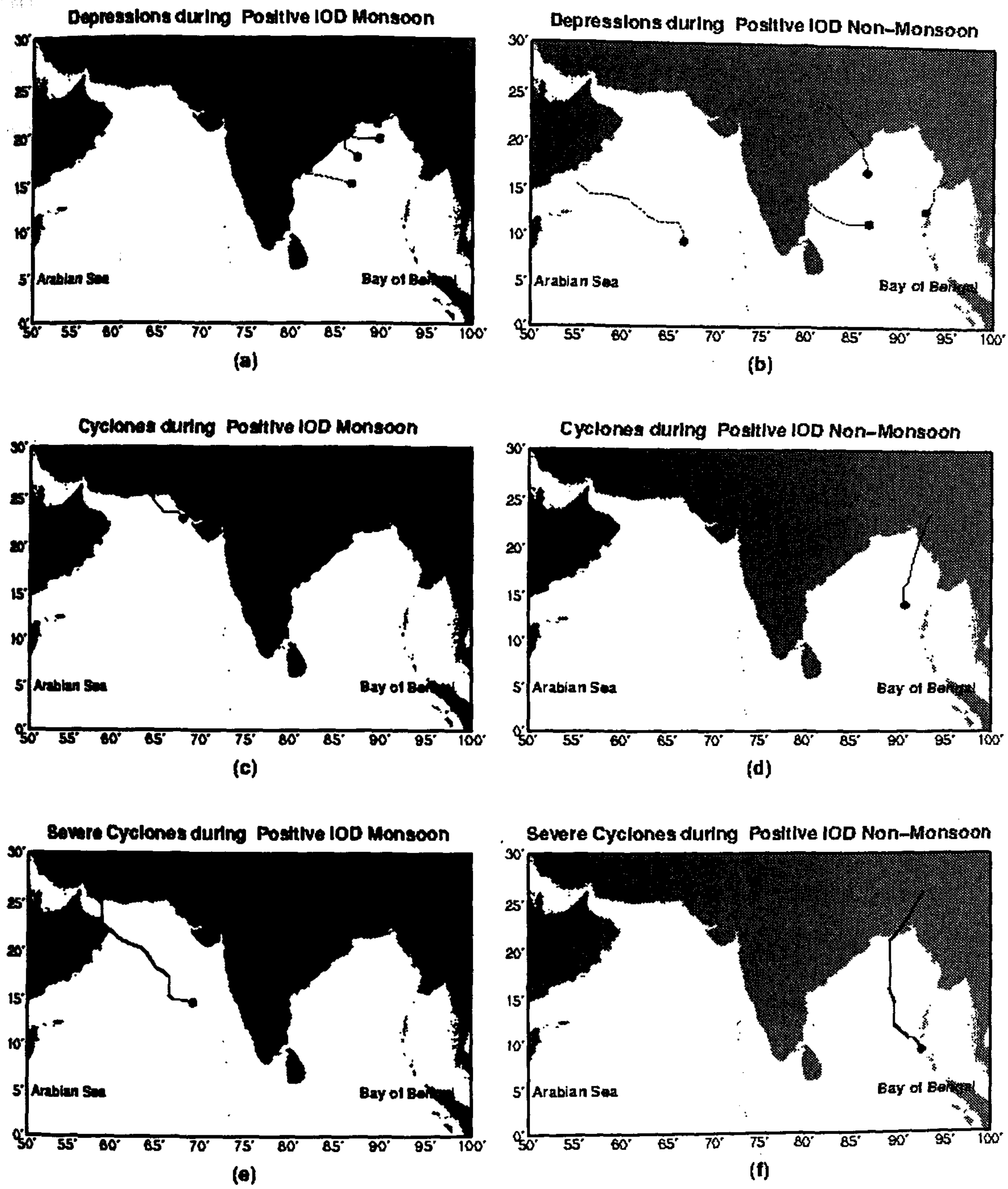

Figure: 6.1 Convective systems formed over NIO during the monsoon and non-monsoon seasons of the PIOD years

Figure 6.1 (c, d) shows the genesis points and tracks of the cyclones formed over NIO during the monsoon and non-monsoon seasons. There was 1 cyclone over AS during the monsoon season but no cyclone was formed over AS during the non-monsoon seasons.

This cyclone has taken a north-westerly direction and entered onto the land and dissipated over there. There were no cyclones over BB during the monsoon season, but there was 1 cyclone during the non-monsoon seasons. This cyclone has taken a long northerly track, entered into the land and dissipated over there. Figure 6.1 (e, f) shows the genesis points and tracks of the severe cyclones formed over NIO during the monsoon and non-monsoon seasons respectively. There was 1 severe cyclone over AS during the monsoon season, but no severe cyclones formed over AS during the non-monsoon seasons. This severe cyclone over AS has taken a north-westerly track, entered into the land and dissipated over there. There were no severe cyclones over BB during the monsoon season, but there was 1 severe cyclone over BB during the non-monsoon seasons. This severe cyclone has taken a northerly track and dissipated over the land.

Table 6.1 List of Depressions formed over AS during the monsoon and non-monsoon seasons in the PIOD years

Arabian Sea			
Monsoon		**Non-monsoon**	
Date of formation	**Date of dissipation**	**Date of formation**	**Date of dissipation**
		27-Oct-2007	02-Nov-2007

Table (6.1) gives the list of all the depressions formed over AS during the monsoon and non-monsoon seasons of the PIOD years. There was only 1 depression over AS formed in the non-monsoon seasons. It was formed on 27-Oct-2007 and dissipated on 02-Nov-2007. Table (6.2) gives the list of all the depressions formed over BB during the monsoon and non-monsoon seasons of the PIOD years. There have been 5 depressions over BB during the monsoon season and 2 depressions during the non-monsoon seasons.

Table 6.2 List of Depressions formed over BB during the monsoon and non-monsoon seasons in the PIOD years

Bay of Bengal			
Monsoon		Non-monsoon	
Date of formation	Date of dissipation	Date of formation	Date of dissipation
21-Jun-2007	23-Jun-2007	03-May-2007	04-May-2007
28-Jun-2007	30-Jun-2007	27-Oct-2007	29-Oct-2007
04-Jul-2007	09-Jul-2007		
05-Aug-2007	07-Aug-2007		
21-Sep-2007	24-Sep-2007		

The first depression in the monsoon season was formed on 21-Jun-2007 and landeded on 23-Jun-2007. The second depression was formed on 28-Jun-2007 and dissipated on 30-Jun-2007. The third depression was formed on 04-Jul-2007 and decayed on 09-Jul-2007. The fourth depression was formed on 05-Aug-2007 and dissipated on 07-Aug-2007. The last depression in the monsoon season was formed on 21-Sep-2007 and dissipated on 24-Sep-2007. The first depression in the non-monsoon season was, formed on 03-May-2007 and dissipated on 04-May-2007. The second depression was formed on 27-Oct-2007 and made landfall on 29-Oct-2007.

Table 6.3 List of Cyclones formed over AS during the monsoon and non-monsoon seasons in the PIOD years

Arabian Sea					
Monsoon			Non-monsoon		
Date of formation	Date of Intensification to Cyclone	Date of dissipation	Date of formation	Date of Intensification to Cyclone	Date of dissipation
25-Jun-2007	25-Jun-2007	26-Jun-2007			

Table (6.3) gives the list of cyclones formed over AS during the monsoon and non-monsoon seasons of the PIOD years. There was only 1 cyclone over AS formed in the monsoon season. It was formed on 25-Jun-2007, intensified into cyclone on 25-Jun-2007 and dissipated on 26-Jun-2007. Table (6.4) gives the list of cyclones formed over BB during the monsoon and non-monsoon seasons of the PIOD years. There was only 1 cyclone over BB, it is formed in the non-monsoon seasons. It was formed on 13-May-2007, intensified into cyclone on 14-May-2007 and made landfall on 15-May 2007.

Table 6.4 List of Cyclones formed over BB during the monsoon and non-monsoon seasons in the PIOD years

Bay of Bengal					
Monsoon			Non-monsoon		
Date of formation	Date of Intensification to Cyclone	Date of dissipation	Date of formation	Date of Intensification to Cyclone	Date of dissipation
			13-May-2007	14-May-2007	15-May 2007

Table 6.5 List of Severe cyclones formed over AS during the monsoon and non-monsoon seasons in the PIOD years

Arabian Sea					
Monsoon			Non-monsoon		
Date of formation	Date of Intensification to severe cyclone	Date of dissipation	Date of formation	Date of Intensification to severe cyclone	Date of dissipation
01-Jun-2007	02-Jun-2007	07-Jun-2007			

Table (6.5) gives the list of severe cyclones formed over AS during the monsoon and non-monsoon seasons of the PIOD years. There was only 1 severe cyclone over AS formed in the monsoon season. It was formed on 01-Jun-2007, intensified into severe cyclone on 02-Jun-2007 and dissipated on 07-Jun-2007. Table (6.6) gives the list of severe cyclones formed over BB during the monsoon and non-monsoon seasons of the PIOD years. There was only 1 severe cyclone over BB formed in the non-monsoon seasons. It was formed on 11-Nov-2007, intensified into severe cyclone on 12-Nov-2007 and landed on 15-Nov- 2007.

Table 6.6 List of Severe cyclones formed over BB during the monsoon and non-monsoon seasons in the PIOD years

Bay of Bengal					
Monsoon			**Non-monsoon**		
Date of formation	**Date of Intensification to severe cyclone**	**Date of dissipation**	**Date of formation**	**Date of Intensification to severe cyclone**	**Date of dissipation**
			11-Nov-2007	12-Nov-2007	15-Nov- 2007

6.3 Variations of CSGP for the convective systems over NIO during the PIOD years

Figure (6.2) shows the variations of CSGP for the convective systems over NIO during the monsoon and non-monsoon seasons of the PIOD years. From figure 6.2 (b), it is seen that the depression was formed against higher magnitude (1.6 x $10^{-10}s^{-2}$ °K) of CSGP. The higher magnitude of CSGP is also found over eastern AS and southern and central BB. From figure 6.2 (c), it is seen that the depressions were formed against lower magnitude (0.0 to 0.2 x $10^{-10}s^{-2}$ °K) of CSGP and the higher magnitudes are found over southern AS. From figure 6.2 (d), it is seen that the depressions were formed against higher magnitudes (0.0 to 1.0 x $10^{-10}s^{-2}$ °K) of CSGP. The higher magnitudes are also found over eastern BB. From figure 6.2 (i), it is observed that the severe cyclone was formed against higher magnitudes of CSGP. From figure 6.2 (l), it is seen that the severe cyclone was formed against higher magnitude (1.0 to 2.0 x $10^{-10}s^{-2}$ °K) of CSGP.

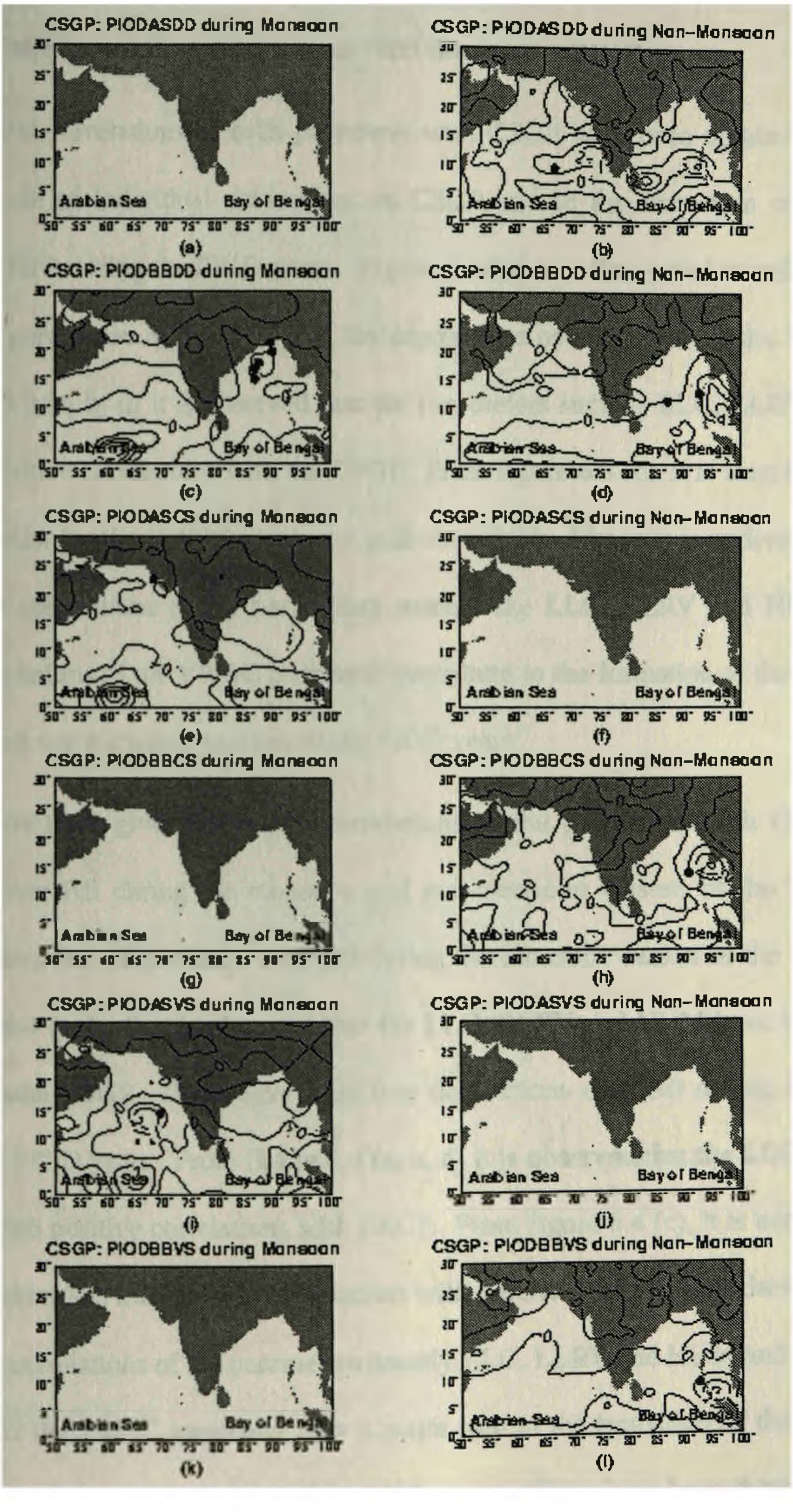

Figure 6.2 Variations of CSGP for the convective systems over NIO during the monsoon and non-monsoon seasons of the PIOD years

6.4 Spatial correlations of the air-sea interaction parameters with CSGP for the formation of the convective systems over NIO during the PIOD years

Spatial correlations of each parameter with CSGP have been obtained to analyse the relative role of individual parameters on CSGP and in the formation of convective systems over NIO during the PIOD years. Figure (6.3) shows the spatial correlations of the cyclogenesis parameters with CSGP for the depressions over AS during the PIOD years. From figure 6.3 (a, b, d) it is observed that the parameters such as LLC, LLRV and HUM have high positive correlations with the CSGP. From figure 6.3 (c), it is seen that negative correlations exist for the VWSC parameter with the CSGP. Hence it is understood that the high positive correlations of the parameters namely the LLC, LLRV and HUM and the negative correlations of the VWSC parameter contribute to the formation of the depressions over AS during non-monsoon seasons of the PIOD years.

Figure (6.4) gives the spatial correlations of the parameters with CSGP for the depressions over BB during the monsoon and non-monsoon seasons of the PIOD years. There have been four depressions over BB during the monsoon season of the PIOD years. From figure 6.4 (a, b, d) it is observed that the LLC, LLRV and HUM have high positive correlations with CSGP. There have been four depressions over BB during the monsoon season of the PIOD years. From figure 6.4 (a, b, d) it is observed that the LLC, LLRV and HUM have high positive correlations with CSGP. From figure 6.4 (c), it is noticed that the VWSC parameter has low positive correlations with CSGP. Hence it is understood that the high positive correlations of the parameters namely LLC, LLRV and HUM and low positive correlations of the VWSC parameter play a major role in the formation of the depressions over BB during the monsoon season of the PIOD years. There have been three depressions over BB during the non-monsoon seasons of the PIOD years.

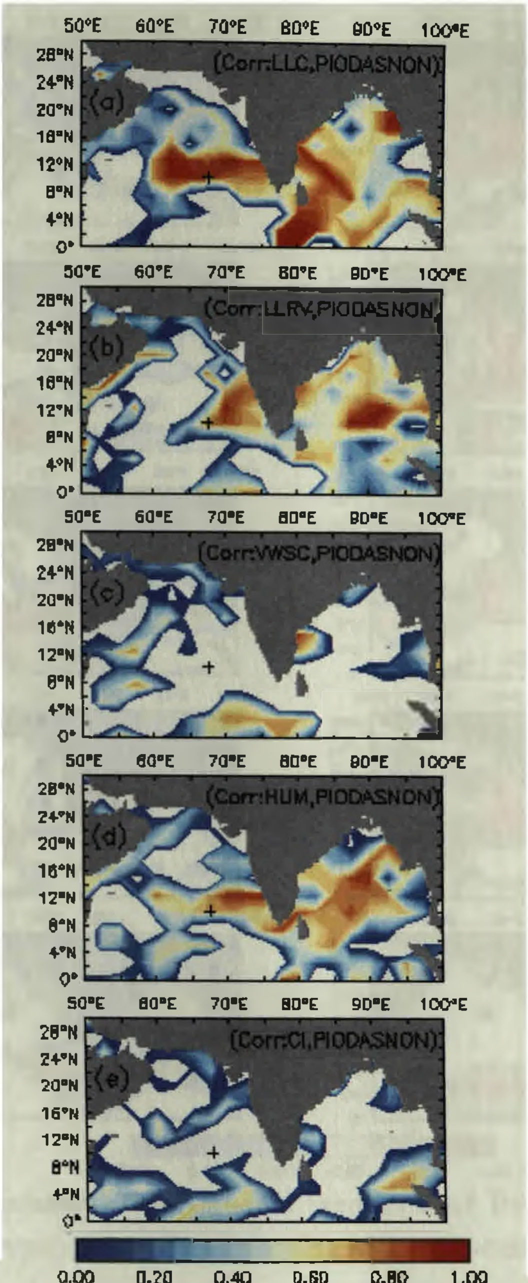

Figure 6.3 Spatial correlations of the parameters with CSGP for the depressions over AS during the non-monsoon seasons of the PIOD years

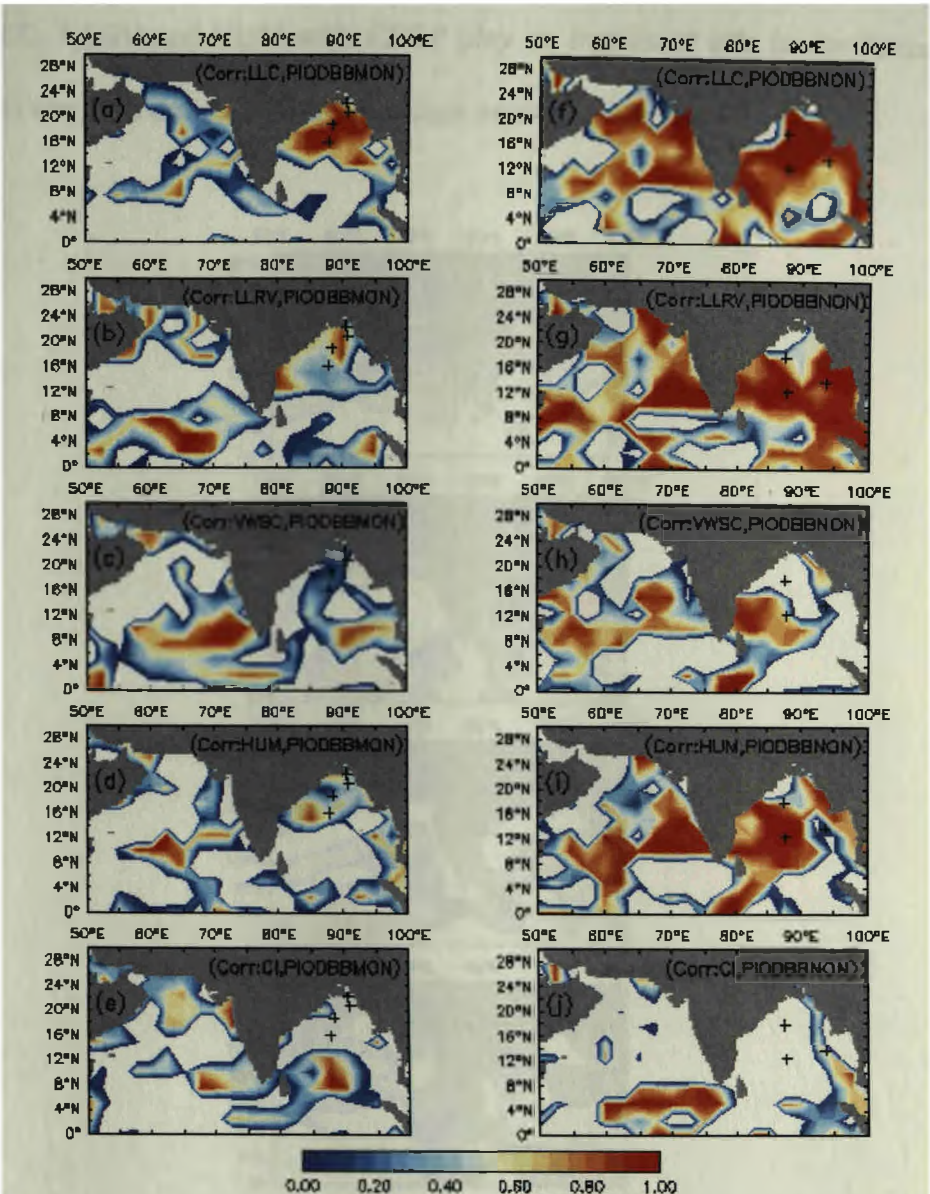

("+" represents the genesis locations of the depressions)

(BB= Bay of Bengal, PIOD=Positive IOD, MON=Monsoon, NON=Non−monsoon)

Figure 6.4 Spatial correlations of the parameters with CSGP for the depressions over BB during the monsoon and non-monsoon seasons of the PIOD years

From figure 6.4 (f, g, i) it is noticed that the parameters namely LLC, LLRV and HUM are having high positive correlations with the CSGP. From figure 6.4 (h) it is seen that there exist high positive correlations for the VWSC parameter with CSGP for one depression and there exist low positive correlations and negative correlations for the other two depressions. Hence it is known that the high positive correlations of the parameters, namely LLC, LLRV and HUM with CSGP play an important role in the formation of the depressions over BB during the non-monsoon seasons of the PIOD years.

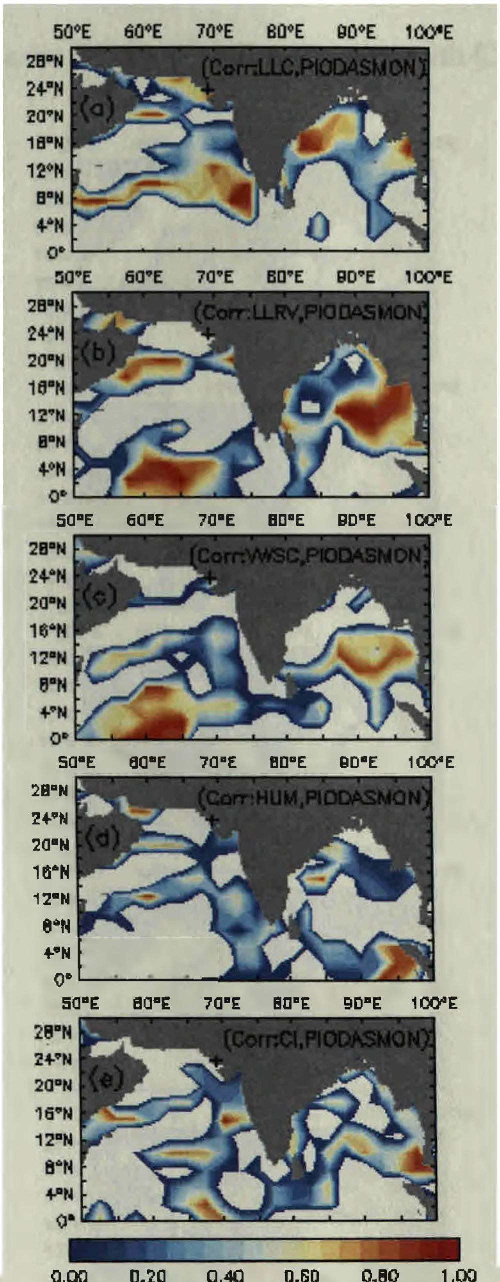

("+" represents the genesis locations of the cyclones)
(AS= Arabian Sea, PIOD=Positive IOD, MON=Monsoon)

Figure 6.5 Spatial correlations of the parameters with CSGP for the cyclones over AS during the monsoon season of the PIOD years

Figure (6.5) shows the spatial correlations of the cyclogenesis parameters with

CSGP for the cyclones formed over AS during the PIOD years. Only one cyclone was formed over AS during the PIOD years. From figure 6.5 (a) it is noticed that there exists a high positive correlation for LLC parameter with CSGP. From figure 6.5 (c), it is seen that low positive correlations exist for the VWSC parameter with CSGP.

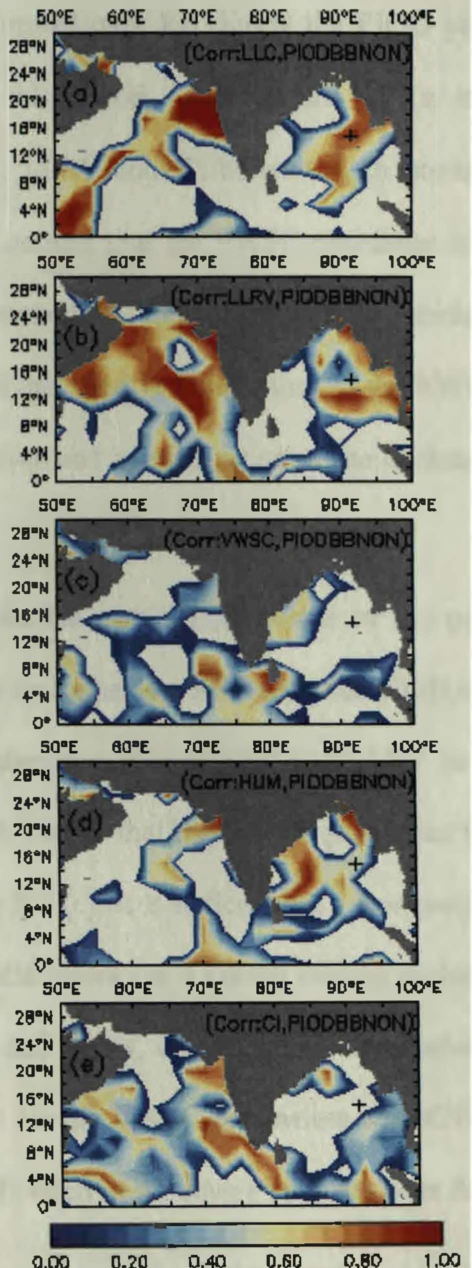

("+" represents the genesis locations of the cyclones)
(BB= Bay of Bengal, PIOD=Positive IOD, Non=Non–Monsoon)

Figure 6.6 Spatial correlations of the parameters with CSGP for the cyclones over BB during the non-monsoon seasons of the PIOD years

Hence it is known that the high positive correlations of the LLC parameter and low positive correlations of the VWSC parameter with CSGP contribute much to the formation and intensification of the cyclone over AS during the monsoon season of the PIOD years.

Figure (6.6) gives the spatial correlations of the cyclogenesis parameters with CSGP for the cyclones formed over BB during the PIOD years. Only one cyclone was formed over BB during this period. From figure 6.6 (a, b, d) it is observed that the parameters such as LLC, LLRV and HUM have high positive correlations with CSGP. From figure 6.6 (c), it is noticed that the VWSC parameter has negative correlations with CSGP. Hence it is understood that the higher positive correlations of the parameters such as LLC, LLRV, HUM and the negative correlations of the VWSC parameter makes a major contribution to the formation and intensification of the cyclones over BB during the PIOD years.

Figure (6.7) gives the spatial correlations of the ocean-atmospheric parameters with CSGP for the severe cyclones over AS during the PIOD years. From figure 6.7 (a, b), it is observed that the parameters namely LLC and LLRV have high positive correlations with CSGP. figure 6.7 (d) shows that the VWSC parameter has low positive correlations with CSGP. From figure 6.7 (c), it is noticed that a low positive correlation exists for the HUM parameter with CSGP. Hence it is known that the higher positive correlations for the parameters namely LLC and LLRV, lower positive correlations form the HUM parameter and negative correlations for the VWSC parameters with CSGP play an important role in the formation and intensification of the severe cyclones over AS during the PIOD years.

Figure (6.8) gives the spatial correlations of the air-sea interaction parameters with CSGP for the severe cyclone over BB during the PIOD years. From figure 6.8 (a, b, d) it is observed that the higher positive correlations of LLC, LLRV and HUM influence the formation of the severe cyclone over BB during the PIOD years.

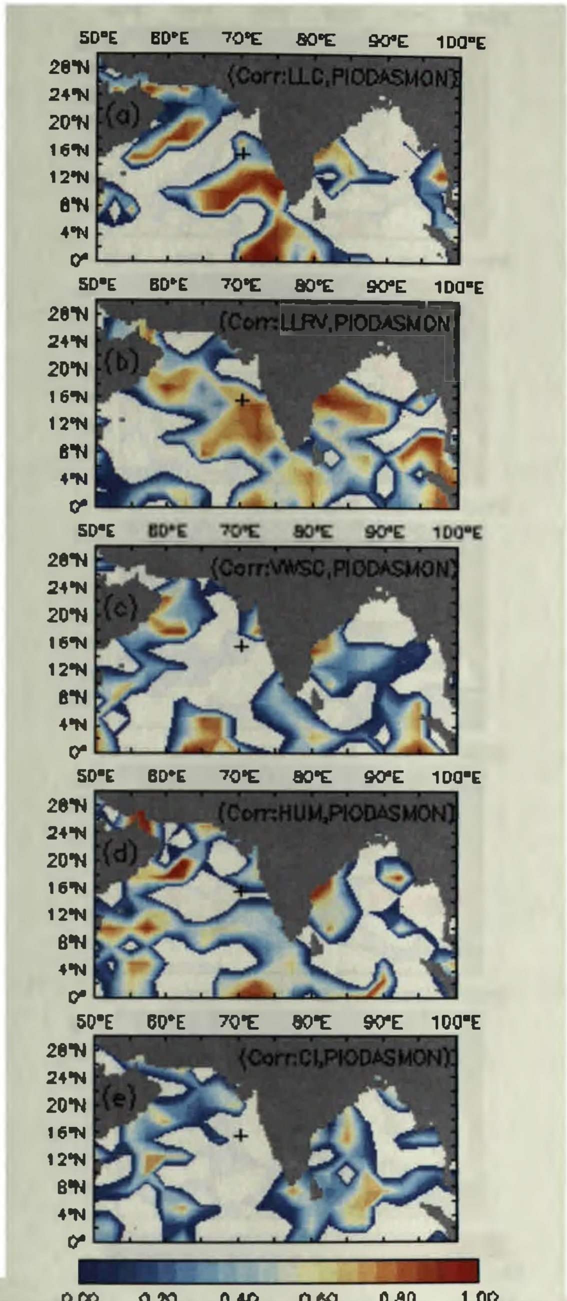

("+" represents the genesis locations of the severe cyclones)
(AS= Arabian Sea, PIOD=Positive IOD,MON=Monsoon)

Figure 6.7 Spatial correlations of the parameters with CSGP for the severe cyclones over AS during the non-monsoon seasons of the PIOD years

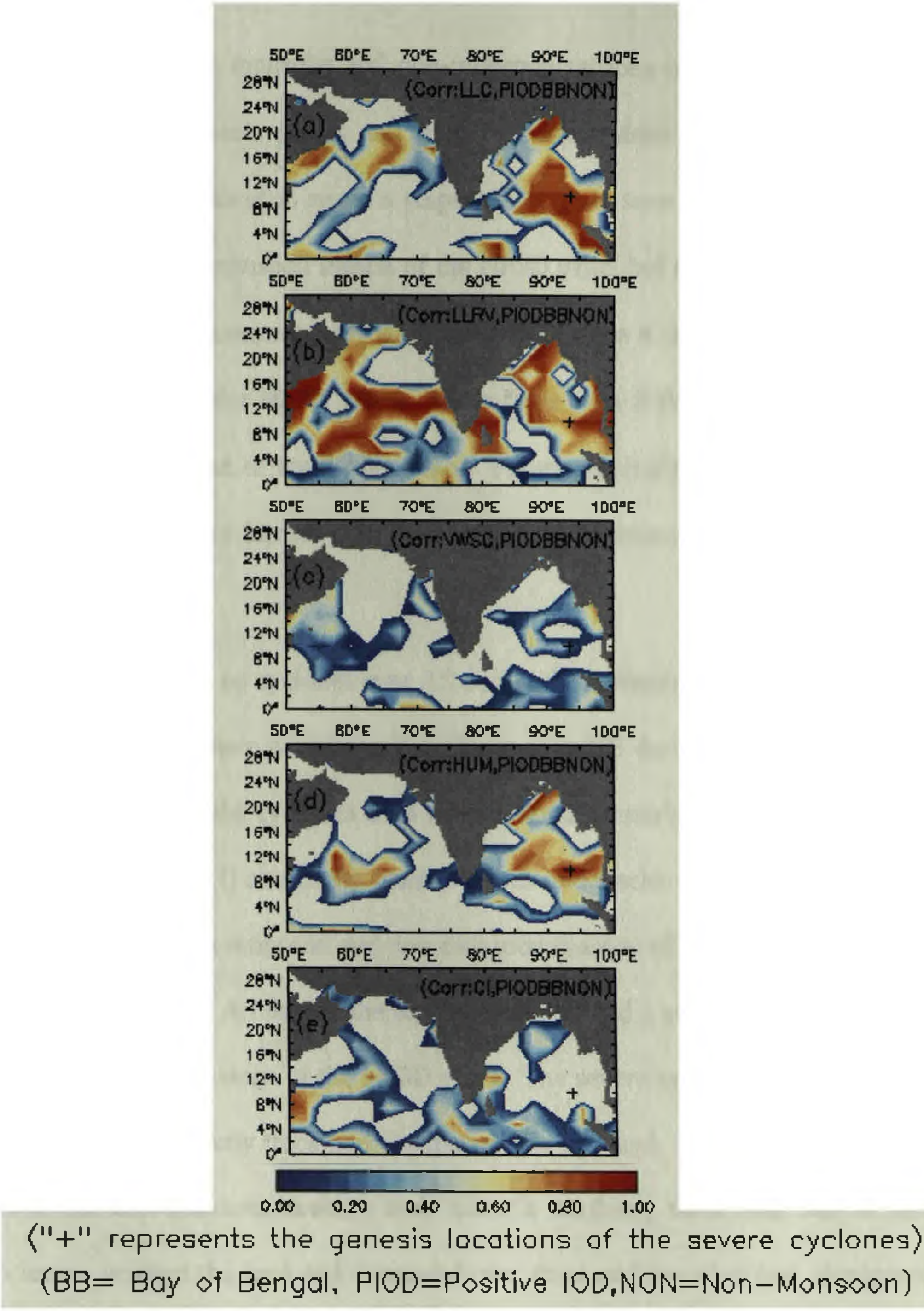

Figure 6.8 Spatial correlations of the parameters with CSGP for the severe cyclones over BB during the non-monsoon seasons of the PIOD years

6.5 Convective systems over NIO during the Negative Indian Ocean Dipole (NIOD) years

Figure (6.9) gives the genesis locations and the tracks of the convective systems over NIO during the monsoon and non-monsoon seasons of the NIOD years. Figure 6.9 (a,b) shows the genesis points and tracks of depressions formed over NIO during the monsoon and non-monsoon seasons respectively. It is seen that there is only 1 depression over AS during the monsoon season of the NIOD years but there were no depressions over AS during the non-monsoon seasons. There have been 4 depressions over BB during the monsoon season of the NIOD years. There have been 8 depressions over BB during the non-monsoon seasons of the NIOD years. Figure 6.9 (c,d) shows the genesis points and tracks of the cyclones formed over NIO during the monsoon and non-monsoon seasons of the NIOD years.

There were no cyclones over AS during the monsoon and non-monsoon seasons of the NIOD years. There have been 2 cyclones over BB during the monsoon season of the NIOD years. Both the cyclones have taken a north westerly track and dissipated over the land. Figure 6.9 (e,f) shows the genesis points and tracks of the severe cyclones formed over NIO during the monsoon and non-monsoon seasons of the NIOD years. There was 1 severe cyclone over AS during the monsoon season and 2 severe cyclones over AS during the non-monsoon seasons of the NIOD years. The severe cyclone over AS in the monsoon season took a northerly track and dissipated over the land. Both the severe cyclones over AS in the non-monsoon seasons have taken a northerly track, and one of these severe cyclones reached the land and dissipated over there and the other one dissipated over the northern AS. There were no severe cyclones over BB during the non-monsoon seasons of the NIOD years. But there have been 5 severe cyclones over BB during the non-monsoon seasons of the NIOD years. Out of the 5 severe cyclones, 4 took a westerly track and reached the land and dissipated over there. The other severe cyclone has taken a northerly track and dissipated over the land.

Figure: 6.9 Convective systems formed over NIO during the monsoon and non-monsoon

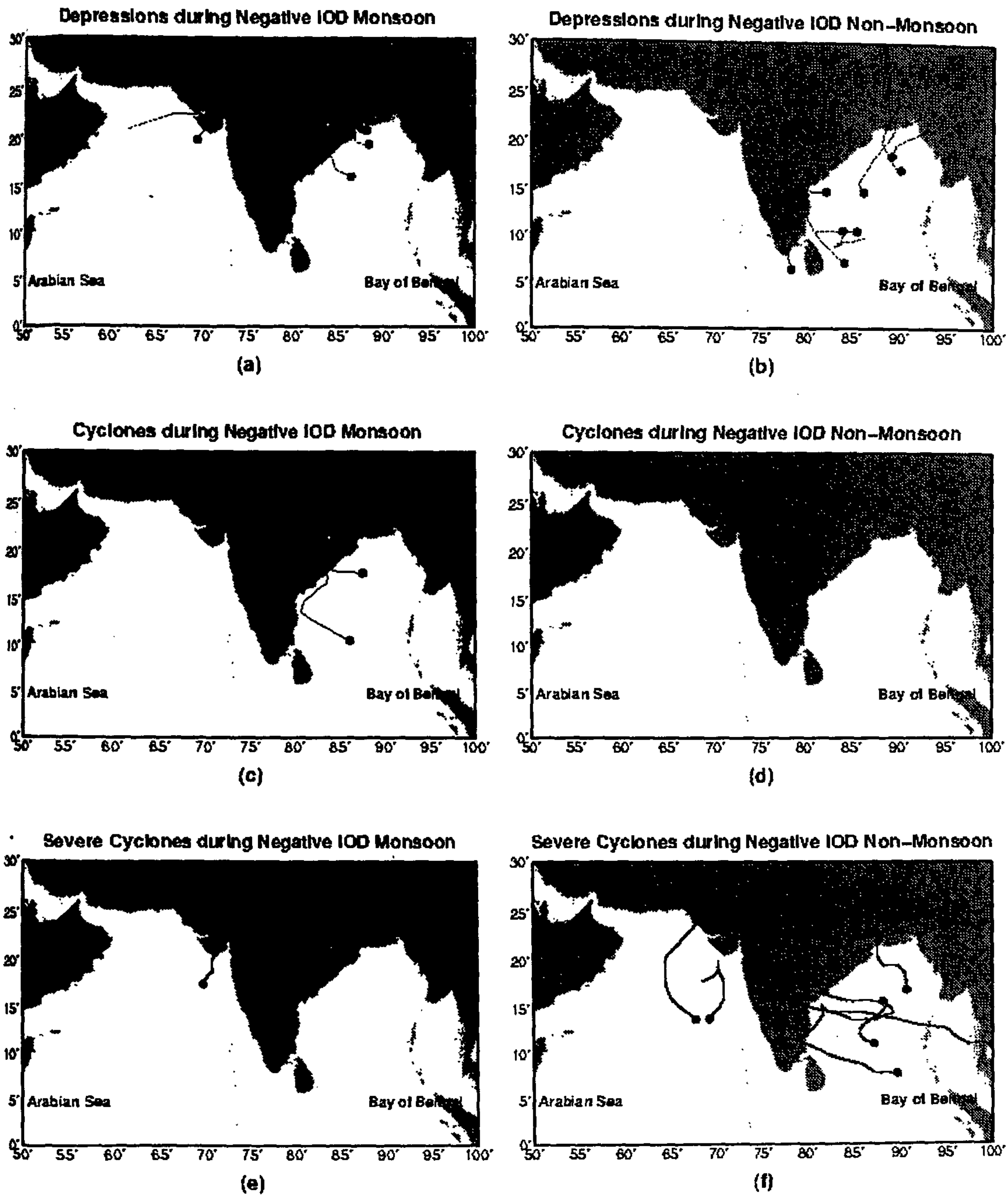

seasons of the NIOD years

Table (6.7) gives the list of the depressions formed over AS during the monsoon and non-monsoon seasons of the NIOD years. Only 1 depression formed over AS in the monsoon season. It was formed on 09-Jun-1989 and dissipated on 12-Jun-1989. Table (6.8) gives the list of all the depressions formed over BB during the monsoon and non-monsoon seasons of the NIOD years. There have been 4 depressions over BB during the monsoon season and 8 depressions during the non-monsoon seasons. In the year 1989, there have been 6 depressions over BB, in which 3 depressions formed during the monsoon season and 3 depressions formed during the non-monsoons seasons.

Table 6.7 List of Depressions formed over AS during the monsoon and non-monsoon seasons of the NIOD years

Arabian Sea			
Monsoon		**Non-monsoon**	
Date of formation	**Date of dissipation**	**Date of formation**	**Date of dissipation**
09-Jun-1989	12-Jun-1989		

The first depression in the monsoon season was formed on 12-Jun-1989 and dissipated on 14-Jun-1989. The second depression was formed on 20-Jun-1989 and decayed on 21-Jun-1989. The third depression was formed on 16-Aug-1989 and landed on 17-Aug-1989. The fourth depression was formed on 17-Jun-1993 and dissipated on 19-Jun-1993. There have been 8 depressions over BB during the non-monsoon seasons. The yearly frequency of the depressions is given as follows: In the year 1989, there were 3 depressions, in the year 1993 there were 2 depressions and in the year 1996 there were 3 depressions over BB. The first depression in the year 1989 formed on 17-Oct-1989 and dissipated on 18-Oct-1989. The second depression in the year formed on 11-Nov-1989 and decayed on 12-Nov-1989. The third depression in the year formed on 17-Nov-1989 and dissipated on 20-Nov-1989. The first depression in the year 1993 formed on 08-Nov-1993 and dissipated on 09-Nov-1993. The second depression in the year formed on 11-Nov-1993 and dissipated on 20-Dec-1993. The first depression in the year 1996 formed on 07-May-1996 and decayed on 08-May-1996. The second depression in the year formed on 01-Oct-1996 and dissipated on 02-Oct-1996. The third depression in the year formed on 27-Oct-1996 and decayed on 29-Oct-1996.

Table 6.8 List of Depressions formed over BB during the monsoon and non-monsoon seasons of the NIOD years

Bay of Bengal			
Monsoon		Non-monsoon	
Date of formation	Date of dissipation	Date of formation	Date of dissipation
12-Jun-1989	14-Jun-1989	17-Oct-1989	18-Oct-1989
20-Jun-1989	21-Jun-1989	11-Nov-1989	12-Nov-1989
16-Aug-1989	17-Aug-1989	17-Nov-1989	20-Nov-1989
17-Jun-1993	19-Jun-1993	08-Nov-1993	09-Nov-1993
		19-Dec-1993	20-Dec-1993
		07-May-1996	08-May-1996
		01-Oct-1996	02-Oct-1996
		27-Oct-1996	29-Oct-1996

There were no cyclones over AS during the NIOD years, but there have been 2 cyclones over BB during the NIOD years. Table (6.9) gives the list of cyclones formed over BB during the monsoon season of the NIOD years. The first cyclone was formed on 22-Aug-1989, intensified into cyclone on 22-Aug-1989 and landed on 25- Aug-1989. The second cyclone was formed on 12-Jun-1996 intensified into cyclone on 14-Jun-1996 and made landfall on 16- Jun-1996.

Table (6.10) gives the list of the severe cyclones formed over AS during the monsoon and non-monsoon seasons of the NIOD years. There was 1 severe cyclone formed over AS in the monsoon season of the NIOD years. It was formed on 17-Jun-1996, intensified into severe cyclone on 18-Jun-1996 and dissipated on 20-Jun-1996. There have been 2 severe cyclones over AS in the non-monsoon seasons. The first severe cyclone was formed on 12-Nov-1993, intensified into severe cyclone on 14-Nov-1993 and decayed on 15-Nov-1993. The second severe cyclone was formed on 22-Oct-1996, intensified into severe cyclone on 23-Oct-1996 and landed on 27-Oct-1996. Table (6.11) gives the list of severe cyclones formed over BB during the monsoon and non-monsoon seasons of the

NIOD years.

Table 6.9 List of Cyclones formed over BB during the monsoon and non-monsoon seasons of the NIOD years

Bay of Bengal					
Monsoon			Non-monsoon		
Date of formation	Date of Intensification to Cyclone	Date of dissipation	Date of formation	Date of Intensification to Cyclone	Date of dissipation
22-Aug-1989	22-Aug-1989	25- Aug-1989			
12-Jun-1996	14-Jun-1996	16- Jun-1996			

There were no severe cyclones over BB in the monsoon season. But there have been 5 severe cyclones over BB in the non-monsoon seasons. In the year 1989, there were 2 severe cyclones over BB. The first severe cyclone has formed on 23-May-1989, intensified into severe cyclone on 25-May-1989 and made landfall on 27-May-1989. The second severe cyclone was formed on 04-Nov-1989, intensified into severe cyclone on 04-Nov-1989 and dissipated on 09-Nov-1989.

In the year 1993, there was 1 severe cyclone over BB. It was formed on 01-Dec-1993, intensified into severe cyclone on 03-Dec-1993 and dissipated on 04-Dec-1993. In the year 1996, there have been 2 severe cyclones over BB. The first severe cyclone formed on 04-Nov-1996, intensified into severe cyclone on 05-Nov-1996 and dissipated on 07-Nov-1996. The second severe cyclone was formed on 28-Nov-1996, intensified into severe cyclone on 03-Dec-1996 and dissipated on 07-Dec-1996.

6.6 Variations of CSGP for the convective systems over NIO during the NIOD years

Figure 6.10 shows the variations of CSGP for the convective systems formed over

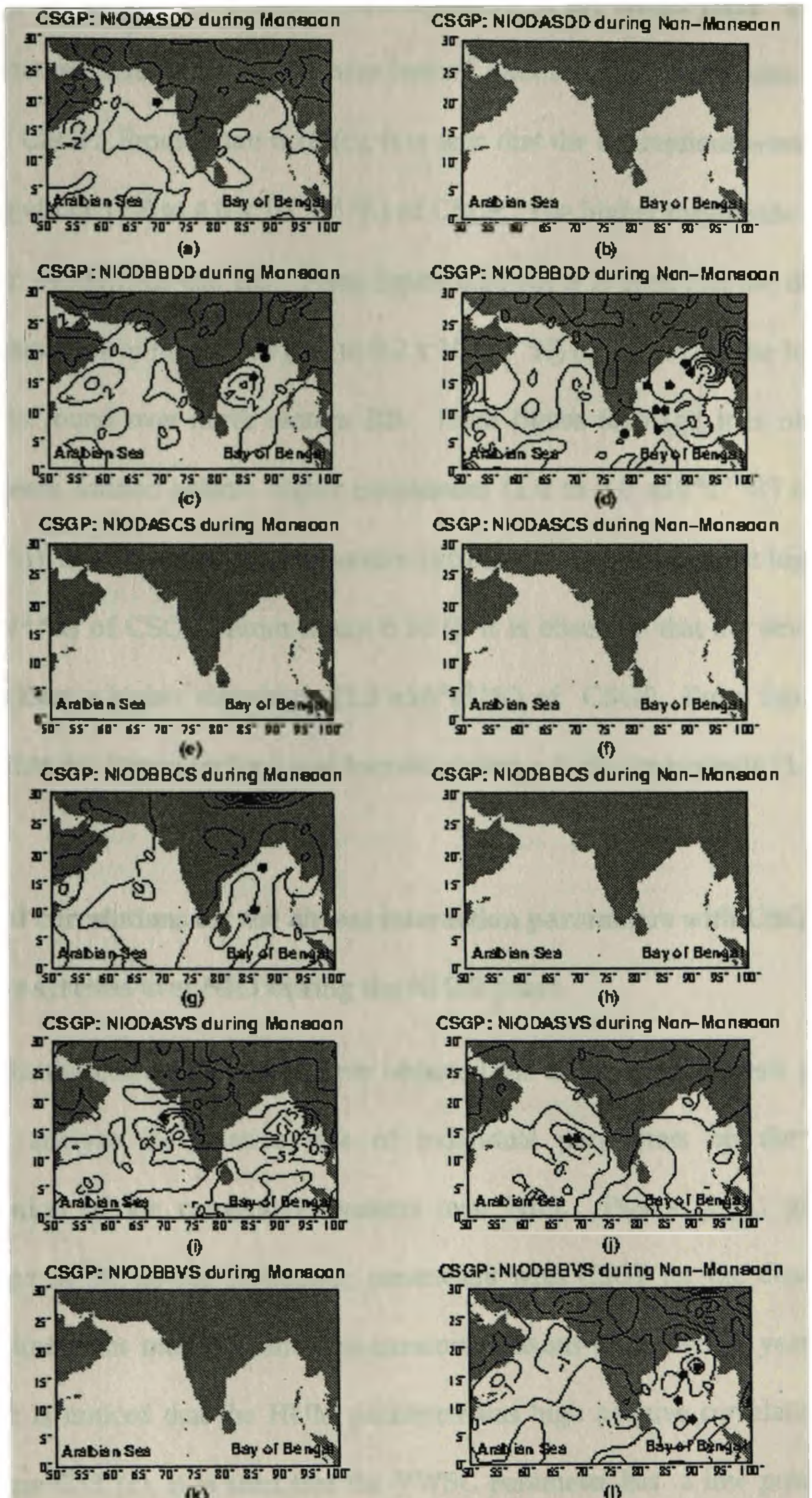

Figure 6.10 Variations of CSGP for the convective systems over NIO during the monsoon and non-monsoon seasons of the NIOD years

NIO during the monsoon and non-monsoon seasons of the NIOD years. From figure 6.10 (a) it is observed that the depression was formed against lower magnitudes (0.0 to 0.2 x $10^{-10}s^{-2}$ °K) of CSGP. From figure 6.10 (c), it is seen that the depressions were formed against higher magnitude (1.0 to 4.0 x $10^{-10}s^{-2}$ °K) of CSGP. The higher magnitude of CSGP is also found over western AS and BB. From figure 6.10 (d) it is seen that the depressions were formed against lower magnitude (0.0 to 0.2 x $10^{-10}s^{-2}$ °K) of CSGP and the higher magnitude of CSGP is found over north eastern BB. From figure 6.10 (g), it is observed that the cyclones were formed against higher magnitudes (1.0 to 2.0 x$10^{-6}s^{-2}$ °K) of CSGP. From figure 6.9 (i), it is observed that the severe cyclone was formed against higher magnitudes (5.0 x$10^{-6}s^{-2}$ °K) of CSGP. From figure 6.10 (j) it is observed that the severe cyclone has formed against a higher magnitude (1.0 x$10^{-6}s^{-2}$ °K) of CSGP. From figure 6.10 (l) it is observed that the severe cyclone was formed against a higher magnitude (1.0 x$10^{-6}s^{-2}$ °K) of CSGP.

6.7 Spatial correlations for the air-sea interaction parameters with CSGP for the convective systems over NIO during the NIOD years

Spatial correlations have been obtained for all the cyclogenesis parameters with CSGP to analyze the relative role of individual parameters on the formation and intensification of the convective systems over NIO. Figure (6.11) gives the spatial correlations of the air-sea interaction parameters with CSGP for the depressions formed over AS during the monsoon and non-monsoon seasons of the NIOD years. From figure 6.11 (d) it is noticed that the HUM parameter has high positive correlations with CSGP. From figure 6.11 (c), it is seen that the VWSC parameter has a low positive correlation with CSGP. Hence it is understood that the parameters such as HUM and VWSC play an important role in the formation of the depressions over AS during the NIOD years.

Table 6.10 List of Severe cyclones formed over AS during the monsoon and non-monsoon seasons in the NIOD years

Arabian Sea					
Monsoon			Non-monsoon		
Date of formation	Date of Intensification to severe cyclone	Date of dissipation	Date of formation	Date of Intensification to severe cyclone	Date of dissipation
17-Jun-1996	18-Jun-1996	20-Jun-1996	12-Nov-1993 22-Oct-1996	14-Nov-1993 23-Oct-1996	15-Nov-1993 27-Oct-1996

Table 6.11 List of Severe cyclones formed over BB during the monsoon and non-monsoon seasons of the NIOD years

Bay of Bengal					
Monsoon			Non-monsoon		
Date of formation	Date of Intensification to severe cyclone	Date of dissipation	Date of formation	Date of Intensification to severe cyclone	Date of dissipation
			23-May-1989	25-May-1989	27-May-1989
			04-Nov-1989	04-Nov-1989	09-Nov-1989
			01-Dec-1993	03-Dec-1993	04-Dec-1993
			04-Nov-1996	05-Nov-1996	07-Nov-1996
			28-Nov-1996	03-Dec-1996	07-Dec-1996

Figure (6.12) gives the spatial correlations of the ocean-atmospheric parameters with CSGP for the depressions over BB during the NIOD years. From figure 6.12 (a) it is noticed that the LLC parameter has high positive correlations with CSGP. From figure 6.12 (b, e) it is observed that the parameters LLRV and CI have low positive correlations with CSGP. From figure 6.12 (c), it is seen that the VWSC parameter has negative correlations with CSGP. Hence it is understood that the parameters such as LLC, LLRV, CI and negative correlations of the VWSC parameter contribute more to the formation of the depressions over BB during the monsoon season of the NIOD years.

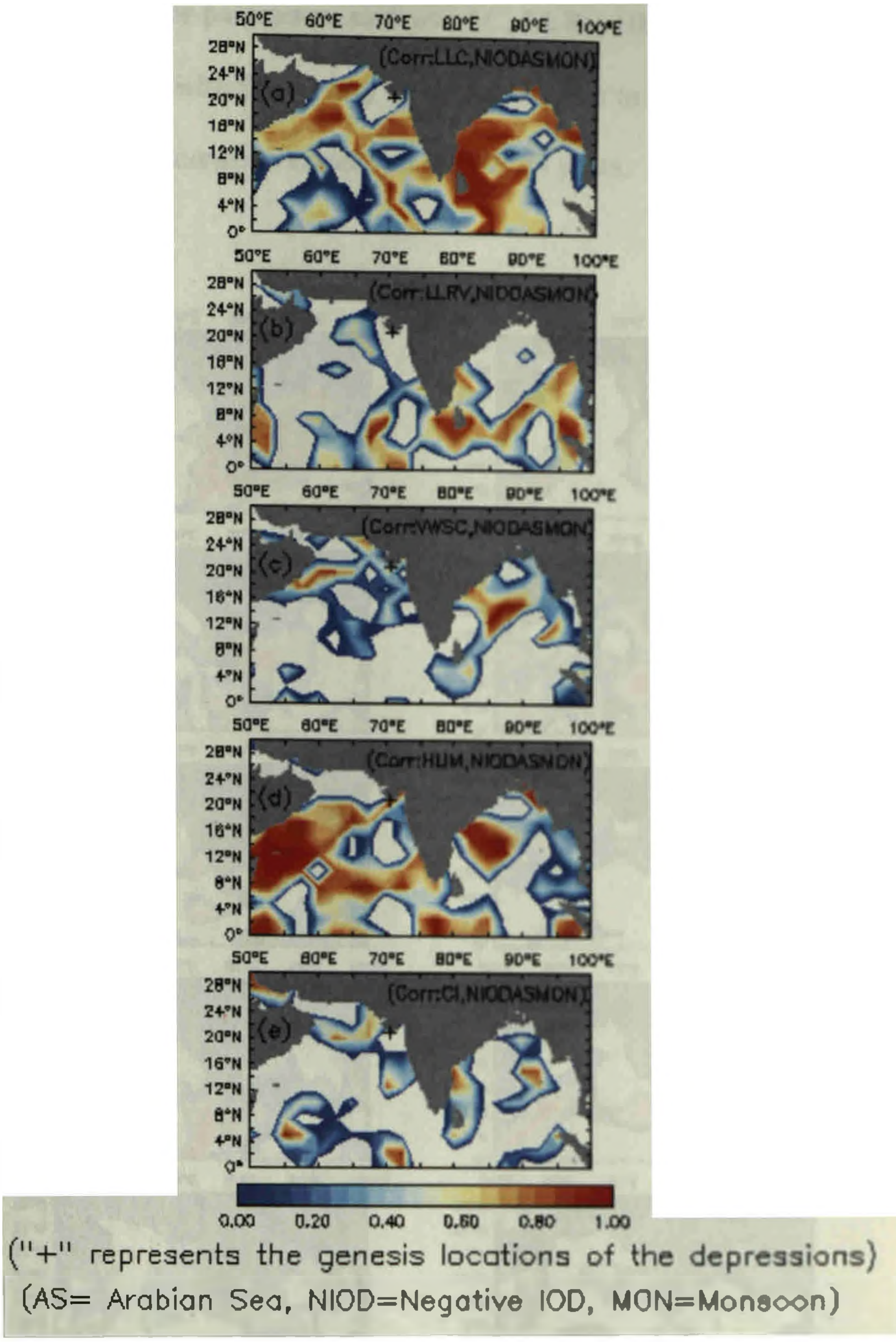

Figure 6.11 Spatial correlations of the parameters with CSGP for the depressions over AS during the monsoon season of the NIOD years

From figure 6.12 (f, g, i) it is observed that the parameters LLC, LLRV and HUM havelow positive correlations with CSGP. From figure 6.12 (h) it is seen that the VWSC parameter has negative correlations for most of the depressions. Hence it is understood that the low positive correlations of the parameters such as LLC, LLRV, HUM and negative correlations of the VWSC parameter with CSGP play an important role in the formation of depressions over BB during the non-monsoon seasons of the NIOD years.

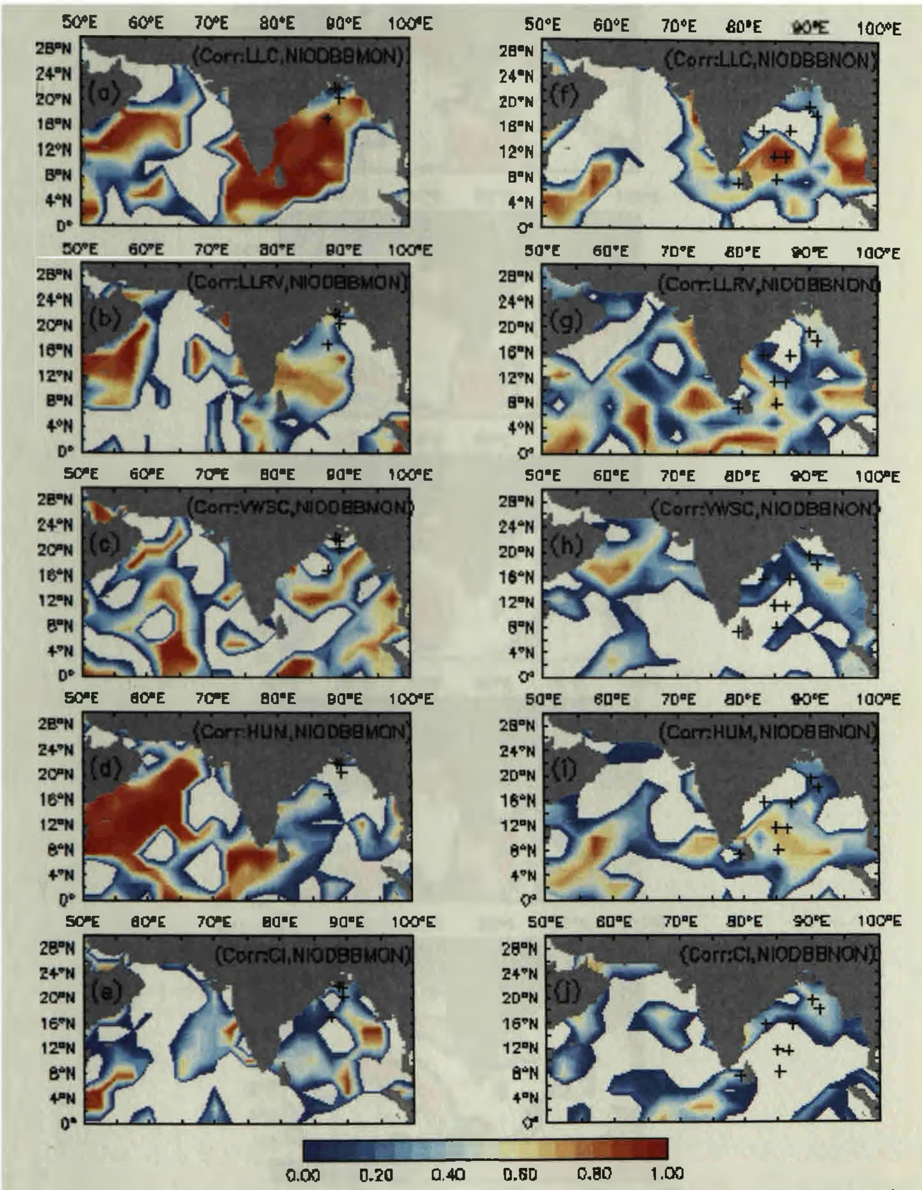

("+" represents the genesis locations of the depressions)

(BB= Bay of Bengal, NIOD=Negative IOD, MON=Monsoon, NON=Non-monsoon)

Figure 6.12 Spatial correlations of the parameters with CSGP for the depressions over BB during the monsoon and non-monsoon seasons of the NIOD years

Figure (6.13) shows the spatial correlations of the cyclogenesis parameters with

CSGP for the cyclones over BB during the NIOD years. From figure 6.13 (a, b, d) it is observed that the parameters such as LLC, LLRV and HUM have positive correlations with CSGP.

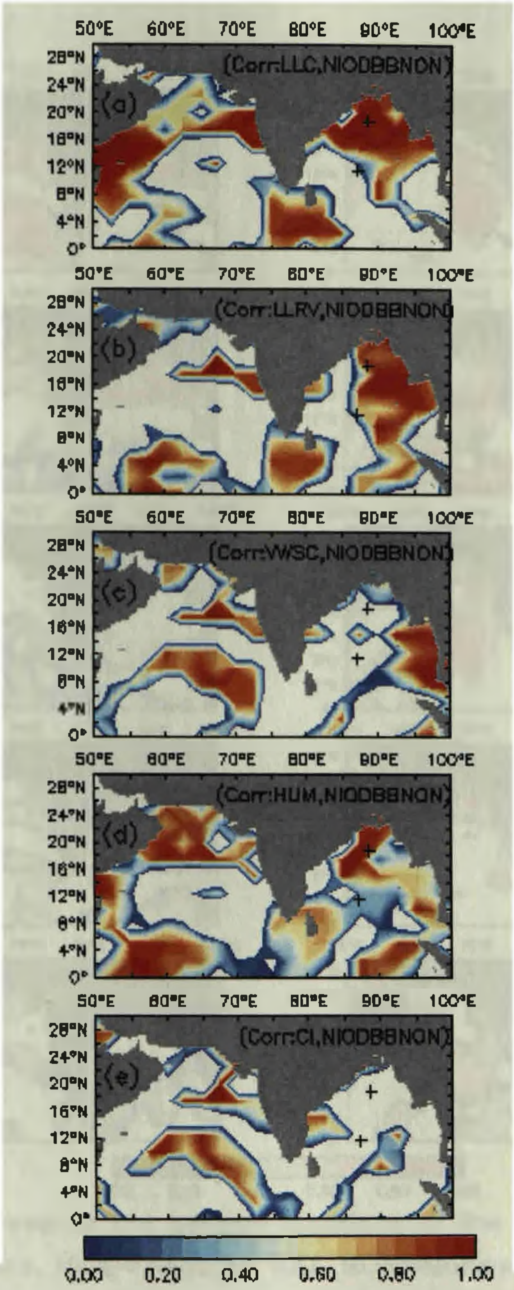

("+" represents the genesis locations of the cyclones)
(BB= Bay of Bengal, NIOD=Negative IOD, MON=Monsoon)

Figure 6.13 Spatial correlations of the parameters with CSGP for the cyclones over BB during the non-monsoon seasons of the NIOD years

From figure 6.13 (c), it is seen that the VWSC parameter has negative correlations with CSGP. Hence it is understood that the positive correlations of the parameters such as LLC, LLRV and HUM and negative correlations of the VWSC parameter contribute much to the formation and intensification of the cyclones over BB during the NIOD years.

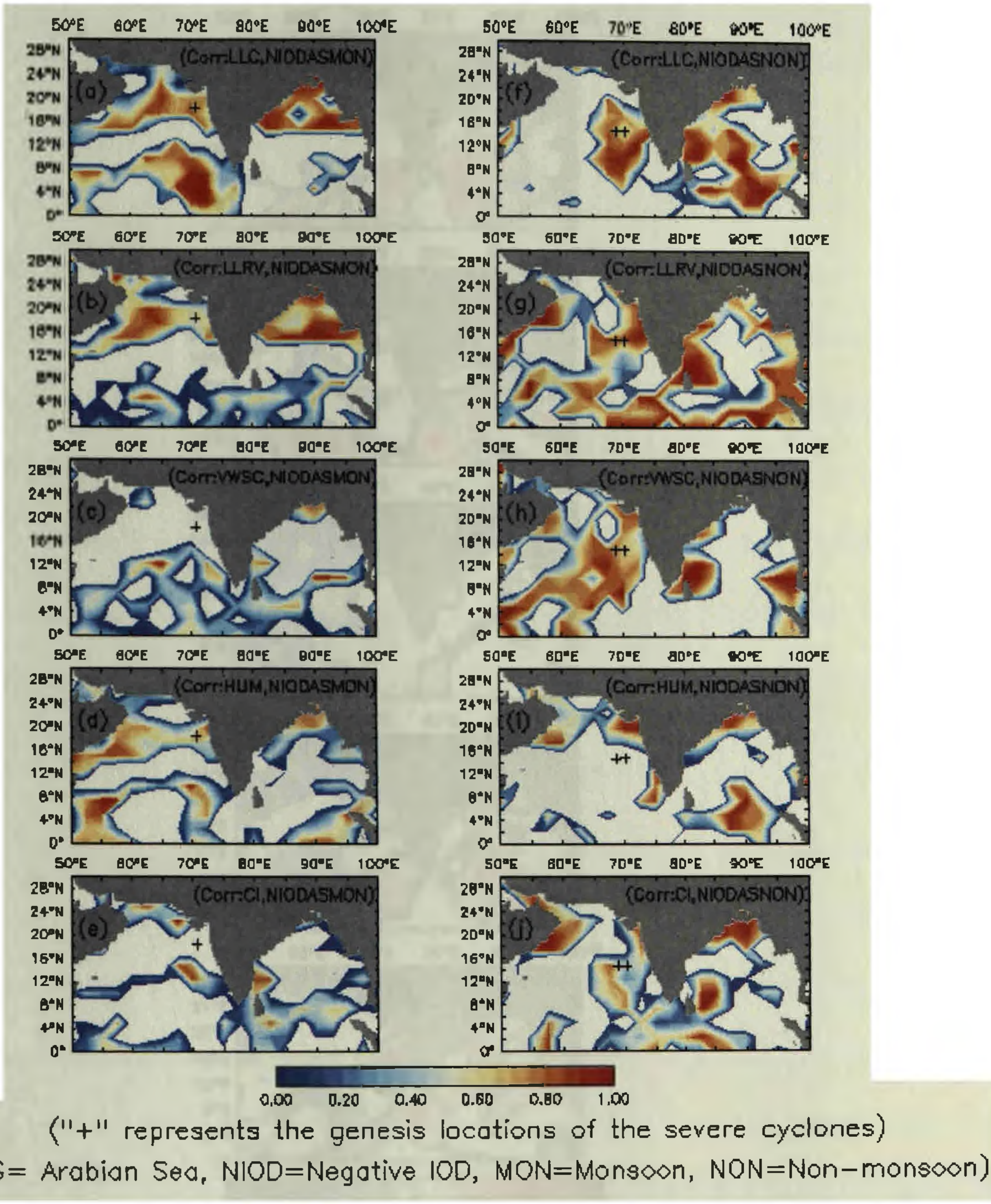

Figure 6.14 Spatial correlations of the parameters with CSGP for the severe cyclones over AS during the monsoon and non-monsoon seasons of the NIOD years

Figure (6.14) gives the spatial correlations of the ocean-atmospheric parameters with CSGP for the severe cyclones formed over AS during the monsoon and non-monsoon seasons of the NIOD years. From figure 6.14 (a, b, d) it is observed that the parameters namely LLC, LLRV and HUM are having high positive correlations with CSGP. From figure 6.14 (c), it is noticed that the VWSC parameter has negative correlations with CSGP.

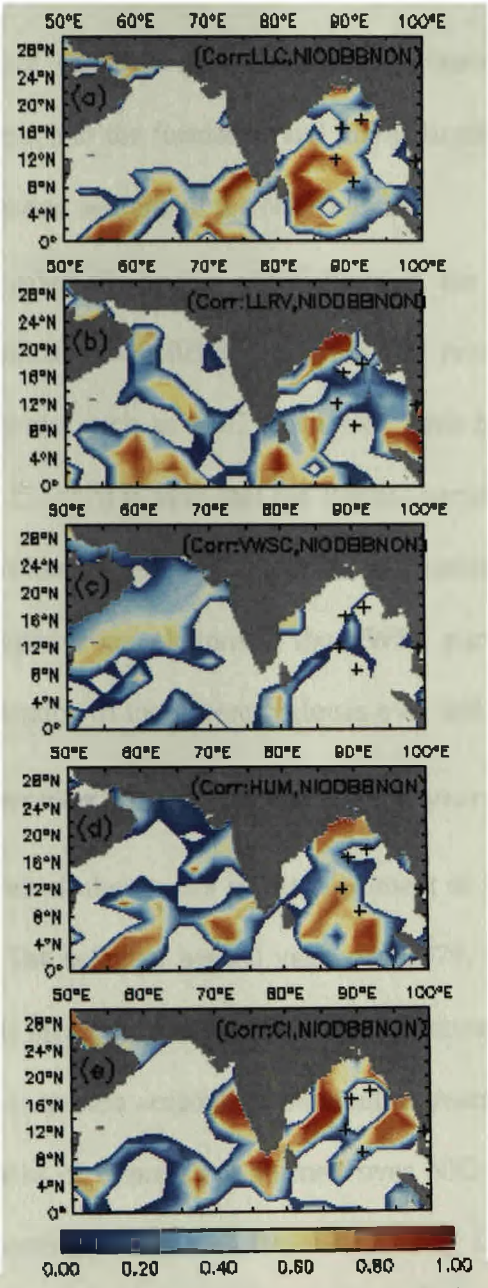

("+" represents the genesis locations of the severe cyclones)
(BB= Bay of Bengal, NIOD=Negative IOD, NON=Non-Monsoon)

Figure 6.15 Spatial correlations of the parameters with CSGP for the severe cyclones over BB during the non-monsoon seasons of the NIOD years

Hence it is understood that the high positive correlations of the parameters such as LLC, LLRV and HUM and negative correlations of the VWSC parameter with CSGP play a major role in the formation and intensification of the severe cyclones over AS during the NIOD years. From figure 6.14 (f, g, j) it is observed that the parameters LLC, LLRV and CI have a high positive correlations with CSGP. Hence it is understood that these parameters contribute much to the formation and intensification of the severe cyclones over AS during the non-monsoon seasons of the NIOD years.

Figure (6.15) gives the spatial correlations of the cyclogenesis parameters with CSGP for the severe cyclones over BB during the NIOD years. From figure 6.15 (a, d) it is noticed that the parameters such as LLC and HUM have high positive correlations with CSGP. From figure 6.15 (c), it is seen that the VWSC parameter has negative correlations with CSGP. Hence it is known that the high positive correlations of the parameters namely LLC and HUM and negative correlations of the VWSC parameter contribute much to the formation and intensification of the severe cyclones over BB during the NIOD years.

6.8 Convective systems over NIO during the neutral years

The years in which there were no establishment of ENSO and IOD are considered as the neutral years. The selected neutral years are 1979, 1980, 1985 and 2001. Figure (6.16) gives the genesis locations and the tracks of the convective systems over NIO during the monsoon and non-monsoon seasons of the neutral years. Figure 6.16 (a,b) shows the genesis points and tracks of depressions formed over NIO during the monsoon and non-monsoon seasons respectively. It is seen that there is only 1 depression over AS during the monsoon season of the neutral years and there have been 4 depressions over AS during the non-monsoon seasons. There have been 10 depressions over BB during the monsoon season and 6 depressions over BB during the non-monsoon seasons of the neutral years. figure 6.16 (c,d) shows the genesis points and tracks of the cyclones formed over NIO

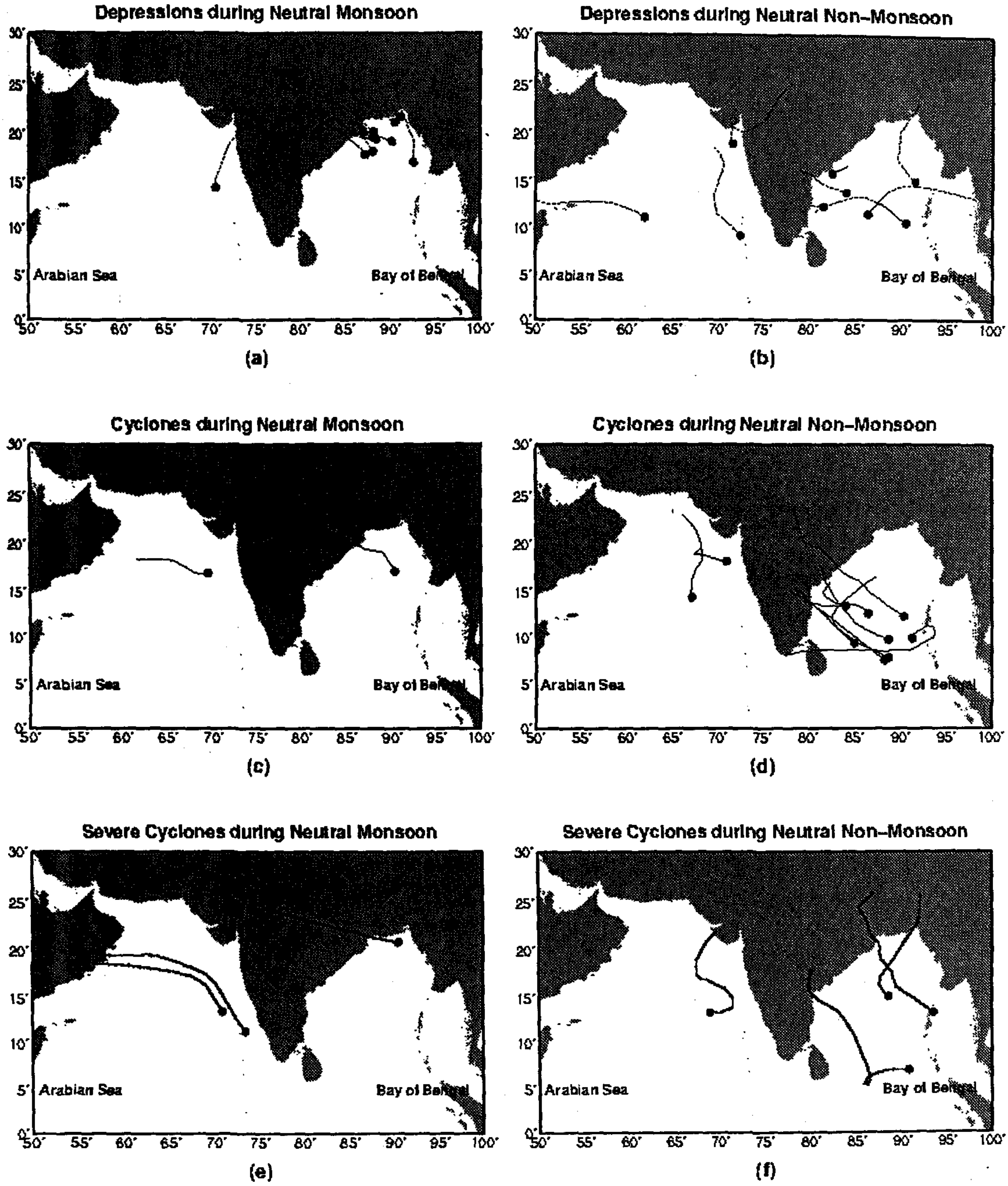

Figure 6.16 Convective systems formed over NIO during the monsoon and non-monsoon seasons of the neutral years

during the monsoon and non-monsoon seasons of the neutral years. There was 1 cyclone over AS during the monsoon season and 2 cyclones over AS during the non-monsoon seasons of the neutral years. It is found that there was 1 cyclone over BB during the monsoon season and 8 cyclones over BB during the non-monsoon seasons of the neutral years. Figure 6.16 (e,f) shows the genesis points and tracks of the severe cyclones formed over NIO during the monsoon and non-monsoon seasons of the neutral years. There have been 2 severe cyclones over AS during the monsoon season and 1 severe cyclone over AS during the non-monsoon seasons of the neutral years. The 2 severe cyclones over AS formed during the monsoon season have taken a westerly track and reached the Oman coast and dissipated over there. It is also found that there was 1 severe cyclone over BB during the monsoon season and 3 severe cyclones over BB in the non-monsoon seasons of the neutral years. It was formed on 04-Jun-1980 and dissipated on 06-Jun-1980. There have been 4 depressions over AS during the non-monsoon seasons of the neutral years. The first depression was formed on 13-Nov-1979 and decayed on 17-Nov-1979. In the year 1980, there were 2 depressions over AS during this period. The first depression in this year was formed on 14-Oct-1980 and dissipated on 18-Oct-1980. The second depression was formed on 14-Nov-1980 and decayed on 20-Nov-1980. The last depression was formed on 06-Oct-1985 and dissipated on 09-Oct-1985.

Table 6.12 List of Depressions formed over AS during the monsoon and non-monsoon seasons of the neutral years

Arabian Sea			
Monsoon		**Non-monsoon**	
Date of formation	**Date of dissipation**	**Date of formation**	**Date of dissipation**
04-Jun-1980	06-Jun-1980	13-Nov-1979	17-Nov-1979
		14-Oct-1980	18-Oct-1980
		14-Nov-1980	20-Nov-1980
		06-Oct-1985	09-Oct-1985

Table (6.12) gives the list of the depressions formed over AS during the monsoon and non-monsoon seasons of the neutral years. There was only 1 depression over AS during the monsoon season of the neutral years. Table (6.13) gives the list of all the depressions formed over BB during the monsoon and non-monsoon seasons of the neutral years. There were 10 depressions over BB during the monsoon season and 6 depressions during the non-monsoon seasons. In the year 1979, there were 5 depressions over BB, in which 4 depressions formed during the monsoon season and 1 depression formed during the non-monsoon seasons.

Table 6.13 List of Depressions formed over BB during the monsoon and non-monsoon seasons of the neutral years

Bay of Bengal			
Monsoon		**Non-monsoon**	
Date of formation	**Date of dissipation**	**Date of formation**	**Date of dissipation**
23-Jun-1979	26-Jun-1979	29-Oct-1979	01-Nov-1979
28-Jun-1979	01-Jul-1979	15-May-1980	19-May-1980
07-Jul-1979	08-Jul-1979	01-Oct-1980	04-Oct-1980
12-Aug-1979	15-Aug-1979	01-Oct-1985	02-Oct-1985
26-Aug-1980	27-Aug-1980	12-Nov-1985	13-Nov-1985
16-Sep-1980	21-Sep-1980	11-Nov-2001	12-Nov-2001
01-Aug-1985	02-Aug-1985		
06-Aug-1985	09-Aug-1985		
14-Aug-1985	15-Aug-1985		
12-Jun-2001	13-Jun-2001		

The first depression in the monsoon season was formed on 23-Jun-1979 and dissipated on 26-Jun-1979. The second depression was formed on 28-Jun-1979 and decayed on 01-Jul-1979. The third depression was formed on 07-Jul-1979 and landed on 08-Jul-1979. The fourth depression was formed on 12-Aug-1979 and made landfall on 15-Aug-1979. The depression in the non-monsoon seasons was formed on 29-Oct-1979 and dissipated on 01-Nov-1979. In the year 1980, there were 4 depressions over BB, in which 2 depressions formed during the monsoon season and the other 2 depressions formed during the non-monsoons seasons. The first depression in the monsoon season was formed on 26-Aug-1980 and dissipated on 27-Aug-1980. The second depression was formed on 16-Sep-1980 and landed on 21-Sep-1980. There have been 2 depressions over BB during the non-monsoon seasons, the first depression in the non-monsoon season was formed on 15-May-1980 and dissipated on 19-May-1980. The second depression was formed on 01-Oct-1980 and decayed on 04-Oct-1980.

In the year 1985, there were 5 depressions over BB, in which 3 depressions formed during the monsoon season and 2 depressions formed during the non-monsoons seasons. The first depression in the monsoon season was formed on 01-Aug-1985 and dissipated on 02-Aug-1985. The second depression was formed on 06-Aug-1985 and landed on 09-Aug-1985. The third depression was formed on 14-Aug-1985 and made landfall on 15-Aug-1985. There have been 2 depressions over BB during the non-monsoon seasons. The first depression in the non-monsoon season was formed on 01-Oct-1985 and dissipated on 02-Oct-1985. The second depression was formed on 12-Nov-1985 and decayed on 13-Nov-1985. In the year 2001, there were 2 depressions over BB in which 1 depression was formed during the monsoon season and the other depression was formed during the non-monsoon seasons. The depression in the monsoon season was formed on 12-Jun-2001 and dissipated on 13-Jun-2001 and the depression in the non-monsoon season was formed on 11-Nov-2001 and decayed on 12-Nov-2001.

Table (6.14) gives the list of the cyclones formed over AS during the neutral years. There were 3 cyclones over AS during the neutral years. In which 1 cyclone formed during the monsoon season and 2 cyclones formed during the non-monsoon seasons. The cyclone in the monsoon season formed on 24-Sep-2001, intensified into cyclone on 25-Sep-2001 and dissipated on 28-Sep-2001. The first cyclone in the non-monsoon season was formed on 28-May-1985, intensified into cyclone on 29-May-1985 and decayed on 31- May-1985. The second cyclone in the non-monsoon season was formed on 08-Oct-2001, intensified into cyclone on 09-Oct-2001 and dissipated on 10-Oct-2001.

Table 6.14 List of Cyclones formed over AS during the monsoon and non-monsoon seasons of the neutral years

Arabian Sea					
Monsoon			Non-monsoon		
Date of formation	Date of Intensification to Cyclone	Date of dissipation	Date of formation	Date of Intensification to Cyclone	Date of dissipation
24-Sep-2001	25-Sep-2001	28-Sep-2001	28-May-1985	29-May-1985	31- May-1985
			08-Oct-2001	09-Oct-2001	10-Oct-2001

Table 6.15 List of Cyclones formed over BB during the monsoon and non-monsoon seasons in the neutral years

Bay of Bengal					
Monsoon			Non-monsoon		
Date of formation	Date of Intensification to cyclone	Date of dissipation	Date of formation	Date of Intensification to cyclone	Date of dissipation
19-Sep-1985	20-Sep-1985	21-Sep-1985	23-Nov-1979	24-Nov-1979	26-Nov-1979
			16-Oct-1980	17-Oct-1980	19-Oct-1980
			03-Dec-1980	04-Dec-1980	07-Dec-1980
			12-Dec-1980	15-Dec-1980	19-Dec-1980
			09-Oct-1985	10-Oct-1985	12-Oct-1985
			15-Nov-1985	16-Nov-1985	17-Nov-1985
			12-Dec-1985	12-Dec-1985	14-Dec-1985
			15-Oct-2001	15-Oct-2001	16-Oct-2001

Table (6.15) gives the list of cyclones formed over BB during the monsoon and non-monsoon seasons of the neutral years. There was 1 cyclone over BB during the monsoon season. There have been 8 cyclones over BB during the non-monsoon seasons of the neutral years. The cyclone in the monsoon season was formed on 19-Sep-1985, intensified into cyclone on 20-Sep-1985 and decayed on 21-Sep-1985. The first cyclone in the non-monsoon seasons was formed on 23-Nov-1979, intensified into cyclone on 24-Nov-1979 and landed on 26-Nov-1979. In the year 1980, there were 3 cyclones over BB during the non-monsoon seasons. The first cyclone was formed on 16-Oct-1980, intensified into cyclone on 17-Oct-1980 and dissipated on 19-Oct-1980. The second cyclone was formed on 03-Dec-1980, intensified into cyclone on 04-Dec-1980 and dissipated on 07-Dec-1980. The third cyclone was formed on 12-Dec-1980, intensified into cyclone on 15-Dec-1980 and made landfall on 19-Dec-1980. In the year 1985, there were 3 cyclones over BB during the non-monsoon seasons. The first cyclone was formed on 09-Oct-1985, intensified into cyclone on 10-Oct-1985 and dissipated on 12-Oct-1985. The second cyclone was formed on 15-Nov-1985, intensified into cyclone on 16-Nov-1985 and dissipated on 17-Nov-1985. The third cyclone was formed on 12-Dec-1985, intensified into cyclone on 12-Dec-1985 and landed on 14-Dec-1985. The last cyclone in the non-monsoon seasons was formed on 15-Oct-2001, intensified into cyclone on 15-Oct-2001 and made landfall on 16-Oct-2001.

Table (6.16) gives the list of severe cyclones formed over AS during the monsoon season of the neutral years. There were 2 severe cyclones over AS during the monsoon season and 1 severe cyclone during the non-monsoon seasons. The first severe cyclone in the monsoon season was formed on 16-Jun-1989, intensified into severe cyclone on 18-Jun-1989 and dissipated on 20-Jun-1989. The second severe cyclone in the monsoon season was formed on 18-Sep-1989, intensified into severe cyclone on 22-Sep-1989 and decayed on 24-Sep-1989. The severe cyclone in the non-monsoon season was formed on 21-May-2001, intensified into severe cyclone on 22-May-2001 and landed on 28-May-2001.

Table 6.16 List of Severe cyclones formed over AS during the monsoon and non-monsoon seasons of the neutral years

Arabian Sea					
Monsoon			**Non-monsoon**		
Date of formation	**Date of Intensification to severe cyclone**	**Date of dissipation**	**Date of formation**	**Date of Intensification to severe cyclone**	**Date of dissipation**
16-Jun-1989	18-Jun-1989	20-Jun-1989	21-May-2001	22-May-2001	28-May-2001
18-Sep-1989	22-Sep-1989	24-Sep-1989			

Table 6.17 List of Severe cyclones formed over BB during the monsoon and non-monsoon seasons of the neutral years

Bay of Bengal					
Monsoon			**Non-monsoon**		
Date of formation	**Date of Intensification to severe cyclone**	**Date of dissipation**	**Date of formation**	**Date of Intensification to severe cyclone**	**Date of dissipation**
06-Aug-1979	07-Aug-1979	10-Aug-1979	06-May-1979	07-May-1979	13-May-1979
			22-May-1985	24-May-1985	25-May-1985
			14-Oct-1985	15-Oct-1985	17-Oct-1985

Table (6.17) gives the list of the severe cyclones formed over BB during the monsoon and non-monsoon seasons of the neutral years. There was 1 severe cyclone over BB during the monsoon season and 3 severe cyclones during the non-monsoon seasons of the neutral years. The severe cyclone in the monsoon season was formed on 06-Aug-1979, intensified into severe cyclone on 07-Aug-1979 and dissipated on 10-Aug-1979. The first severe cyclone in the non-monsoon seasons was formed on 06-May-1979, intensified into severe cyclone on 07-May-1979 and dissipated on 13-May-1979. The second severe cyclone in the non-monsoon seasons was formed on 22-May-1985, intensified into severe cyclone on 24-May-1985and dissipated on 25-May-1985. The third severe cyclone in the non-monsoon seasons was formed on 14-Oct-1985, intensified into severe cyclone on 15-

Oct-1985 and dissipated on 17-Oct-1985.

6.9 Variations of CSGP for the convective systems over NIO during the neutral years

Figure 6.17 (a, b, c, d) gives the variations of CSGP for the depressions over the NIO during the monsoon and non-monsoons seasons of the neutral years. From figure 6.17 (a) it is observed that the depression was formed against lower magnitudes (0.2 $x10^{-6}s^{-2}$ °K) of CSGP and the higher magnitudes are found over southern AS. From figure 6.17 (b) it is observed that the depressions were formed against a lower magnitude (0.0 to 0.2 $x10^{-6}s^{-2}$ °K) of CSGP and the higher magnitudes are observed over southern BB. From figure 6.15 (c) it is observed that the depressions were formed against a higher magnitude (0.0 to 2.0 $x10^{-6}s^{-2}$ °K) of CSGP. From figure 6.17 (d) it is observed that the depressions have formed against a lower magnitude (0.0 to 0.2 $x10^{-6}s^{-2}$ °K) of CSGP and the higher magnitudes are observed over the land.

Figure 6.17 (e, f, g, h) gives the variations of CSGP for the cyclones over the NIO during the monsoon and non-monsoons seasons of the neutral years. From figure 6.17 (e), it is observed that the cyclone was formed against lower magnitudes (0.0 to 0.1 $x10^{-6}s^{-2}$ °K) of CSGP. From figure 6.17 (f), it is observed that the cyclones have formed against a lower magnitude (0.0 to 0.2 $x10^{-6}s^{-2}$ °K) of CSGP. From figure 6.17 (g) it is observed that the cyclone was formed against a lower magnitude (0.2 to 0.5 $x10^{-6}s^{-2}$ °K) of CSGP and the higher magnitudes are found over eastern BB.From figure 6.15 (h) it is observed that the cyclones were formed against a higher magnitude (1.0 to 4.0 $x10^{-6}s^{-2}$ °K) of CSGP.

Figure 6.17 (i, j, k, l) gives the variations of CSGP for the severe cyclones over the NIO during the monsoon and non-monsoon seasons of the neutral years. From figure 6.17 (i), it is observed that the severe cyclone was formed against higher magnitudes (2.0 $x10^{-6}s^{-2}$ °K) of CSGP. From figure 6.17 (j), it is observed that the severe cyclone was formed against lower magnitude (0.0 to 0.2 $x10^{-6}s^{-2}$ °K) of CSGP.

Figure 6.17 Variations of CSGP for the convective systems over NIO during the monsoon and non-monsoon seasons of the neutral years

From figure 6.17 (k), it is observed that the severe cyclone was formed against higher magnitude (1.0 to 2.0 $x10^{-6}s^{-2}$ °K) of CSGP. From figure 6.17 (l) it is observed that the severe cyclones were formed against a higher magnitude (0.0 to 2.0 $x10^{-6}s^{-2}$ °K) of CSGP.

6.10 Spatial correlations for the air-sea interaction parameters with CSGP for the convective systems over NIO during the neutral years

Figure (6.18) gives the spatial correlations of the cyclogenesis parameters with CSGP for the formation of depressions over AS during the monsoon and non-monsoon seasons of the neutral years. From figure 6.18 (a, d) it is observed that the parameters LLC and HUM have high positive correlations with CSGP. Hence it is understood that these parameters contribute much for the formation of depressions over AS during the monsoon season of the neutral years. There have been 3 depressions over AS during the non-monsoon seasons of the neutral years. From figure 6.18 (f, g) it is observed that the parameters such as LLC and LLRV have positive correlations with CSGP for two of these depressions. Hence it is understood that the positive correlations of LLC and LLRV with CSGP have a major role in the formation of the depressions over AS during the non-monsoon seasons of the neutral years.

Figure (6.19) shows the spatial correlations of the air-sea interaction parameters with CSGP for the formation of depressions over BB during the monsoon and non-monsoon seasons of the neutral years. From figure 6.19 (a, b) it is noticed that the parameters LLC and LLRV have high positive correlations with CSGP. From figure 6.19 (c), it is seen that the VWSC parameter has negative correlations with CSGP. From figure 6.19 (d), it is clear that the HUM parameter has low positive correlations with CSGP. Hence it is understood that the high positive correlations of LLC and LLRV and the low positive correlations of the HUM parameter and negative correlations of the VWSC parameter contribute more to the formation of the depressions over BB during the monsoon

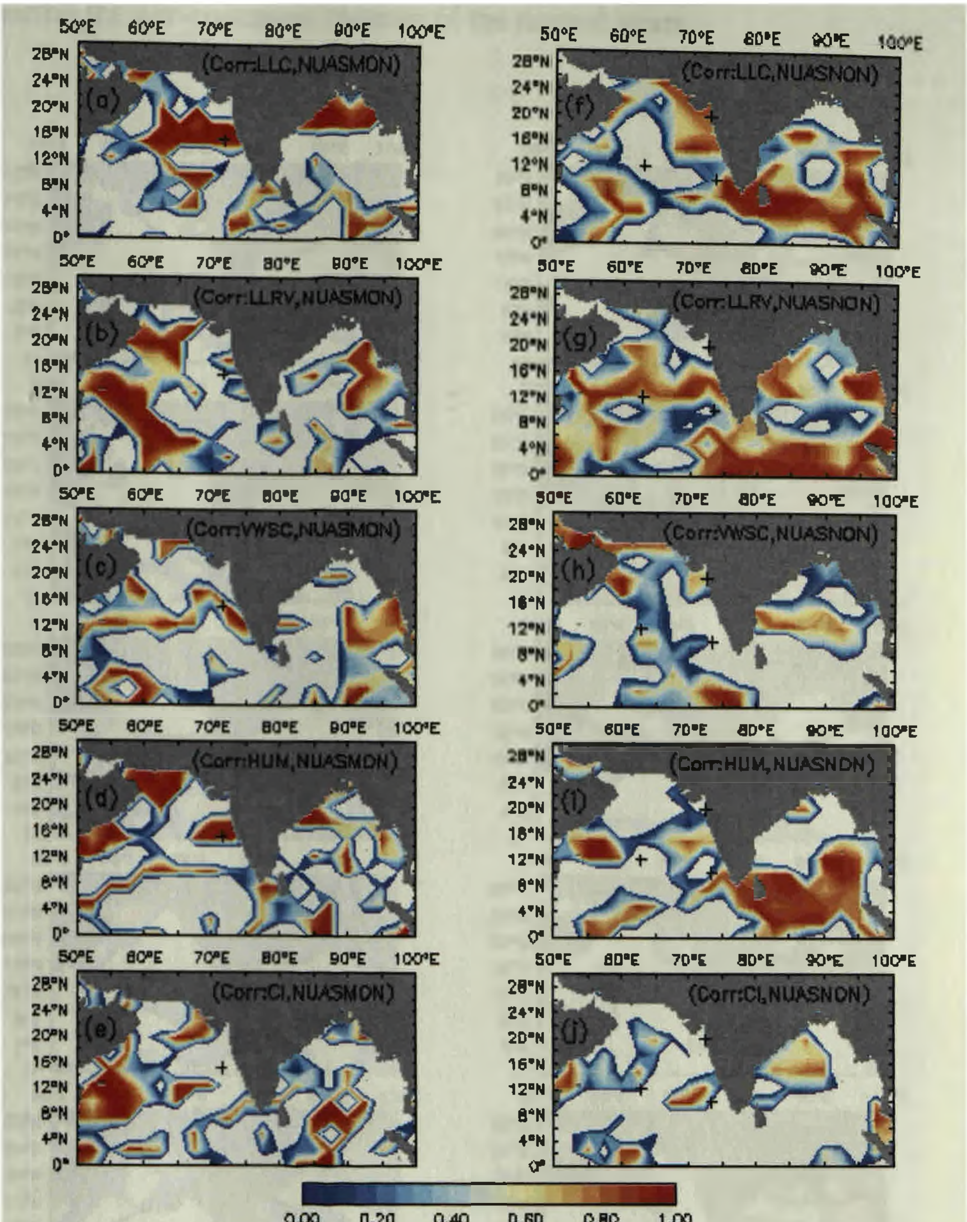

Figure 6.18 Spatial correlations of the parameters with CSGP for the depressions over AS during the monsoon and non-monsoon seasons of the neutral years

seasons of the neutral years. From figure 6.19 (f, g) it is observed that the parameters such as LLC and LLRV have high positive correlations with CSGP. From figure 6.19 (h) it is seen that the VWSC parameter has negative correlations with CSGP. Hence it is understood that the high positive correlations of the parameters LLC, LLRV and negative correlations of the VWSC parameter contribute much to the formation of the depressions over BB during the non-monsoon seasons of the neutral years.

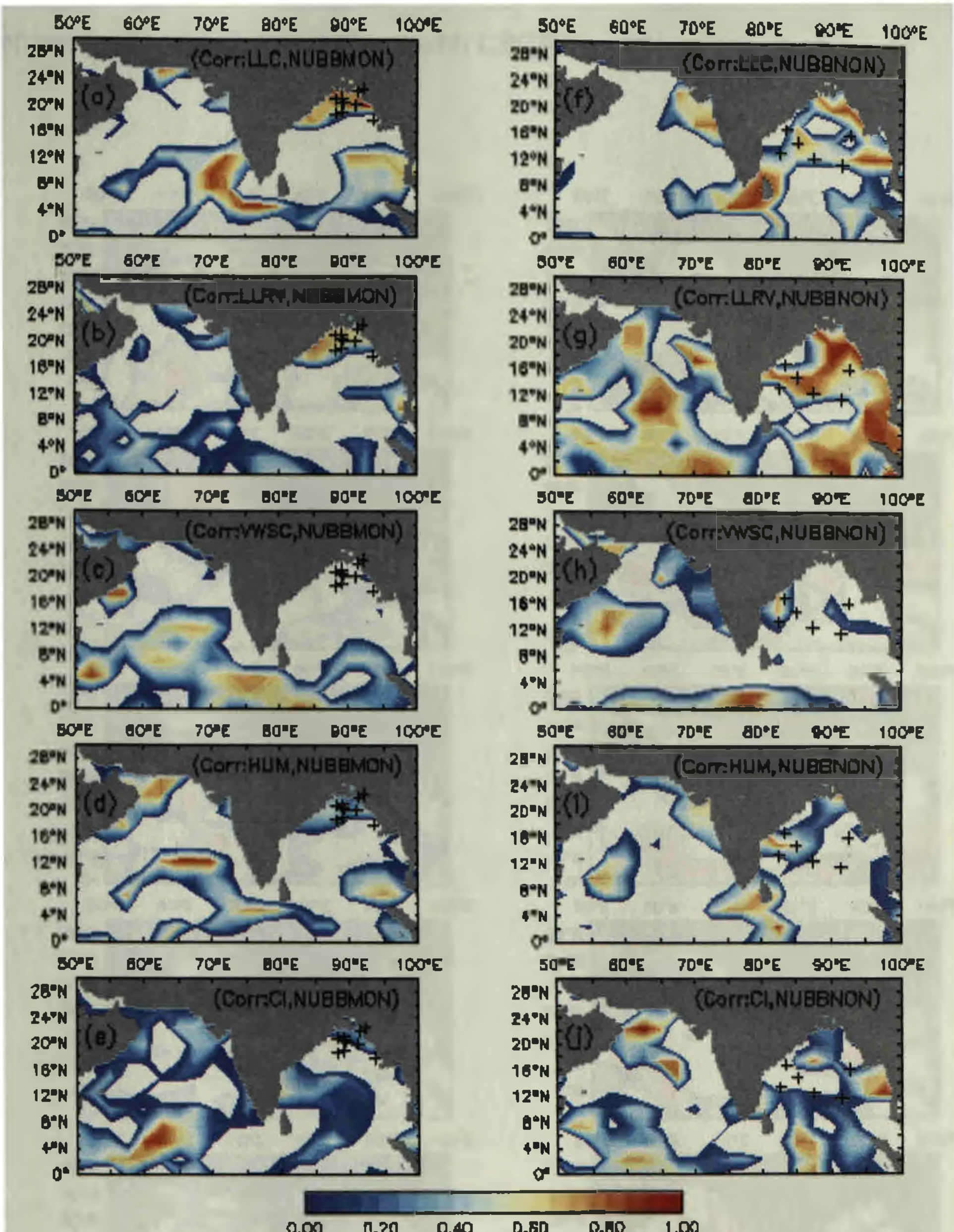

("+" represents the genesis locations of the depressions)
(BB= Bay of Bengal, NU=Neutral, MON=Monsoon, NON=Non-monsoon)

Figure 6.19 Spatial correlations of the parameters with CSGP for the depressions over BB during the monsoon and non-monsoon seasons of the neutral years

Figure (6.20) shows the spatial correlations of the ocean-atmospheric parameters with CSGP for the cyclones formed over AS during the monsoon and non-monsoon seasons of the neutral years. From figure 6.20 (a), it is observed that the LLC parameter has high positive correlations with CSGP. From figure 6.20 (c), it is noticed that the VWSC parameter has low positive correlations with CSGP.

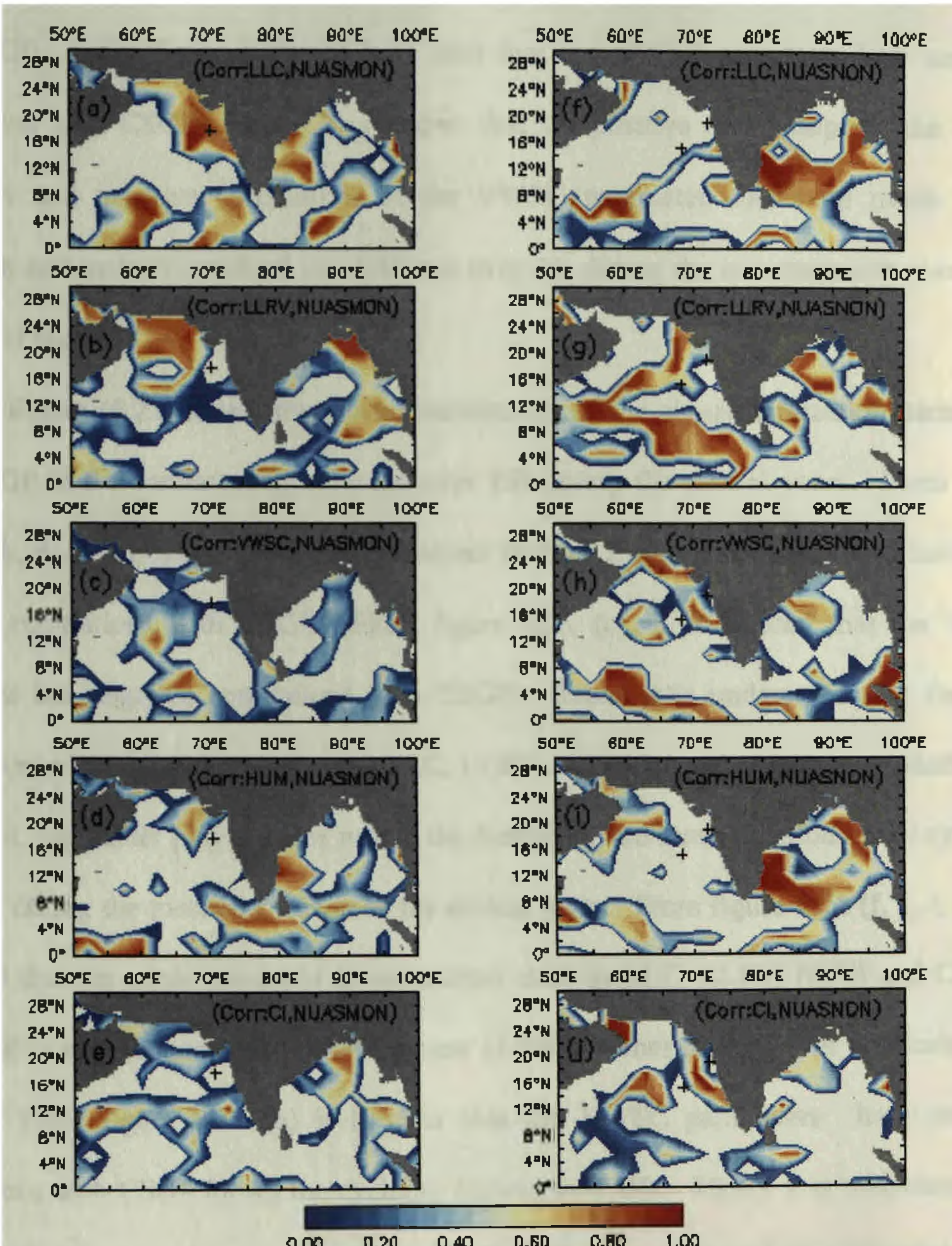

("+" represents the genesis locations of the cyclones)
(AS= Arabian Sea, NU=Neutral, MON=Monsoon, NON=Non–monsoon)

Figure 6.20 Spatial correlations of the parameters with CSGP for the cyclones over AS during the monsoon and non-monsoon seasons of the neutral years

Hence it is understood that the high positive correlations of the LLC parameter and low positive correlations of the VWSC parameter play a major role in the formation and intensification of the cyclones over AS during the monsoon season of the neutral years. From figure 6.20 (g), it is noticed that the LLRV parameter has low positive correlations with CSGP. From figure 6.20 (h) it is seen that the VWSC parameter has negative correlations with CSGP. Hence it is known that the positive correlations of the LLRV parameter and negative correlations of the VWSC parameter contribute much to the formation and intensification of the cyclones over AS during the non-monsoon seasons of the neutral years.

Figure (6.21) shows the spatial correlations of the air-sea interaction parameters with CSGP in the formation of cyclones over BB during the neutral years. From figure 6.18 (a, b, d) it is observed that the parameters such as LLC, LLRV and HUM have high positive correlations with CSGP. From figure 6.21 (c), it is noticed that the VWSC parameter has negative correlations with CSGP. Hence it is understood that the high positive correlations of the parameters LLC, LLRV and HUM and negative correlations of the VWSC parameter play a major role in the formation and intensification of the cyclones over BB during the monsoon season of the neutral years. From figure 6.21 (f, g, i, j) it is observed that the ocean-atmospheric parameters such as LLC, LLRV, HUM and CI have low positive correlations with CSGP for most of the cyclones formed over BB during this period. From figure 6.21 (h) it is clear that the VWSC parameters have negative correlations with CSGP for all the cyclones formed over BB. Hence it is understood that all the cyclogenesis parameters contribute equally to the formation and intensification of the cyclones over BB during the non-monsoon seasons of the neutral years.

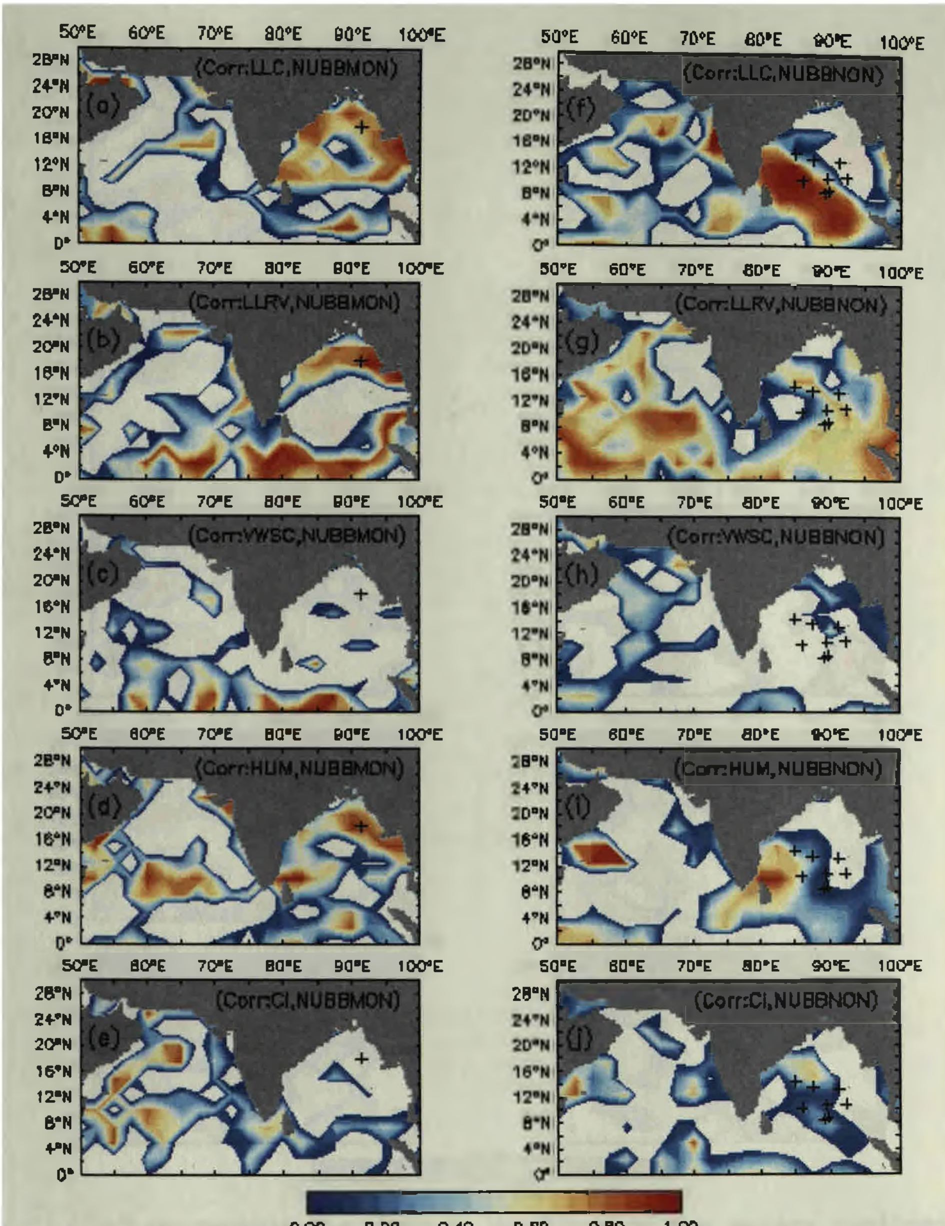

("+" represents the genesis locations of the cyclones)

(BB= Bay of Bengal, NU=Neutral, MON=Monsoon, NON=Non-monsoon)

Figure 6.21 Spatial correlations of the parameters with CSGP for the cyclones over BB during the monsoon and non-monsoon seasons of the neutral years

Figure (6.22) gives the spatial correlations of the cyclogenesis parameters with CSGP in the formation and intensification of the severe cyclones over AS during the monsoon and non-monsoon seasons of the neutral years.

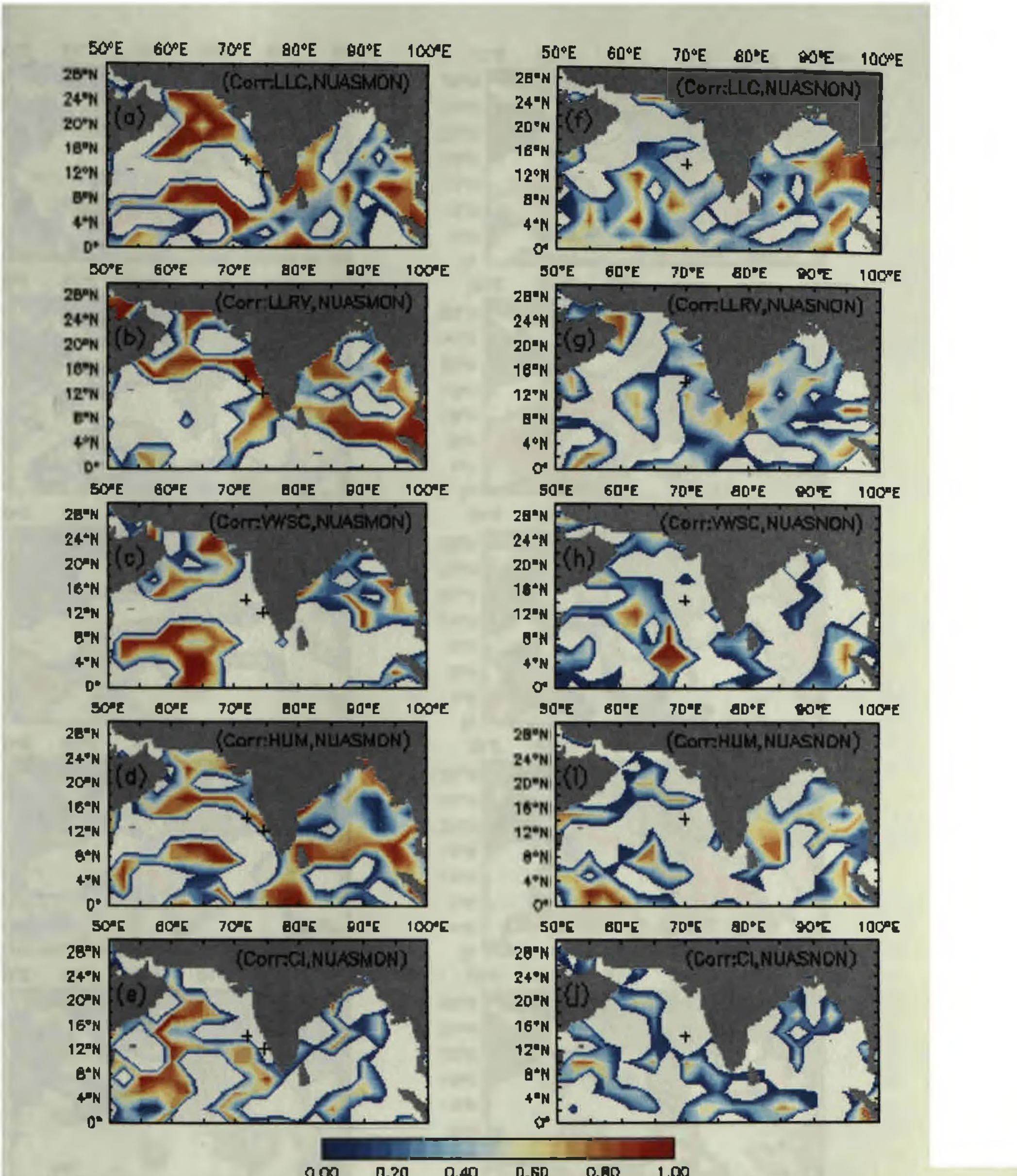

("+" represents the genesis locations of the severe cyclones)
(AS= Arabian Sea, NU=Neutral, MON=Monsoon, NON=Non–monsoon)

Figure 6.22 Spatial correlations of the parameters with CSGP for the severe cyclones over AS during the neutral years

From figure 6.22 (a, b, d) it is observed that the ocean-atmospheric parameters such as LLC, LLRV and HUM have positive correlations with CSGP. From the figure 6.22 (c), it is noticed that the VWSC parameter has negative correlations with CSGP. Hence it is understood that the positive correlations of the air-sea interaction parameters LLC, LLRV

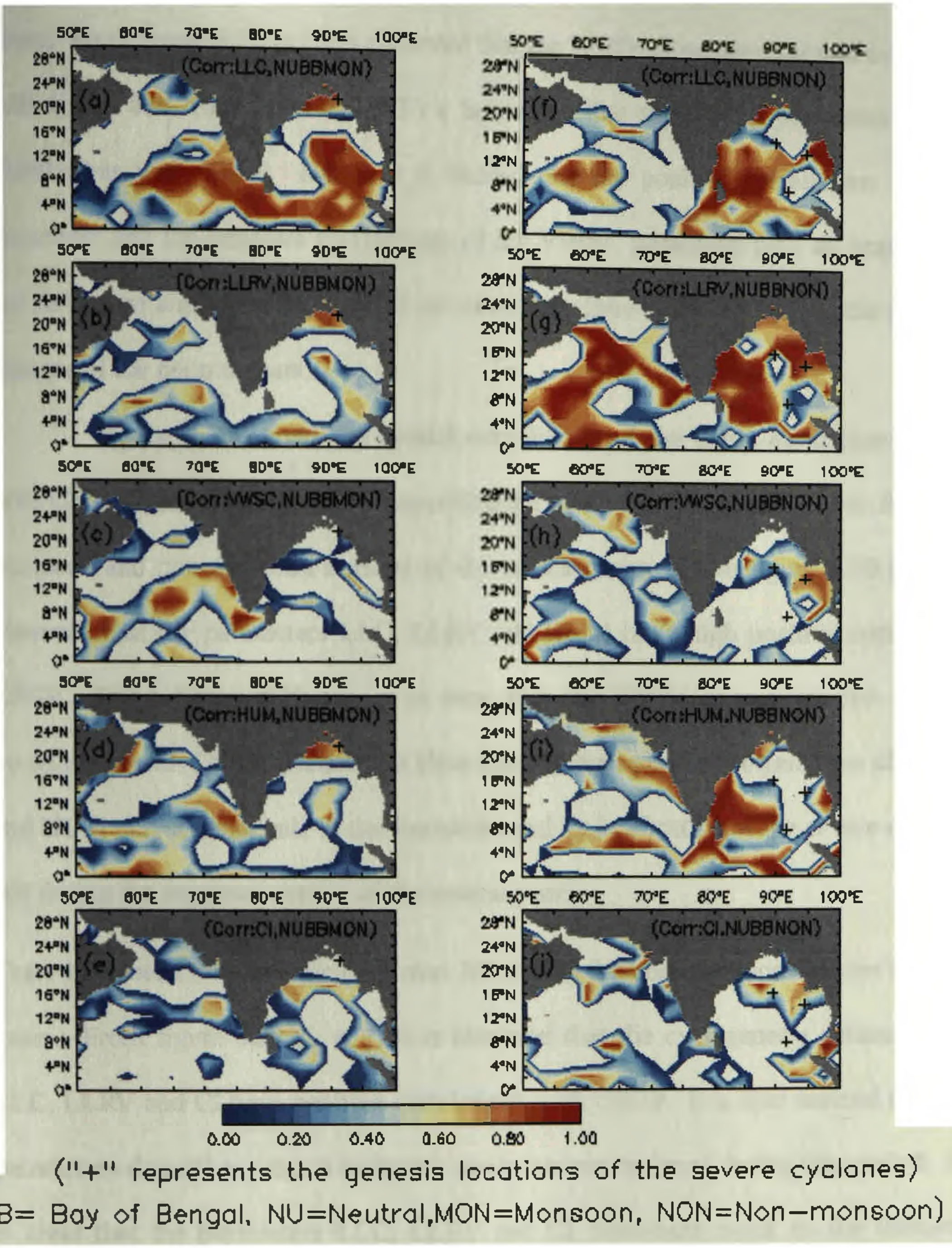

Figure 6.23 Spatial correlations of the parameters with CSGP for the severe cyclones over BB during the monsoon and non-monsoon seasons of the neutral years

and HUM and negative correlations with VWSC contribute much to the formation and intensification of the severe cyclones over AS during the monsoon season of the neutral years. From figure 6.22 (g) it is observed that the LLRV parameter has positive correlations with CSGP and from figure 6.22 (h) it is noticed that the VWSC parameter has negative correlations with CSGP. Hence it is known that the positive correlations of the LLRV parameter and the negative correlations of the VWSC parameter play an important role in the formation and intensification of the severe cyclones over AS during the non-monsoon seasons of the neutral years.

Figure (6.23) gives the spatial correlations of the ocean-atmospheric parameters with CSGP in the formation and intensification of the severe cyclones over BB during the monsoon and non-monsoon seasons of the neutral years. From figure 6.20 (a, b, d), it is observed that the parameters LLC, LLRV and HUM have high positive correlations with CSGP. From figure 6.20 (c), it is seen that the VWSC parameter has low positive correlations with CSGP. Hence it is clear that the high positive correlations of LLC, LLRV and HUM play a major role in the formation and intensification of the severe cyclones over BB during the monsoon season of the neutral years.

There have been 3 severe cyclones over BB during the non-monsoon seasons of the neutral years. From figure 6.20 (f, g, j) it is observed that the cyclogenesis parameters such as LLC, LLRV and CI have positive correlations with CSGP. It is also noticed that the other parameters do not have much influence on the severe cyclones during this period. Hence it is clear that the parameters LLC, LLRV and CI contribute much to the formation and intensification of the severe cyclones over BB during the non-monsoon seasons of the neutral years.

6.11 Conclusion

The relative role of the cyclogenesis parameters in the formation and intensification of the convective systems over NIO during the IOD and neutral years have been investigated. It reveals that the IOD events and the neutral conditions have got higher influence on the formation and intensification of the convective systems over NIO. It is observed that there is a great chance of getting cyclones during the monsoon months, when there is an IOD activity in this basin. It is noticed that the frequency of the depressions over AS are more during the monsoon season of the NIOD years compared to that in the monsoon season of the PIOD and neutral years. It is noticed that the frequency of the depressions is more during the non-monsoon seasons of the PIOD, and neutral years than the non-monsoon seasons of the NIOD years. The frequency of the cyclones is more during the monsoon season of the PIOD years than the monsoon season of the NIOD and neutral years and the frequency of the cyclones is more during the non-monsoon seasons of the neutral years compared to the non-monsoon seasons of the PIOD and NIOD years. More severe cyclones have formed over AS during the monsoon season of the PIOD years compared to the monsoon season of the NIOD and neutral years. It is also found that the frequency of the severe cyclones over AS is more during the non-monsoon seasons of the NIOD years compared to the PIOD and neutral years.

It is noticed that the frequency of the depressions over BB is more during the monsoon season of the PIOD years than the monsoon season of the NIOD and neutral years. It is also seen that the frequency of the depressions is more during the non-monsoon seasons of the NIOD years than the non-monsoon seasons of the PIOD and neutral years. The frequency of the cyclones is more during the monsoon season of the NIOD years compared to the monsoon season of the PIOD and neutral years. More cyclones have formed over BB during the non-monsoon seasons of the neutral years than the non-monsoon seasons of the PIOD and NIOD years. No severe cyclones were formed over BB during the monsoon season of the PIOD and NIOD years and it is noticed that 1 severe cyclone formed over BB during the monsoon season of the neutral years. The frequency of the severe cyclones is more during the non-monsoon seasons of the NIOD years compared to the non-monsoon seasons of the PIOD and neutral years.

In the PIOD years, the warmer than normal SST over the western equatorial Indian Ocean and colder than normal SST over the eastern equatorial Indian Ocean produce high convective activity over the AS and large scale air subsidence over the BB this environmental conditions over the tropical equatorial Indian Ocean enhances the formation and intensification of the cyclones and severe cyclones over AS. While during the NIOD years, the ocean atmosphere system gets reversed over the tropical equatorial Indian Ocean in such a way that the eastern equatorial Indian Ocean gets the warmer than normal SST and the western equatorial Indian Ocean gets the colder than normal SST. This environmental condition over the tropical equatorial Indian Ocean enhances the formation and intensification of the severe cyclones over BB. It is also noticed that the frequency per year of the cyclones over BB is more in the neutral years compared to the PIOD and the NIOD years.

The depressions and cyclones have formed against lower magnitudes of CSGP and the severe cyclones have formed against the larger magnitudes of CSGP during the PIOD years. It is observed that the depressions, cyclones and severe cyclones have formed against higher magnitudes of CSGP during monsoon seasons of the NIOD years . During the neutral years it is observed that the depressions, cyclones and severe cyclones in the non-monsoon seasons have formed against the lower magnitudes of CSGP and the severe cyclones in the monsoon seasos have formed against higher magnitudes of CSGP.

The analysis reveals that various combinations of the cyclogenesis parameters contribute much to the formation of the depressions over NIO during different climatic episodes. The high positive correlations of the parameters such as LLC and LLRV play major role in the formation of depressions over NIO during the neutral years. It is observed that the high positive correlations of the parameters namely LLC and HUM contribute much to the formation of the depressions over NIO during the NIOD years. It is noticed that the high positive correlations of the parameters such as LLC, LLRV and HUM contribute more to the formation of the depressions over NIO during the PIOD years. In the case of cyclones and severe cyclones over NIO, this study further reveals that the high positive correlations of the parameters such as LLC, LLRV and HUM contribute more to the formation and intensification of the convective systems over NIO during the monsoon and non-monsoon seasons of the PIOD, the NIOD and the neutral years.

Further it is also observed that there is a northward shift in the genesis locations of the depressions for the monsoon season and southward shift for the non-monsoon seasons during the PIOD, NIOD and neutral years. It is noticed that the cyclones dissipate immediately after the landfall during the PIOD and neutral years but they are living further after their landfall during the NIOD years. It is seen that there are possibilities to form a severe cyclone over NIO during the monsoon season of the PIOD, NIOD and neutral years. It is also found that the cyclones and severe cyclones dissipate immediately after their landfall during the NIOD and neutral years.

Chapter 7

Summary and Conclusion

The cyclogenesis over the NIO is a complex phenomenon, as it is influenced by several coupled ocean atmospheric phenomena such as El-Niño, El-Niño Modoki, La-Niña, La-Niña Modoki, IOD and MJO. The influence of the air-sea interaction parameters in the formation and intensification of the convective ststems have been investigated in this research work. This study reveals that the frequency and intensity of the convective systems are highly influenced and controlled by the so called climatic forcings namely El-Niño, La-Niña, El-Niño Modoki, La-Niña Modoki, PIOD, NIOD and neutral conditions. There exists large variability in the distribution of the genesis points of the convectve systems and their tracks with respect to these climatic episodes. There is a tendency for the tracks of cyclones and severe cyclones over BB to deflect towards north-east to easterly direction. It is also noticed that, the convective systems live longer even after their landfall or dissipate over the ocean or decay immediately after the landfall depeding up on the influence of the large scale ocean atmospheric system.

A new cyclogenesis indec (CSGP) is developed as a part of this research work. It is observed that this index is capable to distinguish the intensity variations of the convective systems. We have combined all the depressions, cyclones and severe cyclones over NIO during the study period. It is observed that all the depressions over NIO, during both the seasons, have formed against low magnitudes of CSGP (~ -0.5 to 0.5 $x10^{-10}s^{-2}\,^{o}K$), all the cyclones have formed against low positive magnitudes of CSGP (~ 0.0 to 0.5 $x10^{-10}s^{-2}\,^{o}K$) and all the severe cyclones are formed against the high positive values of CSGP (~0.0 to 2.0 $x10^{-10}s^{-2}\,^{o}K$).

The role of the background state of El-Niño and El-Niño Modoki on the convective system activity is presented in chapter 4. Variations in the genesis, intensity and tracks of these systems over north Indian Ocean are presented in this chapter. We have looked at these systems during the monsoon and non monsoon seasons separately. Important findings in the study are:

During the El-Niño years the cyclones and severe cyclones form over the central and western BB or in the Head Bay have longer tracks over the ocean and live longer even after thei landfall. But the systems form over the eastern BB (above 95°E) they dissipate over the sea or deceay immediately after their landfall. During the El-Niño Modoki years the cyclones and severe cyclones are having longer tracks over the ocean some of them dissipate over the ocean or decay immediately after their landfall. Our present study suggests that concurrent occurrence PIOD and El-Niño events can significantly alter cyclogenesis parameters over the AS as compared to a pure El-Niño Modoki year. It is observed that the depressions and cyclones over NIO have formed against lower magnitudes of CSGP during the El-Niño and El-Niño Modoki years. It is also noticed that the severe cyclones are formed against higher values of CSGP during the El-Niño years and they formed against lower magnitudes of the El-Niño Modoki years.

The role of La-Niña and La-Niña Modoki events on the formation of convective systems over the north Indian Ocean is presented in chapter 5. Some of the main findings of the study are: During the La-Niña years the cyclones and severe cyclones over AS are having longer tracks over the ocean and they live longer even after their landfall. But in the case of the cyclones and severe cyclones formed during the monsoon season have longer tracks over the ocean and shorter tracks over the ocean in the non-monsoon seasons of the La-Niña years. During the La-Niña Modoki years the cyclones and severe cyclones have longer tracks over the ocean and they live further even after their landfall. This study also suggets that the La-Niña Modoki events are not conducive for the formation of cyclones over the AS, which is due to the low values of mid tropospheric instability, mid tropospheric humidity and low level relative vorticity. The frequency of severe cyclones are more ovr BB during the non-monsoon seasons of the La-Niña Modoki years. The depressions and cyclones formed agianst lower magnitudes of CSGP and the severe cyclones have formed against the larger magnitudes of CSGP during the La-Niña and La-Niña Modoki years.

The role of PIOD, NIOD and neutral events on the formation of convective systems over the north Indian Ocean is presented in chapter 6. The main findings of the study are: During the PIOD years the severe cyclones are are having longer tracks over the ocean. During the NIOD years the cyclones are having longer tracks over the ocean and the severe cyclones are having shorter tracks over the ocean. During the neutral years the cyclones and severe cyclones are having longer tracks over the ocean.

During the PIOD years it is seen that the depressions and cyclones havae formed against lower magnitudes of CSGP and the severe cyclones have formed against higher magnitudes of CSGP. It is also noticed that the depressions, cyclones and severe cyclones have formed against higher magnitudes of CSGP during the monsoon season of the NIOD years. It is found that the depressions, cyclones and severe cyclones in the non-monsoon seasons have formed against the lower magnitudes of CSGP and the severe cyclones in the monsoon seasos have formed against higher magnitudes of CSGP during the neutral years .

Spatial correlations of the air-sea interaction parameters such as LLC, LLRV, VWSC, HUM and CI with CSGP have been obtained in order to study their role in the formation and intensification of the convective systems over NIO. It is noticed that different combinations of the air-sea interaction parameters are influenceing the formation of the convective systems over NIO. In the El-Niño years, the higher positive correlations of LLC, LLRV, HUM and CI with CSGP are found to be the major contributors in the formation of the depressions over AS during the monsoon season. While the larger positive correlations of LLRV, CI and the smaller positive correlations of VWSC with CSGP are found responsible for the formation of the depressions over AS during the non-monsoon seasons. Where as in BB, the higher positive correlations of LLC, LLRV, HUM and negative correlations of VWSC with CSGP play an important role in the formation of depressions over BB during the monsoon season. While the higher positive correlations of LLC, LLRV and HUM with CSGP contribute much to the formation of the depressions over BB during the non-monsoon seasons. It is noticed that the larger positive correlations of LLC with CSGP is responsible for the formation and intensification of cyclones over BB during the monsoon season. It is also noticed that the smaller positive correlations of VWSC and CI with CSGP is found to be supportive for the development of this cyclone over BB during this period. While the higher positive correlations for the parameters such as LLC, LLRV and HUM with CSGP contribute more to the genesis and further intensification of the cyclones over BB during the non-monsoon seasons.

It is noticed that the higher positive correlations of LLC, CI and negative correlations of VWSC with CSGP are found to be the major contributors in the formation and intensification of the severe cyclones over AS during the non-monsoon seasons. Where as in BB, it is observed that the of HUM with CSGP contribute much to the development and further intensification of the severe cyclones over BB during the monsoon season. It is also noticed that the lower positive correlations of other parameters such as the LLC, LLRV and VWSC with CSGP are found to be supportive for the formation and intensification of the severe cyclones over BB during this period. While the higher positive correlations of the parameters such as LLC, LLRV and HUM with CSGP are found to be major contributors in the formation and intensification of the severe cyclones over BB during the non-monsoon seasons.

In the El-Niño Modoki years, higher positive correlations of LLC, lower positive correlations of LLRV and HUM and the negative correlations of VWSC with CSGP are found responsible for the formation of the depressions over AS during the monsoon season. While the lower positive correlations of LLC and negative correlations of VWSC with CSGP are found to be responsible for the formation of the depressions over AS during the non-monsoon seasons. Where as in BB, the higher positive correlations of LLC and lower positive correlations for the parameters such as LLRV and HUM and negative correlations of VWSC with CSGP are found to be the major contributors for the depressions over BB during the monsoon season. While the higher positive correlations of LLC and HUM and lower positive correlations of LLRV with CSGP are found to be responsible for the formation of the depressions over BB during non-monsoon seasons.

It is clear that the lower positive correlations of LLRV and negative correlations of VWSC are found to be the major contributors to the formation and intensification of the cyclone over AS during the monsoon season. While the larger positive correlations of LLC and LLRV and CI and the negative correlations of VWSC are found to be responsible for the formation and intensification of the cyclones over AS during the non-monsoon seasons. Where as in BB, the higher positive correlations of the parameters such as LLC and LLRV with CSGP are found to be the major contributors to the formation and intensification of the cyclones over BB during the monsoon season. It is also observed that the lower positive correlations of VWSC, HUM and CI with CSGP are found to be supportive for the formation and intensification of the cyclones over BB during this period. While the higher positive correlations of HUM with CSGP is responsible for the formation and intensification of the cyclones over BB during the non-monsoon seasons. It is also found that the lower positive correlations of LLRV, VWSC, HUM and CI with CSGP are found to be supportive for the formation and intensification of the cyclones during this period.

It is noticed that, the lower positive correlations of LLC, LLRV, HUM and CI and the negative correlations of VWSC with CSGP are found to be responsible for the formation of severe cyclones over AS during the monsoon season. While the higher positive correlations of LLRV, HUM and CI are found to be the major contributors to the formation and intensification of the severe cyclones over AS during the non-monsoon seasons. It is also noticed that the lower positive correlations of LLC and VWSC are found to be supportive for the formation and intensification of the severe cyclones over AS during this period. Where as in BB the higher positive correlations of LLC, LLRV and CI are found to be responsible for the formation and intensification of the severe cyclones over BB during the non-monsoon seasons. It is also observed that the lower positive correlations of VWSC and HUM are found to be supportive in the formation and intensification of the severe cyclones over BB during this period.

In the La-Niña years, the lower positive correlations of LLRV and the VWSC with CSGP are found responsible for the formation of the depressions over AS during the monsoon season. While the higher positive correlations of LLC, LLRV and HUM with CSGP are found to be responsible for the formation of the depressions over AS during the non-monsoon seasons. Where as in BB, the correlation values are less for the parameters such as LLC, LLRV and HUM and negative correlations exist for VWSC with CSGP. Hence it is noticed that these parameters equally contribute to the formation of the depressions over BB during the monsoon season. While the higher positive correlations of the parameters namely the LLC and HUM and lower positive correlations of LLRV with CSGP and negative correlations of VWSC parameter are found to be responsible for the formation of the depressions over BB during non-monsoon seasons.

It is noticed that, the higher positive correlations of LLC and LLRV and the negative correlations of the VWSC parameter contribute much to the formation and intensification of the cyclone over AS during the non-monsoon seasons. Where as in BB, the higher positive correlations of LLC and negative correlations of the VWSC parameter with CSGP contribute to the formation and intensification of the cyclones over BB during the monsoon season. It is also observed that the higher positive correlations for the LLRV parameter and the negative correlations of the VWSC parameter with CSGP contribute to the formation and intensification of the cyclones over BB during the non-monsoon seasons.

The higher positive correlations of LLC and HUM and negative correlations of VWSC with CSGP are found to be responsible for the formation of severe cyclones over AS during the monsoon season. While the higher positive correlations of LLC, LLRV and HUM with CSGP are found to be the major contributors to the formation and intensification of the severe cyclones over AS during the non-monsoon seasons. Where as in BB the higher positive correlations of LLC, LLRV and HUM and negative correlations of the VWSC parameter contribute more to the formation and intensification of the severe cyclones over BB during the non-monsoon seasons.

In the La-Niña Modoki years, the lower positive correlations of LLC, LLRV and HUM and the negative correlations of VWSC with CSGP are found responsible for the formation of the depressions over BB during the monsoon season. While the higher positive correlations of LLC, LLRV, HUM and CI and the negative correlations of the VWSC with CSGP contribute equally to the formation of the depressions over BB during the non-monsoon seasons. It is clear that, the lower positive correlations of LLC, LLRV and HUM and the negative correlations of VWSC play a major role in the formation and intensification of the cyclones over BB during the non-monsoon seasons. It is also seen that the lower positive correlations of LLC, LLRV, HUM and the negative correlations of VWSC with CSGP are found to be responsible for the formation of severe cyclones over BB during the non-monsoon seasons.

In the PIOD years, the higher positive correlations of LLC, LLRV and HUM and the negative correlations of VWSC with CSGP are found responsible for the formation of the depression over AS during the non-monsoon seasons. Where as in BB, it is observed that the higher positive correlations of LLC, LLRV and HUM with CSGP are found to be the major contributors for the depressions over BB during the monsoon and non-monsoon seasons. The higher positive correlations of LLC and lower positive correlations of VWSC with CSGP are found to be responsible for the formation and intensification of the cyclone over AS during the monsoon season. Where as in BB, the higher positive correlations of LLC, LLRV and HUM and negative correlations of the VWSC with CSGP play a major role in the formation and intensification of the cyclone over BB during the non-monsoon seasons. It is observed that the higher positive correlations of LLC and LLRV and the negative correlations of the VWSC with CSGP contribute to the formation and intensification of the severe cyclones over AS during the monsoon season. Where as in BB, the higher positive correlations of the parameters such as LLC, LLRV and HUM are found to be responsible for the formation and intensification of the severe cyclones over BB during the non-monsoon seasons.

In the NIOD years, the higher positive correlations of HUM with CSGP have been found responsible for the formation of the depressions over AS during the monsoon season. Where as in BB, the higher positive correlations of LLC, LLRV and CI contribute much to the formation of depressions over BB during the monsoon season. It is observed that the lower positive correlations of LLC, LLRV and HUM with CSGP are found to be responsible for the formation of the depressions over BB during non-monsoon seasons. It is noticed that the higher positive correlations of LLC, LLRV and HUM and negative correlations of the VWSC parameter contribute much to the formation and intensification of the cyclones over BB during the non-monsoon seasons. It is observed that the higher positive correlations of the parameters LLC, LLRV, HUM and the negative correlations of the VWSC with CSGP are found to be responsible for the formation of severe cyclone over AS during the monsoon season. While the higher positive correlations of LLC, LLRV and CI are found to be the major contributors to the formation and intensification of the severe cyclones over AS during the non-monsoon seasons. Where as in BB the higher positive correlations of LLC and HUM are found to be responsible for the formation and intensification of the severe cyclones over BB during the non-monsoon seasons.

In the neutral years, the higher positive correlations of LLC and HUM with CSGP contribute more to the formation of the depressions over AS during the monsoon season. While the lower positive correlations of LLC, LLRV and HUM play a major role in the formation of the depressions over AS during the non-monsoon seasons. Where as in BB, the higher positive correlations of LLC, LLRV and HUM and negative correlations of the VWSC with CSGP are found to be the major contributors for the depressions over BB during the monsoon season. While the higher positive correlations of LLC and LLRV contribute much to the formation of the depressions over BB during non-monsoon seasons.

It is noticed that, the higher positive correlations of LLC and negative correlations of VWSC are found to be the major contributors of the formation and intensification of the cyclones over AS during the monsoon season. While the higher positive correlations of LLRV and the negative correlations of the VWSC are found to be responsible for the formation and intensification of the cyclones over AS during the non-monsoon seasons. Where as in BB, the higher positive correlations of LLC, LLRV and HUM and negative correlations of the VWSC with CSGP contribute more to the formation and intensification of the cyclones over BB during the monsoon season. It is also observed that the higher positive correlations of LLRV and the negative correlations of the VWSC with CSGP contribute much to the formation and intensification of the cyclones over BB during the non-monsoon seasons.

It is observed that the higher positive correlations of LLC, LLRV, HUM and the negative correlations of VWSC with CSGP are found to be responsible for the formation of severe cyclones over AS during the monsoon season. While the lower positive correlations of LLRV and the negative correlations of the VWSC parameter contribute much to the formation and intensification of the severe cyclones over AS during the non-monsoon seasons. It is noticed that the higher positive correlations of LLC, LLRV and HUM and the negative correlations of the VWSC are found to be responsible for the formation and intensification of the severe cyclones over BB during the monsoon season. It is also noticed that the higher positive correlations of LLC, LLRV and CI are found to be responsible for the formation and intensification of the severe cyclones over BB during the non-monsoon seasons.

7.1 Future work

The role of air-sea interaction parameters in the formation and intensification of the convective systems over NIO during different climatic episodes have been explained in this research work. It is understood that the cyclogenesis parameters LLC, LLRV, VWSC and HUM have a major influence on the convective systems in almost all the climate modes. It reveals that the CI had a supportive role in formation and intensification of most of the convective systems over NIO. In order to improve the accuracy in the forecast it is needed to test different air-sea interaction parameters such as SST, OLR and LHF to optimize the new index. If a suitable combination of the parameters is obtained the accuracy of new index will be improved and it can provide better forecasts for the convective systems over NIO.

References

Amato TE, Camargo SJ (2010) A climatology of Arabian Sea Cyclonic storms. Journal of Climate. American Meteorological Society, Vol. 24, pp 140-158.

Ashok K, Guan Z and Yamagata T (2003) Influence of the Indian Ocean Dipole on the Australian winter rainfall. Geophysical Research Letters, Vol. 30, No. 15, 1821, doi:10.1029/2003GL017926.

Ashok K, Behera SK, Rao SA, Weng H (2007) El-Niño Modoki and its possible teleconnections. Journal. Geophys. Res 112, C11007, doi:10.1029/2006JC003798

Ashok K and Yamagata T (2009) The El-Niño with a difference?. Nature 461: pp 481-484, doi:10.1029/2001GL013294.

Behera SK and Yamagata T (2001) Subtropical SST dipole events in the southern Indian Ocean. Geophysical Research Letters. Vol,. 28, No. 2, pp 327-330.

Bove MC, Elsner JB, Landsea CW, Niu X, and O'Brien J (1998) Effect of El Niño on U.S. landfalling hurricanes, revisited. Bull. Amer. Meteor. Soc., 79, pp 2477–2482.

Camargo SJ and Sobel AH (2005) Western North Pacific tropical cyclone intensity and ENSO. J. Climate, 18, pp 2996–3006.

Camargo SJ, Emanuel KA, Sobel AH (2007) Use of a Genesis Potential Index to diagnose ENSO effects on tropical cyclone genesis. J Clim 20: pp 4819–4834. doi:10.1175/JCLI4282.1

Chan JCL (1985) Tropical cyclone activity in the northwest Pacific in relation to the El-Niño/Southern Oscillation phenomenon. Mon Weather Rev 113: pp 599–606.

Chia HH and Ropelewski CF (2002) The interannual variability in the genesis location of tropical cyclones in the north west Pacific. J Clim 15: pp 2934–2944

Chu PS (2004) ENSO and tropical cyclone activity. Hurricanes and Typhoons, Past, Present and Future, R.J. Murnane and K.B. Liu, Eds., Columbia University Press, pp 297-332.

Chu PS and Wang J (1997) Tropical cyclone occurrences in the vicinity of Hawaii: Are the differences between El Niño and non–El Niño years significant? J. Climate, 10, pp 2683–2689.

Clark II C, Nnaji GA, and Huang W (2014): Effects of El-Niño and La-Niña Sea Surface

Temperature Anomalies on Annual Precipitations and Streamflow Discharges in Southeastern United States. Journal of Coastal Research: Special Issue 68 - Climate Change Impacts on Surface Water Systems: pp. 113 – 120.

Clark JD and Chu PS (2002) Interannual variation of tropical cyclone activity over the central north Pacific. J. Meteor. Soc. Japan, 80, pp 403-418.

Cyclone eAtlas – IMD; Version 2.0 / 2011, Technical Note; Tracks of Cyclones and Depressions over North Indian Ocean, (from 1891 onwards), Cyclone Warning & Research centre, India Meteorological Department, Regional Meteorological Centre, Chennai, 48pp

Dash et.al (2004): S.K. Dash, Jenamani Rajendra Kumar and M.S. Shekhar.: On the decreasing frequency of monsoon depressions over the Indian region. Current Science, 86, pp 1404-1411.

DeMaria M, Knaff JA, Bernadette HC (2001) A tropical cyclone genesis parameter for the tropical Atlantic. Weather Forecast 16: pp 219–233. doi: 10. 1175/ 1520-0434 (2001) 016 \ 0219: ATCGPF [2.0.CO; 2]

Dong K (1988) El-Niño and tropical cyclone frequency in the Australian region and the North-western Pacific. Aust Meteor Mag 36: pp 219–255

Dube SK, Rao, AD., Sinha PC, Murty, TS. and Bahuleyan N (1997) Storm surge in Bay of Bengal and Arabian Sea: the problem and its prediction. Mausam 48: pp 288–304

Elsner JB, Kara AB (1999) Hurricanes of the North Atlantic: Climate and Society. Oxford University Press 488pp.

Elsner JB and Liu KB (2003) Examining the ENSO-typhoon hypothesis. Climate Res., 25, pp 43–54.

Emanuel KA (1986) Air sea interaction theory for tropical cyclones. Part I: Steady state maintenance. J. Atmos. Sci., 43, pp 585-604.

Emanuel KA (2005) Increasing destructiveness of tropical cyclones over the past 30 years. Nature, 436, pp 686-688.

Emanuel KA and Nolan DS (2004) Tropical cyclone activity and global climate. Preprints 26th conf. on hurricanes and Tropical Meteorology, Miami, FL, Amer Meteorol soc: pp 240-241

Francis PA, Sulochana Gadgil, Vinayachandran PN (2007) Triggering of the positive Indian Ocean Dipole events by severe cyclones over the Bay of Bengal. Tellus 59A: pp 461- 475

Frank WM (1976) The structure and energetics of the tropical cyclone: Dept. Atmospheric sciences, Colorado state University, Fort Collins, Colorado.

Frank WM (1977) The structure and energetics of the tropical cyclone. I. Storm structure.

Monthly. Weather. Review. Volume 105, pp 1119-1135.

Frank WM and Roundy PE (2006) The role of Tropical waves in tropical cyclogenesis. Month. Weather. Review. Volume 134, pp 2397-2417.

Goldenberg Sb and Shapiro LJ (1996) Physical mechanisms for the association of El-Niño and west African rainfall with Atlantic major hurricane activity. J. Climate, 9, pp 1169-1187.

Graham NE and Barnett TP (1987) Sea Surface Temperature, Surface Wind Divergence, and Convection over Tropical Oceans. Science, Reports, Vol.238. Pp 687-659

Gray WM (1967b) Global view of the origin of the tropical disturbances and storms. Atmos. Sci. Pap. No.14, Colorado State University, Fort Collins, 105 pp.

Gray WM (1968) Global view of the origin of tropical disturbances and storms. Monthly Weather Review. Volume 96, Number 10, pp 669-699

Gray WM and Shea DJ (1973) The hurricanes inner core region II: Thermal stability and dynamic characteristics. J. Atmos. Sci., 8, pp 1565-1576.

Gray WM (1975) Tropical cyclone genesis. Dept of Atmos Sc Paper No. 232 Colorado State University Port Collins Co USA, p 121

Gray WM (1984) Atlantic seasonal hurricane frequency. Part I: El-Niño and 30 mb quasi-biennial oscillation influences. Mon Weather Rev 112: pp 1649–1668

Gray WM (1998) The formation of tropical cyclones. Meteorology and Atmospheric physics, Volume 67, issue 1, pp 37-69.

Gray WM and Shea DJ (1973b) The hurricanes inner core region. II. Thermal stability and dynamic characteristics. J. of Atmos. Scie. Volume 30, pp 1565-1576.

Gray WM (1979) Hurricanes: Their formation, structure and likely role in the tropical circulation. Meteorology over the Tropical Oceans, D. B. Shaw, Ed., Royal Meteorological Society, pp 155–218.

Gray WM and Sheaffer JD (1991) El-Niño and QBO influences on tropical cyclone activity. Teleconnections Linking Worldwide Anomalies, M. H. Glantz, R. W. Katz, and N. Nicholls, Eds., Cambridge University Press, pp 257–284.

Gray WM, Landsea CW, Mielke Jr. PW, and Berry KJ (1993) Predicting Atlantic basin seasonal tropical cyclone activity by 1 August. Wea. Forecasting, 8, pp 73–86.

Hsu PC, Ho CR, Liang SJ, and Kuo NJ (2013): Impacts of Two Types of El Niño and La Niña Events on Typhoon Activity, Advances in Meteorology, Volume 2013 (2013), Article ID 632470, 8 pages, http://dx.doi.org/10.1155/2013/632470.

Holland GJ (1997) The maximum potential intensity of the tropical cyclones. J. Atmos. Sci. Volume 54, pp 2519-2541.

Ind. Met. Dept., 1964, „Tracks of storms and depressions"

Ind. Met. Dept., 1979, „Tracks of storms and depressions"

Ind. Met. Dept., 1996, „Tracks of storms and depressions"- An addendum to the StormTrack Atlas (1891-1970)

Joseph PV, Bindu G and Preethi B (2016) Impact of the upper tropospheric cooling trend over central Asia on the Indian summer monsoon rainfall and the Bay of Bengal cyclone tracks: CURRENT SCIENCE, VOL.110, NO.11, 10 JUNE 2016.

Kalnay E et.al (1996) The NCEP NCAR 40- Year Reanalysis Project. Bull. Amer. Meteor. Soc., 77, pp 437-471.

Kanamitsu M, Ebisuzaki W, Woollen J, Shi-Keng Yang, Hnilo JJ, Fiorino M, and Potter GL (2002) NCEP–DOE AMIP-II Reanalysis (R-2). Bull. Amer. Meteor. Soc., 83, pp 1631–1643, doi: 10.1175/BAMS-83-11-1631.

Kaplan J (2010) A Revised Tropical Cyclone Rapid Intensification Index for the Atlantic and Eastern North Pacific Basins. Weather and Forecasting. Volume 25, pp 220-241.

Kimball SK (2006) A modelling study of Hurricane landfall in a dry environment. Mon. Weather. Review. Volume 134, pp 1901-1918.

Kotal SD, Kundu PK, and Roy Bhowmik SK (2009) Analysis of cyclogenesis parameter for developing and non-developing low pressure systems over the Indian Sea. Nat Hazards 50: pp 389–402. DOI 10.1007/s11069-009-9348-5.

Knaff, JA (1997) Implications of summertime sea level pressure anomalies in the tropical Atlantic region. J. Climate, 10, pp 789–804.

Kripalani RH and Pankaj Kumar (2004) Northeast monsoon rainfall variability over south peninsular india vis-a-vis the indian ocean dipole mode. Int J Climatol 24: pp 1267–1282.

Lander, M. A., 1994: An exploratory analysis of the relationship between tropical storm formation in the western North Pacific and ENSO. Mon. Wea. Rev., 122, pp 636–651.

Lander, M. A., 1996: Specific tropical cyclone track types and unusual tropical cyclone motions associated with a reverse-oriented monsoon trough in the western North Pacific. Wea. Forecasting, 11, pp 170–186.

Landsea CW (1993) A climatology of intense (or major) Atlantic hurricanes. Month. Weather. Review., 121, pp 1703-1713.

Landsea CW, Pielke Jr RA, Mestas-Nuñez AM, Knaff JA (1999) Atlantic basin hurricanes: Indices of climatic changes. Clim Change 42: pp 89–129.

Landsea, CW (2000) El Niño–Southern Oscillation and the seasonal predictability of tropical cyclones. El Niño: Impacts of Multiscale Variability on Natural Ecosystems and Society, H. F. Díaz and V. Markgraf, Eds., Cambridge University Press, 149–181.

Li W, Zhang P, Ye J, Li L and Baker PA (2011): Impact of two different types of ElNiño events on the Amazon climate and ecosystem productivity, Journal of Plant Ecology, VOLUME 4, NUMBER 1–2, PAGES 91–99, MARCH 2011, doi: 10.1093/jpe/rtq039.

Li T, Zhang Y, Er Lu and Wang D (2002) Relative role of dynamic and thermodynamic processes in the development of the Indian Ocean dipole: An OGCM diagnosis. Geophysical Research Letters. Vol. 29, No. 23, 2110, doi:10.1029/2002GL015789.

Mandal GS (1991) Tropical cyclones and their forecastig and warning systems in the North Indian Ocean. WMO/TD-No.430, Tropical cyclones Program, Report No. TCP-28, WMO, Geneva

McBride JL (1981) Observational analysis of tropical cyclone formation. Part III: budget analysis.J.Atmos.Sci.38:1152–1166.doi:10.1175/1520-0469(1981)038<1152:OAOTCF>2.0.CO;2

McBride JL and Zehr RM (1981) Observational analysis of tropical cyclone formation. Part II:comparison of non-developing and developing systems. J Atmos Sci 38: pp 1132–1151. doi:10.1175/1520-0469(1981)038<1132:OAOTCF>2.0.CO;2

Merrill RT (1984) A comparison of large and small tropical cyclones. Mon. Weather. Review. Volume. 112, pp 1408-1418.

Mooley DA (1980) Severe cyclonic storms in the Bay of Bengal,1877-1976. Mon Weather Rev 108: pp 1647-1655.

Mooley DA (1981) Increase in the frequency of the severe cyclonic storms of the Bay after 1964-Possible causes. Mausam 32: pp 35-40

Munikrishna K (2009) Intensifying tropical cyclones over the North Indian Ocean during summer monsoon—Global warming. Global and Planetary Change. Volume 65, Issues 1–2, pp 12–16.

Pai DS and Rajeevan M (1998) Upper tropospheric circulation anomalies over Asia-Pacific region associated with the inter-annual variation of Indian summer monsoon. Mausam, 49, pp 461-468.

Palmen E (1948) On the distribution of temperature and wind in the upper westerlies. J. Meteorol. 5, pp 20-27.

Patwardhan SK and Bhalme HN (2001) A study of cyclonic disturbances over India and the adjacent ocean. Int. J. Climatol. 21, pp 527-534.

Pielke Jr.RA and Landsea CW (1999) La Niña, El Niño and Atlantic hurricane damages in the United States. Bull. Amer. Meteor. Soc., 80, pp 2027–2033.

Philander SGH (1983) El-Niño Southern Oscillation phenomena. Nature 302: 295-301.

Philander SG and Rasmusson EM (1985) The Southern Oscillation and El Niño. Advances in Geophysics. Volume 28, pp 197-215.

Pradhan PK, Preethi B, Ashok K, Krishnan R, and Sahai AK (2011) Modoki, Indian Ocean Dipole, and western North Pacific typhoons: Possible implications for extreme events. J Geophys Res vol. 116:D18108, doi: 10.1029/2011JD015666.

Pradhan PK, Preethi B, Ashok K Krishnan and Sahai AK (2011) Modoki, Indian Ocean Dipole, and western North Pacific typhoons: Possible implications for extreme events. Journal of Geophysical Research. Vol. 116, D18108, doi:10.1029/2011JD015666.

Rajeevan M, Khole M, De US (2000a) Variability of Sea Surface Temperature and tropical storms in the Indian ocean in the recent years. Proc. Of TROPMET-2000. National symposium on Tropical Meteorology, Cochin, India. 1-4 February2000, pp 234-237.

Rajeevan M, De U.S. and Prasad R.K. (2000b) Decadal variation of sea surface temperatures, cloudiness and monsoon depressions in the north Indian ocean. Current Science 79, pp 283-285.

Ramesh Kumar MR, Anu K Babu and Chris Reason (2009) On the role of convective systems over northwest Pacific Ocean and monsoon activity over the Indian subcontinent. Meteorol. Appl.16: pp 353 – 360. DOI: 10.1002/met.131.

Ramesh kumar MR and Byju (2010) A multi sensor study of conditions leading to the formation of a cyclone over the Arabian sea during 5-9 May 2004, International journal of Remote sensing,31:17,4683-4697.

Ramesh Kumar MR and Sankar S (2010) Impact of global warming on cyclonic storms over north Indian Ocean. Indian J Geo-Mar Sci. Vol. 39(4):December 2010, pp. 516–520.

Roy Bhowmik SK (2003) An evaluation of cyclone genesis parameter over the Bay of Bengal using model analysis. Mausam (New Delhi) 54: pp 351–358

Royer JF, Chauvin F, Timbal B, Araspin P, Grimal D (1998) A GCM study of the impact of greenhouse gas increase on the frequency of occurrence of tropical cyclone. Clim Change 38: pp 307–343. doi: 10.1023/A:1005386312622.

Ryan BF, Watterson IG and Evans JL (1992) Tropical cyclone frequencies inferred from Gray's yearly genesis parameter: Validation of GCM tropical climates. Geophys. Res. Lett., 19, 1831–1834.

Saji NH, Goswami BN, Vinayachandran PN, Yamagata T (1999) A dipole mode in the tropical Indian Ocean. Nature 401: pp 360-363.

Saji NH and Yamagata T (2003) Possible impacts of Indian Ocean Dipole mode events on global climate.

Saunders MA, Chandler RE, Merchant CJ, and Roberts FP (2000) Atlantic hurricanes and NW Pacific typhoons: ENSO spatial impacts on occurrence and landfall. Geophys. Res. Lett., 27, pp 1147–1150.

Shea DJ and Gray WM (1973a) The hurricanes inner core region. I. Symmetric and asymmetric structure. J. of Atmos. Scie. Volume 30, pp 1544-1564.

Sikora CR (1976) An investigation of equivalent potential temperature as a measure of tropical cyclone intensity. Technical note, JTWC, 76-3, 12 pp

Singh OP,Khan TMA,Rahman S (2000) Changes in the frequency of tropical cyclones over the North Indian Ocean. Meteorol Atmos Phys 75: pp 11-20

Singh OP (2007) Long-term trends in the frequency of severe cyclones of Bay of Bengal: obseervations and simulations. Mausam 58: pp 59-66

Singh OP, Ali Kahn TM, Rahman (2001) Has the frequency of intense tropical cyclones increased in the north Indian Ocean? Curr Sci 80: pp 575-580.

Shapiro LJ (1987) Month-to-month variability of the Atlantic tropical circulation and its relationship to tropical storm formation. Mon. Wea. Rev., 115, pp 2598–2614.

Shinoda T, Hurlburt HE and Metzget EJ (2011) Anomalous tropical ocean circulation associated with La Niña Modoki. J. Geophys. Research. Volume 116, C12001, doi:10.1029/2011JC007304.

Smith TM and Reynolds RW (2003) Extended Reconstruction of Global Sea Surface Temps based on COADS 1854-1997. Journal of Climate, 16, 1495-1510.

Smith TM, Reynolds RW, Peterson TC and Lawrimore J (2008) Improvements NOAAs Historical Merged Land Ocean Tem Analysis (1880-2006), Journal of Climate, 21, 2283-2296.

Srivastav AK, Sinha RayKC, De US (2000) Trends in the frequency of cyclonic disturbances and their intensification over Indian Seas. Mausam 51: pp 113-118

Sumesh KG and Ramesh Kumar MR (2013) Tropical cyclones over North Indian Ocean during El-Niño Modoki years. Nat. Haz.

Sumesh KG and Ramesh Kumar MR (2015) Tropical cyclones over North Indian Ocean during La-Niña Modoki years. IJGMS.

Tang BH and Neelin JD (2004) ENSO influence on Atlantic hurricanes via tropospheric warming. Geophys. Res. Lett., 31.L24204, doi:10.1029/2004GL021072.

Trenberth KE (1997) The definition of El-Niño. Bull. Amer. Met. Soc., 78, pp 2771-2777.

Trenberth KE and Stepaniak DP (2001) Indices of El-Niño evolution. J. Climate, 14, pp 1697-1701.

Wang B, Chan JCL (2002) How strong ENSO events affect tropical storm activity over the western North Pacific. J Clim 15: pp 1643–1658

Webster PJ, Moore AM, Loschnigg JP, Leben RR (1999) Coupled Oceanic-Atmospheric dynamics in the Indian Ocean during 1997-98. Nature 401: pp 356-360

Weng, H., K. Ashok, S. K. Behera, S. A. Rao, and T. Yamagata (2007) Impacts of recent El Niño Modoki on dry/wet condidions in the Pacific rim during boreal summer. Climate Dynamics, 29, pp 113-129.

Weng, H., S. K. Behera, and T. Yamagata (2009) Anomalous winter climate conditions in the Pacific rim during recent El Niño Modoki and El Niño events. Climate Dynamics, 32, pp 663-674.

Wu MC, Chang WL and Leung WM (2004) Impacts of El Niño–Southern Oscillation events on tropical cyclone landfalling activity in the western North Pacific. J. Climate, 17, pp 1419–1428.

Wu G and Lau NC (1992) A GCM simulation of the relationship between tropical-storm formation and ENSO. Mon. Wea. Rev., 120, pp 958–977.

Wu et.al (2015) Impact of environmental moisture on tropical cyclone intensification Atmos. Chem. Phys., Volume 15, pp 14041-14053.

Xavier PK, Joseph PV (2000) Vertical wind shear in relation to frequency of monsoon depressions and tropical cyclones of Indian seas, Proc. Of TROPMET-2000, National symposium on Tropical Meteorology, 1-4 February 2000, Cochin, India, pp 242-245.

Xue Y, Smith TM and Reynolds RW (2003) Inter decadal changes of 30-Yr SST Normals during 1871-2008. Journal of Climate, 16, 1601-1612.

Yu L and Weller RA (2007) Objectively Analyzed air-sea heat Fluxes for the global ice-free oceans (1981–2005). Bull. Ameri. Meteor. Soc., 88, 527–539.

Yuan J and Cao J (2013) North Indian Ocean tropical cyclone activities influenced by the Indian Ocean Dipole mode. J. Sci. China Earth Sci. Vol. 56: pp 855-865. doi:10.1007/s11430-012-4559-0.

Zehr RM (1992) Tropical cyclogenesis in the western north Pacific. NOAA Tech. Rep. NESDIS 61, 181pp.